École Doctorale des Sciences Chimiques (ED250)
Aix-Marseille Université
Campus Scientifique de Luminy
Marseille, France

Université de Médecine de Kaohsiung
Département de Chimie Médicale et Appliquée
Kaohsiung, Taïwan

Centre Interdisciplinaire de Nanoscience de Marseille (CINaM)
CNRS UMR 7325, France

Thèse de Doctorat
en vue d'obtenir le grade de Docteur de Aix-Marseille Université
et Université de Médecine de Kaohsiung

spécialité : Chimie
présentée par

Adela Ya-Ting Huang

Avancée dans la synthèse de dendrimères, sur support solide et par auto-assemblage

Soutenance prevue le 11 Juillet 2017
devant le jury compisé de:

Anne-Marie Caminade	Directeur de Recherche, LCC CNRS UPR 8241	Rapporteur
Yun-Ming Wang	Professeur, Université de Chiao-Tung de Nationale	Rapporteur
Jean-Louis Reymond	Professeur, Université de Berne	Jury
Frédéric Fages	Professeur, Aix-Marseille Université	Jury
Chun-Cheng Lin	Professeur, Université de Tsing Hua de Nationale	Jury
Sodio Chih-Neng Hsu	Professeur, Université de Médecine de Kaohsiung	Jury
Ling Peng	Directeur de Recherche, CINaM, CNRS UMR 7325	Directeur de thèse
Chai-Lin Kao	Professeur, Université de Médecine de Kaohsiung	Directeur de thèse

Department of Medicinal and Applied Chemistry

Kaohsiung Medical University, Taiwan

and

École Doctorale des Sciences Chimiques (ED250)

Aix-Marseille University, CINaM, CNRS UMR 7325, France

Co-tutorship PhD Dissertation

Supervisor: **Dr. Chai-Lin Kao**

                              Dr. Ling Peng

Co-supervisor：   **Dr. Aura Tintaru**

Advancing Dendrimer Synthesis:
Solid-phase and Self-assembly Approach

Avancée dans la synthèse de dendrimères, sur support solide
et par auto-assemblage

Adela Ya-Ting Huang

July 2017

Table of Contents

Acknowledgements

First of all, I would like to acknowledge my committee, Dr. Anne-Marie Caminade, Dr. Yun-Ming Wang, Dr. Jean-Louis Reymond, Dr. Frédéric Fages, Dr. Chun-Cheng Lin, Dr. Sodio Chih-Neng Hsu, Dr. Ling Peng and Dr. Chai-Lin Kao. Thank you for your kind acceptance serving on my committee, as the jury of my PhD defense.

Secondly, I would like to express my sincere gratitude to all the people who helped me during my PhD period. My deepest gratitude goes to my supervisor Dr. Ling Peng and Dr. Chai-Lin Kao, who gave me many instructive advices and valuable suggestions both in the academic studies and daily life. During my PhD degree pursuing, I learned a lot about scientific thinking and methodical working, which broadened my horizons and allowed me to acquire good habits. I am really grateful of their assistances. In particular, in the preparation of my dissertation, the insightful guidance and careful revision is of great importance for the completion with present quality.

I am also greatly indebted to my co-supervisor, Dr. Aura Tintaru. She taught and helped me a lot during my working and thesis preparation. She is playing a role of a director as well as a friend. What I learned from her was not only about the science and work but also her attitude to life.

I do appreciate Dr. Gilles Quéléver and Dr. Alain Maggiani at AMU who gave me a lot of help and suggestions as well as thesis revision.

To Dr. Hui-Ting Chen and Dr. Horng-Huey Ko at KMU, thank you for listening to me, supporting me, and giving me advice whenever it was needed. Thanks to Dr. Chi-Yu Lu and Dr. Hsing-Yin Chen at KMU who did many efforts in MS characterizations and computational simulations for my PhD projects.

I would also like to gratefully acknowledge all the members: of the Kao group at KMU: Dr. Kuang-Chan Hsieh, Dr. Yi-Hsuan Tang, Ms. Ching-Hua Tsai, Mr. Anand Selvaraj, Mr. Yu-Wen

Abstract

Dendrimers hold great promise for a wide range of applications thanks to their unique structural architecture and multivalent cooperativity. Unfortunately, dendrimer synthesis often suffers from inherent problems of structural defects caused by incomplete reactions and difficulties associated with dendrimer purification because of the presence of highly similar side-products. For these reasons, alternative synthetic approaches to overcome the limitations of current dendrimer synthesis are in high demand. The objective of my PhD thesis is to contribute to advances in dendrimer synthesis by exploring solid-phase method and self-assembly approaches to enable the creation of structurally diverse dendrimers as new molecular paradigms and functional materials for future applications, in particular in the biomedical field.

The first part of my PhD project mainly focuses on establishing novel strategies and methodologies for solid-phase dendrimer synthesis (SPDS) because SPDS has advantages of convenient synthesis and easy purification procedures. We first developed a new and concise solid-phase synthesis of PAMAM dendrimers based on the adoption of peptide synthesis chemistry. High-generation dendrimers were successfully achieved using solid supports with a reduced loading ratio. We then constructed a small library of triazine dendrimers varying in generations and surface groups with a view to rapidly synthesizing dendrimers with structural diversity. We also strived to synthesize poly(aminoester) dendrimers using the solid-phase method. However, due to the labile nature of poly(aminoester) dendrimers, we were not able to obtain the desired dendrimers. We are still pursuing our efforts in this direction.

The second part of my PhD program aims to apply the self-assembly approach for constructing supramolecular dendrimers, because self-assembly is a powerful yet convenient strategy to create supramolecular nanoassemblies. In particular, we would like to build a supramolecular dendrimer nanosystem as a nanotheranostic for simultaneous molecular imaging and drug delivery. For this purpose, a small DOTA-conjugated amphiphilic dendrimer with Gd(III)-chelation has been established. This dendrimer was able to self-assemble into supramolecular dendrimer nanomicelles to encapsulate the anticancer drug doxorubicin in the interior, while at the same time bearing Gd/DOTA-entities on the dendrimer surface. It constitutes a novel multivalent nanotheranostic to improve imaging sensitivity and resolution as well as therapeutic efficacy.

In summary, my PhD program mainly contributes to elaborating strategies for dendrimer synthesis using both solid-phase method and self-assembly approach. Results from these studies have allowed us to advance dendrimer synthesis and will further help us to improve our knowledge with a view to constructing versatile dendritic molecules and broaden their applications in the arenas of biomedical and material sciences.

Keywords: solid-phase synthesis, inverse PAMAM dendrimers, triazine dendrimer library, poly(aminoester) dendrimers, self-assembly, amphiphilic dendrimers, nanotheranostics

Résumé

Les dendrimères sont des outils extrêmement prometteurs pour un très large éventail d'applications du fait de leur architecture structurelle unique et à leur multivalence. Cependant, leur synthèse souffre encore de problèmes inhérents aux défauts de structure causés par des réactions incomplètes ainsi qu'à des difficultés associées à leur purification liées à la présence de produits secondaires très similaires aux dendrimères escomptés. Pour ces différentes raisons et afin de surmonter les limitations rencontrées lors de la synthèse de dendrimères, des approches synthétiques alternatives sont fortement requises. L'objectif de mon doctorat consiste à réaliser des avancées dans la synthèse de dendrimères en explorant notamment une approche sur support solide ainsi que des approches d'auto-assemblage pour faciliter la synthèse de dendrimères et permettre la création de nouveaux dendrimères structurellement diversifiés et pouvant être utilisés en tant que nouveaux paradigmes moléculaires et matériaux fonctionnels pour une large gamme d'applications.

La première partie de mon projet de thèse se concentre principalement sur la mise au point d'une stratégie et d'une méthodologie novatrices pour la synthèse de dendrimères en phase solide (SPDS). Nous avons tout d'abord développé une nouvelle méthode de synthèse sur support solide de dendrimères poly(amidoamines) (PAMAM) basée sur l'utilisation des principes de la chimie de synthèse de peptides. Les dendrimères de hautes générations sont obtenus efficacement en utilisant un taux de charge réduit des supports solides. Nous avons ensuite construit une petite bibliothèque de dendrimères de type triazine en faisant varier la taille des dendrimères et donc la génération mais aussi la nature des groupes de surface dans le but de construire une variété de dendrimères de très grande pureté afin d'étendre la diversité d'applications de ces dendrimères. Cette approche nous a permis d'accéder rapidement à ce type de dendrimères de la triazine et d'utiliser des molécules pour des applications biomédicales spécifiques. Nous nous sommes également efforcés de synthétiser des dendrimères poly(aminoesters) en utilisant les principes de la synthèse sur support solide. Néanmoins, du fait du caractère labile de ces dendrimères, nous n'avons pu les obtenir, mais nous poursuivons tout de même nos efforts dans ce domaine.

L'auto-assemblage est également une alternative très intéressante pour générer des nanostructures supramoléculaires, qui peuvent se comporter comme étant plus que la somme de leurs unités constitutives individuelles et être dotées de propriétés totalement nouvelles. La deuxième partie de mon programme de thèse vise justement à appliquer une approche d'auto-assemblage pour la construction de dendrimères supramoléculaires comme nanothéranostiques pour l'imagerie moléculaire simultanée et l'administration de médicaments. A cet effet, nous avons construit un petit dendrimère amphiphile modifié par DOTA présentant des propriétés chélatantes pour le Gd (III). Ce dendrimère est capable de s'auto-assembler en dendrimère supramoléculaire et par la même occasion d'encapsuler l'agent anticancéreux doxorubicine dans sa structure interne. Du fait de la présence également d'entités Gd / DOTA à la surface de ce dendrimère, nous avons ainsi constitué de nouveaux agents théranostiques à base de dendrimères multivalents afin d'améliorer la sensibilité et la résolution pour l'imagerie ainsi que l'efficacité des agents thérapeutiques.

En résumé, les principaux efforts de ma thèse ont été orientés vers le développement de stratégies innovantes pour la synthèse de dendrimères en utilisant les principes de la synthèse en phase solide mais aussi ceux de l'auto-assemblage. Les résultats issus de ces études nous ont permis de mieux comprendre et de faire avancer nos connaissances actuelles en vue de construire davantage de molécules dendritiques polyvalentes et ainsi d'élargir leurs applications dans les domaines des sciences biomédicales et des sciences des matériaux.

Mots-clés: synthèse en phase solide, dendrimères PAMAM inversés, bibliothèque de dendrimères de triazine, dendrimères poly(aminoesters), dendrimères auto-assemblés, dendrimères amphiphiles, nanothéranostique

中文摘要

　　樹枝狀高分子具有可精確調控的高度分支結構與多價特性，是當前正在蓬勃發展的新型合成高分子。近年來，隨著對樹枝狀高分子各方面研究的不斷深入，其多價性與協同性，以及可形成奈米級球型結構等許多獨特的分子性質，在在引起相關領域的關注與探討。然而，樹枝狀高分子的合成是一個繁瑣、耗時且費力的過程，由於製備過程中常存在結構高度相似的副產物，因此導致純化與分離上的困難與複雜，進而削弱了它們在開發與應用上的潛力。因此，開拓新的合成方法是目前發展樹枝狀高分子的重點方向之一。我的博士論文主要以開發固相合成和自組裝方法有效製備樹枝狀高分子為研究重點。

　　在本博士論文中第一部分的重點為建立固相合成法，利用其產物易純化及分離之優點，作為樹枝狀高分子合成的新策略。首先，在胜肽合成化學的基礎上，設計了相對應的單體分子作為固相合成的材料，以達合成新型的反式聚乙二胺樹枝狀高分子之目標。論文中亦經由減少固相樹脂載體的負載率，成功建構了高代數樹枝狀高分子。而為增加固相合成樹枝狀高分子之應用性與多樣性，更利用組合化學建立了具多種表面官能機修飾的三嗪樹枝狀高分子樣品庫，該方法可快速獲取具分子多樣性的三嗪樹枝狀高分子庫，進一步提高樹枝狀高分子可供應用的機會。另外，於本論文研究中亦使用固相方法合成聚胺酯樹枝狀高分子，以克服此類分子在液相合成中的限制和挑戰。

　　本博士研究之第二部分旨在以自組裝樹枝狀超分子，並將其應用於奈米科學、分子成像和藥物傳輸。論文研究利用自組裝非共價鍵結合小代數樹枝狀分子，將其組裝成高分子複合物，解決了樹枝狀高分子在傳統合成中的問題。研究中設計並合成了具1,4,7,10-四氮雜環十二烷-1,4,7,10-四羧酸修飾之兩親性樹枝狀高分子，作為釓的螯合劑，將其應用於醫學影像顯影劑，以提高成像靈敏度和分辨率。

　　綜上所述，此博士論文主要致力於發展固相合成與自組裝作為樹枝狀高分子之合成策略與其相關應用。利用已知之相關知識探討及研究成果，進一步結合固相合成與自組裝方法，開發具多功能性及創新性的樹枝狀高分子，並將其應用擴展到生物醫學和材料科學領域。

關鍵詞：固相合成、反式聚乙二胺樹枝狀高分子、三嗪樹枝狀高分子、聚胺酯樹枝狀高分子、自組裝、兩親性樹枝狀高分子、奈米材料、醫學影像。

List of Publications

I. Publications

1. Chai-Lin Kao; **Adela Y.-T. Huang**; Hui-Ting Chen. Solid-phase synthesis of a seventh-generation inverse poly(amidoamine) dendrimer: importance of the loading ratio on the resin. *Macromol. Rapid Commun.,* **2017**, marc.201700062R. (IF: 4.638, 8/85)

2. **Adela Y.-T. Huang**; Chai-Lin Kao; Ling Peng. Solid-phase synthesis: A promising and valuable means to transform dendrimer synthesis. *Chem. Soc. Rev.,* **2016**, in revision. (IF: 34.09, 2/163)

3. **Adela Y.-T. Huang**; Subrata Patra; Hui-Ting Chen; Chai-Lin Kao; Eric E. Simanek. Solid-phase Synthesis of Libraries of Triazine Dendrimers and Orthogonal Staining Methods for Tracking Reactions on Resin. *Asian J. Org. Chem.,* **2016**, *5*, 860-864. (IF: 3.318, 16/59)

4. Yi-Han Chen; Rajendranath Kirankumar; **Adela Y.-T. Huang;** Chi-Yu Lu; Chai-Lin Kao; Po-Yu Chen. Electrochemical study of a new non-heme iron complex-modified carbon ionic liquid electrode with electrocatalytic activity towards hydrogen peroxide reduction. *Electrochimica Acta.*, **2015**, *184*, 316-322. (IF: 4.504, 3/27)

5. Subrata Patra; Brittany Kozura; **Adela Y.-T. Huang**; Alan E. Enciso; Xiankai Sun; Jer-Tsong Hsieh; Chai-Lin Kao; Hui-Ting Chen; Eric E. Simanek. Dendrimers Terminated with Dichlorotriazine Groups Provide a Route to Compositional Diversity. *Org. Lett.*, **2013**, *15*, 3808-3811. (IF: 6.324, 3/58)

6. **Adela Y.-T. Huang**; Ching-Hua Tsai; Hsing-Yin Chen; Hui-Ting Chen; Chi-Yu Lu; Yu-Ting Lin; Chai-Lin Kao, Concise solid-phase synthesis of inverse poly(amidoamine) dendrons using AB2 building blocks. *Chem. Commun.*, **2013**, *49*, 5784-5786. (IF: 6.718, 20/148)

7. Yi-Hsuan Tang; **Adela Y.-T. Huang**; Po-Yu Chen; Hui-Ting Chen; Chai-Lin Kao, Metallodendrimers and Dendrimer Nanocomposites. *Curr. Pharm. Design*, **2011**, *17*, 2308-2330. (IF: 3.87, 46/261)

8. **Adela Y.-T. Huang**, Introduction of Intense Pulse Light and Cosmetic Laser as Medical Beauty Treatments, *Quarterly of Kaohsiung Medical University Innovation Incubation Center*, **2009**, *17*, 3-5.

II. Oral communications

1. **<u>Adela Y.-T. Huang.</u>** Solid-phase Synthesis as a Promising Approach for Dendrimer Synthesis. Rencontres Scientifiques des Doctorants en Chimie de Marseille-7$^{\text{ème}}$ edition, 04/2017, Marseille, France

2. **<u>Adela Y.-T. Huang</u>**; Chai-Lin Kao, Ling Peng. Solid-phase Synthesis as a Promising Approach for Dendrimer Synthesis. Journées Méditerranéennes des Jeunes Chercheurs 2016 (JMJC 2016), 10/2016, Nice, France.

3. **<u>Adela Y.-T. Huang</u>**; Chai-Lin Kao. The Development of Solid-phase Dendrimer Synthesis. 2015 PST Medicinal Chemistry Symposium, 05/2015, Xitou, Taiwan. **(The third prize)**

4. **<u>Adela Y.-T. Huang</u>**; Chai-Lin Kao. Synthesis of Poly(amidoamine) (PAMAM) Dendron Analogue by Using AB$_2$ Monomers through Solid-Phase Peptide Synthesizer. 8$^{\text{th}}$ International Dendrimer Symposium, 06/2013, Madrid, Spain.

III. Posters presentations

1. **<u>Adela Y.-T. Huang.</u>** Solid-phase Synthesis of Libraries of Triazine Dendrimers and Orthogonal Staining Methods for Tracking Reactions on Resin. Rencontres Scientifiques des Doctorants en Chimie de Marseille-6$^{\text{ème}}$ edition, 05/2016, Marseille, France

2. **<u>Adela Y.-T. Huang</u>**; Subrata Patra; Hui-Ting Chen; Eric E. Simanek; Chai-Lin Kao. Preparation of Triazine Dendrimers Library through Solid-phase Method. 4th International Symposium on Biomedical Applications of Dendrimers. 06/2014, Lugano, Switzerland.

3. Yu-Ting Lin, **<u>Adela Y.-T. Huang</u>**, Hui-Ting Chen. Solid phase synthesis of poly(amino) ester dendrimers. 4th International Symposium on Biomedical Applications of Dendrimers. 06/2014, Lugano, Switzerland.

4. **<u>Adela Y.-T. Huang</u>**. Solid-phase Synthesis of A Small Library of Triazine Dendrimers with Amine Nucleophiles to Poly(dichlorotriazines). Poster Competition 2014, 04/2014, College of Life Science, Kaohsiung Medical University, Kaohsiung, Taiwan. **(The Outstanding Award)**

5. Ying-Yu Chen; **<u>Adela Y.-T. Huang</u>**. Preparation of Triazine Dendrons with Diverse Nucleophilic Linkers through Solid-phase Synthesis. Poster Competition 2014, 04/2014,

College of Life Science, Kaohsiung Medical University, Kaohsiung, Taiwan. **(Honorable Mention Award)**

6. Yu-Ting Lin; **Adela Y.-T. Huang**. A Method for the Poly(amino) Ester Dendrimers of *tert*-butyl-Derivatized Solid Phase Supports. Poster Competition 2014, 04/2014, College of Life Science, Kaohsiung Medical University, Kaohsiung, Taiwan.

7. **Adela Y.-T. Huang**; Chai-Lin Kao, Synthesis of Poly(amidoamine) (PAMAM) Dendron Analogue by Using AB_2 Monomers through Solid-Phase Peptide Synthesizer. 8th International Dendrimer Symposium, 06/2013, Madrid, Spain.

8. **Adela Y.-T. Huang;** Ching-Hua Tsai and Yu-Ting Lin. Synthesis of inverse poly(amidoamine) (PAMAM) dendrons by using AB_2 monomers through solid-phase synthesizer. Poster Competition 2013, 04/2013, College of Life Science, Kaohsiung Medical University, Kaohsiung, Taiwan. **(Merit Award)**

9. **Adela Y.-T. Huang**; Chai-Lin Kao. A facile solid-supported approach of dendritic macromolecules synthesis. Medicinal Chemistry Symposium 2013, 01/2013, Pingtung.

10. **Adela Y.-T. Huang**; Yu, S. K.; Lin, J. Y.; Chen, H. T. Evaluation of the Affinity of Peptides and Hydroxyapatite. ISCMC2010, 10/2010, Taipei.

Abbreviations

4-AMP	4-Aminomethylpiperidine
Ac_2O	Acetic anhydride
AliR	Alizarin R (Mordant orange)
Boc	*tert*-Butoxycarbonyl
Boc_2O	Di-*tert*-butyl dicarbonate
DBU	1,8-Diazabicyclo[5.4.0]undec-7-ene
DCC	*N,N'*-Dicyclohexylcarbodiimide
DCM	Dichloromethane
DCU	Dicyclohexyl urea
DIPEA	*N,N*-Diisopropylethylamine
DLS	Dynamic light scattering
DMAP	4-Dimethylaminopyridine
DMB	1,3-Dimethoxybenzene
DMF	Dimethylformamide
DOSY	Diffusion-ordered spectroscopy
DOTA	1,4,7,10-Tetraazacyclododecane-1,4,7,10-tetraacetic acid
DOX	Doxorubicin
DTPA	Diethyltriaminepentaacetic acid
EA	Ethyl acetate
EDA	Ethylenediamine
ESI	Electrospray ionization
EtOH	Ethanol
Fmoc	9-Fluorenylmethyloxycarbonyl
G	Generation
Gd	Gadolinium
GPC	Gel permeation chromatography
HEEP	1-Hydroxyethoxyethylpiperazine
HPLC	High performance liquid chromatography

HRMS	High-resolution mass spectrometry
IR	Infrared spectroscopy
MALDI	Matrix-assisted laser desorption/ionization
MAP	Multiple antigenic peptide
MeCN	Acetonitrile
MeOH	Methanol
MG	Malachite green
MRI	Magnetic resonance imaging
MS	Mass spectrometry
NMM	N-Methylmorpholine
NMR	Nuclear magnetic resonance
NOTA	1,4,7,10-Tetraazacyclododecane-1,4,7,10-tetraacetic acid
PAMAM	Poly(amidoamine)
PDI	Polydispersity index
PEG	Poly(ethylene glycol)
PET	Positron emission tomography
PS	Polystyrene
PyBOP	Benzotriazol-1-yl-oxytripyrrolidinophosphonium hexafluorophosphate
SPDS	Solid-phase dendrimer synthesis
SPECT	Single photon emission computed tomography
SPOS	Solid-phase organic synthesis
SPS	Solid-phase synthesis
TBAI	Tetrabutylammonium iodide
*t*Bu	*tert*-Butyl
TEA	Triethylamine
TETA	1,4,8,11-Tetraazacyclotetradecane-N,N',N'',N'''-tetraacetic acid
TFA	Trifluoroacetic acid
THF	Tetrahydrofuran
TIS	Triisopropylsilane
TOF	Time-of-flight

Chapter I: General introduction

1. Dendrimers

Dendrimers are a special class of synthetic macromolecules with a precisely-controlled molecular structure and a unique radiating ramified architecture (**Figure 1**). They were first reported in 1978[1] by Vögtle and referred to as "cascade molecules". Later on, the term "dendrimer" was coined and proposed by Tomalia and his co-workers based on the Greek words "dendron" (tree) and "meros" (part).[2] Structurally speaking, a dendrimer is composed of three main components: (i) the central core from which the dendrimer emanates, (ii) the repetitive branching units which allow dendrimer growth in geometrically-organized radial layers called generations, and (iii) the large number and dense distribution of terminal groups on the surface (**Figure 1**). In 1985, Tomalia reported the synthesis of the first family of dendrimers, the poly(amidoamine) (PAMAM) dendrimers from generation 1 to generation 10.[3] Shortly after, dendrimers such as polyether dendrimers[4], polypropylamine dendrimers[5], polypeptide dendrimers[6] and phosphor dendrimers[7] etc. also emerged.[8,9] Nowadays, over 100 types of different dendrimers have been reported with an impressive diversity in the core, repeating units and terminal functionalities, ranging from pure hydrocarbons to peptides or coordination compounds.[10-12]
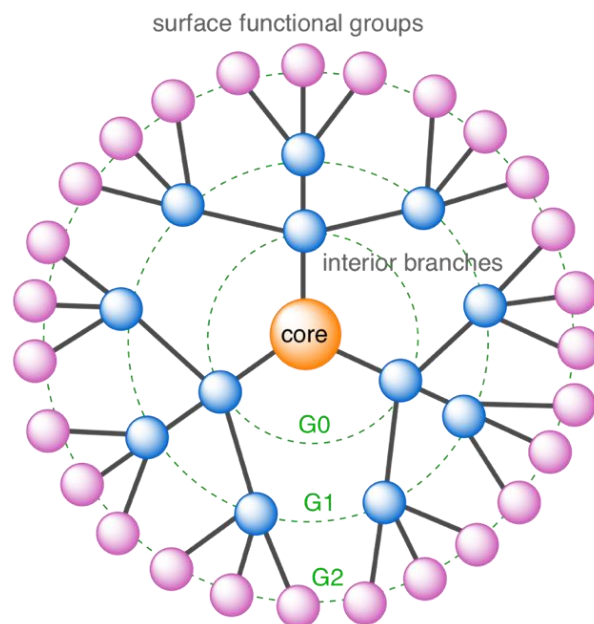
Figure 1. General presentation of a dendrimer composed of a central core (in orange: ⬤), radiating branch units defining the number of generations (in blue: ⤙), and surface terminals (in pink: ⬤).

Since the seminal report of Tomalia et al., dendrimers have always been intriguing and fascinating to the scientific community because of their unique structural properties such as the well-defined, regular and highly branched 3D-structure with various cavities in the interior, and the numerous terminals on the surface which result in multivalent cooperativity.[8,13-15] These distinct properties of dendrimers have been widely exploited in various fields such as catalysis,[16] molecular recognition and sensors[17-19], host-guest chemistry[8,13,20,21], energy storage and production[22-24], and biomedical applications.[10,25] We are particularly interested in the biological applications of dendrimers and will give a quick introduction to this field below.

2. Biomedical applications of dendrimers

As we mentioned above, the major structural characteristics of a dendrimer consist of: (i) the outer surface bearing a high number of functionalities; (ii) the inner and outer shells having a well-defined branching structure and microenvironment; and (iii) the core which gradually becomes more shielded from the outside as the dendrimer grows bigger and bigger. These features together

with the precisely controlled chemical composition and molecular size can be specifically tailored towards a desired property or function that is often required for biological applications such as enzyme mimicry, drugs and drug delivery, vaccines, bio-imaging, tissue engineering etc. We present some brief examples to illustrate these aspects, with a view to giving a perspective on the promising biological applications of dendrimers.

2.1.   Enzyme mimics

Dendrimer-based enzyme mimics are considered to be among the best candidates for creating biomimetic catalysts and artificial enzymes by virtue of their protein-like globular 3D-structure, their shielded inner microenvironment, and their exposed and easily accessible surfaces with numerous functionalities.[26] In fact, the first PAMAM dendrimers were synthesized by Tomalia et al as protein mimics,[27] because PAMAM dendrimers are composed of repeated amide units, similar to peptides and proteins. Dendrimer-based catalysis has gained considerable interest[12] since the first report by Brunner et al. using an optically active phosphine dendrimer, a so-called "dendrizyme", for enantioselective cyclopropanation of styrene with ethyl diazoacetate,[28,29] and later by Knapen et al., who used a Ni(II)-functionalized silane dendrimer (**1**) (**Figure 2**) for regiospecific reaction of Kharasch addition of polyhalogenoalkanes.[30] There are two major advantages of using dendrimers as catalysts. One is creating a large dendritic molecule with many active sites on the dendrimer surfaces. These types of catalysts can be considered as a hybrid of heterogeneous and homogeneous catalysts, featuring high reactivity and selectivity.[31] The other is the encapsulation of catalytic agents such as metal catalysts, which are transported into the interior of the dendrimer, where their activities can be enhanced by dendritic effects.[32,33] Many studies in this field have been reviewed and reported, including different types of dendrimer catalysts generated using dendrimers ranging from organic[34,35]/inorganic dendrimers[12], peptide dendrimers,[11,36,37] phosphor dendrimers[12,31] and metallodendrimers,[38] with various geometrical constructions in the core or on the terminals and branches, and in either homogenous or heterogeneous forms.[31]

1
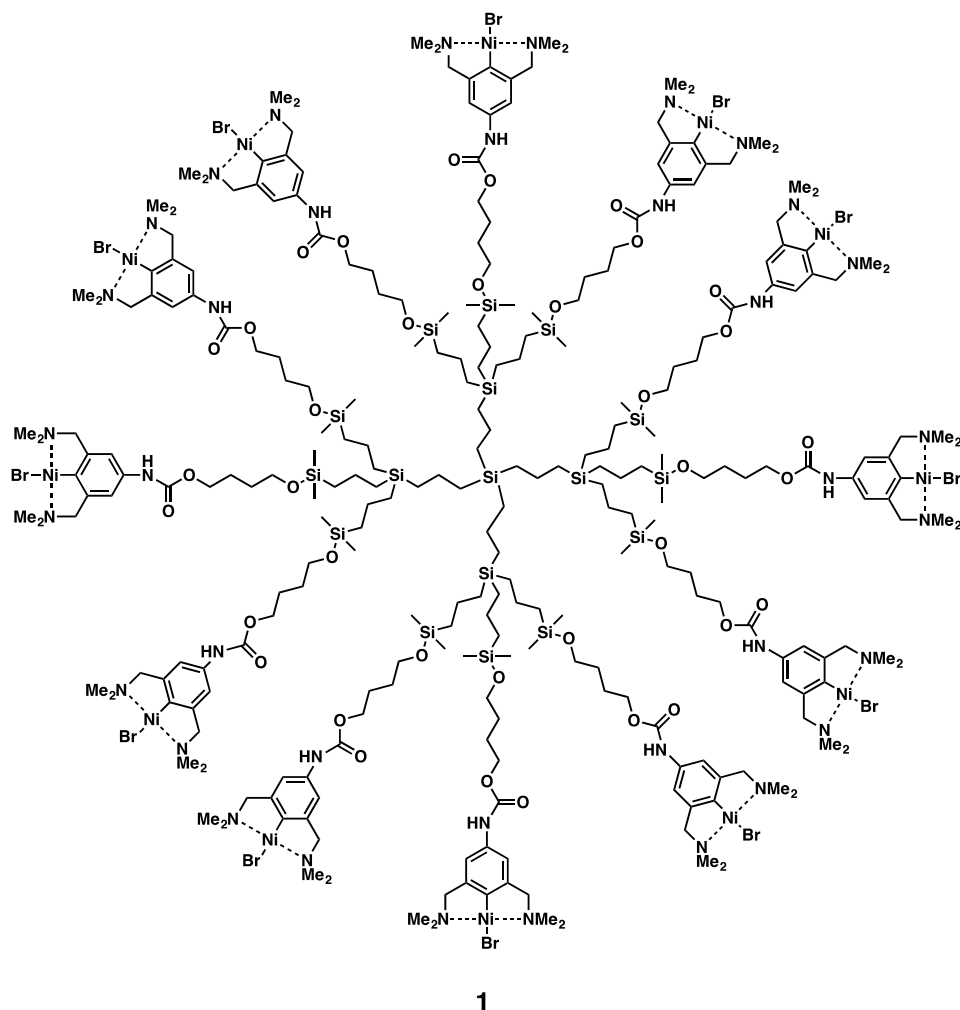
Figure 2. Ni(II)-functionalized silane dendrimers as regiospecific catalysts reported by Knapen et al. in 1994.

2.2. Drug and drug delivery

The most successful biomedical application of dendrimers as drug is the sulfonate-terminated polylysine dendrimer with antiviral and antimicrobial activity, which has been trade-marked as VivaGel[TM], and recommended by WHO for anti-HIV use in Africa.[39] Also, various dendrimers such as PAMAM, peptide dendrimers, glycodendrimers and phosphor dendrimers with antiviral, antibacterial and anti-inflammatory activities have been explored and studied.[40-48]

Dendrimers have also been extensively studied as drug delivery systems. For example, cisplatin was complexed to the surface groups of a carboxylate-terminated PAMAM dendrimer which led to a 10-fold increase in the solubility of the cisplatin compared to the free drug.[49] This cisplatin-

dendrimer conjugate was shown to target to the tumors in mice via the enhanced permeation and retention effect.[49] Amine-terminated PAMAM dendrimers were employed for chemical conjugation with various drug molecules such as the anticancer drug methotrexate,[50] which significantly enhanced the anticancer and anti-tumor activities. In addition, cationic dendrimers have been studied as vectors for nucleic acid delivery in gene therapy.[51,52] This approach exploits the ability of the positively charged dendrimer to interact with the negatively charged nucleic acid to form stable and nanosized complexes, which can prevent nucleic acid from degradation and promote cellular update in order to bring the nucleic acid cargo either to the nucleus for gene transfection or to the RNAi machinery for gene silencing.[53-56] **Figure 3** illustrates one of the structurally flexible PAMAM dendrimers (**2**) developed in our laboratory, which bears a large and extensive core of triethanolamine (TEA) and is very effective for both DNA and RNA delivery.[57] Generation 5 of this dendrimer family has been scheduled in clinical studies for cancer treatment.[58]

2
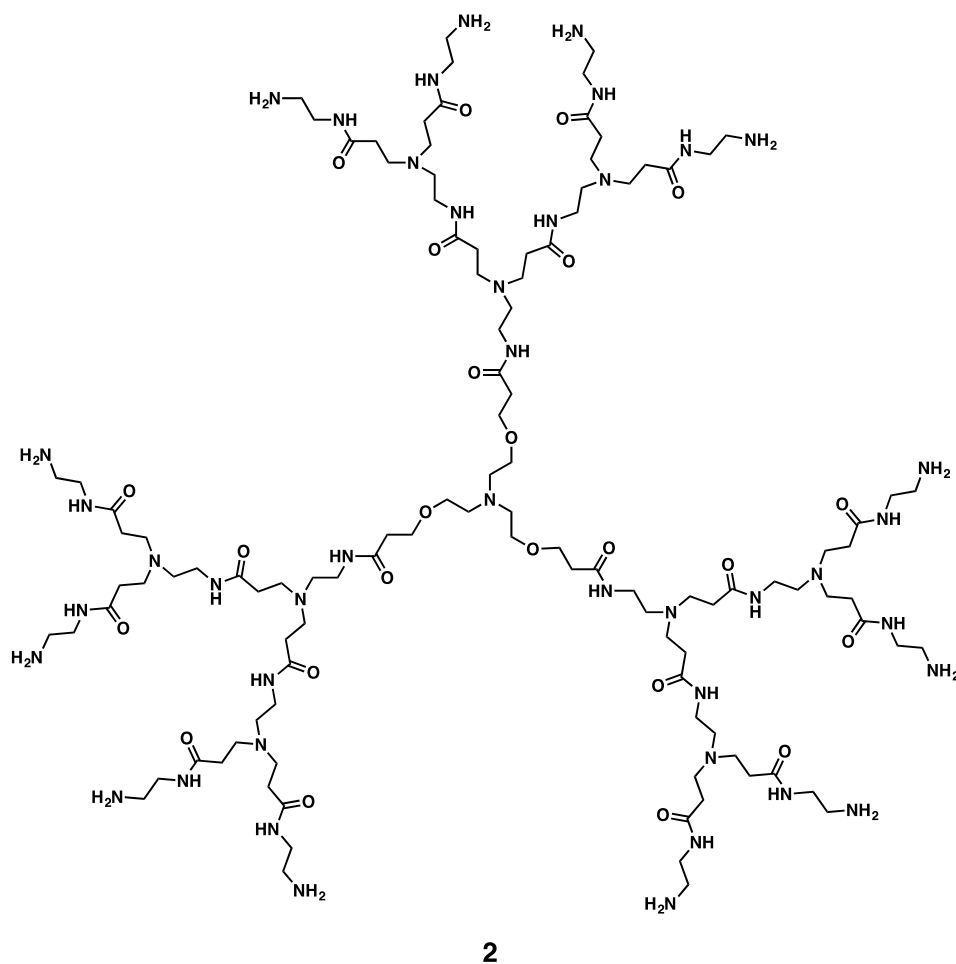
Figure 3. TEA-core PAMAM dendrimer for nucleic acid delivery.[57]

2.3. Vaccines

Dendrimers such as peptide dendrimers and glycodendrimers have also been explored and investigated as vaccines. The multiple antigenic peptide (MAP) dendrimer systems (**Figure 4**) established by Tam et al.[6,59,60] used defined mixtures of B- and T-cell epitopes to decorate the dendrimer terminals. By further conjugating the dendrimer with cancer-related peptides, the obtained MAPs could be processed in antigen-presenting cells in a similar way as antigens derived from intracellular pathogens (e.g. viruses), thereby providing a powerful immune response including cytotoxic T-cells.[61]
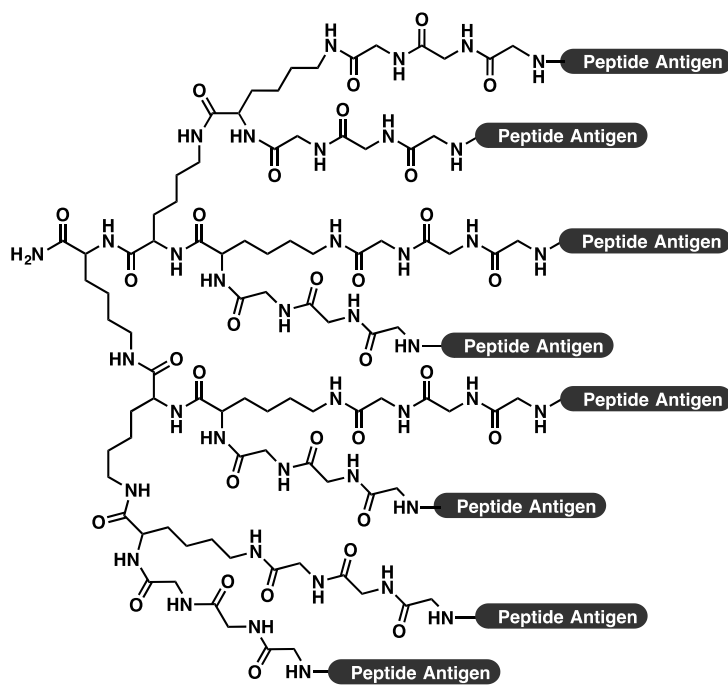
3

Figure 4. Multiple antigenic peptide (MAP) dendrimer.

2.4. Imaging

The earliest report of dendrimers for bio-imaging purposes is the use of PAMAM dendrimers conjugated with a contrast agent for magnetic resonance imaging (MRI).[62] In that study, PAMAM dendrimers were decorated with Gd(III)-DTPA (diethylenetriaminepentaacetic acid) functional entities through a thiourea linkage.[63,64] The so-obtained dendrimer conjugates had a long blood circulation time in mice (or other animals) and showed excellent MRI images of blood vessels. Later, polypropylenimine (PPI) dendrimers appended with Gd(III)-DTPA ligands were also developed.[65-67] In the same direction, gadomer 17 was established based on dendrimers with a 1,3,5-benzoic acid core and lysine residues as branching units with Gd-DOTA (1,4,7,10-tetraazacyclododecane-1,4,7,10-tetraacetic acid) moieties attached at the dendrimer terminals (**Figure 5**). Gadomer 17 has been entered into clinical development and showed a good intravascular distribution and a rapid renal elimination. In addition, dendrimers were constructed with both targeting and imaging components.[68,69] Several reviews provide further details of the development of nanomaterials for bio-imaging purposes.[66,70-73]
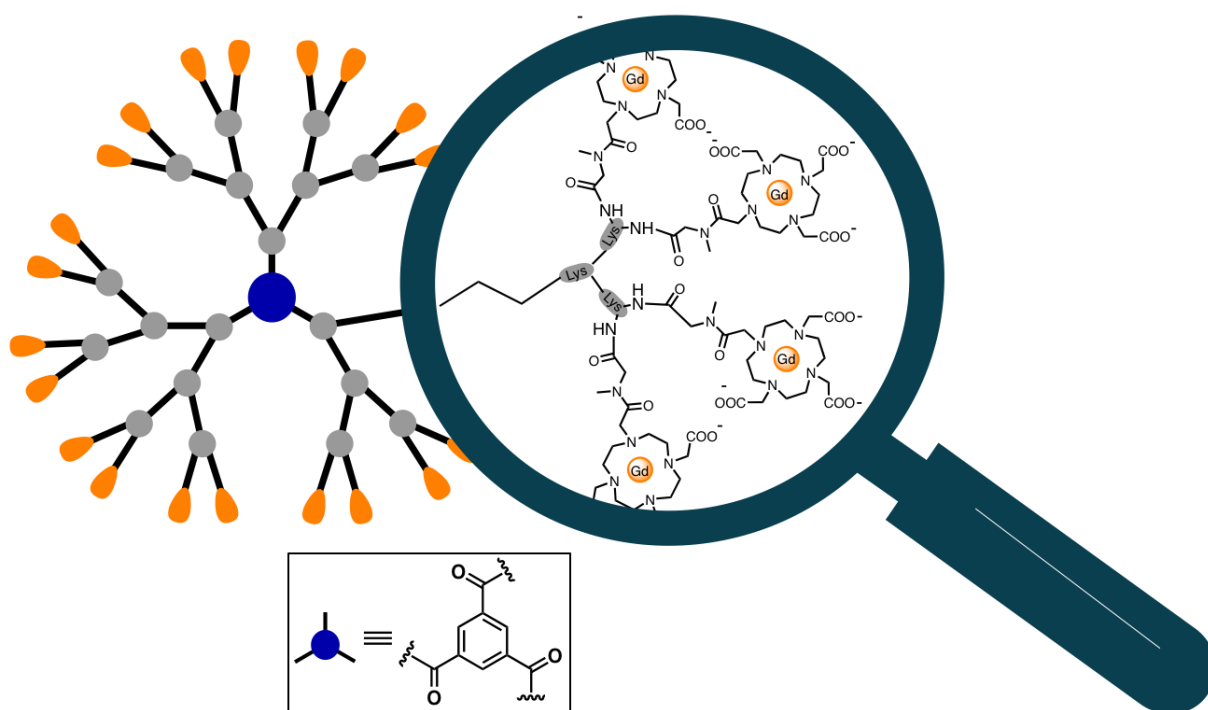
Figure 5. Structural illustration of gadomer 17 based on a polylysine dendrimer with Gd-DOTA moieties.

2.5.   Tissue engineering

Besides the above-mentioned biomedical applications, dendrimers have also been explored for use in tissue engineering. Grinstaff et al. reported polyester dendrimers as injectable sealants for corneal wounds, thanks to the high density of functional-groups and low viscosity in solution.[74-76] In their work, they functionalized the peripheries of biodegradable polyester dendrimers (**Figure 6**) with reactive groups capable of cross-linking and forming an insoluble hydrogel matrix upon UV irradiation. Using this procedure, the authors successfully sealed experimental corneal lacerations and are currently investigating the use of these materials for additional ophthalmic surgeries.
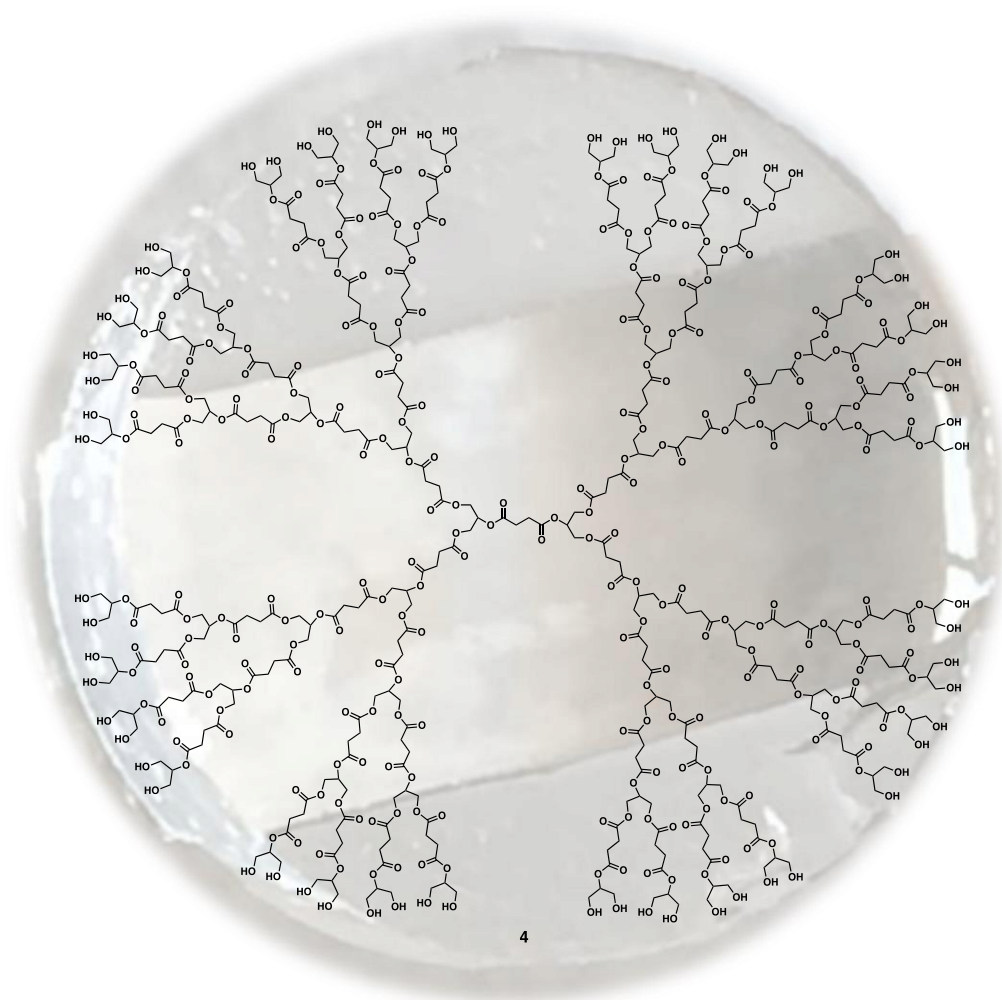
Figure 6. Biodegradable polyester dendrimers for sealing corneal wound in tissue engineering.

3. Conventional dendrimer synthesis and limitations

As we mentioned above, dendrimers have various biological and biomedical applications. However, translation of these applications into therapeutic interventions has often been hampered by the quality and the consistency of dendrimer products.[77] Dendrimer production requires a stepwise synthesis, which is similar to that of proteins and nucleic acids, yet completely different from conventional polymer preparation using one-pot synthesis. Consequently, dendrimer synthesis is tedious, time-consuming and laborious. In addition, dendrimer purification is particularly difficult and complicated due to the presence of impurities in the form of highly similar side-products and/or lower generation dendrimers. This situation gets even worse when preparing higher generation dendrimers.

In general, dendrimer synthesis can be achieved via two classic strategies, namely divergent and convergent approaches (**Figure 7**). In the divergent approach, pioneered by Tomalia[78] and Newkome[79], and currently widely used, dendrimer growth proceeds "inside outward", that is to say, starting from the core and building out towards the outer arms by stepwise multiplication of the branching units (**Figure 7A**).[1,79-81] While this approach can achieve higher generation dendrimers, it is limited by structural defects generated from side reactions and/or incomplete reactions alongside difficulties with purification and separation.[82] Conversely, in the convergent approach as developed by Hawker and Fréchet,[80,81,83-85] a dendrimer is constructed from the outer terminal and inward towards the core, by coupling of dendritic wedges, so-called dendrons, from lower to higher generations (**Figure 7B**). In the convergent approach, the size and generation number of the final dendrimer is pre-determined, providing greater structural control than the divergent method because there are fewer reaction steps and structural defects. The final products are therefore easier to purify. However, the convergent strategy is limited to the preparation of rather low-generation dendrimers due to the steric hindrance of high-generation dendrimers.[82]

A. Divergent method
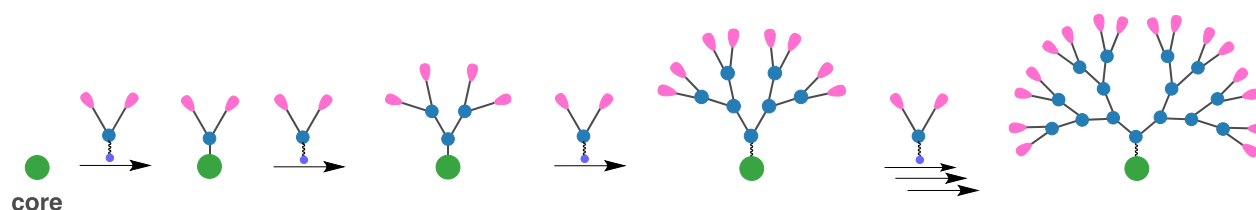
B. Convergent method
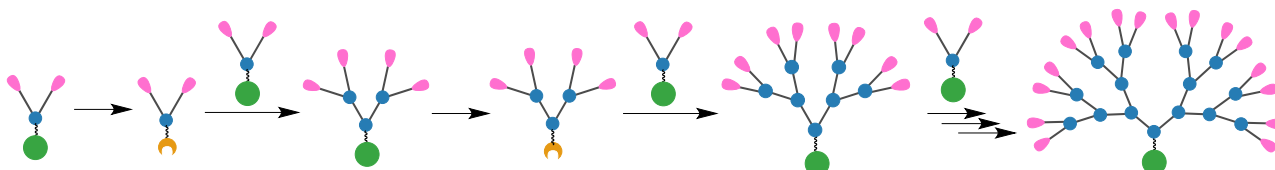
Figure 7. Illustration of **(A)** divergent and **(B)** convergent approaches for dendrimer synthesis.

A further strategy based on a combined divergent/convergent method, called the double-stage approach,[86] has also been developed which can accelerate dendrimer synthesis. More recently, a strategy based on "click" chemistry[82] has shown good promise for rapid and efficient dendrimer synthesis. Nevertheless, both of these new approaches maintain essentially the same chemistry as divergent and convergent synthesis, and hence inevitably inherit the problems concerning structural defects and impurities encountered in divergent and convergent synthesis as well as the problems with the purification procedure. Therefore, a method for convenient synthesis of dendrimers with structural consistency and high quality is in great demand.[81]

4. Alternative strategies for dendrimer construction

As we mentioned above, both divergent and convergent dendrimer synthesis as well as the double-stage and click chemistry methods suffer from inherent problems of synthesis and purification of high-generation dendrimers.[77] Therefore, alternative strategies such as solid-phase synthesis (SPS) and self-assembly approaches have been proposed and explored for dendrimer construction.

Solid-phase synthesis (SPS), first developed by Merrifield for peptide synthesis,[87] has multiple advantageous features such as efficient and complete reaction, ease of practical implementation, a simple purification process and the possibility of eventual automation. Therefore, it constitutes a promising alternative for overcoming the problems encountered during dendrimer synthesis in solution. In addition, the stepwise synthesis of dendrimers resembles that of peptides/proteins and oligonucleotides/nucleic acids, which can be prepared routinely in large quantities and high quality using solid-phase synthesis nowadays. Therefore, we expect that solid-phase synthesis may open up new avenues to transform dendrimer synthesis for constructing functional and dendritic materials for various applications.

Meanwhile, self-assembly is a fundamental concept and an appealing approach for the creation of new molecular architectures and functional materials in modern molecular science.[88-90] It relies on the cumulative effects of non-covalent interactions to assemble molecular building blocks into supramolecular entities in a specific, controllable and reversible way, yet with relatively little synthetic effort.[91] Recently, convergent self-assembly of small dendrons into supramolecular nanostructures for biomedical applications has become of considerable interest. In particular, our group has introduced the concept of self-assembling small amphiphilic dendrons into supramolecular nanomicellar dendrimers as nanovectors for the delivery of nucleic acids and anticancer drugs for gene therapy and cancer treatment.[56,92-94] Given these encouraging results, self-assembly of small amphiphilic dendrons to create supramolecular dendrimers constitutes a promising new strategy for dendrimer constructions.

5. Aim of this PhD thesis

Based on the brief overview of dendrimers and dendrimer synthesis presented above, I would like my PhD project to contribute to the development of dendrimer synthesis using the solid-phase synthesis and self-assembly approach. The first part of my PhD project (chapter II) mainly focuses on establishing a novel strategy and methodology for solid-phase dendrimer synthesis (SPDS) in the hope that SPDS will transform dendrimer synthesis and enable the creation of structurally diverse dendrimers as new molecular paradigms and functional materials for a wide range of applications. Different types of dendrimers, such as PAMAM dendrimers, triazine dendrimers and poly(aminoester) dendrimers, were synthesized using the solid-phase approach in my PhD project, and some of them were realized with great success. In the second part of my PhD program (chapter III), I further explored the self-assembly approach for constructing supramolecular dendrimers as nanotheranostics for simultaneous molecular imaging and drug delivery. Motivated by the promising results that we have obtained from self-assembled amphiphilic dendrimer nanomicelles for drug delivery,[93] a DOTA-modified amphiphilic dendrimer with Gd(III)-chelation has been established. This dendrimer will be used to create novel dendrimer-based MRI contrast agents with multivalence to improve imaging sensitivity and resolution. In the following chapters, I will present my PhD research in the hope that further work will deliver more efficient methods for advancing the synthesis of dendrimers, which can be explored and extended into the arenas of biomedical and material sciences.[95]

6. References

[1] E. Buhleier; W. Wehner; F. Vögtle. "Cascade"- and "nonskid-chain-like" syntheses of molecular cavity topologies. *Synthesis*, **1978**, *2*, 155-158.

[2] D. A. Tomalia; J. R. Dewald; M. R. Hall; S. J. Martin; P. B. Smith, Preprints of the 1st SPSJ International Polymer Conference, Society of Polymer Science, Kyoto, Japan, **1984**, p.65

[3] D. A. Tomalia; H. Baker; J. Dewald; M. Hall; G. Kallos; S. Martin; J. Roeck; J. Ryder; P. Smith. A new class of polymers: Starburst-dendritic macromolecules. *Polym. J.*, **1985**, *17*, 117-132.

[4] C. Hawker; J. M. J. Fréchet. A new convergent approach to monodisperse dendritic macromolecules. *J. Chem. Soc., Chem. Commun.*, **1990**, 1010-1013.

[5] E. M. M. de Brabander-van den Berg; E. W. Meijer. Poly(propylene imine) dendrimers: Large-scale synthesis by hetereogeneously catalyzed hydrogenations. *Angew. Chem. Int. Ed. Engl.*, **1993**, *32*, 1308-1311.

[6] J. P. Tam. Synthetic peptide vaccine design: Synthesis and properties of a high-density multiple antigenic peptide system. *PNAS*, **1988**, *85*, 5409-5413.

[7] N. Launay; A.-M. Caminade; R. Lahana; J.-P. Majoral. A general synthetic strategy for neutral phosphorus-containing dendrimers. *Angew. Chem. Int. Ed. Engl.*, **1994**, *33*, 1589-1592.

[8] J. M. Fréchet. Functional polymers and dendrimers: Reactivity, molecular architecture, and interfacial energy. *Science*, **1994**, *263*, 1710-1715.

[9] F. Vögtle; S. Gestermann; R. Hesse; H. Schwierz; B. Windisch. Functional dendrimers. *Prog. Polym. Sci.*, **2000**, *25*, 987-1041.

[10] U. Boas; J. B. Christensen; P. M. H. Heegaard. Dendrimers in medicine and biotechnology: New molecular tools. RSC Publishing: **2006**.

[11] J.-L. Reymond; T. Darbre. Peptide and glycopeptide dendrimer apple trees as enzyme models and for biomedical applications. *Org. Biomol. Chem.*, **2012**, *10*, 1483-1492.

[12] A.-M. Caminade. Inorganic dendrimers: Recent advances for catalysis, nanomaterials, and nanomedicine. *Chem. Soc. Rev.*, **2016**, *45*, 5174-5186.

[13] D. A. Tomalia; A. M. Naylor; W. A. Goddard. Starburst dendrimers: Molecular-level control of size, shape, surface chemistry, topology, and flexibility from atoms to macroscopic matter. *Angew. Chem. Int. Ed. Engl.*, **1990**, *29*, 138-175.

[14] B. I. Voit. Dendritic polymers: From aesthetic macromolecules to commercially interesting materials. *Acta Polym.*, **1995**, *46*, 87-99.

[15] T. Kehat; K. Goren; M. Portnoy. Dendrons on insoluble supports: Synthesis and applications. *New J. Chem.*, **2007**, *31*, 1218-1242.

[16] F. Zeng; S. C. Zimmerman. Dendrimers in supramolecular chemistry: From molecular recognition to self-assembly. *Chem. Rev.*, **1997**, *97*, 1681-1712.

[17] S. Stevelmans; J. C. M. van Hest; J. F. G. A. Jansen; D. A. F. J. van Boxtel; E. M. M. de Brabander-van den Berg; E. W. Meijer. Synthesis, characterization, and guest−host properties of inverted unimolecular dendritic micelles. *J. Am. Chem. Soc.*, **1996**, *118*, 7398-7399.

[18] J. Satija; V. V. R. Sai; S. Mukherji. Dendrimers in biosensors: Concept and applications. *J. Mater. Chem.*, **2011**, *21*, 14367-14386.

[19] L. Pu, 8. Dendrimer-based sensors. *Chemosensors: Principles, strategies, and applications*, John Wiley & Sons, Inc.: **2011**.

[20] M. W. P. L. Baars; A. J. Karlsson; V. Sorokin; B. F. W. de Waal; E. W. Meijer. Supramolecular modification of the periphery of dendrimers resulting in rigidity and functionality. *Angew. Chem. Int. Ed.*, **2000**, *39*, 4262-4265.

[21] M. W. P. L. Baars; E. W. Meijer, Host-guest chemistry of dendritic molecules. *Dendrimers II: Architecture, Nanostructure and Supramolecular Chemistry*, Springer Berlin Heidelberg: **2000**.

[22] X. Zhou; D. S. Tyson; F. N. Castellano. First Generation light-harvesting dendrimers with a [Ru(bpy)3]2+ core and aryl ether ligands functionalized with Coumarin 450. *Angew. Chem.*, **2000**, *112*, 4471-4475.

[23] A. Adronov; S. L. Gilat; J. M. J. Fréchet; K. Ohta; F. V. R. Neuwahl; G. R. Fleming. Light harvesting and energy transfer in laser−dye-labeled poly(aryl ether) dendrimers. *J. Am. Chem. Soc.*, **2000**, *122*, 1175-1185.

[24] T. Sato; D.-L. Jiang; T. Aida. A blue-luminescent dendritic rod: Poly(phenyleneethynylene) within a light-harvesting dendritic envelope. *J. Am. Chem. Soc.*, **1999**, *121*, 10658-10659.

[25] S. Svenson; D. A. Tomalia. Dendrimers in biomedical applications-Reflections on the field. *Adv. Drug Del. Rev.*, **2012**, *64*, 102-115.

[26] R. Esfand; D. A. Tomalia. Poly(amidoamine) (PAMAM) dendrimers: From biomimicry to drug delivery and biomedical applications. *Drug Discovery Today*, **2001**, *6*, 427-436.

[27] D. A. Tomalia; J. M. J. Fréchet. Discovery of dendrimers and dendritic polymers: A brief historical perspective*. *J. Polym. Sci., Part A: Polym. Chem.*, **2002**, *40*, 2719-2728.

[28] H. Brunner. Dendrizymes: Expanded ligands for enantioselective catalysis. *J. Organomet. Chem.*, **1995**, *500*, 39-46.

[29] H. Brunner; S. Altmann. Optisch aktive stickstoffliganden mit dendrimer-struktur. *Chem. Ber.*, **1994**, *127*, 2285-2296.

[30] J. W. J. Knapen; A. W. van der Made; J. C. de Wilde; P. W. N. M. van Leeuwen; P. Wijkens; D. M. Grove; G. van Koten. Homogeneous catalysts based on silane dendrimers functionalized with arylnickel(II) complexes. *Nature*, **1994**, *372*, 659-663.

[31] Anne-Marie Caminade; Cédric-Olivier Turrin; Régis Laurent; Armelle Ouali; B. Delavaux-Nicot. Dendrimers: Towards catalytic, material and biomedical uses. John Wiley & Sons, Inc.: **2011**.

[32] A.-M. Caminade; A. Ouali; R. Laurent; C.-O. Turrin; J.-P. Majoral. The dendritic effect illustrated with phosphorus dendrimers. *Chem. Soc. Rev.*, **2015**, *44*, 3890-3899.

[33] A. Mansour; T. Kehat; M. Portnoy. Dendritic effects in catalysis by Pd complexes of bidentate phosphines on a dendronized support: Heck vs. carbonylation reactions. *Org. Biomol. Chem.*, **2008**, *6*, 3382-3387.

[34] J. N. H. Reek; S. Arévalo; R. van Heerbeek; P. C. J. Kamer; P. W. N. M. van Leeuwen, Dendrimers in catalysis. *Advances in Catalysis*, Academic Press: **2006**.

[35] R. K. Gopalakrishna Panicker; S. Krishnapillai. Synthesis of on resin poly(propylene imine) dendrimer and its use as organocatalyst. *Tetrahedron Lett.*, **2014**, *55*, 2352-2354.

[36] N. A. Uhlich; T. Darbre; J.-L. Reymond. Peptide dendrimer enzyme models for ester hydrolysis and aldolization prepared by convergent thioether ligation. *Org. Biomol. Chem.*, **2011**, *9*, 7071-7084.

[37] J. Kofoed; J.-L. Reymond. Dendrimers as artificial enzymes. *Curr. Opin. Chem. Biol.*, **2005**, *9*, 656-664.

[38] T. Yi-Hsuan; H. Adela Ya-Ting; C. Po-Yu; C. Hui-Ting; K. Chai-Lin. Metallodendrimers and dendrimer nanocomposites. *Curr. Pharm. Des.*, **2011**, *17*, 2308-2330.

[39] R. Rupp; S. L. Rosenthal; L. R. Stanberry. VivaGel(™) (SPL7013 Gel): A candidate dendrimer-microbicide for the prevention of HIV and HSV infection. *Int. J. Nanomedicine*, **2007**, *2*, 561-566.

[40] C. Z. Chen; S. L. Cooper. Interactions between dendrimer biocides and bacterial membranes. *Biomaterials*, **2002**, *23*, 3359-3368.

[41] Y. Lu; D. L. Slomberg; A. Shah; M. H. Schoenfisch. Nitric oxide-releasing amphiphilic poly(amidoamine) (PAMAM) dendrimers as antibacterial agents. *Biomacromolecules*, **2013**, *14*, 3589-3598.

[42] S. Vembu; S. Pazhamalai; M. Gopalakrishnan. Potential antibacterial activity of triazine dendrimer: Synthesis and controllable drug release properties. *Biorg. Med. Chem.*, **2015**, *23*, 4561-4566.

[43] Y. Gong; B. Matthews; D. Cheung; T. Tam; I. Gadawski; D. Leung; G. Holan; J. Raff; S. Sacks. Evidence of dual sites of action of dendrimers: SPL-2999 inhibits both virus entry and late stages of herpes simplex virus replication. *Antiviral Res.*, **2002**, *55*, 319-329.

[44] E. Kolomiets; M. A. Swiderska; R. U. Kadam; E. M. V. Johansson; K.-E. Jaeger; T. Darbre; J.-L. Reymond. Glycopeptide dendrimers with high affinity for the fucose-binding lectin LecB from pseudomonas aeruginosa. *ChemMedChem*, **2009**, *4*, 562-569.

[45] M. Stach; T. N. Siriwardena; T. Köhler; C. van Delden; T. Darbre; J.-L. Reymond. Combining topology and sequence design for the discovery of potent antimicrobial peptide dendrimers against multidrug-resistant *Pseudomonas aeruginosa*. *Angew. Chem. Int. Ed.*, **2014**, *53*, 12827-12831.

[46] G. Michaud; R. Visini; M. Bergmann; G. Salerno; R. Bosco; E. Gillon; B. Richichi; C. Nativi; A. Imberty; A. Stocker; T. Darbre; J.-L. Reymond. Overcoming antibiotic resistance in Pseudomonas aeruginosa biofilms using glycopeptide dendrimers. *Chemical Science*, **2016**, *7*, 166-182.

[47] E. Blattes; A. Vercellone; H. Eutamène; C.-O. Turrin; V. Théodorou; J.-P. Majoral; A.-M. Caminade; J. Prandi; J. Nigou; G. Puzo. Mannodendrimers prevent acute lung inflammation by inhibiting neutrophil recruitment. *PNAS*, **2013**, *110*, 8795-8800.

[48] J. Ledall; S. Fruchon; M. Garzoni; G. M. Pavan; A.-M. Caminade; C.-O. Turrin; M. Blanzat; R. Poupot. Interaction studies reveal specific recognition of an anti-inflammatory polyphosphorhydrazone dendrimer by human monocytes. *Nanoscale*, **2015**, *7*, 17672-17684.

[49] B. A. Howell; D. Fan. Poly(amidoamine) dendrimer-supported organoplatinum antitumour agents. *Proc. R. Soc. A*, **2010**, *466*, 1515-1526.

[50] J. F. Kukowska-Latallo; K. A. Candido; Z. Cao; S. S. Nigavekar; I. J. Majoros; T. P. Thomas; L. P. Balogh; M. K. Khan; J. R. Baker. Nanoparticle targeting of anticancer drug improves therapeutic response in animal model of human epithelial cancer. *Cancer Res.*, **2005**, *65*, 5317-5324.

[51] J. D. Eichman; A. U. Bielinska; J. F. Kukowska-Latallo; J. R. Baker Jr. The use of PAMAM dendrimers in the efficient transfer of genetic material into cells. *Pharm. Sci. Technolo. Today*, **2000**, *3*, 232-245.

[52] C. Dufès; I. F. Uchegbu; A. G. Schätzlein. Dendrimers in gene delivery. *Adv. Drug Del. Rev.*, **2005**, *57*, 2177-2202.

[53] S. Biswas; V. P. Torchilin. Dendrimers for siRNA delivery. *Pharmaceuticals*, **2013**, *6*, 161-183.

[54] C. Liu; X. Liu; P. Rocchi; F. Qu; J. L. Iovanna; L. Peng. Arginine-terminated generation 4 PAMAM dendrimer as an effective nanovector for functional siRNA delivery in vitro and in vivo. *Bioconj. Chem.*, **2014**, *25*, 521-532.

[55] X. Liu; L. Peng, Dendrimer nanovectors for siRNA delivery. *SiRNA Delivery Methods: Methods and Protocols*, Springer New York: **2016**.

[56] C. Chen; P. Posocco; X. Liu; Q. Cheng; E. Laurini; J. Zhou; C. Liu; Y. Wang; J. Tang; V. D. Col; T. Yu; S. Giorgio; M. Fermeglia; F. Qu; Z. Liang; J. J. Rossi; M. Liu; P. Rocchi; S. Pricl; L. Peng. Mastering dendrimer self-assembly for efficient siRNA delivery: From conceptual design to in vivo efficient gene silencing. *Small*, **2016**, *12*, 3667-3676.

[57] X. Liu; J. Wu; M. Yammine; J. Zhou; P. Posocco; S. Viel; C. Liu; F. Ziarelli; M. Fermeglia; S. Pricl; G. Victorero; C. Nguyen; P. Erbacher; J.-P. Behr; L. Peng. Structurally flexible triethanolamine core PAMAM dendrimers are effective nanovectors for DNA transfection *in vitro* and *in vivo* to the mouse thymus. *Bioconj. Chem.*, **2011**, *22*, 2461-2473.

[58] X. Liu; C. Liu; C. V. Catapano; L. Peng; J. Zhou; P. Rocchi. Structurally flexible triethanolamine-core poly(amidoamine) dendrimers as effective nanovectors to deliver RNAi-based therapeutics. *Biotechnol. Adv.*, **2014**, *32*, 844-852.

[59] L. Zhang; J. P. Tam. Synthesis and application of unprotected cyclic peptides as building blocks for peptide dendrimers. *J. Am. Chem. Soc.*, **1997**, *119*, 2363-2370.

[60] K. Sadler; J. P. Tam. Peptide dendrimers: Applications and synthesis. *Rev. Mol. Biotechnol.*, **2002**, *90*, 195-229.

[61] S. Ota; T. Ono; A. Morita; A. Uenaka; M. Harada; E. Nakayama. Cellular processing of a multibranched lysine core with tumor antigen peptides and presentation of peptide epitopes recognized by cytotoxic T lymphocytes on antigen-presenting cells. *Cancer Res.*, **2002**, *62*, 1471-1476.

[62] E. Wiener; M. W. Brechbiel; H. Brothers; R. L. Magin; O. A. Gansow; D. A. Tomalia; P. C. Lauterbur. Dendrimer-based metal chelates: A new class of magnetic resonance imaging contrast agents. *Magn. Reson. Med.*, **1994**, *31*, 1-8.

[63] H. C. Roberts; M. Saeed; T. P. L. Roberts; A. Mühler; D. M. Shames; J. S. Mann; M. Stiskal; F. Demsar; R. C. Brasch. Comparison of albumin-(Gd-DTPA)30 and Gd-DTPA-24-cascade-polymer for measurements of normal and abnormal microvascular permeability. *J. Magn. Reson. Imaging*, **1997**, *7*, 331-338.

[64] G. Schuhmann-Giampieri; H. Schmitt-Willich; T. Frenzel; W.-R. Press; H.-J. Weinmann. In vivo and in vitro evaluation of Gd-DTPA-polylysine as a macromolecular contrast agent for magnetic resonance imaging. *Invest. Radiol.*, **1991**, *26*, 969-974.

[65] S. Langereis; Q. G. de Lussanet; M. H. P. van Genderen; W. H. Backes; E. W. Meijer. Multivalent contrast agents based on gadolinium−diethylenetriaminepentaacetic acid-terminated poly(propylene imine) dendrimers for magnetic resonance imaging. *Macromolecules*, **2004**, *37*, 3084-3091.

[66] Z. Dai. Advances in nanotheranostics I: Design and fabrication of theranosic nanoparticles. Springer Berlin Heidelberg: **2016**.

[67] S. Langereis; Q. G. de Lussanet; M. H. P. van Genderen; E. W. Meijer; R. G. H. Beets-Tan; A. W. Griffioen; J. M. A. van Engelshoven; W. H. Backes. Evaluation of Gd(III)DTPA-terminated poly(propylene imine) dendrimers as contrast agents for MR imaging. *NMR Biomed.*, **2006**, *19*, 133-141.

[68] Q. Dong; D. R. Hurst; H. J. Weinmann; T. L. Chenevert; F. J. Londy; M. R. Prince. Magnetic resonance angiography with Gadomer-17: An animal study. *Invest. Radiol.*, **1998**, *33*, 699-708.

[69] B. Misselwitz; H. Schmitt-Willich; W. Ebert; T. Frenzel; H.-J. Weinmann. Pharmacokinetics of Gadomer-17, a new dendritic magnetic resonance contrast agent. *Magn. Reson. Mater. Phys., Biol. Med.*, **2001**, *12*, 128-134.

[70] Y. Huang; S. He; W. Cao; K. Cai; X.-J. Liang. Biomedical nanomaterials for imaging-guided cancer therapy. *Nanoscale*, **2012**, *4*, 6135-6149.

[71] S. S. Kelkar; T. M. Reineke. Theranostics: Combining imaging and therapy. *Bioconj. Chem.*, **2011**, *22*, 1879-1903.

[72] B. T. Luk; L. Zhang. Current advances in polymer-based nanotheranostics for cancer treatment and diagnosis. *ACS Appl. Mater. Interfaces*, **2014**, *6*, 21859-21873.

[73] P. Sharma; S. Brown; G. Walter; S. Santra; B. Moudgil. Nanoparticles for bioimaging. *Adv. Colloid Interface Sci.*, **2006**, *123-126*, 471-485.

[74] M. W. Grinstaff. Biodendrimers: New polymeric biomaterials for tissue engineering. *Chem. Eur. J.*, **2002**, *8*, 2838-2846.

[75] A. J. Velazquez; M. A. Carnahan; J. Kristinsson; S. Stinnett; M. W. Grinstaff; T. Kim. New dendritic adhesives for sutureless ophthalmic surgical procedures: In vitro studies of corneal laceration repair. *Arch. Ophthalmol.*, **2004**, *122*, 867-870.

[76] M. Wathier; P. J. Jung; M. A. Carnahan; T. Kim; M. W. Grinstaff. Dendritic macromers as in situ polymerizing biomaterials for securing cataract incisions. *J. Am. Chem. Soc.*, **2004**, *126*, 12744-12745.

[77] S. Svenson. The dendrimer paradox-high medical expectations but poor clinical translation. *Chem. Soc. Rev.*, **2015**, *44*, 4131-4144.

[78] D. A. Tomalia; H. Baker; J. Dewald; M. Hall; G. Kallos; S. Martin; J. Roeck; J. Ryder; P. Smith. Dendritic macromolecules: synthesis of starburst dendrimers. *Macromolecules*, **1986**, *19*, 2466-2468.

[79] G. R. Newkome; Z. Yao; G. R. Baker; V. K. Gupta. Micelles. Part 1. Cascade molecules: A new approach to micelles. A [27]-arborol. *J. Org. Chem.*, **1985**, *50*, 2003-2004.

[80] D. A. Tomalia; J. B. Christensen; U. Boas. Dendrimers, dendrons and dendritic polymers. Cambridge University Press: **2012**.

[81] E. Abbasi; S. F. Aval; A. Akbarzadeh; M. Milani; H. T. Nasrabadi; S. W. Joo; Y. Hanifehpour; K. Nejati-Koshki; R. Pashaei-Asl. Dendrimers: Synthesis, applications, and properties. *Nanoscale Res. Lett.*, **2014**, *9*, 247-247.

[82] M. V. Walter; M. Malkoch. Simplifying the synthesis of dendrimers: Accelerated approaches. *Chem. Soc. Rev.*, **2012**, *41*, 4593-4609.

[83] Z. Xu; J. S. Moore. Rapid construction of large-size phenylacetylene dendrimers up to 12.5 nanometers in molecular diameter. *Angew. Chem. Int. Ed. Engl.*, **1993**, *32*, 1354-1357.

[84] C. J. Hawker; J. M. J. Fréchet. Preparation of polymers with controlled molecular architecture. A new convergent approach to dendritic macromolecules. *J. Am. Chem. Soc.*, **1990**, *112*, 7638-7647.

[85] K. L. Wooley; C. J. Hawker; J. M. J. Fréchet. Hyperbranched macromolecules via a novel double-stage convergent growth approach. *J. Am. Chem. Soc.*, **1991**, *113*, 4252-4261.

[86] H. Ihre; A. Hult; J. M. J. Fréchet; I. Gitsov. Double-stage convergent approach for the synthesis of functionalized dendritic aliphatic polyesters based on 2,2-bis(hydroxymethyl)propionic acid. *Macromolecules*, **1998**, *31*, 4061-4068.

[87] R. B. Merrifield. Solid phase peptide synthesis. I. The synthesis of a tetrapeptide. *J. Am. Chem. Soc.*, **1963**, *85*, 2149-2154.

[88] J.-M. Lehn. Toward self-organization and complex matter. *Science*, **2002**, *295*, 2400-2403.

[89] M. J. Webber; E. A. Appel; E. W. Meijer; R. Langer. Supramolecular biomaterials. *Nat. Mater.*, **2016**, *15*, 13-26.

[90] T. Aida; E. W. Meijer; S. I. Stupp. Functional supramolecular polymers. *Science*, **2012**, *335*, 813-817.

[91] A. Whitty. Cooperativity and biological complexity. *Nat. Chem. Biol.*, **2008**, *4*, 435-439.

[92] X. Liu; J. Zhou; T. Yu; C. Chen; Q. Cheng; K. Sengupta; Y. Huang; H. Li; C. Liu; Y. Wang; P. Posocco; M. Wang; Q. Cui; S. Giorgio; M. Fermeglia; F. Qu; S. Pricl; Y. Shi; Z. Liang; P. Rocchi; J. J. Rossi; L. Peng. Adaptive amphiphilic dendrimer-based nanoassemblies as robust and versatile siRNA delivery systems. *Angew. Chem. Int. Ed.*, **2014**, *53*, 11822-11827.

[93] T. Wei; C. Chen; J. Liu; C. Liu; P. Posocco; X. Liu; Q. Cheng; S. Huo; Z. Liang; M. Fermeglia; S. Pricl; X.-J. Liang; P. Rocchi; L. Peng. Anticancer drug nanomicelles formed by self-assembling amphiphilic dendrimer to combat cancer drug resistance. *PNAS*, **2015**, *112*, 2978-2983.

[94] Y. Cao; X. Liu; L. Peng. Molecular engineering of dendrimer nanovectors for siRNA delivery and gene silencing. *Front. Chem. Sci. Eng.*, **2017**, In Press, DOI: 10.1007/s11705-11017-11623-11705

[95] A. Y.-T. Huang; C.-H. Tsai; H.-Y. Chen; H.-T. Chen; C.-Y. Lu; Y.-T. Lin; C.-L. Kao. Concise solid-phase synthesis of inverse poly(amidoamine) dendrons using AB2 building blocks. *Chem. Commun.*, **2013**, *49*, 5784-5786.

Chapter II: Solid-phase synthesis of dendrimers

Section 1. Solid-phase dendrimer synthesis: a brief overview (manuscript in revision)

1. Background of solid-phase synthesis (SPS)

Since its advent, solid-phase synthesis (SPS) has generated a revolution in the synthesis of biological macromolecules. The seminal work of Merrifield in the early 1960s,[1] comprised the solid-phase synthesis of peptides, in which an amino acid was first attached to an insoluble resin and then assembled into peptides via stepwise and iterative synthesis through peptide bond formation.[1] Compared to solution-phase synthesis, this approach was proved to be very effective and yet could be performed conveniently in a short time frame with minimal side reactions and easy purification procedures. As such, this inaugural solid-phase synthesis strategy revolutionized peptide synthesis and earned Merrifield the Nobel Prize in 1984.[2] Based on this pioneering work,[1] solid-phase synthesis can be defined as a process involving the anchoring to an insoluble support of a molecular component onto which other molecular motifs are subsequently added to construct the desired target molecule (**Figure 1.1**). Each synthetic step in solid-phase synthesis is followed by a purification process involving simple washing and filtration in order to collect the desired product on a resin ready for the next stage of preparation. The whole synthesis process hence consists of iterative assembly and purification steps until the final step involving cleavage of the final product from the solid support (**Figure 1.1**).[3]
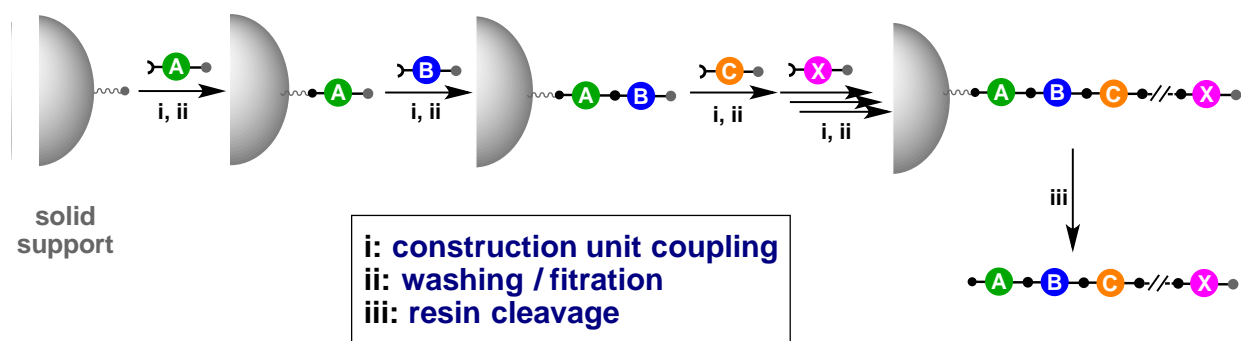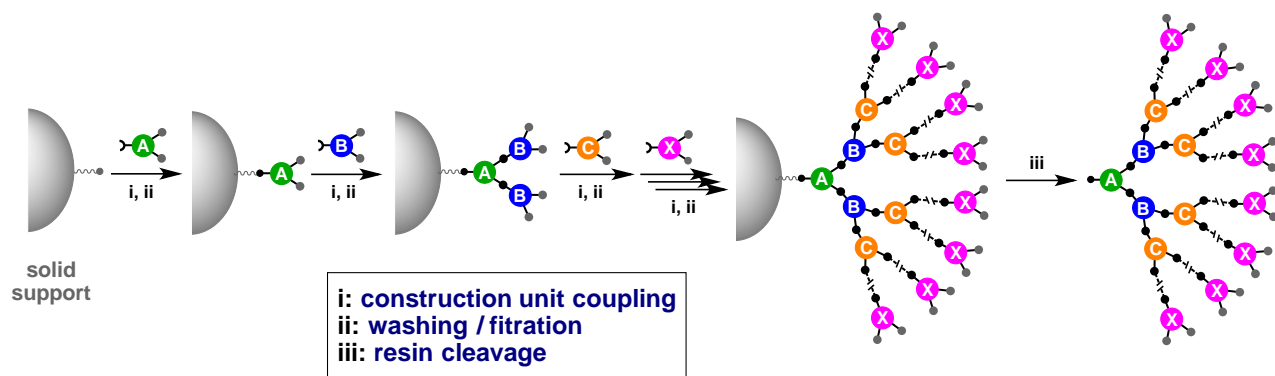
Figure 1.1. Principle of solid-phase organic synthesis (SPOS).

Compared to a solution-phase synthesis for which each reaction step requires, time-consuming and tedious separation of the desired product from the reaction mixture, the solid-phase strategy allows easy removal of excess reagents and unbound by-products by simple washing and filtration procedures at each synthetic step. The ease of purification allows chemists to use a large excess of reagents, which often drives the reaction towards product formation in high yields, while minimizing and/or suppressing the formation of by-products, and at the same time, speeding up the reaction. Consequently, the SPS approach is very effective and straightforward, enabling the synthesis to be achieved rapidly and conveniently yet in high yields. Following the initial success in generating peptides,[4] solid-phase synthesis has since rapidly gained in popularity[3] and made readily accessible the synthesis of complex biological macromolecules such as polypeptides,[4] oligonucleotides,[5] or oligosaccharides[6], that are otherwise difficult to accomplish in solution. In addition, solid-phase synthesis has been implemented in the fabrication of structurally diverse small molecules[7] and polymers,[8] as well as in combinatorial chemistry to construct new chemical entities and natural product-like libraries.[9,10] Nowadays, solid-phase synthesis has widely employed for both academic research and industrial production.

Solid-phase synthesis (SPS) is expected to overcome the synthetic and purification problems encountered for dendrimer synthesis by offering complete chemical reactions via using a large excess of reagents yet an extremely efficient purification process consisting of simple washing and filtration (**Figure 1.2**). The first solid-phase dendrimer synthesis was explored by Tam in 1988 for preparing peptide dendrimers.[11] Since then, solid-phase synthesis has successfully generated a large array of dendrimers including oligonucleotide dendrimers, carbohydrate dendrimers,

PAMAM dendrimers, polyester dendrimers, polyurea dendrimers, polyether/polythioether and triazine dendrimers etc, illustrating the remarkable structural and chemical diversity of dendrimers which can be achieved with this approach. Below, we will briefly comment the general considerations for solid-phase synthesis before presenting some pioneering and archetypal examples for dendrimer synthesis.

Figure 1.2. Principle of solid-phase dendrimer synthesis (SPDS).

Considerations for solid-phase synthesis (SPS)

A successful solid-phase synthesis (SPS) starts with the judicious choice of the solid support and the linker bearing the reactive functionality in order to be compatible with the chemical reactions to construct the dendrimers.[3] The choice of solid support with appropriate loading, solvent and monitoring method for ensuring dendrimer growth towards high generations is also crucial.[12] These considerations will be discussed below to provide some general information and knowledge.

1.1. Solid supports[13]

When selecting a solid support, stability under acidic, basic, reducing and oxidizing conditions, mechanical properties and recyclability are all concerns which should be taken into account. Two categories of solid support are commonly used: (i) inorganic materials such as silica, alumina, glass or clays, and (ii) organic polymeric resins which are often composed of polystyrene cross-

linked with divinylbenzene. Inorganic supports often have relatively poor mechanical stability and low loading of functional groups, while organic polymeric supports are able to provide high loading capacity alongside varied physical and chemical properties. Polymeric supports are the most commonly used solid-support, the network of which is flexible and can expand or exclude solvent to accommodate the growing molecules within the resin matrix. There are commonly three types commercial available polymeric resin classified: polystyrene (PS) resins, poly(ethylene glycol)-polystyrene (PEG-PS) resins and hydrophilic PEG-based resins.

1.2. Linkers[13]

The linker harboring the reactive functionality which connects the solid support to the substrate[12] is also another critical issue to consider for SPS (**Figure 1.3**). The linker can be designed to be either acid/base labile, or nucleophile labile or photolabile, in order to efficiently immobilize the substrate on the support while ensuring the trouble-free cleavage of the final product from the resin. A good linker should be easily functionalized with a variety of reagents, stable under various reaction conditions and able to undergo efficient cleavage without endangering the final products. Also, the influence of linker length and chemical composition (hydrophobic/hydrophilic) is a key factor for solid support. For example, the TentaGel™ resin-linker carrying a long and flexible polyethylene glycol (PEG) spacer, which was designed to make the reactive sites accessible to reagents while avoiding steric hindrance for the synthesis in the solid-phase.
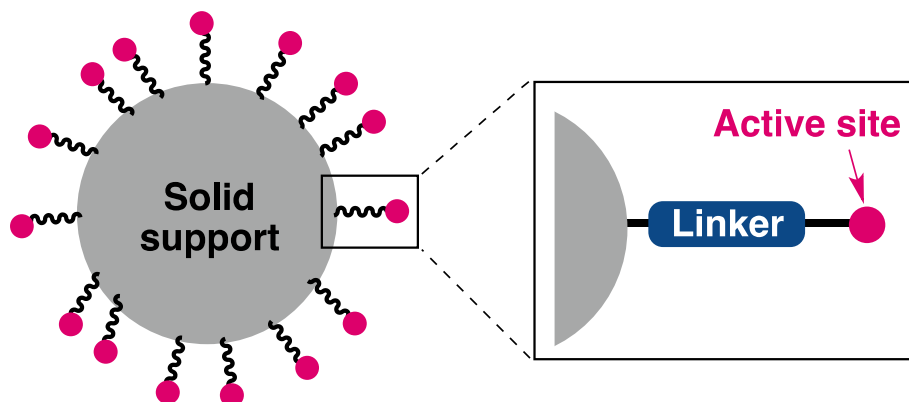
Figure 1.3. Schematic presentation of a solid support for solid-phase synthesis.

1.3. Resin swelling and solvents

Regarding to polymeric resin, folding of the polymer chains may deeply bury reactive sites of the linker within the resin matrix, thereupon limiting accessibility to reaction reagents and impeding the reaction (**Figure 1.4**). Long-term storage may further deactivate the reactive sites, which can impair the reaction, hence compromising the reaction efficiency. The ratio of cross-linking bridges between the polymer chains is another factor to impart mechanical stability and swelling properties to the resin matrix.[14-16] Degree of cross-linking impacts the swellability. Low level of cross-linkage (under 1%) yields exceedingly swellable but mechanically weak resin networks, while highly cross-linked polymers, though mechanically stronger, do not swell much even in good solvents, impeding high yielding for solid-phase synthesis. For these reasons, properly pre-rinsing and swelling the resin is important to release the polymeric chains and expose the reactive sites to ensure that substrates bound to the solid support are accessible to reagents. A swollen polymeric resin is like a solvent influencing the reaction efficiency.[17] Thus, the selection of solvents can be critical, as well as considerations of mesh size, loading capacity and the composition of the resin.
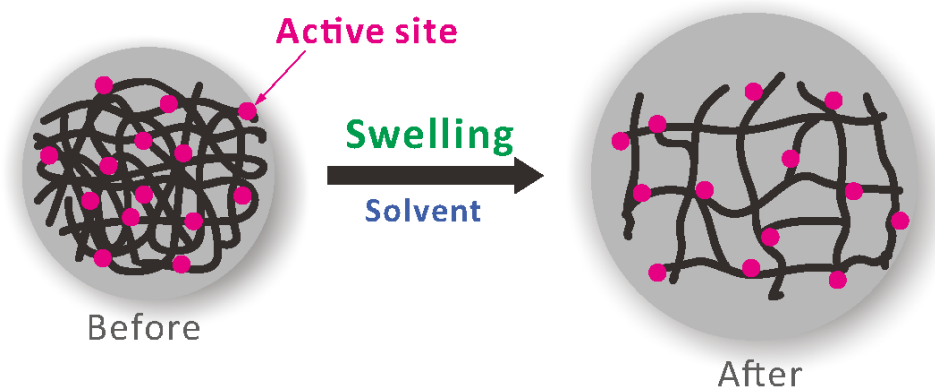
Figure 1.4. Pre-rinsing and swelling the polymeric resin is important to release and expose the reactive sites.

1.4. Loading capacity of solid support[18,19]

Various solid supports with different loading capacity of the linker are nowadays commercially available. High loading amount of resin can host more compounds on resin than the one with the lower loading one, leading to higher production. Although loading capacity will not influence greatly the chemistry in classical solid-phase synthesis such as solid-phase peptide synthesis, it needs to be considered seriously in the solid-phase dendrimer synthesis. Because of the dendritic structure, dendrimer will occupy more space with increasing generation. Therefore, when using high loading resin, the distance between two dendrimers on the same resin bead may be getting too closed while preparing large dendrimer; and eventually, the repulsion between two neighboring dendrimers will impede the reaction and cause incomplete reaction as well as side product. Therefore, suitably reduced the loading ratio is important in the preparation of high generation of dendrimers through SPDS (**Figure 1.5**).
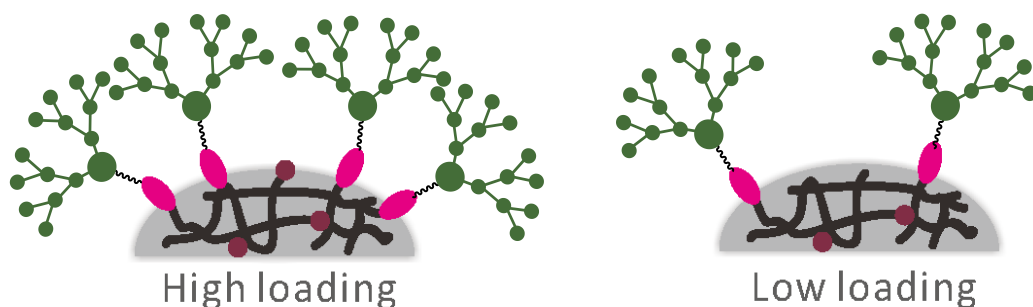
Figure 1.5. Resin with lower loading capacity is able to decrease steric congestion when synthesizing higher generation dendrimers.

1.5. Reactions

It is also worth mentioning that the reactions used in SPS should be highly effective and efficient, devoid of possible side reactions and by-products, and at the same time, compatible with the solid supports, intermediates and final products that will be present during the synthesis. A

variety of classical and modern metal-catalyzed reactions have been successfully implemented on various insoluble supports, including silica, clays and organic polymers and recently documented.[3] This offers a great promise for synthesizing dendrimers with broad chemical and structural diversity.

1.6. Monitoring chemical reaction

Monitoring the progress of the reaction during SPS is essential for controlling and assessing the synthesis. Conventional methods rely on analyzing the products released from the solid supports or using a facile colorimetric test to track the appearance and disappearance of a chemical functionality or entity on the solid support.[20] Recently, emerging technological advances have made solid-state NMR, IR and Raman spectroscopy suitable non-destructive methods for tracking the progress of the reaction in situ in the solid-phase.[21,22] However, these methods are limited to certain special chemistry and functional groups for selectively detection, not yet generally applicable to all SPS in particular to SPDS. Therefore, the development of on-site analytical methods to follow the progress of reactions will greatly accelerate and facilitate SPDS.

2. Selected examples of solid-phase dendrimer synthesis (SPDS)

In view of the above-mentioned considerations, some pioneering and archetypal studies on solid-phase dendrimer synthesis were presented below, showcasing the promise, scope and limitation of solid-phase dendrimer synthesis.

2.1. Peptide dendrimers

A peptide dendrimer can be broadly defined as any dendrimer which contains peptide backbones in the core and/or as branching units. Peptide dendrimers have often been conceived as protein mimics, antiviral and anticancer agents, vaccines, drugs and drug delivery systems.[23] In 1988, Tam described the first solid-phase synthesis of peptide dendrimers using a general but chemically explicit approach for the preparation of multiple antigen peptide systems (MAPs)

29

(**Figure 1.6**).[11] These MAPs are composed of a polylysine dendrimer as skeleton, with peptide antigens appended on the dendrimer periphery to provide multivalent immunoactivity. Both the polylysine dendrimer core and the peptide antigens at the terminals were achieved via stepwise peptide synthesis in the solid-phase. The synthesis started with the assembly of the polylysine dendrimer on a solid support, which involved attaching the protected lysine (**5**) via its free carboxylic acid terminus to the amine-bearing resin. Subsequent deprotection freed the two amine functions for further coupling with the free C-terminus of the next protected lysine (**5**). Iterative synthesis allowed increasingly high generations of the peptide dendrimer to be made in this way, and the final product was cleaved from the solid resin once the desired peptide antigen sequence was achieved (**Figure 1.6**). The so-obtained dendritic MAPs were used as immunogens for various immune response investigations as well as for antibody production.
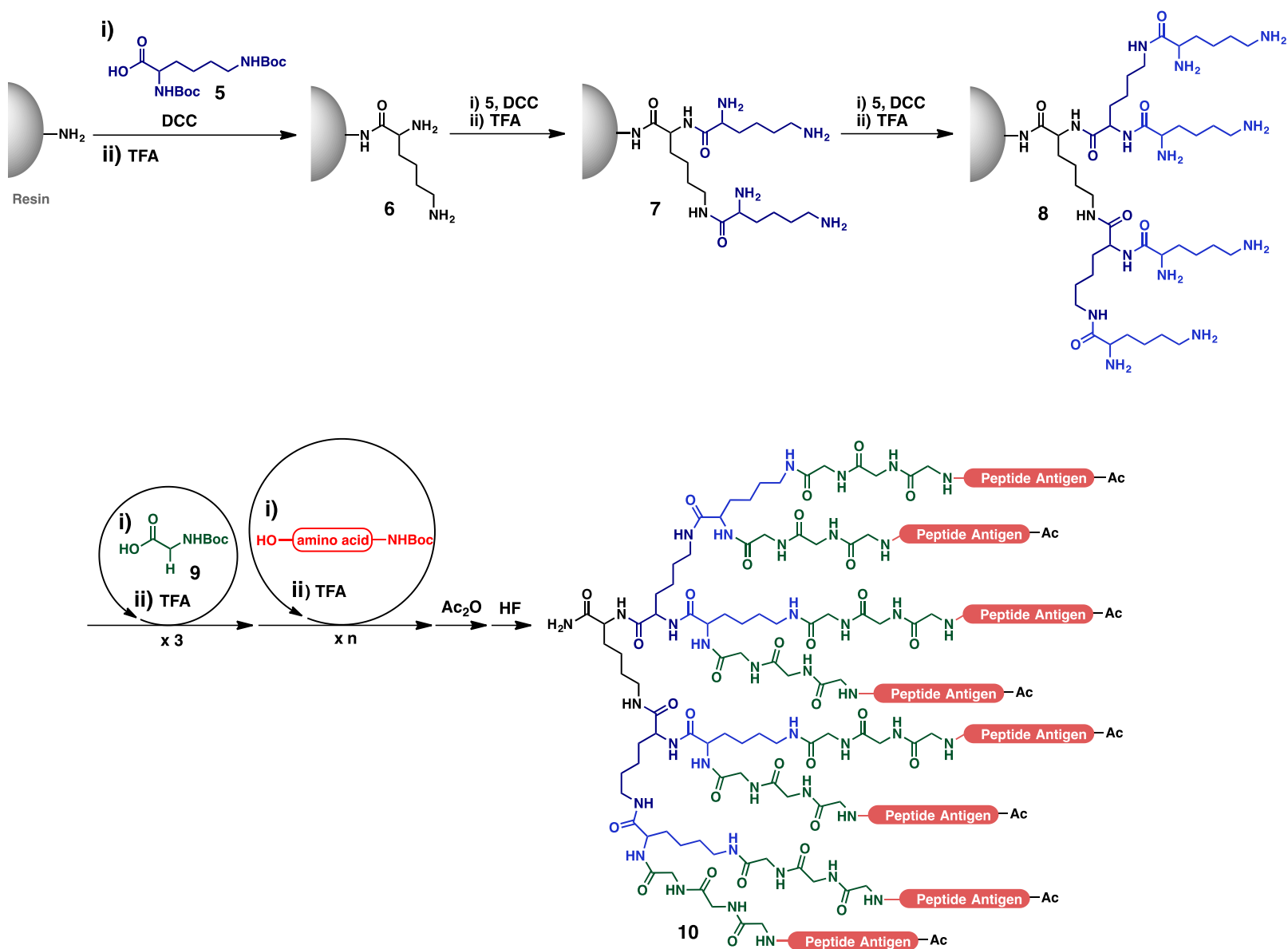
Figure 1.6. Solid-phase synthesis of multiple antigen peptide systems, the first peptide dendrimers.[11]

Following the successful synthesis of MAPs, many peptide dendrimers such as poly(glutamic acid), polyarginine, polyproline and polyglycine were also prepared using solid-phase synthesis.[24] It is worth mentioning that linear polyproline oligomers have unusual conformational plasticity due to the unique rigidity of proline, which originates from the pyrrolidine ring and the secondary amide bond. Remarkably, linear polyproline displays solvent-dependent secondary conformations, generating a right-handed helix in organic solvents such as ethanol or propanol, and a left-handed helix in aqueous solution.[24] Using solid-phase synthesis, Crespo et al. prepared polyproline dendrimers using L-proline (**11**) as the building block and protected *cis*-4-amino-L-proline (**13**) as branching unit (**Figure 1.7**).[25] Indeed, the polyproline dendrimers were also endowed with this conformational plasticity. When the dendrimers were moved from an organic media to an aqueous solution, the same conformational transition occurred, but at a faster rate.[25] This feature can be harnessed as a conformational switch for potential functional materials to encapsulate and release guest molecules, for example as a drug vehicle.
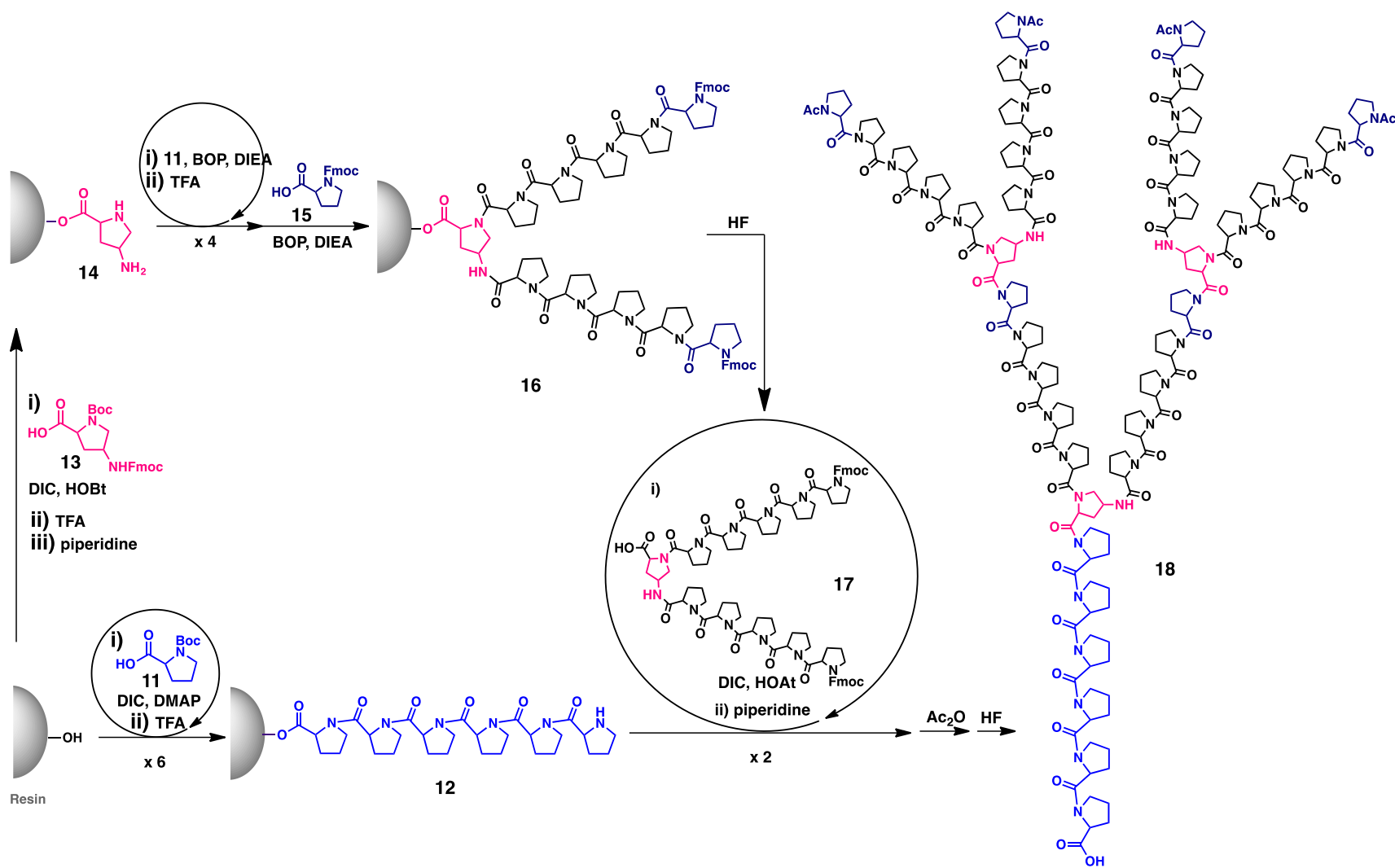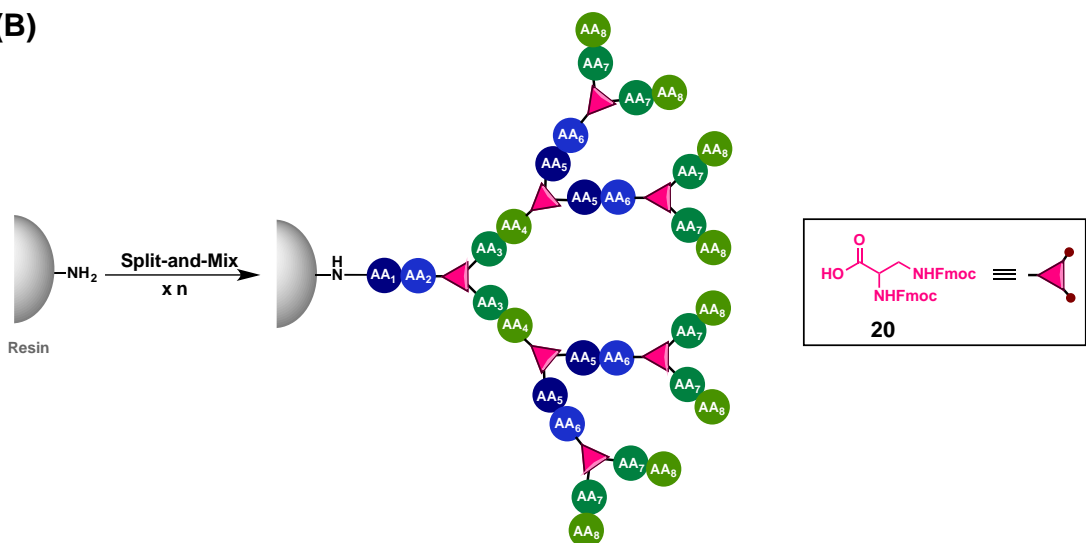
Figure 1.7. Solid-phase synthesis of polyproline dendrimers using a combined divergent/convergent approach.[25]

Later on, Reymond and co-workers pioneered the use of solid-phase synthesis to prepare peptide dendrimer libraries (**Figure 1.8**).[26,27] For example, they inventively incorporated the catalytic triad serine-histidine-aspartate at variable positions while employing Fmoc-protected 3,5-diaminobenzoic acid (**19**) as branching point to create dendritic motifs that mimic esterases (**Figure 1.8A**).[26] In addition, they introduced cysteine within the dendrimer structure, allowing construction of larger dendrimers via disulfide bridges. They further generated peptide dendrimer libraries using a split-and-mix approach (**Figure 1.8B**).[27] These peptide dendrimers contain eight variable amino acid positions spanning outwards along three continuous branching units made of L-2,3-diaminopropanoic acid (**20**). With four different amino acids per variable position, a combinatorial library of peptide dendrimers was constructed and then screened to search for artificial enzymes. In this way, effective aldolases were identified with enhanced activity through positive dendritic effects. The combinatorial construction of dendrimer libraries using a solid-phase strategy has since provided versatile and rapid access to peptide dendrimers with both sequence and structural diversity useful in various biological applications such as enzyme mimicry, drug screening as well as drug and gene delivery.[23,28]

(A)
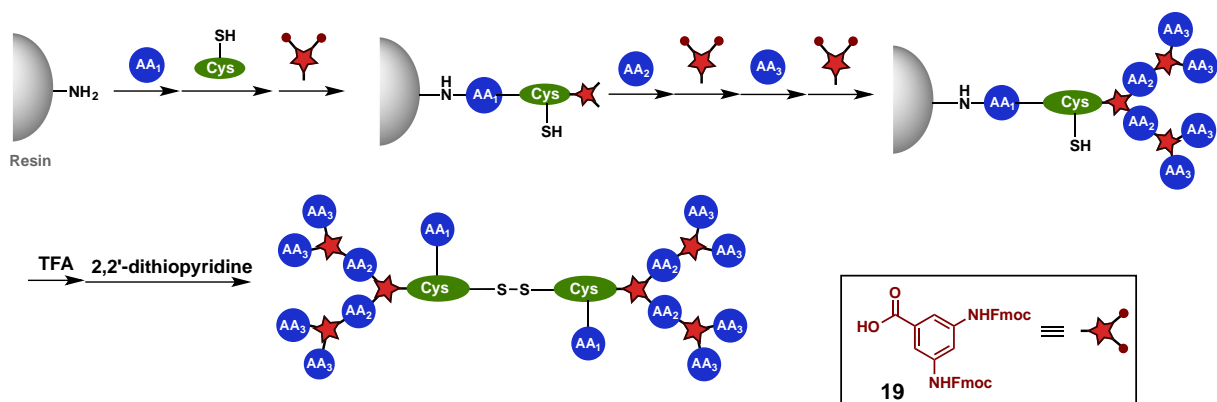
(B)

Figure 1.8. (A) Solid-phase synthesis of peptide dendrimer libraries;[26] **(B)** Solid-phase synthesis of peptide dendrimer libraries using the split-and-mix approach.[27] *AA_n: amino acid residues; Cys: Cysteine.

2.2. Carbohydrate dendrimers (glycodendrimers)

Carbohydrate dendrimers, also named as glycodendrimers, are of particular interest for protein interaction and recognition by virtue of their glycomimetic properties, especially cooperative multivalency allowing their enhanced binding affinity to protein receptors. In 1993, Roy et al. applied solid-phase synthesis to construct the first glycodendrimer based on a polylysine peptide dendrimer (**Figure 1.9**).[29] They decorated the periphery of the polylysine dendrimer with sialic

acid via a diglycine linker through thiolation (**Figure 1.9**, route **A**). More recently, they reported a highly efficient strategy to synthesize mannosylated dendrimers via click chemistry.[30] In this process, they transformed the amine terminals of polylysine to azido functions, followed by copper catalyzed azide-alkyne cycloaddition with propargyl-α-D-mannopyranoside (**26**) (**Figure 1.9**, route **B**).
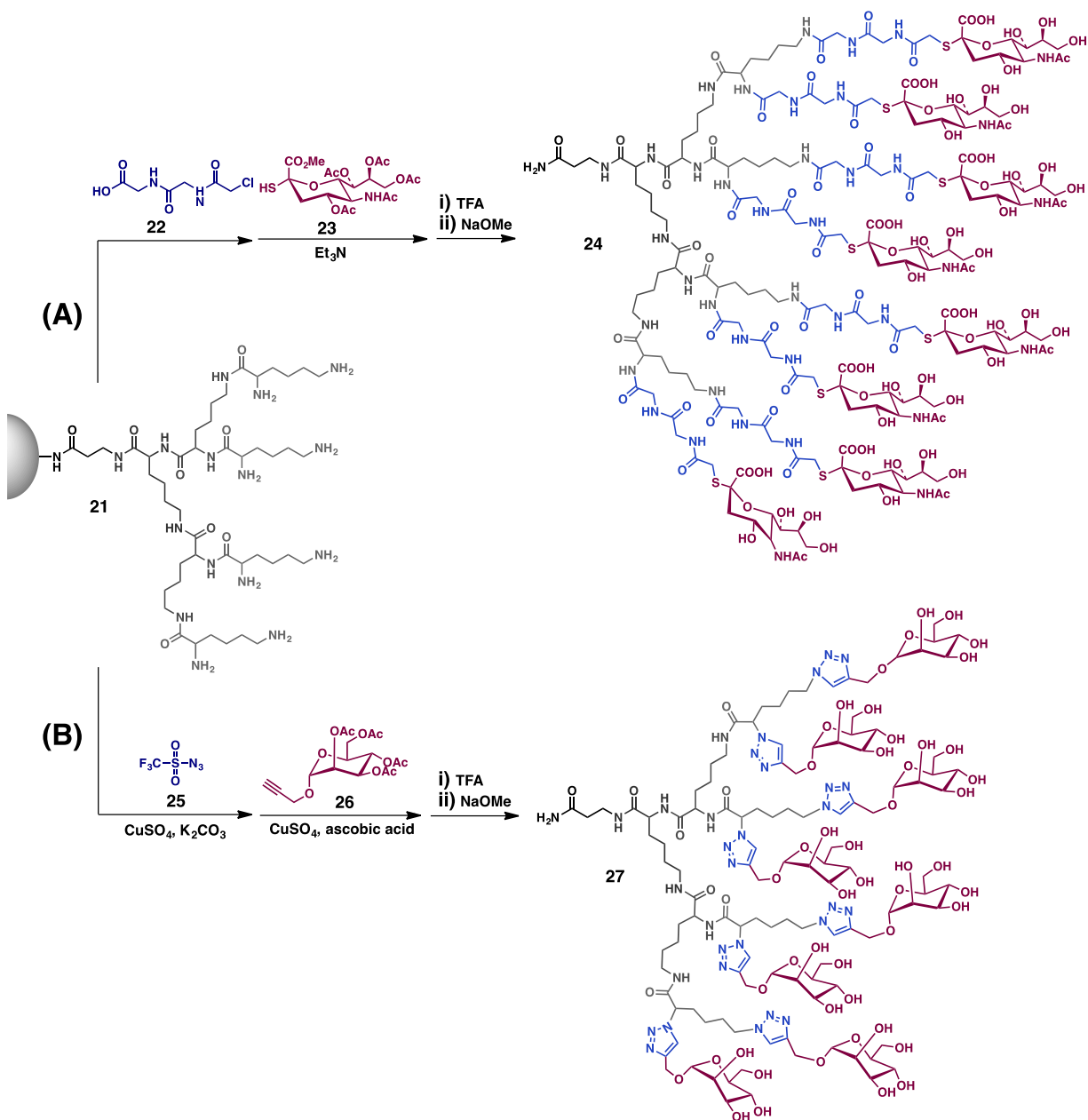
Figure 1.9. Solid-phase synthesis of glyco-polylysine dendrimers via **(A)** thiolation and **(B)** click reaction.[29,30]

Most glycodendrimers have their peripheries decorated with carbohydrate units. However, those dendrimers have carbohydrate introduced into their core were also reported. Indeed, using a special safety-catch resin, Fernandez and co-workers introduced carbohydrate units such as glucose or even β-cyclodextrin into the glycodendrimer core at the resin cleavage step (**Figure 1.10**).[31] To do this, the dendrimer-anchored linker was first activated using iodoacetonitrile (**32**) and then subjected to chemo-selective treatment with the carbohydrate-bearing amine nucleophile to deliver the core-substituted glycodendrimer (**33**) (**Figure 1.10**). This method offers a practical and convenient way to diversify the structure and chemistry of the glycodendrimer core.
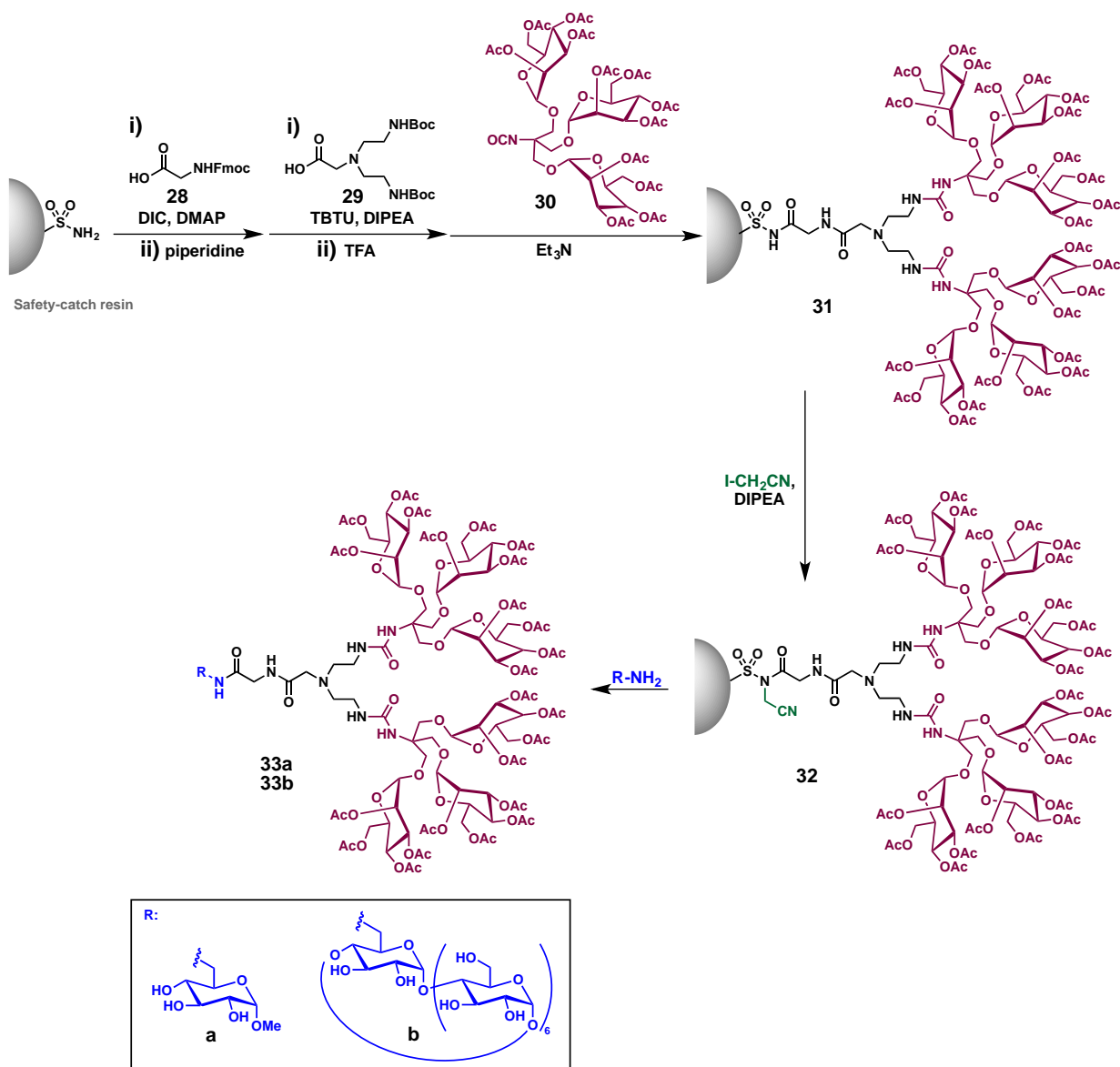
Figure 1.10. Solid-phase synthesis of glycodendrimers using safety-catch resin for core diversification.[31]

2.3. Nucleic acid dendrimers

Besides peptide dendrimers and glycodendrimers, nucleic acid dendrimers have also been prepared by taking advantage of the solid-phase synthesis of oligonucleotides via phosphoramidite chemistry. Both convergent and divergent approaches have been applied to solid-phase synthesis of nucleic acid dendrimers (**Figure 1.11**).[32,33] Hudson and Dhama prepared a second-generation

nucleic acid dendrimer with the convergent strategy using the protected adenosine-2',3'-*O*-bis(phosphoramidite) (**34**) as focal point to link neighboring branches together (**Figure 1.11A**).[32] Although this method has successfully delivered nucleic acid dendrimers, the reaction steps must be carefully and stringently controlled, which means it is less suitable for synthesizing high-generation dendrimers.

Therefore, the divergent method (**Figure 1.11B**) was developed to overcome this limitation by implementing chemical synthesis of oligonucleotides in the 5' → 3' ("backward") direction rather than the conventional 3' → 5' direction.[33] To achieve this, the oligonucleotides were first assembled onto the surface of a controlled-pore glass based solid support with an automated DNA synthesizer, then the branching unit (**34**) was used in large excess to force branching construction to completion, followed by divergent growth to generate full-length dendrimers. These oligonucleotide dendrimers have potential applications in the selective modulation of gene expression.

Figure 1.11. Solid-phase synthesis of nucleotide dendrimers using **(A)** a convergent strategy[32] and **(B)** a divergent strategy.[33]

2.4. PAMAM dendrimers

Poly(amidoamine) (PAMAM) dendrimers have been the most extensively investigated dendrimers since the seminal report in 1985.[34] With a large number of amide functionalities in the interior and primary amine terminals on the surface, PAMAM dendrimers were originally devised and synthesized by Tomalia to mimic proteins.[35] Since then, numerous PAMAM dendrimers with different core structures, branching units and terminal groups have been established with a myriad of applications ranging from sensors, light harvesters, dendritic supports and catalysts, to imaging agents, drugs and drug delivery.[35-37]
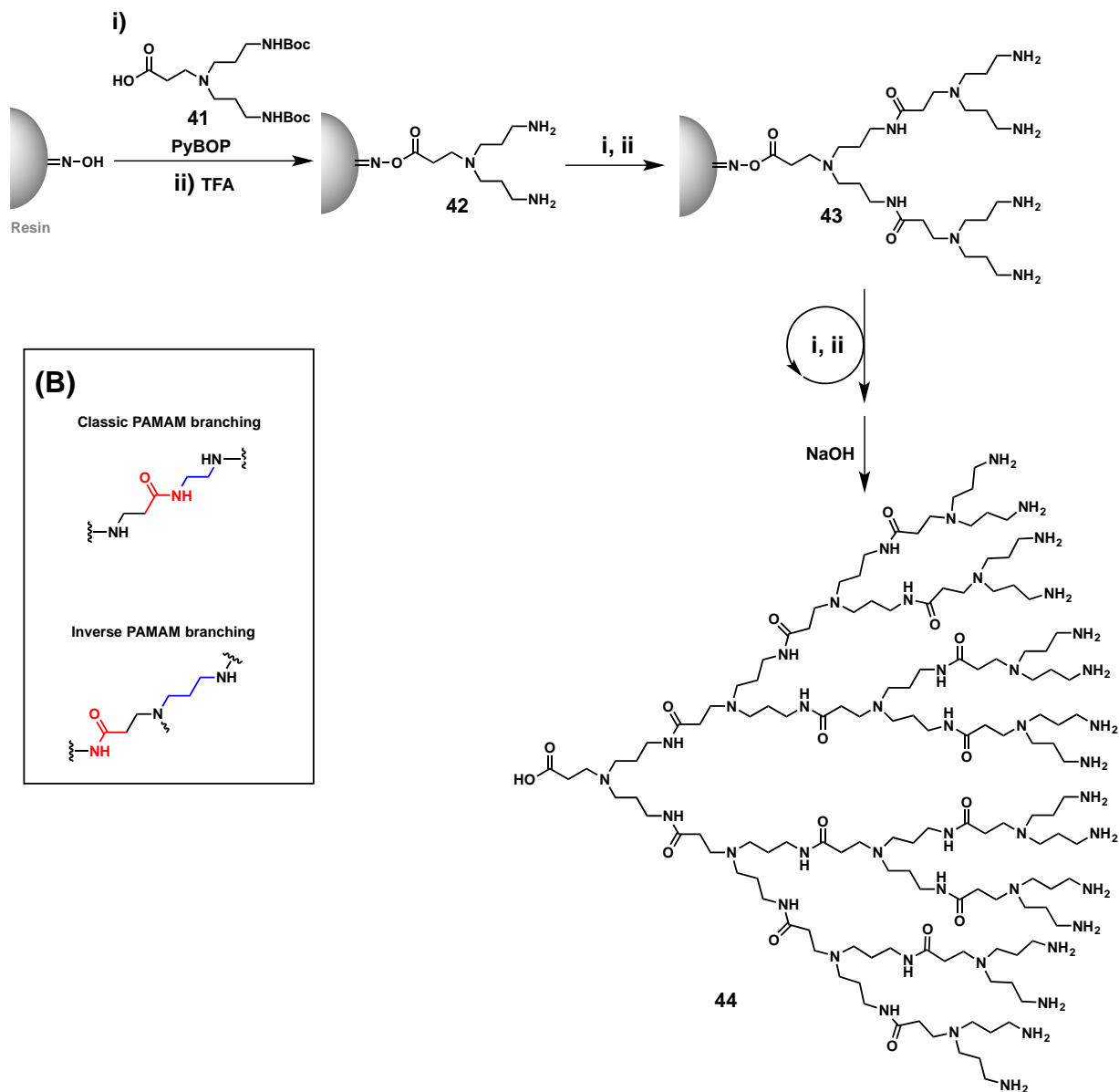
The first solid-phase synthesis of PAMAM dendrimers was reported by Bradley and co-workers in 1997.[18] They used a TentaGel™ resin-linker conjugate carrying a long and flexible polyethylene glycol (PEG) spacer, which was designed to make the reactive sites accessible to reagents while avoiding steric hindrance for the preparation of high-generation dendrimers in the solid-phase. The synthesis was carried out using an iterative two-reaction sequence consisting of Michael addition of the terminal amine to methyl acrylate (**35**) and subsequent amidation with diamine (**37**) (**Figure 1.12**), similar to the traditional synthesis of PAMAM dendrimers in solution. Bradley further promoted the use of so-obtained supported dendrimers as super high-loading resins for solid-phase synthesis.[19] This approach capitalizes on the multivalency of the dendrimers and the resulting increase in the number of reactive sites. For example, the above-mentioned PAMAM dendrimers anchored on TentaGel resin were used as super high-loading reagents for solid-phase synthesis to prepare peptides, amidines and aryl ethers etc.[19]
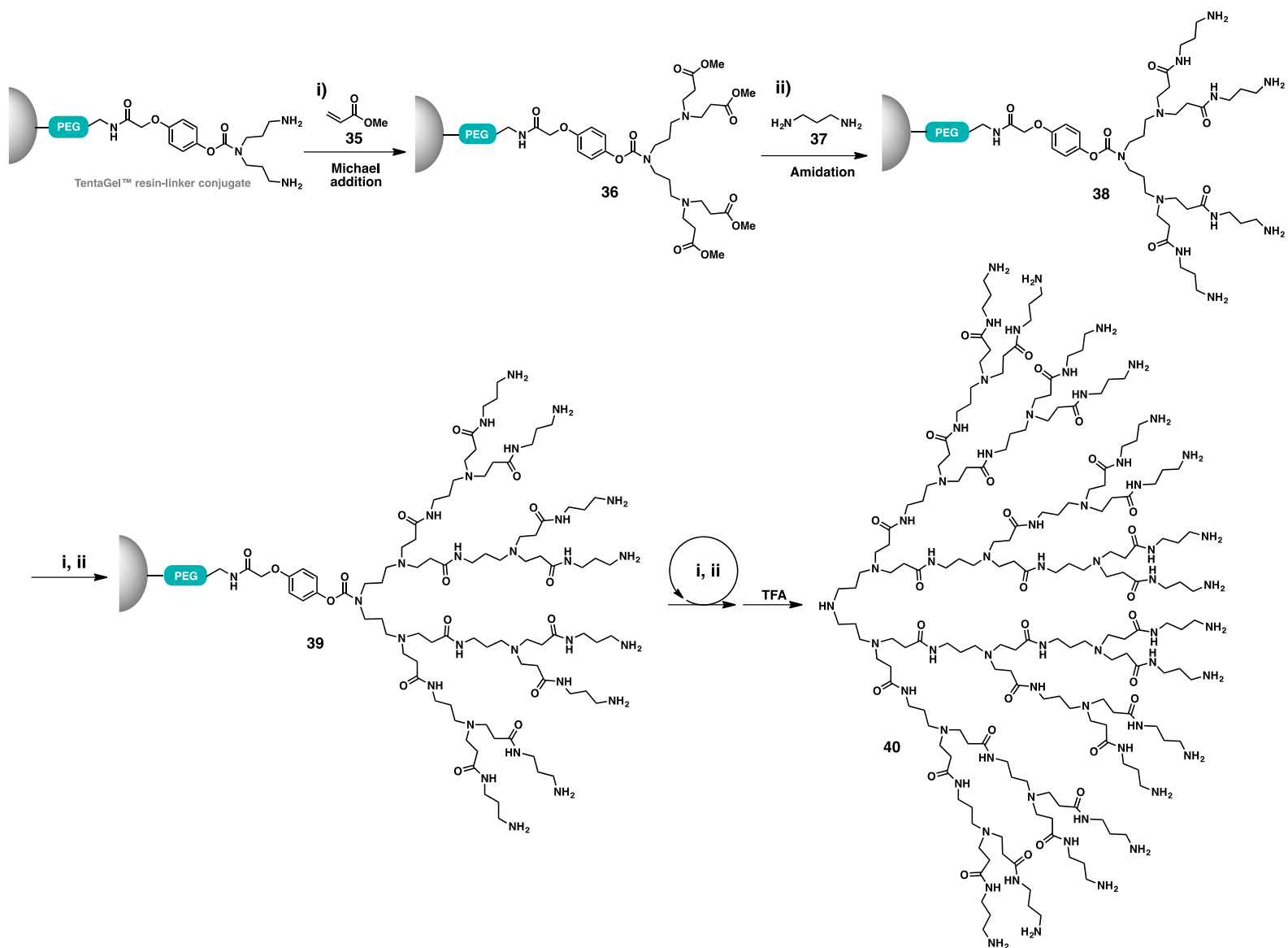
Figure 1.12. Solid-phase synthesis of PAMAM dendrimers via iterative Michael addition and amidation.[18]

It should be mentioned that the synthetic protocol for PAMAM dendrimers, which consists of iterative Michael addition and amidation, unavoidably creates structural defects in the resulting dendrimers. These defects are similar to those identified in dendrimer synthesis in solution and include lost or broken branching arms, cyclized peripheral groups, and dimerized forms.[38] To circumvent this problem, we developed a concise solid-phase synthesis for PAMAM dendrimers in 2013.[39] We harnessed solid-phase peptide synthesis approach to enable PAMAM dendrimer synthesis via iterative amide bond formation by employing a construction unit (**41**) harboring both a carboxylic acid function and amine terminals along with a tertiary amine branching point (**Figure 1.13A**). In contrast to the conventional 2-step iterative synthetic protocol for PAMAM synthesis, this synthetic protocol significantly shortened the reaction steps, and at the same time prevented the structural defects originating from Michael addition and amidation. This highly efficient protocol was carried out using a solid-phase peptide synthesizer, which enabled automatic dendrimer synthesis. Compared to conventional PAMAM dendrimers, these dendrimers have the amide bond linkage in the opposite direction (**Figure 1.13B**) as a result of the peptide synthesis chemistry. Therefore, these dendrimers are also referred as inverse PAMAM dendrimers. We will present this study in details in section 2.
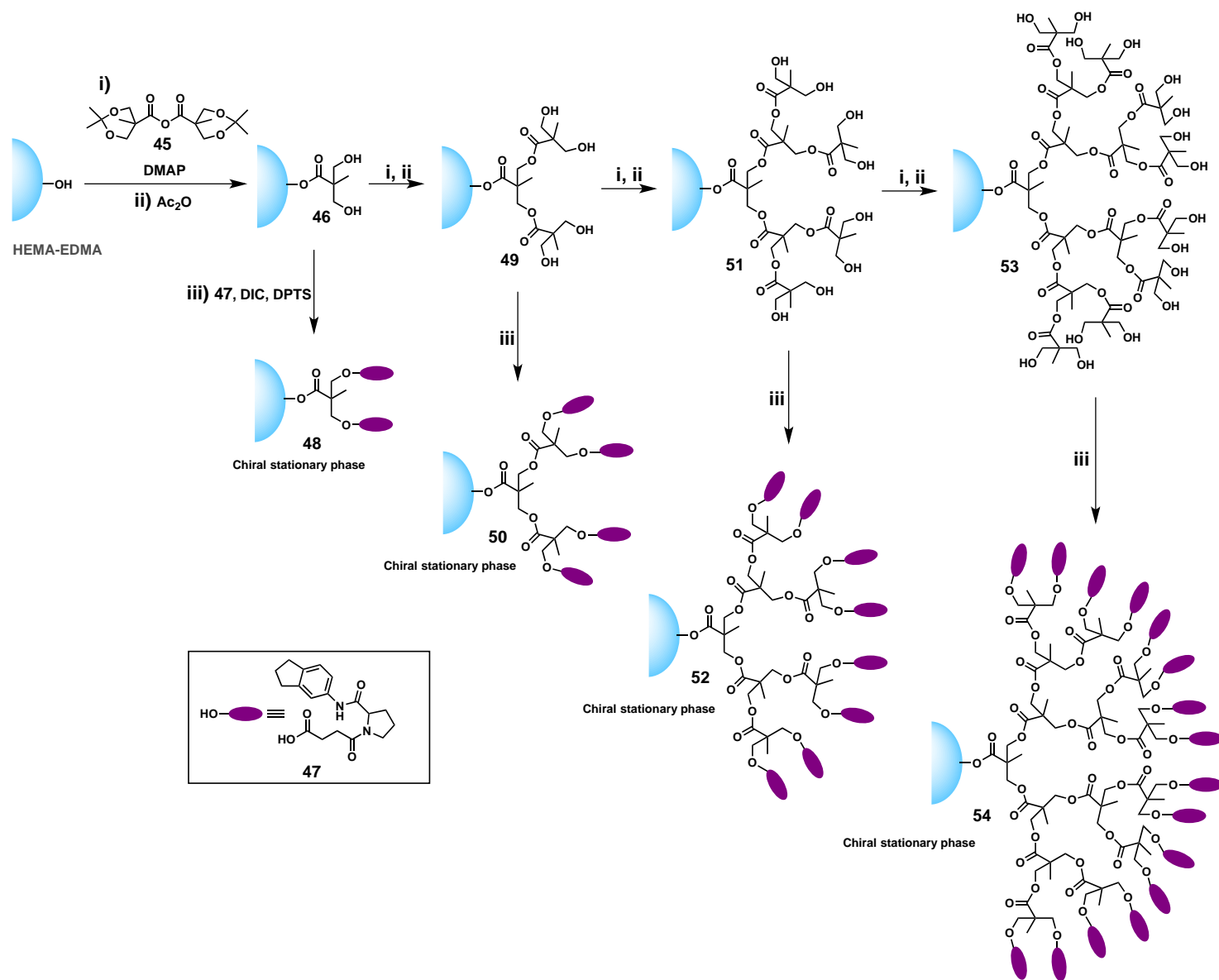
Figure 1.13. Solid-phase synthesis of inverse PAMAM dendrimers using peptide synthesis chemistry.[39]
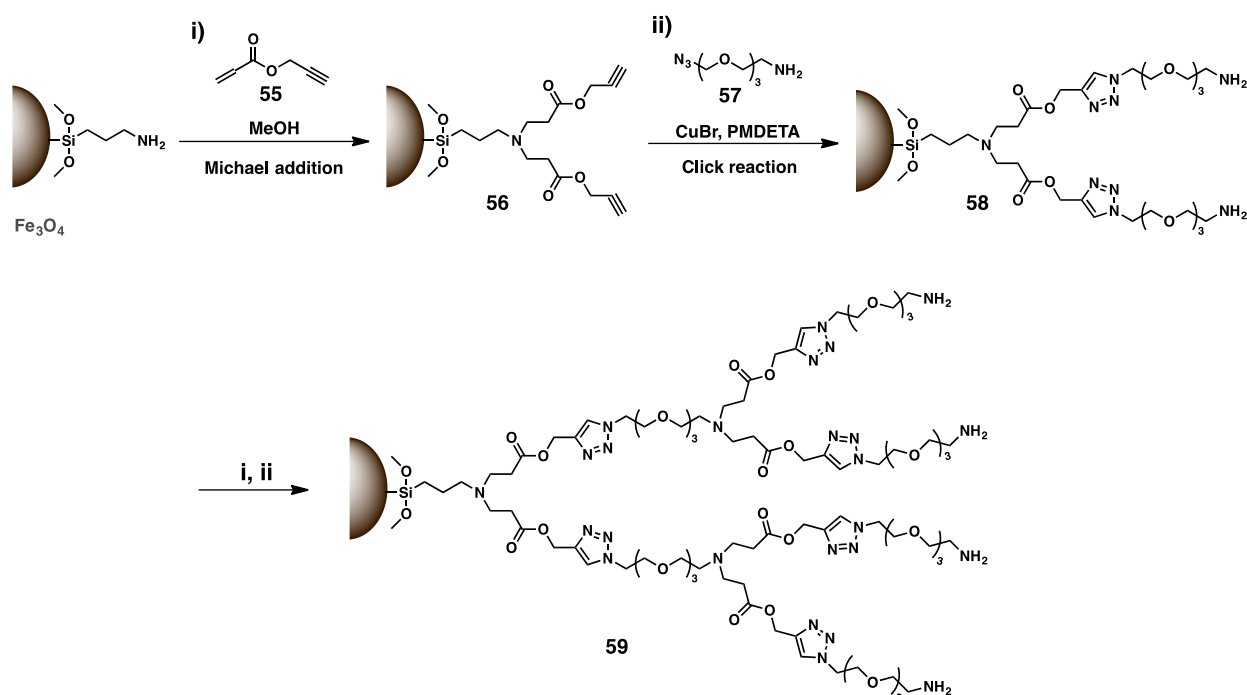
2.5. Polyester dendrimers

Polyester dendrimers containing ester backbones were first reported in the early 1990s.[40] Later, Fréchet and co-workers explored the solid-phase synthesis of polyester dendrimers on a polymer resin.[41] Their aim was to create stationary phases for HPLC-based chiral separation by capitalizing on the multivalent properties of the dendrimers to enhance the separation efficiency. The dendrimer construction mainly relied on isopropylidene-2,2-bis(methoxy)propionic anhydride (**45**) for ester bond formation, while an L-proline derivative (**47**) was appended to the dendrimer terminals to provide a chiral environment (**Figure 1.14**). The so-obtained supported dendrimer resins were successfully applied as chiral stationary phases for HPLC, enabling effective separation of enantiomers of amino acid derivatives.

Among the various ester dendrimers, poly(aminoester) dendrimers have emerged as promising biodegradable and biocompatible materials for biomedical applications by virtue of the presence of numerous ester and amine functions.[42] The ester backbones can be easily disassembled by enzymatic action or in acidic/basic conditions, imparting biodegradability. The numerous amine functionalities can serve as buffers to neutralize the acids generated from ester hydrolysis, hence providing a neutral and benign environment during and after dendrimer degradation. With the aim of developing Fe_3O_4 as a magnetic resonance imaging agent for biomedical applications, Li et al. enclosed Fe_3O_4 nanoparticles within a poly(aminoester) dendrimer shell. They used consecutive iteration of Michael addition and azide-alkyne Huisgen cycloaddition (Cu(I)-mediated click reaction) to construct poly(aminoester) dendrimers on the surface of Fe_3O_4 nanoparticles (**Figure 1.15**). Their synthetic protocol was devoid of any protection/deprotection chemistry, providing the desired product in good yield.[43]

Figure 1.14. Solid-phase synthesis of polyester dendrimer-bound polymer beads as a stationary phase for chiral HPLC separation.[41]
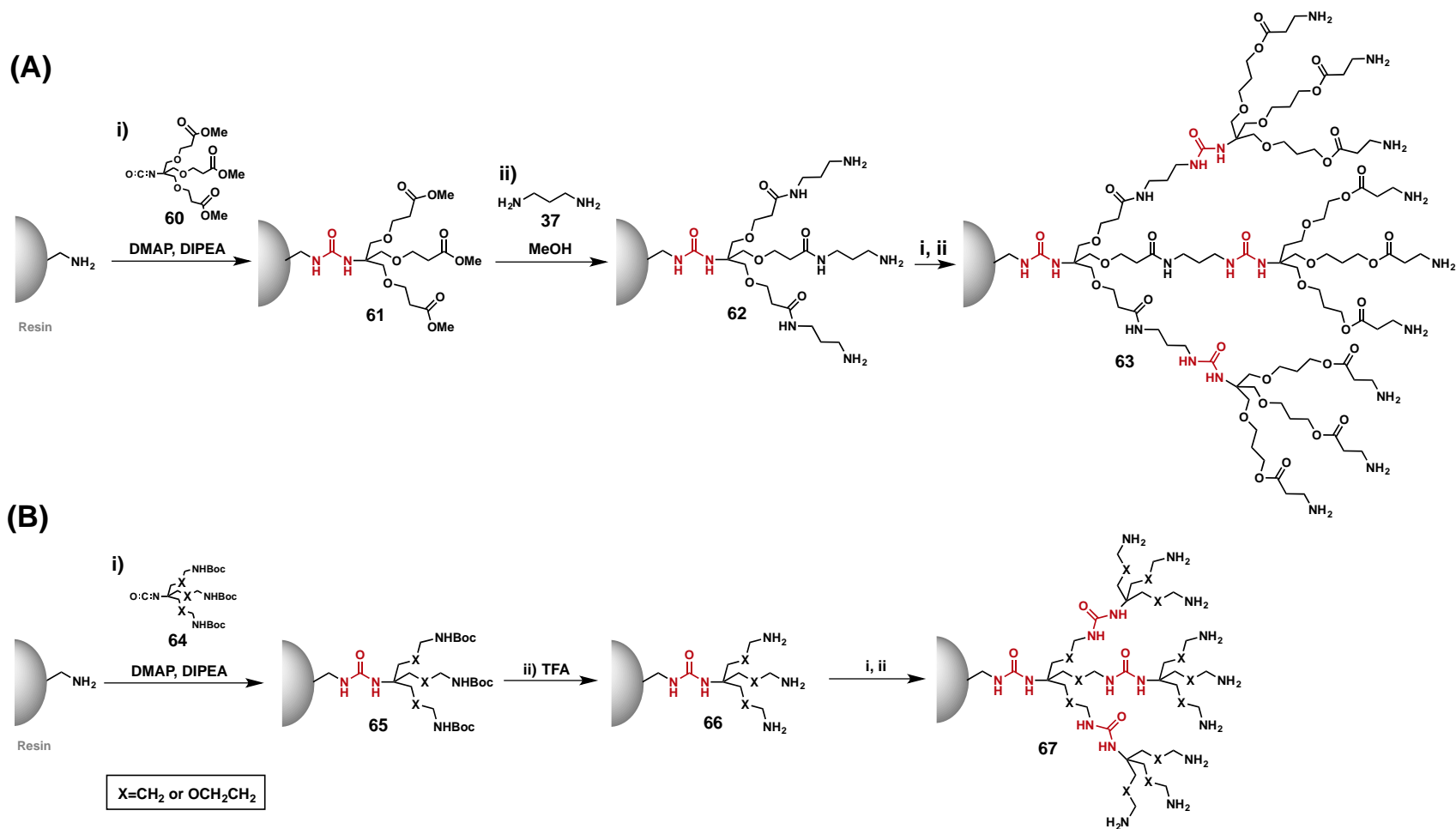
Figure 1.15. Solid-phase synthesis of poly(amino)ester dendrimers to decorate Fe_3O_4 nanoparticles as magnetic resonance imaging agents.[43]

2.6. Polyurea dendrimers

Polyurea dendrimers are a relatively new family of biocompatible dendrimers which harbor urea functionalities.[44,45] In 2000, Bradley reported solid-phase synthesis of polyurea dendrimers using an AB₃-type building block (**60**), which harbors an isocyanate moiety and three ester functions (**Figure 1.16A**).[46] The synthesis started by anchoring the isocyanate unit onto the amine-bearing solid support via the formation of urea, and followed with subsequent amidation of the terminal ester functions with propylenediamine (**37**). The resulting amine-terminated resin was then subjected to iterative reaction with the isocyanate-bearing construction unit (**60**) to generate the polyurea dendrimers (**Figure 1.16A**).

It should be mentioned that amidation of the ester terminals of polyurea dendrimers with a diamine often generates intra-molecular cyclization, a side-reaction also observed during PAMAM dendrimer synthesis. In order to avoid this side-reaction, Bradley and co-workers devised new construction units (**64**) bearing protected amine terminals to replace the previous ester functions.

In this way, they bypassed the amidation step, thereby preventing side-reactions while significantly shortening and simplifying the synthesis (**Figure 1.16B**).[47]
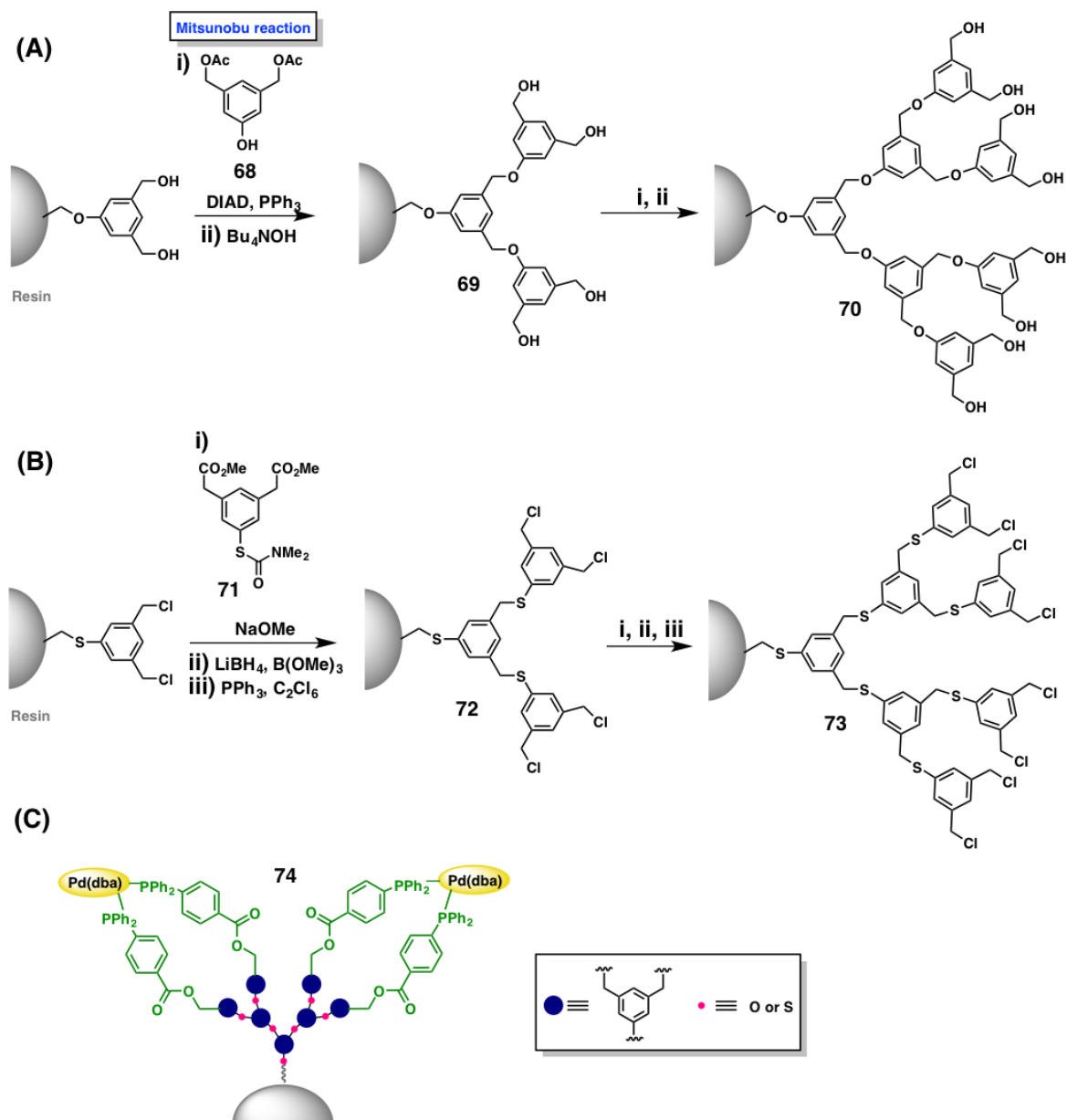
Figure 1.16. Solid-phase synthesis of polyurea dendrimers via an iterative synthesis process consisting of **(A)** branching unit condensation and subsequent amidation;[43] and **(B)** branching unit condensation and subsequent deprotection.[47]

2.7. Polyether/polythioether dendrimers

Compared with the PAMAM, polyester and polyurea dendrimers mentioned above, polyether dendrimers are expected to display better chemical inertness and stability by virtue of their ether linkage, which is much more robust and resistant to reductive, hydrolytic and nucleophilic reactions than amide, ester and urea functionalities. Bradley established the first solid-phase synthesis of polyether dendrimers based on a 3,5-bis(acetoxymethyl)phenol building block (**68**).[48] They used a two-step synthetic sequence composed of a Mitsunobu reaction and ester hydrolysis to successfully construct polyether dendrimers (**Figure 1.17A**).

Later, Portnoy developed an improved strategy to synthesize polyether and poly(thioether) dendrimers. They replaced the Mitsunobu reaction with a nucleophilic substitution reaction using a thiol nucleophile generated in situ from hydrolysis of **71** (**Figure 1.17B**), which can be easily prepared from commercially available reagent.[49] This new method avoided the Mitsunobu reaction, which requires expensive reagents with limited shelf-life. The polyether and polythioether dendrimers (**74**) bearing phosphine ligands were also prepared and complexed to Pd and Co precursors to create multivalent catalysts for cross-coupling reactions (**Figure 1.17C**).[50] Indeed, these supported dendrimer catalysts significantly improved the selectivity and reactivity with a positive dendritic effect.

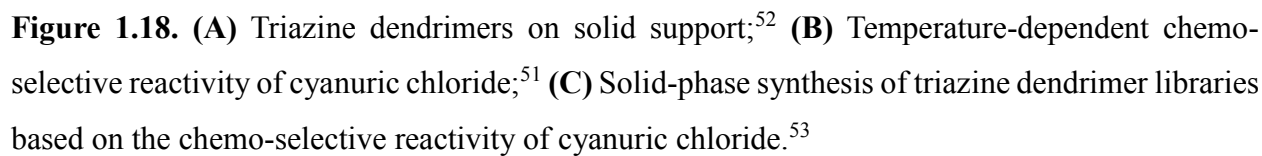**Figure 1.17. (A)** Solid-phase synthesis of polyether dendrimers via an iterative synthesis process involving Mitsunobu coupling and ester hydrolysis;[45] **(B)** Solid-phase synthesis of polythioether dendrimers using a chlorodehydroxylation-nucleophilic substitution reaction;[49] **(C)** Polyether/polythioether dendrimer based supported catalysts for Heck and Suzuki reactions.[50]

2.8. Triazine dendrimers

Triazine dendrimers (**Figure 1.18**), composed of 1,3,5-triazine rings, which are further connected with diamine units,[51] were first outlined in the patent filed by Meijer et al in the 1990s. Since then, their potential for use in drug and gene delivery has been intensively investigated by Simanek and co-workers over the past two decades. Today, a variety of triazine dendrimers with different diamine linkers and surface functionalities has been established. Solid-supported triazine dendrimers (**Figure 1.18A**) have also been prepared to serve as supported reagents and devices. These supported dendrimer reagents can be endowed with multivalent properties yet easily recovered, regenerated and reused for applications such as scavenging agents and protein library screening.[52]

The synthesis of triazine dendrimers is mainly based on nucleophilic aromatic substitutions of cyanuric chloride (**76**). By exploiting the different reactivity of the cyanuric chlorides towards amine nucleophiles, it is possible to obtain mono-, di- or tri-substituted triazines through the control of the temperature and reaction time (**Figure 1.18B**). This constitutes the chemistry foundation for the construction of triazine dendrimers.

By taking advantages of the chemo-selective substitution of cyanuric chloride (**76**), we developed solid-phase synthesis to prepare a library of triazine dendrimers with various combinations of terminal functionalities originated from the cyclic secondary amines and the primary amines of amino acids (**Figure 1.18C**).[53] We also established orthogonal staining methods using the Kaiser ninhydrin test and Alizarin R (AliR) to reveal, respectively, alkyl amines and aryl chlorides on the dendrimer terminals after each synthetic step. These staining methods allowed us to track the progress of the reactions and hence easily and efficiently control the dendrimer synthesis.

Figure 1.18. (A) Triazine dendrimers on solid support;[52] **(B)** Temperature-dependent chemoselective reactivity of cyanuric chloride;[51] **(C)** Solid-phase synthesis of triazine dendrimer libraries based on the chemo-selective reactivity of cyanuric chloride.[53]

3. Conclusions and perspectives

In this section, we have highlighted the development and current state of solid-phase dendrimer synthesis. Most endeavors have been directed towards generating peptide and PAMAM dendrimers, as well as biologically relevant dendrimers of carbohydrates and oligonucleotides, and their related conjugates. Efforts have also been devoted to synthesizing polyester, polyether/polythioether, polyurea and triazine dendrimers, using various solid supports and diverse chemistry for dendrimer growth on and cleavage from the resin.

Solid-phase dendrimer synthesis with its efficient synthesis, simple operation and purification as well as possibility for automation, offers not only highly efficient and effective synthesis of dendrimers but also a unique method to construct dendrimers on various solid supports to provide supported functional materials such as solid-support reagents, catalysts and devices etc.[54] Nevertheless, heterogeneity is the main drawback of solid-phase dendrimer synthesis. In addition, substrates anchored to a solid support may have limited access to the reagents due to issues related to immobilization, steric hindrance and size selectivity, which may slow down or even impede the reaction. As described in the example of PAMAM dendrimer synthesis by Bradley, using a solid support which bears a long and flexible PEG spacer may overcome this problem.[18] It is important to note that even a few side-reactions with tiny by-products in each step can create a complex mixture of products and by-products at the end of a synthetic procedure. Chemists thus strive to find optimized chemical reactions involving the most appropriate building units, and use the convergent/divergent double strategy as well as click chemistry to construct dendrimers more efficiently and in fewer steps.[55] Yet the optimization of solid-phase dendrimer synthesis is laborious and tedious. One remarkable reason is that it is seldom possible to track the reactions without cleaving the products from their solid supports. Consequently, easy and convenient online and non-destructive analytical methods, such as the solid-state NMR, IR and Raman spectroscopy which have been used in solid-phase peptide synthesis, would be extremely advantageous for dendrimer synthesis.

Since their conception, dendrimers have been considered and appreciated as admirable chemical entities and functional materials, holding great promise for a wide range of applications by virtue of their unique structural properties and multivalent cooperativity.[37] Three decades on, their characteristic multi-step synthesis still requires tremendous effort, which greatly handicaps

their development and limits their applications.[36] Continuing improvements in solid-phase dendrimer synthesis, alongside solution-phase synthesis, are of high demand. We hope that these improvements will transform dendrimer synthesis and enable the creation of structurally diverse dendrimers as new molecular paradigms and functional materials in a wide range of applications, including energy production, environmental protection, health care, cosmetics etc. We expect that further research will deliver more efficient methods for advancing the synthesis of dendrimers, which can be explored and extended into the arenas of biomedical and materials science.

4. References

[1]   R. B. Merrifield. Solid phase peptide synthesis. I. The synthesis of a tetrapeptide. *J. Am. Chem. Soc.*, **1963**, *85*, 2149-2154.

[2]   R. B. Merrifield. Solid phase synthesis. *Angew. Chem. Int. Ed. Engl.*, **1985**, *24*, 799-810.

[3]   P. H. Toy; Y. Lam. Solid-phase organic synthesis: Concepts, strategies, and applications. John Wiley & Sons, Inc.: **2012**.

[4]   J. M. Palomo. Solid-phase peptide synthesis: An overview focused on the preparation of biologically relevant peptides. *RSC Advances*, **2014**, *4*, 32658-32672.

[5]   M. J. Gait; R. C. Sheppard. Rapid synthesis of oligodeoxyribonucleotides: A new solid-phase method. *Nucleic Acids Res.*, **1977**, *4*, 1135-1158.

[6]   P. H. Seeberger. The logic of automated glycan assembly. *Acc. Chem. Res.*, **2015**, *48*, 1450-1463.

[7]   R. C. D. Brown. Recent developments in solid-phase organic synthesis. *J. Chem. Soc., Perkin Trans. 1*, **1998**, 3293-3320.

[8]   L. Spasser; M. Portnoy. Solid-phase synthesis of uniform linear oligoethers with repeating functional arms as multivalent spacers. *J. Polym. Sci., Part A: Polym. Chem.*, **2010**, *48*, 6009-6013.

[9]   K. Kumar; H. Waldmann. Synthesis of natural product inspired compound collections. *Angew. Chem. Int. Ed.*, **2009**, *48*, 3224-3242.

[10]   J. P. Nandy; M. Prakesch; S. Khadem; P. T. Reddy; U. Sharma; P. Arya. Advances in solution- and solid-phase synthesis toward the generation of natural product-like libraries. *Chem. Rev.*, **2009**, *109*, 1999-2060.

[11]   J. P. Tam. Synthetic peptide vaccine design: Synthesis and properties of a high-density multiple antigenic peptide system. *PNAS*, **1988**, *85*, 5409-5413.

[12]   K. Gordon; S. Balasubramanian. Solid phase synthesis–Designer linkers for combinatorial chemistry: A review. *J. Chem. Technol. Biotechnol.*, **1999**, *74*, 835-851.

[13]   J. Tulla-Puche; F. Albericio. The power of functional resins in organic synthesis. John Wiley & Sons, Inc.: **2008**.

[14]   S. Rana; P. White; M. Bradley. Influence of resin cross-linking on solid-phase chemistry. *J. Comb. Chem.*, **2001**, *3*, 9-15.

[15] D. Hudson. Matrix assisted synthetic transformations: A mosaic of diverse contributions. I. The pattern emerges. *J. Comb. Chem.*, **1999**, *1*, 333-360.

[16] M. Kempe; G. Barany. CLEAR: A novel family of highly cross-linked polymeric supports for solid-phase peptide synthesis. *J. Am. Chem. Soc.*, **1996**, *118*, 7083-7093.

[17] A. W. Czarnik. Solid-phase synthesis supports are like solvents. *Biotechnol. Bioeng.*, **1998**, *61*, 77-79.

[18] V. Swali; N. J. Wells; G. J. Langley; M. Bradley. Solid-phase dendrimer synthesis and the generation of super-high-loading resin beads for combinatorial chemistry. *J. Org. Chem.*, **1997**, *62*, 4902-4903.

[19] S. Lebreton; S. Monaghan; M. Bradley. Solid-phase dendrimer chemistry: Synthesis and applications. *Aldrichimica Acta*, **2001**, *43*, 75-82.

[20] F. Gaggini; A. Porcheddu; G. Reginato; M. Rodriquez; M. Taddei. Colorimetric tools for solid-phase organic synthesis. *J. Comb. Chem.*, **2004**, *6*, 805-810.

[21] C. Dhalluin; C. Boutillon; A. Tartar; G. Lippens. Magic angle spinning nuclear magnetic resonance in solid-phase peptide synthesis. *J. Am. Chem. Soc.*, **1997**, *119*, 10494-10500.

[22] S. S. Rahman; D. J. Busby; D. C. Lee. Infrared and Raman spectra of a single resin bead for analysis of solid-phase reactions and use in encoding combinatorial libraries. *J. Org. Chem.*, **1998**, *63*, 6196-6199.

[23] J.-L. Reymond; T. Darbre. Peptide and glycopeptide dendrimer apple trees as enzyme models and for biomedical applications. *Org. Biomol. Chem.*, **2012**, *10*, 1483-1492.

[24] L. Crespo; G. Sanclimens; M. Pons; E. Giralt; M. Royo; F. Albericio. Peptide and amide bond-containing dendrimers. *Chem. Rev.*, **2005**, *105*, 1663-1682.

[25] L. Crespo; G. Sanclimens; B. Montaner; R. Pérez-Tomás; M. Royo; M. Pons; F. Albericio; E. Giralt. Peptide dendrimers based on polyproline helices. *J. Am. Chem. Soc.*, **2002**, *124*, 8876-8883.

[26] C. Douat-Casassus; T. Darbre; J.-L. Reymond. Selective catalysis with peptide dendrimers. *J. Am. Chem. Soc.*, **2004**, *126*, 7817-7826.

[27] A. Clouet; T. Darbre; J.-L. Reymond. A combinatorial approach to catalytic peptide dendrimers. *Angew. Chem. Int. Ed.*, **2004**, *43*, 4612-4615.

[28] N. Maillard; A. Clouet; T. Darbre; J.-L. Reymond. Combinatorial libraries of peptide dendrimers: Design, synthesis, on-bead high-throughput screening, bead decoding and characterization. *Nat. Protocols*, **2009**, *4*, 132-142.

[29] R. Roy; D. Zanini; S. J. Meunier; A. Romanowska. Solid-phase synthesis of dendritic sialoside inhibitors of influenza A virus haemagglutinin. *J. Chem. Soc., Chem. Commun.*, **1993**, 1869-1872.

[30] A. Papadopoulos; T. C. Shiao; R. Roy. Diazo transfer and click chemistry in the solid phase syntheses of lysine-based glycodendrimers as antagonists against *Escherichia coli FimH*. *Mol. Pharm.*, **2012**, *9*, 394-403.

[31] A. Díaz-Moscoso; J. M. Benito; C. Ortiz Mellet; J. M. García Fernández. Efficient use of Ellman safety-catch linker for solid-phase assisted synthesis of multivalent glycoconjugates. *J. Comb. Chem.*, **2007**, *9*, 339-342.

[32] R. H. E. Hudson; M. J. Damha. Nucleic acid dendrimers: Novel biopolymer structures. *J. Am. Chem. Soc.*, **1993**, *115*, 2119-2124.

[33] R. H. E. Hudson; S. Robidoux; M. J. Damha. Divergent solid-phase synthesis of nucleic acid dendrimers. *Tetrahedron Lett.*, **1998**, *39*, 1299-1302.

[34] D. A. Tomalia; H. Baker; J. Dewald; M. Hall; G. Kallos; S. Martin; J. Roeck; J. Ryder; P. Smith. A new class of polymers: Starburst-dendritic macromolecules. *Polym. J.*, **1985**, *17*, 117-132.

[35] D. A. Tomalia; A. M. Naylor; W. A. Goddard. Starburst dendrimers: Molecular-level control of size, shape, surface chemistry, topology, and flexibility from atoms to macroscopic matter. *Angew. Chem. Int. Ed. Engl.*, **1990**, *29*, 138-175.

[36] S. Svenson. The dendrimer paradox-high medical expectations but poor clinical translation. *Chem. Soc. Rev.*, **2015**, *44*, 4131-4144.

[37] D. A. Tomalia; J. B. Christensen; U. Boas. Dendrimers, dendrons and dendritic polymers. Cambridge University Press: **2012**.

[38] J. Peterson; V. Allikmaa; J. Subbi; T. Pehk; M. Lopp. Structural deviations in poly(amidoamine) dendrimers: A MALDI-TOF MS analysis. *Eur. Polym. J.*, **2003**, *39*, 33-42.

[39] A. Y.-T. Huang; C.-H. Tsai; H.-Y. Chen; H.-T. Chen; C.-Y. Lu; Y.-T. Lin; C.-L. Kao. Concise solid-phase synthesis of inverse poly(amidoamine) dendrons using AB2 building blocks. *Chem. Commun.*, **2013**, *49*, 5784-5786.

[40] C. J. Hawker; J. M. J. Fréchet. Monodispersed dendritic polyesters with removable chain ends: A versatile approach to globular macromolecules with chemically reversible polarities. *J. Chem. Soc., Perkin Trans. 1*, **1992**, 2459-2469.

[41] F. H. Ling; V. Lu; F. Svec; J. M. J. Fréchet. Effect of multivalency on the performance of enantioselective separation media for chiral HPLC prepared by linking multiple selectors to a porous polymer support via liphatic dendrons. *J. Org. Chem.*, **2002**, *67*, 1993-2002.

[42] Y. Wang; G. Quéléver; L. Peng. The seemingly trivial yet challenging synthesis of poly(aminoester) dendrimers. *Curr. Med. Chem.*, **2012**, *19*, 5011-5028.

[43] M. Li; L. Q. Xu; L. Wang; Y. P. Wu; J. Li; K.-G. Neoh; E.-T. Kang. Clickable poly(ester amine) dendrimer-grafted Fe3O4 nanoparticles prepared via successive Michael addition and alkyne-azide click chemistry. *Polym. Chem.*, **2011**, *2*, 1312-1321.

[44] R. B. Restani; P. I. Morgado; M. P. Ribeiro; I. J. Correia; A. Aguiar-Ricardo; V. D. B. Bonifácio. Biocompatible polyurea dendrimers with pH-dependent fluorescence. *Angew. Chem. Int. Ed.*, **2012**, *51*, 5162-5165.

[45] R. B. Restani; J. Conde; P. V. Baptista; M. T. Cidade; A. M. Braganca; J. Morgado; I. J. Correia; A. Aguiar-Ricardo; V. D. B. Bonifacio. Polyurea dendrimer for efficient cytosolic siRNA delivery. *RSC Advances*, **2014**, *4*, 54872-54878.

[46] C. Fromont; M. Bradley. High-loading resin beads for solid phase synthesis using triple branching symmetrical dendrimers. *Chem. Commun.*, **2000**, 283-284.

[47] S. Lebreton; S.-E. How; M. Buchholz; B.-E. Yingyongnarongkul; M. Bradley. Solid-phase construction: High efficiency dendrimer synthesis using AB3 isocyanate-type monomers. *Tetrahedron*, **2003**, *59*, 3945-3953.

[48] A. Basso; B. Evans; N. Pegg; M. Bradley. Solid phase synthesis of aryl-ether dendrimers. *Chem. Commun.*, **2001**, 697-698.

[49] A. Dahan; A. Weissberg; M. Portnoy. Preparation of novel polythioether dendrons on a solid support. *Chem. Commun.*, **2003**, 1206-1207.

[50] A. Mansour; T. Kehat; M. Portnoy. Dendritic effects in catalysis by Pd complexes of bidentate phosphines on a dendronized support: Heck vs. carbonylation reactions. *Org. Biomol. Chem.*, **2008**, *6*, 3382-3387.

[51] M. B. Steffensen; E. Hollink; F. Kuschel; M. Bauer; E. E. Simanek. Dendrimers based on [1,3,5]-triazines. *J. Polym. Sci. A Polym. Chem.*, **2006**, *44*, 3411-3433.

[52] A. Marsh; S. J. Carlisle; S. C. Smith. High-loading scavenger resins for combinatorial chemistry. *Tetrahedron Lett.*, **2001**, *42*, 493-496.

[53] A. Y.-T. Huang; S. Patra; H.-T. Chen; C.-L. Kao; E. E. Simanek. Solid-phase synthesis of libraries of triazine dendrimers and orthogonal staining methods for tracking reactions on resin. *Asian J. Org. Chem.*, **2016**, *5*, 860-864.

[54] T. Kehat; K. Goren; M. Portnoy. Dendrons on insoluble supports: Synthesis and applications. *New J. Chem.*, **2007**, *31*, 1218-1242.

[55] M. V. Walter; M. Malkoch. Simplifying the synthesis of dendrimers: Accelerated approaches. *Chem. Soc. Rev.*, **2012**, *41*, 4593-4609.

Section 2. Solid-phase synthesis of inverse PAMAM dendrimers
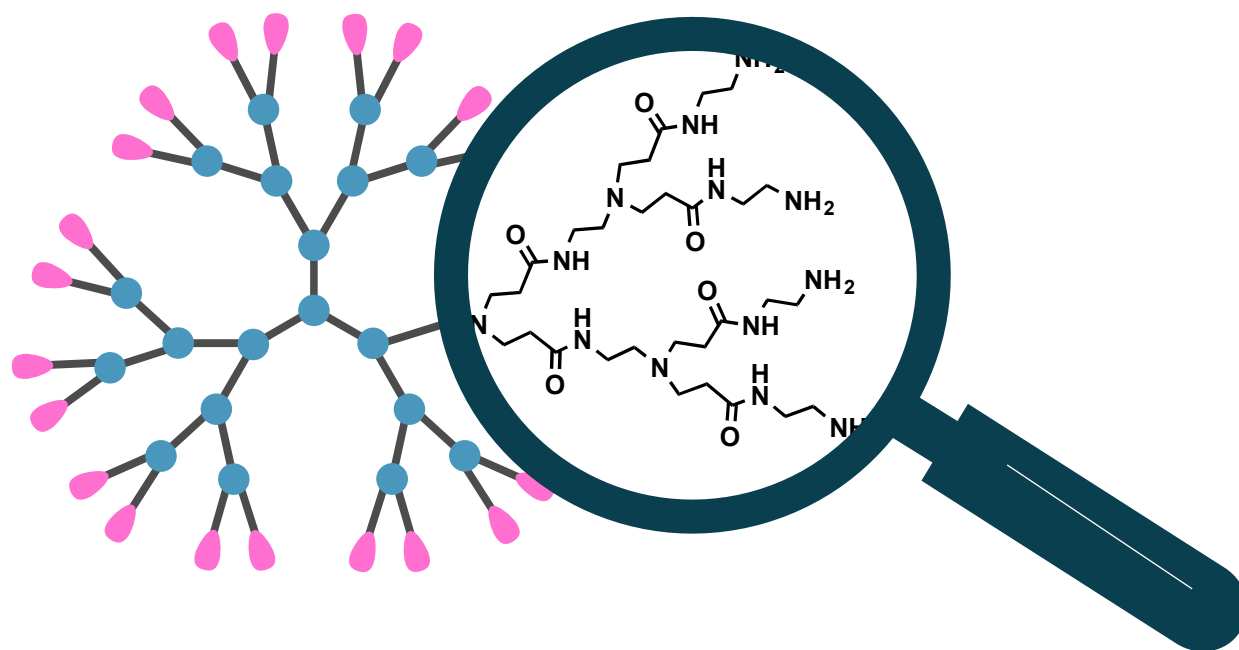
1. Background

PAMAM dendrimer stands for **P**oly(**AM**ido**AM**ine) dendrimer harbors repeating amide functionalities with tertiary amines as branching points (**Figure 2.1**), which was first reported by Tomalia and co-workers in 1985.[1] PAMAM dendrimers have been the most widely studied dendrimers. PAMAM dendrimers exhibit excellent biocompatibility thanks to their peptide-mimic amide backbones alongside the numerous interior tertiary amine functions and surface primary amine terminals.[2] Generous solubility in water, low cytotoxicity when bearing neutral terminal functionalities, and readily modifiable surface groups altogether make PAMAM dendrimers particularly interesting for biological applications.[3] Consequently, PAMAM dendrimers has been

extensively studied as a platform for multivalent conjugates combining specific targeting,[4-7] drug delivery,[8-10] gene and nucleic acid delivery,[11] as well as imaging agents,[12-14] etc.
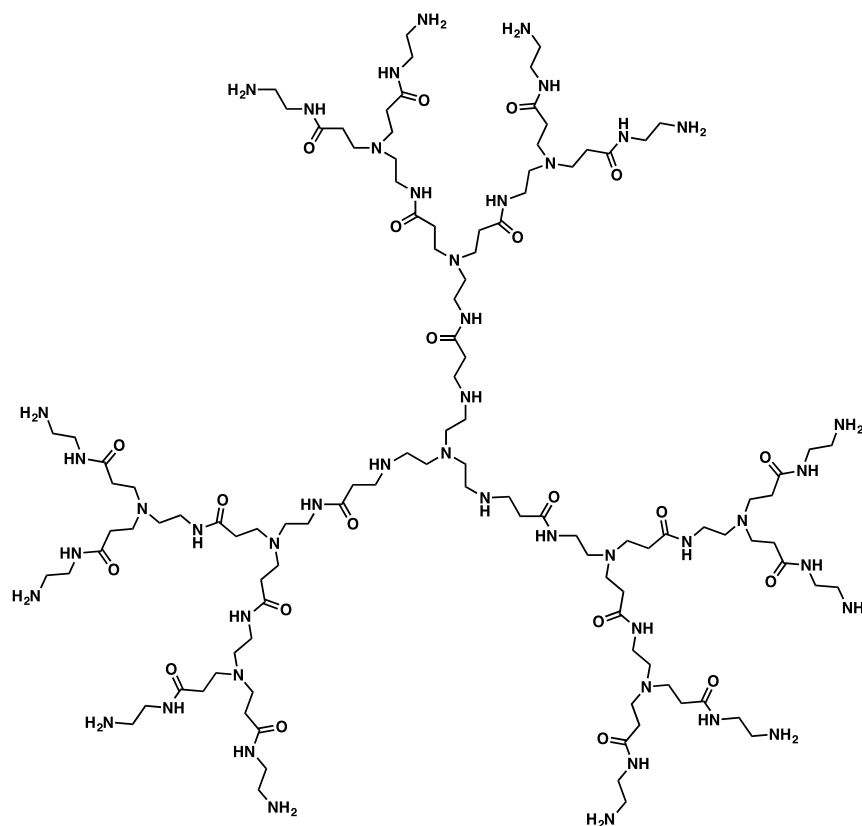

87

Figure 2.1. The structure of classical G2 PAMAM dendrimer firstly reported by Tomalia et al.

PAMAM dendrimer synthesis reported by Tomalia and co-workers involves an iterative two-step process of Michael addition and amidation.[1] The synthesis starts with an amine or a compounds with multiple amine functions such as ethylenediamine (EDA, **88**), which undergo double Michael addition with methyl acrylate (**35**). The Michael addition proceeds generally fast with a good yield, resulting in the ester-terminating product. The resulting compound represents the so-called half generation of the PAMAM dendrimer (**89** and **91**) (**Scheme 2.1**). The second step of the synthesis is the amidation of the ester terminals using a large excess of ethylenediamine to build up the full generation PAMAM dendrimer (**90**). By repeating these two steps, dendrimers

with generations up to 10 could be obtained.[15-17]

In addition to amidation, methylester in half generation PAMAM dendrimers can undergo hydrolysis to deliver the corresponding carboxylic acid. These functional terminals can be easily modified or derived to achieve further dendrimers with various other chemical entities such as alkyl chains, oligomers, polymers, peptides, proteins, drugs, and so on.[2,16,18]
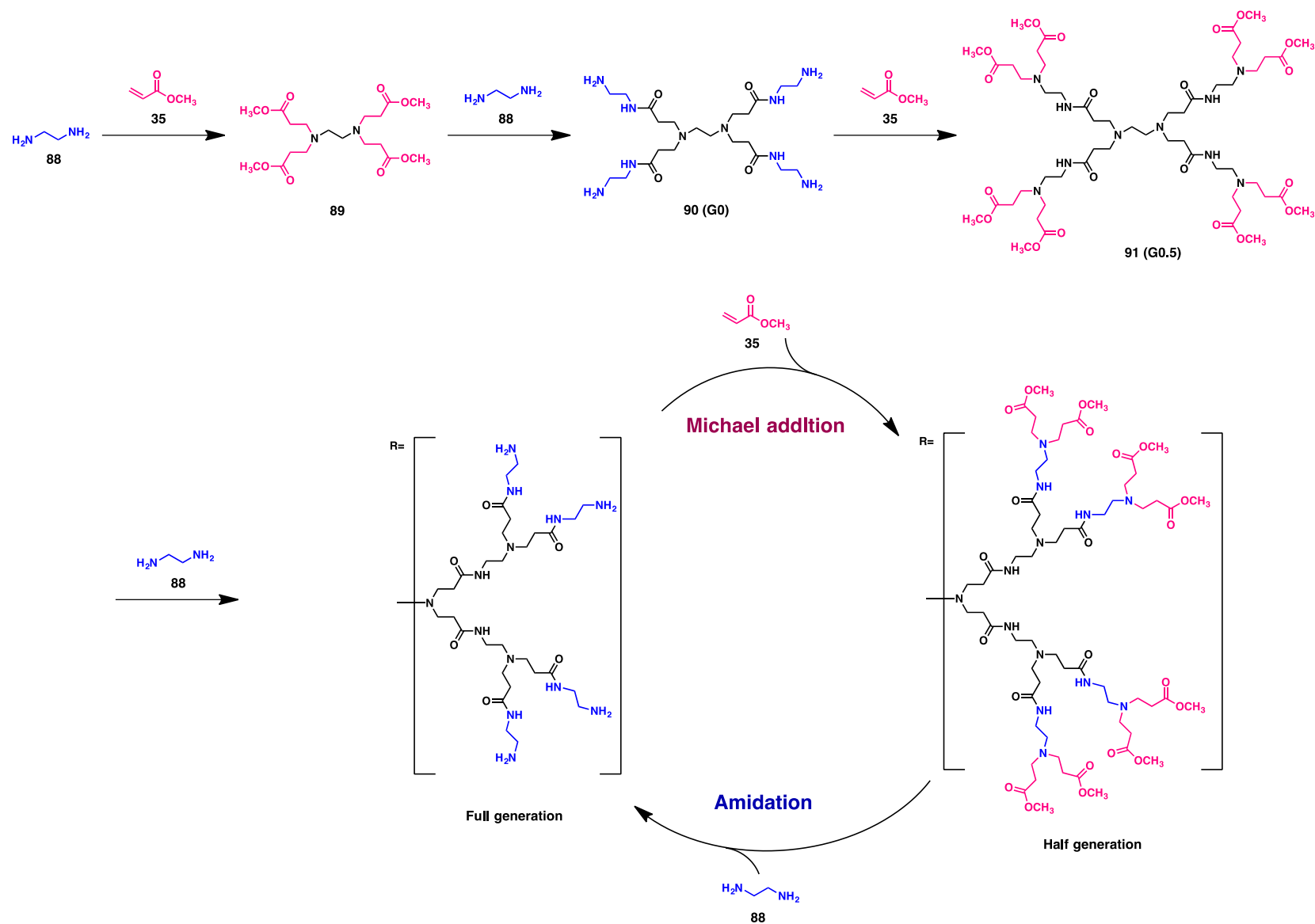
Scheme 2.1. General procedure for PAMAM dendrimer synthesis via two-repeating step of Michael addition and amidation.

On the basis of the iterative synthesis using Michael addition and amidation for PAMAM dendrimers, a variety of structural defects can be resulted from various side-reactions including incomplete Michael addition, *retro*-Michael reaction, intramolecular cyclization and/or dimerization during amidation.[19] Incomplete Michael reaction yields dendrimers with missing branching arms (**Scheme 2.2**, route **I**), whereas the close proximity of the terminal groups and the dendrimer molecules gives rise to intramolecular cyclization (**Scheme 2.2**, route **II**)[16] and intermolecular dimerization (**Scheme 2.2**, route **III**) during amidation step.[16] Also, *retro*-Michael reaction is a common problem at elevated temperatures ($>60^{\circ}$C), although it can be reduced considerably at reaction temperature below 60°C (**Scheme 2.2**, route **IV**).[16] As a consequence of the *retro*-Michael reaction, *N*-(2-aminoethyl) acryl amide chain is cleaved and a defective dendrimer with one missing branch is formed. The resulted defective dendrimer is able to undergo the further Michael addition with ethylenediamine to generate additional defective dendrimers.

In the case of PAMAM dendrimers, the defects occur inevitably beyond generation 4 because of the crowded terminal groups. Very often, the defective dendrimers are difficult to separate from desired intact dendrimers because of their similar chemical compositions and physicochemical properties.[19]
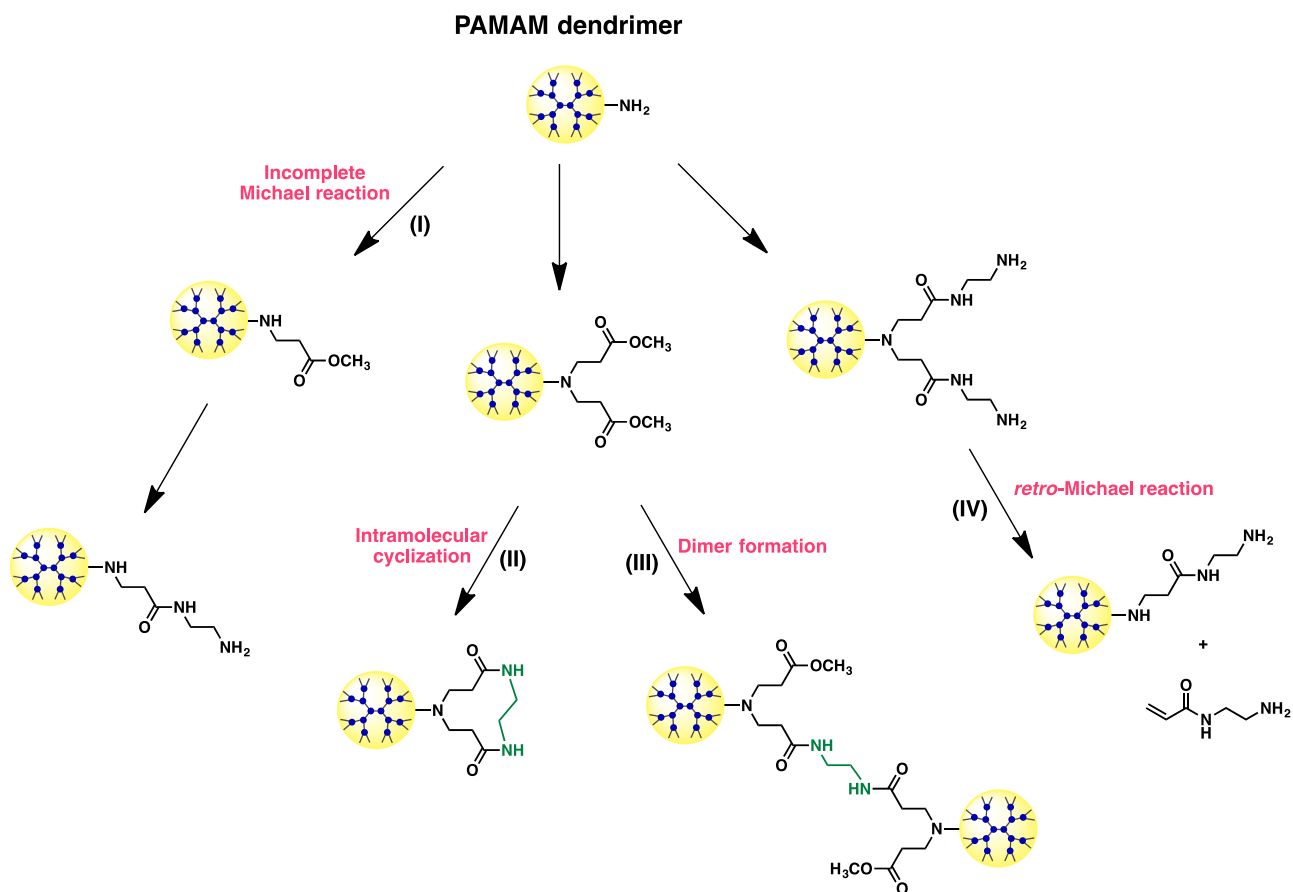
Scheme 2.2. Possible side-reactions in PAMAM dendrimer growth through two-step procedure.

To solve the problems encountered during dendrimer synthesis in solution, solid-phase synthesis (SPS) was proposed to prepare PAMAM dendrimers by making use of excess reagents to complete all reactions together with simple washing and filtration procedures for easy and convenient purification. As we mentioned in the introduction of solid-phase dendrimer synthesis (SPDS), Bradley et al. reported the first PAMAM dendrimer synthesis on solid supports using the two-step iterative synthetic procedure of amidation/Michael addition developed for solution synthesis.[20] They achieved PAMAM dendrimer synthesis up to G4 on the solid support and promoted the obtained solid support harboring dendrimers as high-loading resins for further solid-phase organic synthesis (SPOS). However, the defective dendrimers remained inevitably because of the implementation of the same chemistry issued from the solution-phase synthesis of PAMAM dendrimers.
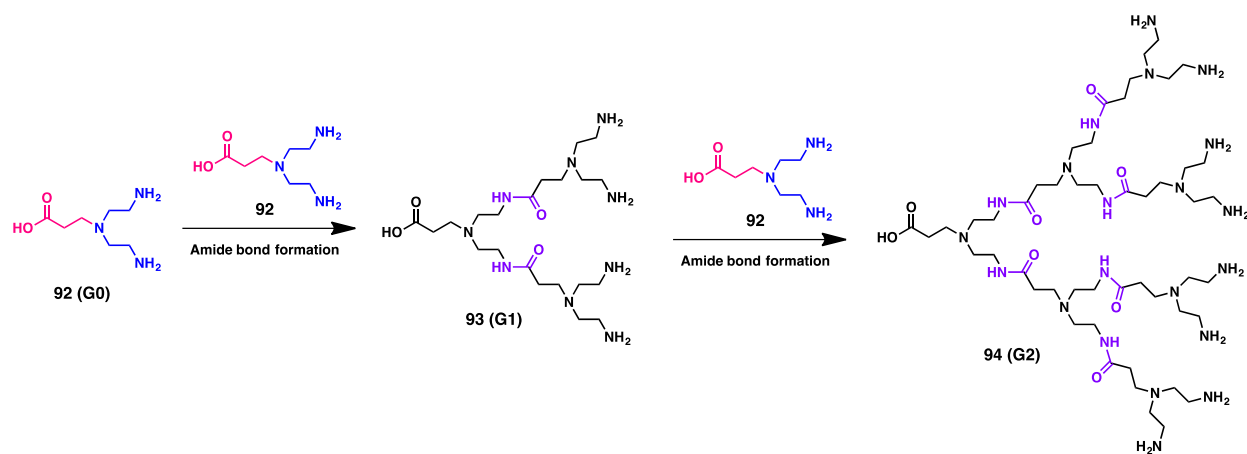
As the defective dendrimers on solid-phase synthesis are mainly originated from Michael and

retro-Michael reaction as well as amidation, it is therefore desirable if we can completely avoid Michael addition and amidation for PAMAM dendrimer synthesis. We therefore came out with the idea to construct PAMAM dendrimer via amide bond formation rather than the conventional synthesis composed of Michael addition and amidation. It is well-known that solid-phase peptide synthesis can deliver, via stepwise amide bond formation, peptides in high quality and large quantity, and most of peptide therapeutics in clinical use are prepared using solid-phase synthesis nowadays. Take into account of all these considerations, we wanted to establish a concise solid-phase synthesis for PAMAM dendrimers by exploiting the solid-phase peptide synthesis chemistry,[21] namely, making use of amide bond formation to construct PAMAM dendrimers (**Scheme 2.3**). To do it, a building block of AB_2 type comprising a carboxylic acid terminal and two amine terminal moieties bridged via a tertiary amine function is require. Using the rationally designed building units, we were able to build up our dendrimers successfully up to generation 6 via simple amide bond formation. By employing solid support with lower loading capacity, we could further achieve the effective synthesis of high generation dendrimer G7. It is to note that the amide functions in our dendrimers compared to classic PAMAM dendrimers were inverted in direction, we therefore refer the so-obtained dendrimers to "inverse PAMAM dendrimers". Basically, the compositions of functionalities such as carboxylic acids, amides and amine terminals are similar to regular PAMAM dendrimers. Thus, we believe that these novel inverse PAMAM dendrimers can complement and enlarge the existing PAMAM dendrimer for the further applications. In this section, we will present our study and results related to the solid-phase synthesis of PAMAM dendrimers.
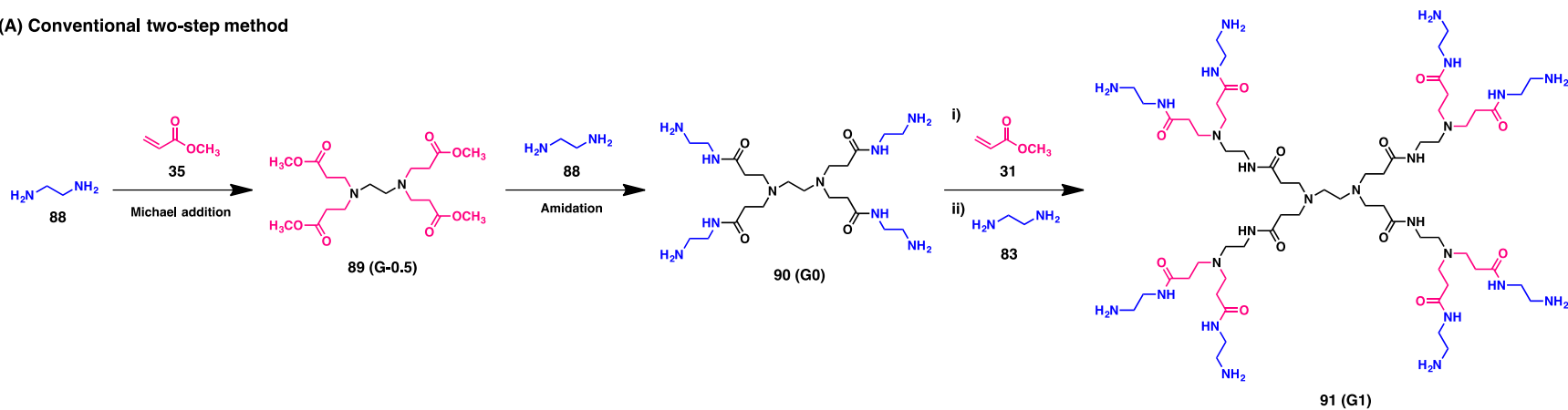
Scheme 2.3. Comparisons of PAMAM dendrimer synthesis using **(A)** conventional two-step protocol and **(B)** amide bond formation.

2. Molecular conception of inverse PAMAM dendrimers

As we mentioned in the Background part, we would like to develop a novel solid-phase synthesis strategy for PAMAM dendrimers. This strategy can be accomplished using AB_2 building units containing both carboxylic acid function and amine terminals for amide bond formation to construct the corresponding PAMAM dendrimers. We therefore devised two building units (**41**) and (**92**) (**Figure 2.2**), consisting of propylene and ethylene at the amine branching point respectively, for the construction of inverse PAMAM dendrimers (**Scheme 2.4**).
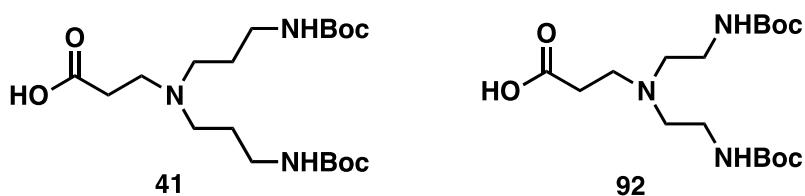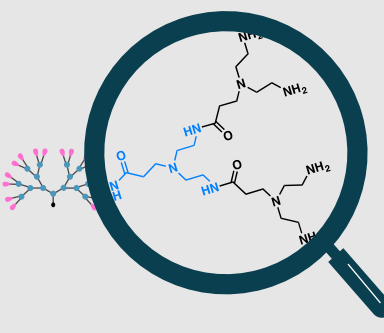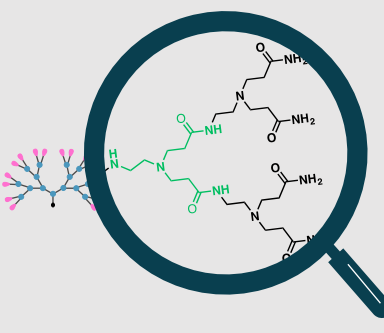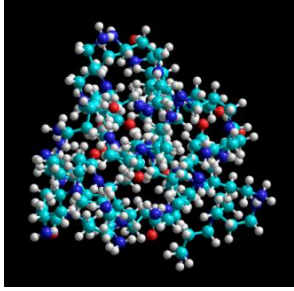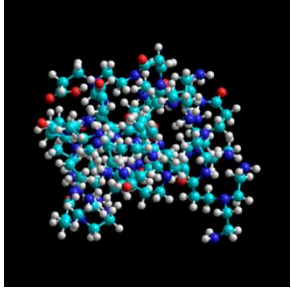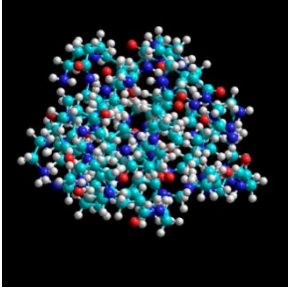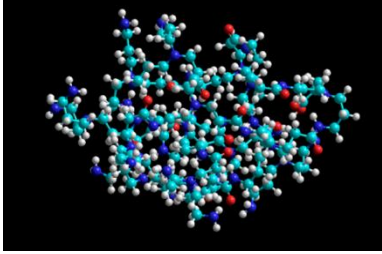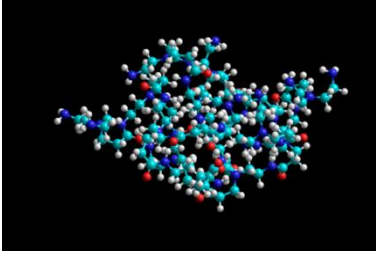

Figure 2.2. Two building blocks, **41** and **92**, consisting of propylene and ethylene at the amine branching point respectively.

Before we had embarked on the synthesis, we first carried out computer modeling to compare the dendrimers constructed from the repeating unit of **41** and **92** in regards to the classical PAMAM dendrimer in the aspects of dendrimer shape and size, solvent accessible surface area and distribution of the terminal groups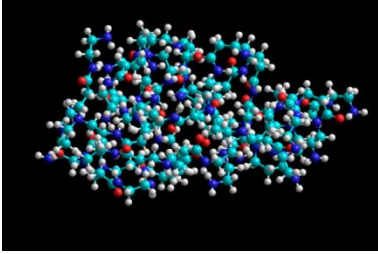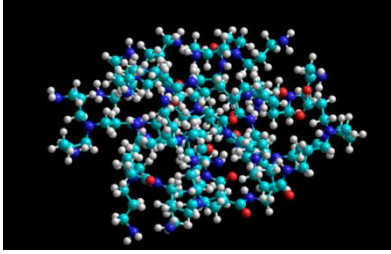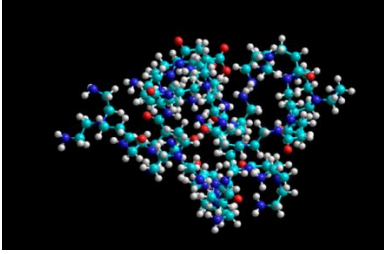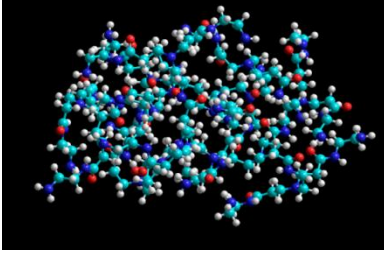 as a function of generation, because all these are important properties for biological applications, such as enzyme mimics, drug and drug delivery etc. In addition, the degree of surface congestion caused by the summation of the excluded volumes for the branching units might influence both the shape and the packing density of the surface.[15] We therefore carried out the simulation calculation to estimate the volume and surface area of G3 inverse PAMAM dendrimers [**A**] and [**B**] built respectively from the repeating unit of **41** and **92**, in comparison to a classical G3 PAMAM dendrimer [**C**]. As an example, **Table 2.1** shows the simulation results of their molecular structures viewed from three different axes. From these results, the inverse PAMAM dendrimer [**A**] resembles much more closely to the classic PAMAM dendrimers in molecular size and shape than the inverse PAMAM dendrimer [**B**], with [**B**] being

obviously smaller than [**C**] and deviated considerable in molecular shape from [**C**] as well. This was further confirmed by the data of their molecular volume and surface area obtained via simulation and listed in **Table 2.2**. Remarkably, inversed PAMAM dendrimer [**A**] possesses similar molecular volume and surface area as the classical PAMAM dendrimer [**C**]. Namely, the molecular volume and surface area of the inverse dendrimer [**A**] are 3421 $Å^3$ and 1859 $Å^2$, similar to those of a classical G3 PAMAM dendrimer [**C**], which are 3976 $Å^3$ and 2084 $Å^2$. In contrast, the inverse dendrimer [**B**] has the molecular volume of 2752 $Å^3$ and surface area of 1613 $Å^2$, which are considerably deviated from those of the classic dendrimer [**C**]. Consequently, we expect the properties such as solubility[22] and site isolation effect[23-25] in the dendrimers [**A**] to be similar to [**C**] owing to the comparable amounts of similar functional groups, including amide linkages, primary and tertiary amines within similar molecular volume and space. We therefore mainly focused our efforts on the synthesis of the dendrimers [**A**].

Table 2.1. Simulation calculation results of G3 PAMAM dendrimers with three branching units viewed along three molecular axes.

[A] **G3 Inverse PAMAM** **[Propylene moiety]**	[B] **G3 Inverse PAMAM** **[Ethylene moiety]**	[C] **G3 Classic PAMAM** **[Ethylene moiety]**

Table 2.2. Volume and surface area of G3 inverse PAMAM dendrimers [**A**], [**B**] and G3 classic PAMAM dendrimer [**C**] with different branching moieties.

|	[**A**]	[**B**]	[**C**]
Volume (Å^3)	3421	2752	3976
Surface area (Å^2)	1859	1613	2084
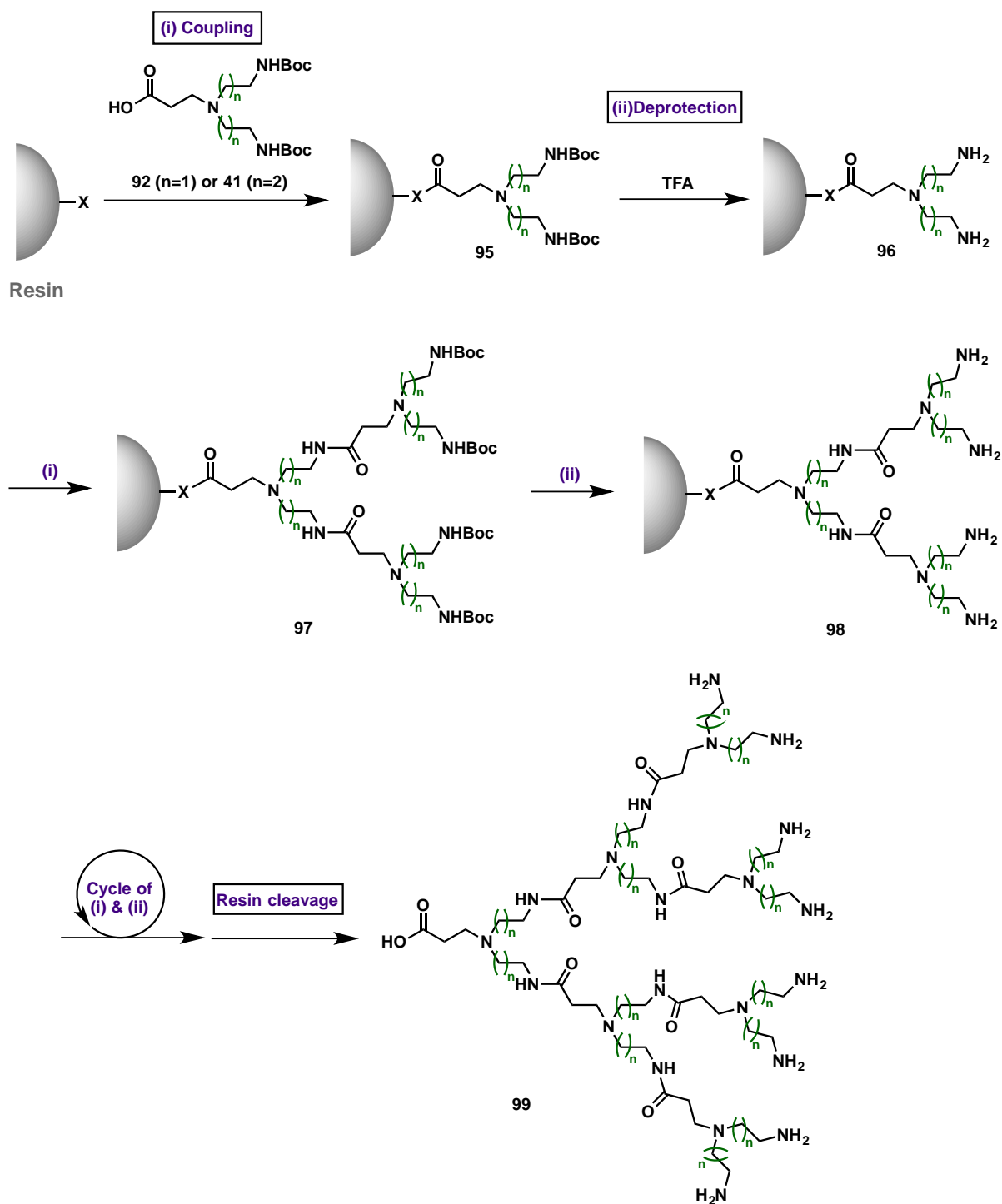
Scheme 2.4. Synthetic plan for solid-phase synthesis of inverse PAMAM dendrimers using designed AB$_2$ building blocks via amide bond formation.

3. Dendrimer synthesis

3.1. Preparation and optimization of the building blocks

For synthesizing the above designed inverse PAMAM dendrimers in solid-phase, we had need of the building units (**92**) and (**41**). We attempted to prepare **92** starting with the β-alanine (**100**) and the protected 2-chloroethylamine (**101**). Unfortunately, we could not get the desired compound **92**, probably because of self-cyclization of **101**. We then turned to prepare **41** by replacing **101** with **102**, which has a 1,3-propylenediamine moiety instead of ethylenediamine to minimize the self-cyclization (**Scheme 2.5**).[26] The desired product **41** was obtained yet in a low yield of 40%, probably owing to the further alkylation of **41** with **102** to generate quaternary ammonium, as tertiary amine is often more reactive with alkyl halide than primary and secondary amines.
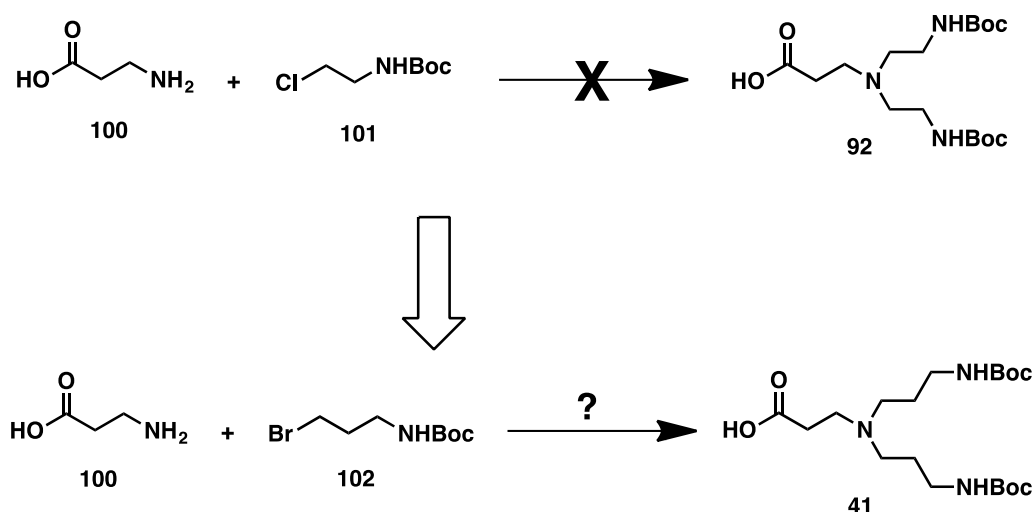
Scheme 2.5. Alternative synthetic plan of building block (**41**).

Since solid-phase synthesis employs a large excess of reagents to complete the reaction, we therefore need to develop an effective synthesis to prepare **41** in large quantity. Replacing the β-alanine (**100**) with the β-alanine methyl ester (**103**), we could successfully obtain the corresponding product **104** in 86% yield (**Scheme 2.6**). Further hydrolysis of **104** delivered the building unit **41** in high yield.
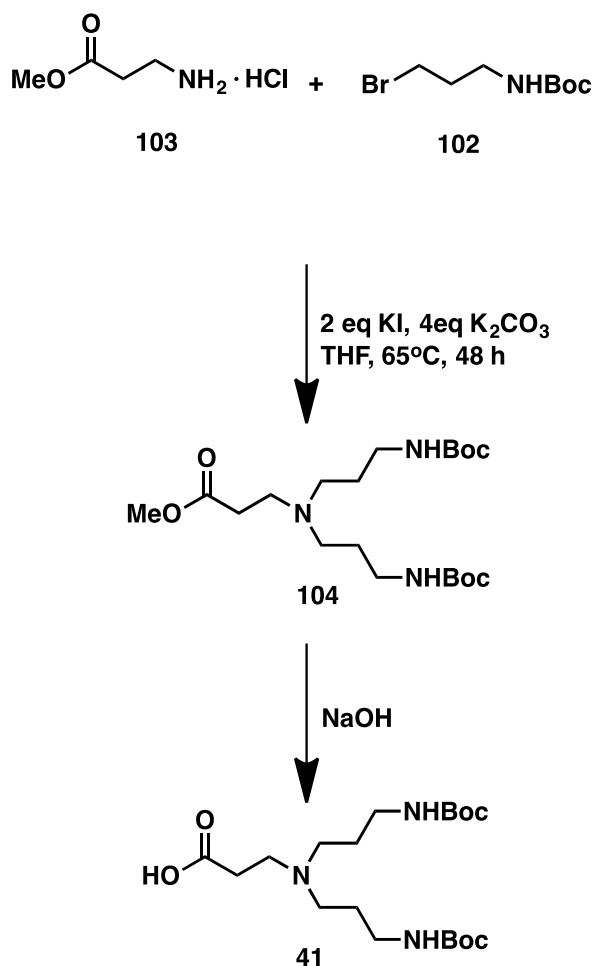
Scheme 2.6. Synthesis of building block (**41**).

We further optimized the synthesis of **104** using different solvents, bases, auxiliary agents, under different temperatures and with different reaction times (**Table 2.3**). Among the different bases used, *N,N*-diisopropylethylamine (DIPEA) and K_2CO_3 were superior to $CsCO_3$ and 1,8-diazabicyclo[5.4.0]undec-7-ene (DBU) for yielding the desired product. We selected K_2CO_3 because of readily removal of inorganic base from the organic reaction mixture. The reaction temperature was also important: raising the reaction temperature increased the yield. We therefore set the reaction temperature at the boiling point of tetrahydrofuran (THF), as THF is the best solvent identified for this reaction. Addition of KI further promoted this synthesis through halide exchange reaction (Finkelstein reaction). To summarize, the best conditions are found to be 2.0 eq of KI , 4.0 eq of K_2CO_3, in THF at 65°C (**Table 2.3**, entry *12*). Subsequent hydrolysis of **104** in

NaOH offered the desired building block **41** in 94% yield. As (**41**) containing both tertiary amine and carboxylic acid, it forms zwitterions.[27] We therefore collected (**41**) by extracting it from the aqueous layer of the reaction media. Using the above optimized synthesis and purification procedure, we could scale up the preparation of both **104** and **41**, yielding **41** in 20-gram scale and in pure form without compromising the high yield over 80% (**Scheme 2.6**). We also employed the similar protocol to prepare **92** but unfortunately it was not effective, probably also because of the self-cyclization of **101**.

Table 2.3. Optimizations for the preparation of building block (**104**).

Entry	Solvent	Base	Auxiliary agent	Temperature (°C)	Time (h)	Yield (%)
1	DCM	TEA	-	rt	20	6
2	DCM	DIPEA	-	rt	20	10
3	DCM	K_2CO_3	KI	rt	48	8
4	THF	TEA	-	rt	20	9
5	THF	DIPEA	-	rt	48	16
6	THF	DIPEA	KI	rt	20	25
7	THF	K_2CO_3	KI	rt	20	27
8	THF	$CsCO_3$	KI	65	20	10
9	THF	DIPEA	KI	65	36	43
10	THF	DBU	KI	65	48	10
11	THF	K_2CO_3	-	65	48	32
12	THF	K_2CO_3	KI	65	48	86
13	THF	DIPEA	KI	65	48	70
14	MeCN	K_2CO_3	KI	65	48	35
15	DMF	K_2CO_3	KI	80	60	22
16	THF	K_2CO_3	TBAI	65	48	57

3.2. Solid-phase synthesis of inverse PAMAM dendrimers

For our solid-phase synthesis, we opted for Kaiser oxime resin as the solid support because of its compatibility with the peptide synthesis strategy involving Boc chemistry. In addition, the final dendrimer cleavage from this resin can be easily accomplished under various basic and nucleophilic conditions. Nevertheless, the oxime ester linkage is susceptible to trifluoroacetic acid (TFA). Therefore, it is critical to employ an appropriate concentration of TFA for deprotection of the Boc groups of **41**. We tried different conditions for deprotecting the Boc groups. Indeed, effective deprotection of the terminal *N*-Boc groups in **41** could be achieved with 33% TFA in dichloromethane (DCM) after 1 h of reaction at room temperature.

To start the synthesis of inverse PAMAM dendrimers [**A**] (**Scheme 2.7**), **41** was first appended to Kaiser oxime resin using the benzotriazol-1-yl-oxytripyrrolidinophosphonium hexafluorophosphate (PyBOP) as the coupling agent, then acetic anhydride (Ac$_2$O) was used to cap the remaining oxime functionalities on the resin followed by deprotection of the Boc groups with 33% TFA in DCM.

For subsequent dendrimer synthesis, the amine-terminating resin (**42**) was further coupled with the building block (**41**) via amide bond formation with the aid of PyBOP and *N*-methylmorpholine (NMM), followed by deprotection of the terminal Boc groups in 33% TFA/DCM. Further dendrimer growth was achieved through the iterative coupling with **41** and subsequent deprotecition of the terminal Boc groups. All steps (except for the first coupling reaction with the oxime resin), including coupling reaction with **41**, capping reaction with Ac$_2$O as well as Boc deprotection in TFA, could be monitored using Kaiser ninhydrin test of the solid support.[28] Upon reaching the desired generation, the final product was cleaved from the solid support using NaOH in dioxane, yielding the dendrimers with a carboxylic acid tail at the focal point. (**Scheme 2.7**).
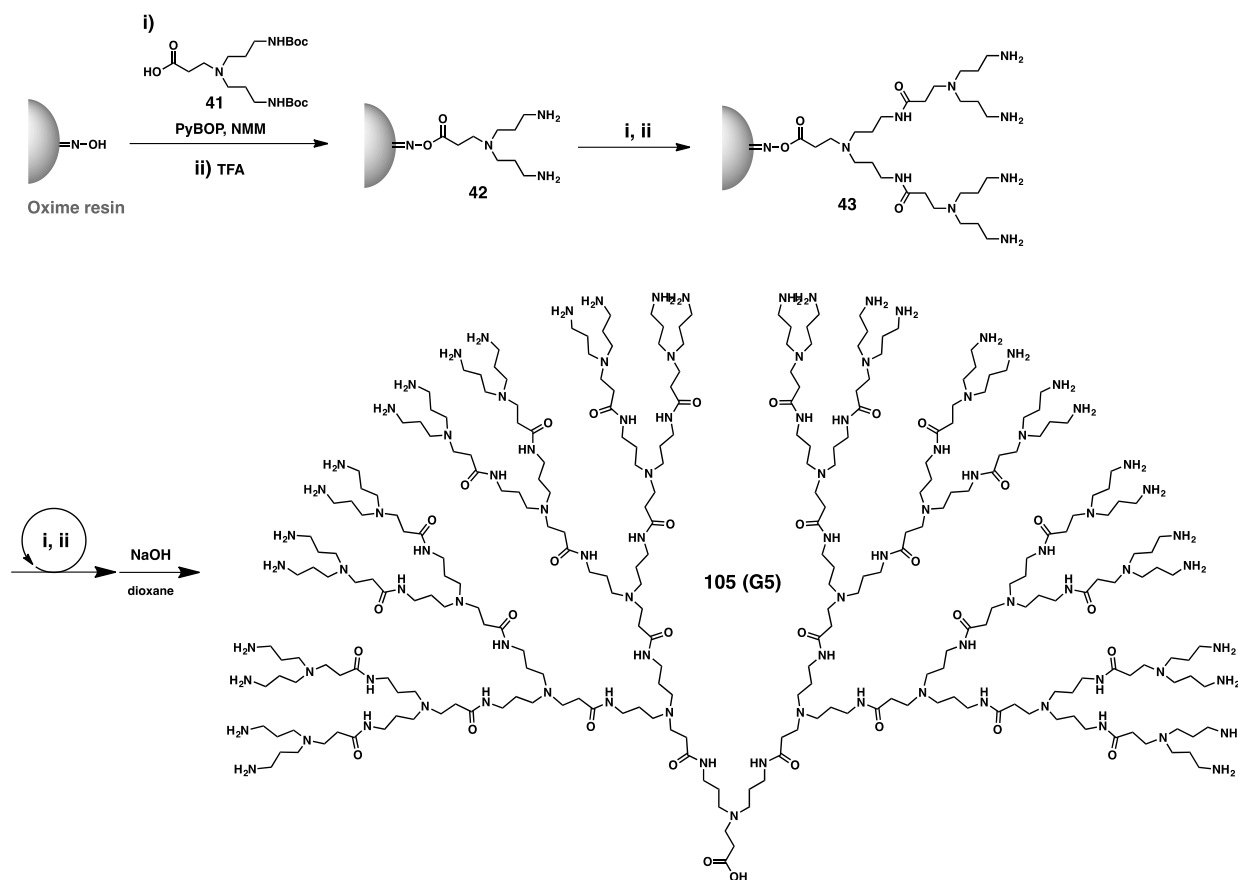
Scheme 2.7. Solid-phase synthesis of inverse PAMAM dendrimers using building block (**41**).

All the final dendrimers were collected using simple filtration without any additional purification process, and the yields for the G2 (**106**), G3 (**107**), G4 (**44**), G5 (**105**) and G6 (**108**) were 91%, 86%, 81%, 80% and 80%, respectively.[29] Also to mention, this reaction procedure was able to proceed not only manually but also with an automatic solid-phase peptide synthesizer to deliver the G2 (**106**), G3 (**107**), G4 (**44**), G5 (**105**) and G6 (**108**) inverse PAMAM dendrimers, with excellent yields of 93%, 89%, 84%, 86% and 82% respectively. All the synthesized dendrimers were characterized using NMR, MALDI-TOF-MS and GPC with the polydispersity index (PDI) falling between 1.07 and 1.18 (**Figure 2.3** and **Table 2.4**).
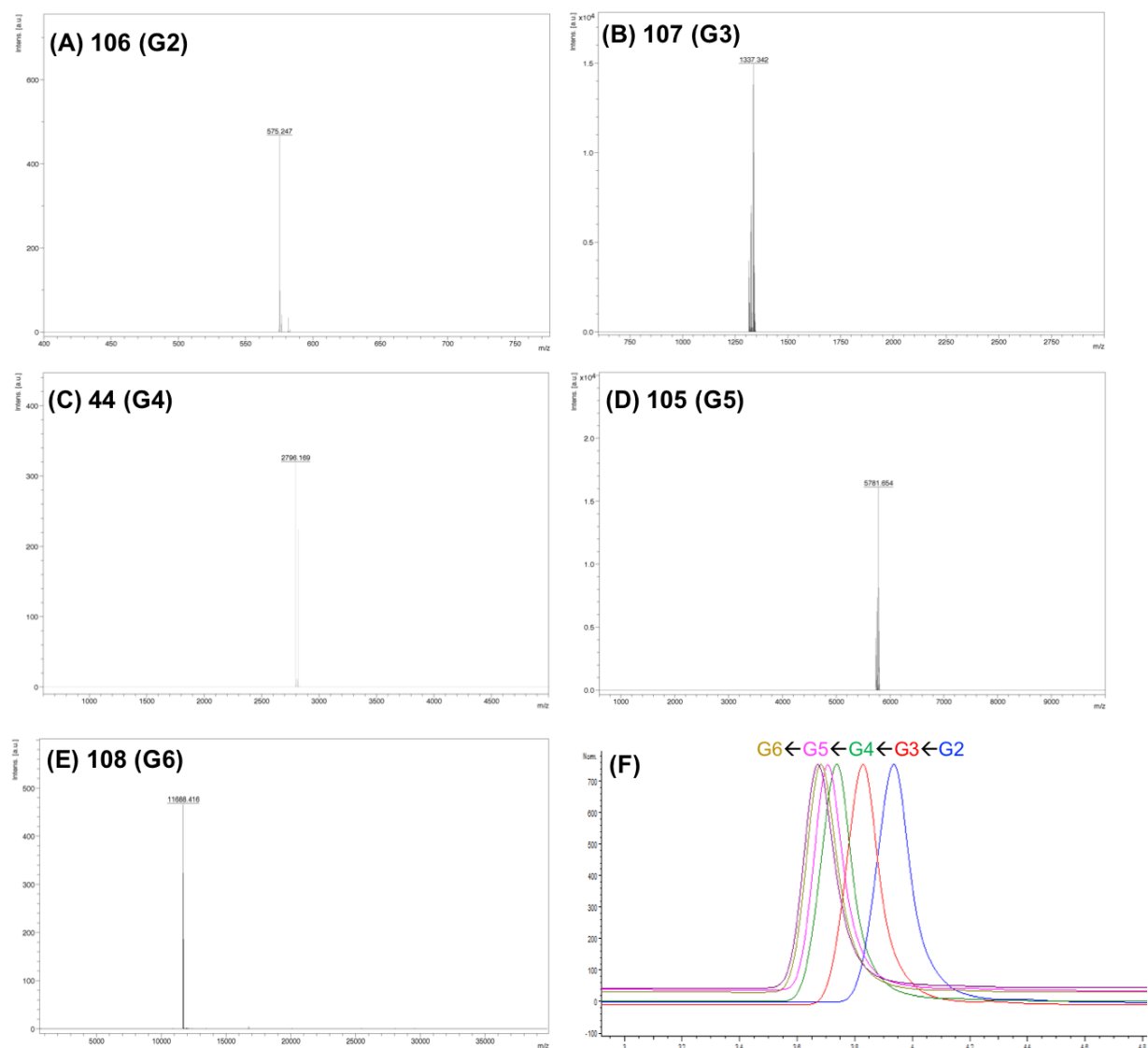
Figure 2.3. (A)-(E) MALDI-TOF-MS spectra; and **(F)** GPC traces of G2-G6 inverse PAMAM dendrimers.

Table 2.4. MALDI-TOF-MS results and PDI values of G2-G6 inverse PAMAM dendrimers.

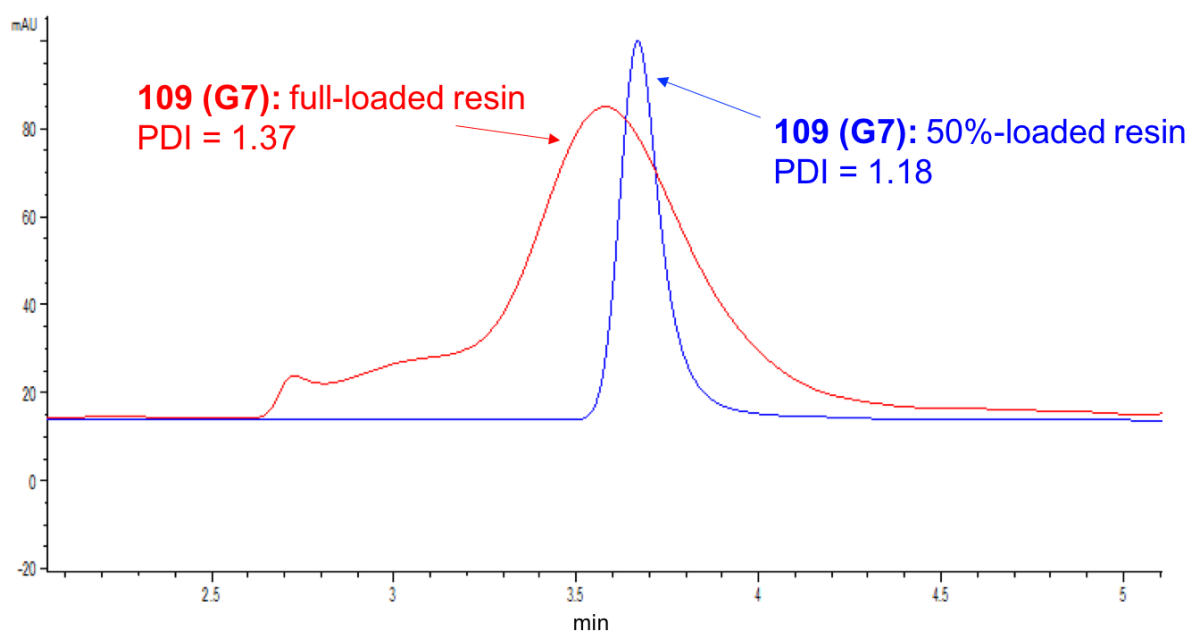| Inverse PAMAM dendrimer	MALDI-TOF-MS		PDI
	Calculated	*Observed*	
106 (G2)	574.5	575.2	1.07
107 (G3)	1315.1	1315.7	1.09
44 (G4)	2796.3	2796.2	1.10
105 (G5)	5782.7	5782.4	1.18
108 (G6)	11687.65	11688.42	1.17

3.3. High generation dendrimer synthesis

Although we successfully synthesized the inverse PAMAM dendrimers G2-G6 on solid support using peptide synthesis strategy, we failed to achieve the synthesis of the G7 inverse PAMAM dendrimer even if we prolonged the coupling reaction time and increased the excess equivalents of the building unit (**41**). The unsuccessful synthesis of the G7 inverse PAMAM dendrimer can be mainly ascribed to the steric hindrance between the neighboring molecules on the same resin and/or the interaction between neighboring branches within the same dendrimer, which generate site-site interaction or steric repulsion to impede further reactions for dendrimer growth (**Figure 2.4**). In addition, the sterically hindered dendrimer terminal branches often have tendency for back-folding, which may burry the terminal reactive functional groups within dendrimers and limit its access to react with building units. Consequently, considerably defective dendrimers will be generated due to the incomplete reactions, requiring hence tedious purification procedures, which are often of limited efficiency for high generation dendrimers.
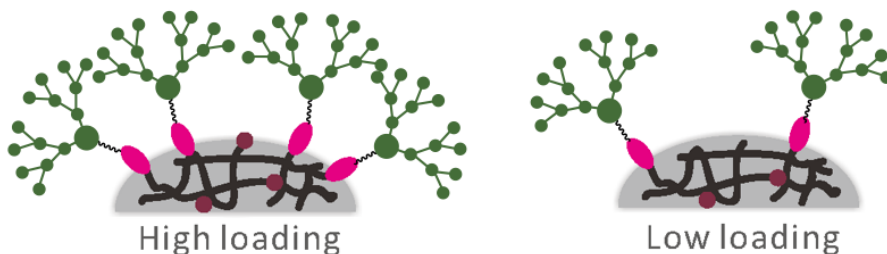
Figure 2.4. Resin with lower loading capacity is able to decrease steric congestion when synthesizing higher generation dendrimers.

In order to release the steric hindrance between the neighboring molecules within the same resin, it is necessary to enlarge the space/distance among the neighboring molecules, which can be achieved via reducing the resin loading. Resin loading capacity refers to the number of reactive sites on the resin. It strongly affects the preparation efficiency of high generation dendrimers in solid-phase synthesis. Decreasing resin loading means more space among reactive sites, thereby enlarging distance between two neighboring molecules and reducing site-site interaction or steric hindrance for high generation dendrimer synthesis. We therefore reduced the loading ratio to 50% of the resin capacity using Ac_2O to cap the oxime groups. Using the so-obtained resin with half loading capacity, we finally secured the G7 inverse PAMAM dendrimer (**109**) in 80% yield following the synthetic protocol which we developed for G2-G6. GPC analysis indicates that the PDI of the final product through reducing loading ratio fell to 1.18 compare to 1.37 of the product obtained using full-loaded resin (**Figure 2.5**). Further MS analysis showed unambiguously the effective synthesis of the G7 inverse PAMAM dendrimer with a clear-cut and clean molecular weight signal when using the half-loaded resin, whereas the G7 inverse PAMAM dendrimer obtained using full-loaded resin was associated with many impurities or defected dendrimers (**Figure 2.6**). Similarly, using the resin with 50% loading ratio, the G6 inverse PAMAM dendrimer was obtained in higher yield of 85% and narrower polydispersity as compare to the product obtained from full-loading resin. Presumably, the increasing steric hindrance among the high generation dendrimers within the same resin will interact and impact each other, hence greatly impeding the reaction with the following building blocks. Notably, reducing the loading ratio of the solid support constitutes an effective means to generate dendrimer products of highly purity (**Figure 2.5** and **Figure 2.6**).

Figure 2.5. GPC traces of the solid-phase synthesized G7 inverse PAMAM dendrimers (109) using full- and 50%-loaded resin.
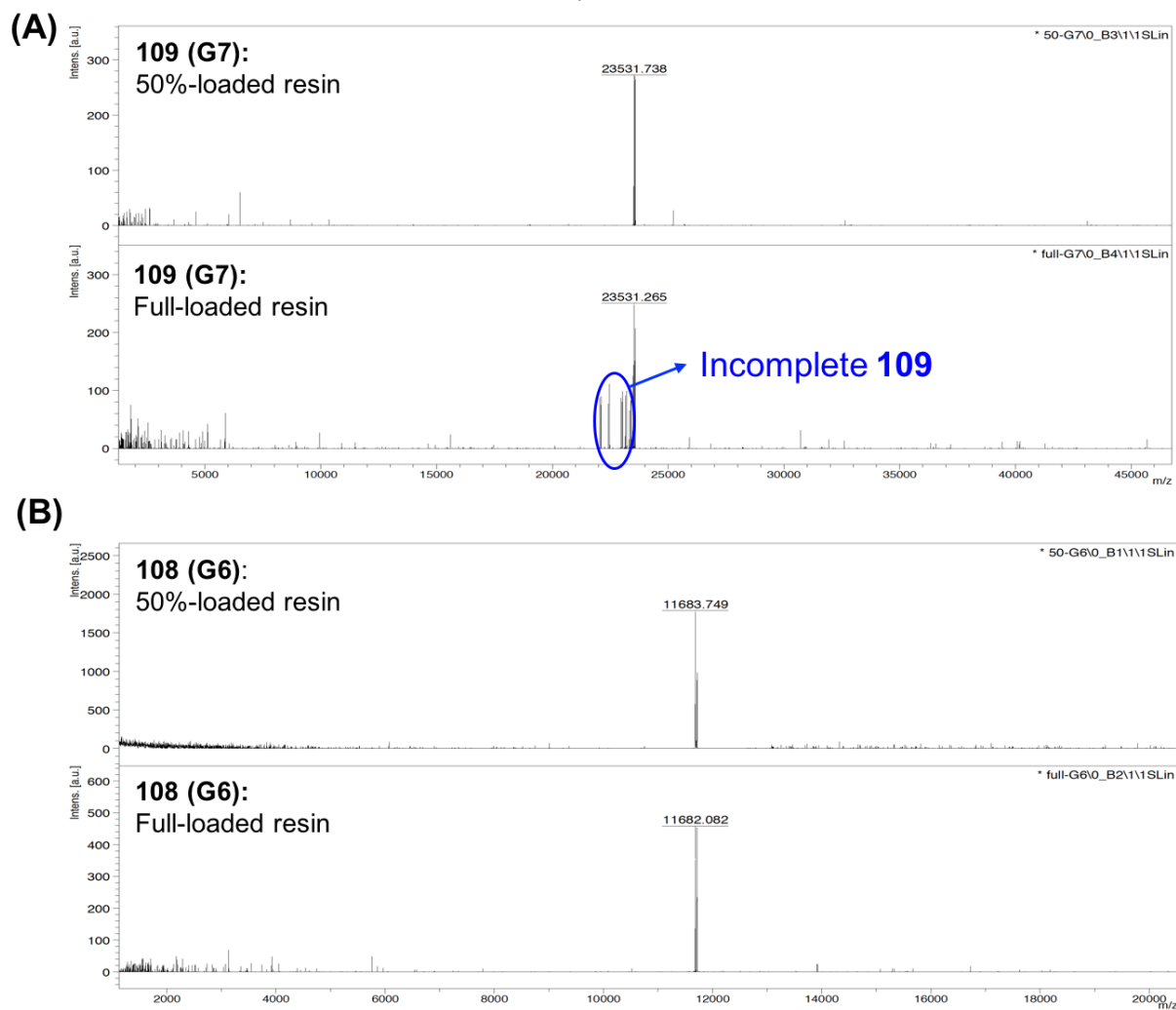
Figure 2.6. MALDI-TOF-MS traces of solid-phase synthesized **(A)** the G7 PAMAM dendrimer (**109**) and **(B)** the G6 PAMAM dendrimer (**108**) using full- and 50%-loaded resin.

4. Summary

In order to overcome the limitation associated with PAMAM dendrimer synthesis using traditional iterative steps of Michael addition and amidation, we established a novel and convenient approach for the solid-phase synthesis of inverse PAMAM dendrimers via amide bond formation using peptide solid-phase synthesis. In this approach, an AB_2 type building block (**41**) harboring both a carboxylic acid and amine functionalities along with the tertiary amine branching as focal points was designed and elaborated for dendrimer synthesis. The dendrimer synthesis starts first with the coupling of the building block (**41**) to Kaiser oxime resin, followed by iterative steps of deprotection using TFA and amide bond formation with **41**. By employing this methodology, inverse PAMAM dendrimers were obtained with high yields using either manual syntheses or a standard solid-phase peptide synthesizer. In addition, reducing the loading ratio of resin allowed effective synthesis of the high generation dendrimers of G6 and G7, suggesting that the steric hindrance among neighboring molecules on solid support may constitute the major obstacle in solid-phase synthesis of high generation dendrimers.

This synthetic approach is based on amide bond formation, the essential of peptide synthesis, hence precluding effectively the formation of side-products that are typically associated with the Michael addition and amidation in the conventional synthesis of PAMAM dendrimers. Also, this method can avoid the use of large excess of reagents and tedious isolation procedures. This solid-phase approach has set the stage as a concise manner to synthesize inverse PAMAM dendrimers, which may further expand the applications in biological and materials sciences.

5. Experimental Section

General

Kaiser oxime resin was obtained from Merck and AK Scientific Inc. The other chemicals, solvents, and reagents were obtained from Acros, Aldrich and TCI, and used without further purification. Mass spectra were acquired on either an Agilent ESI-MS-TOF and MALDI-MS-TOF (positive mode electrospray) mass spectrometer instruments as indicated. NMR spectra were obtained on a Varian 400MHz spectrometer. High-performance liquid chromatography (HPLC) and gel permeation chromatography (GPC) experiments were performed using an Agilent HPLC system (1100 series).

General MALDI-TOF-MS protocol

A dendrimer solution was prepared by dissolving 1 mg of each final product in 1 ml of MeOH. Additionally, a 1:10 dilution of this solution was made. The matrix solution was prepared by dissolving 10 mg of the matrix in 1 ml of MeOH. The analytical sample was prepared by mixing the dendrimer solution (0.5 μl) with the matrix solution (0.5 μl) on a stainless steel probe tip, and this mixture was allowed to dry at room temperature. MALDI-TOF MS system (model Autoflex III Smartbeam) equipped with a 355 nm Nd: YAG laser was purchased from Bruker Daltonics (Billerica, MA, USA). Mass spectra were acquired in positive ion reflector mode for the summing of 600 laser shots and data were processed by FlexAnalysis software (Bruker Daltonics).

Preparation of building block (41)

Synthesis of 103
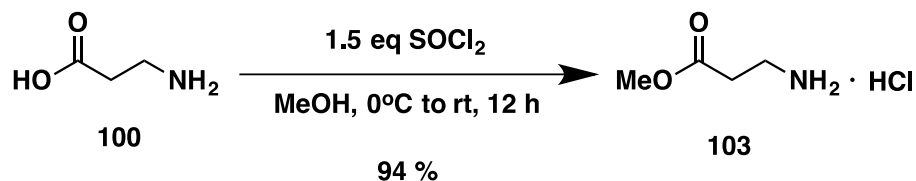
To a solution of β-alanine (**100**) (2.02 g, 22.45 mmol) in methanol (MeOH), was added thionyl chloride (SOCl$_2$) (2.50 mL, 34.04 mmol, 1.5 eq) slowly and the reaction mixture was stirred at 0 °C to rt under N$_2$ for 12 h. The solvent was then evaporated under reduced pressure. The crude product was purified by precipitation with DCM/ether at 4 °C three times. The precipitate was collected, washed with ether and dried under high vacuum, giving the corresponding final product **103** as a white solid (2.95 g, 94 %). ^{1}H NMR (400 MHz, D$_2$O) δ 2.71 (t, J = 8.0 Hz, 2H), 3.19 (t, J = 8.0 Hz, 2H), 3.65 (s, 3H); ^{13}C NMR (100 MHz, D$_2$O) δ 31.10, 35.13, 52.67, 173.21; HRMS (FAB): calcd for C$_4$H$_9$NO$_2$ [M]$^+$ 103.0633; found at m/z 103.0630.

Synthesis of 102
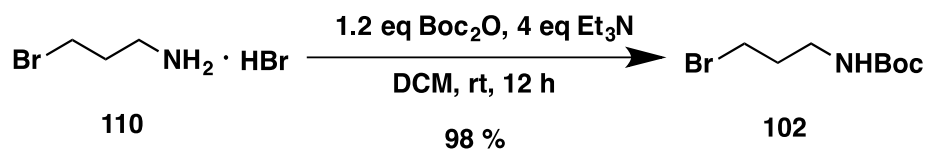
To a solution of **110** (2.05 g, 9.36 mmol) in DCM under N$_2$, was added triethylamine (TEA) (5.2 mL, 37.45 mmol, 4.0 eq). The reaction mixture was stirred at rt for 30 min until the starting material **110** dissolved completely. To the resulting solution was added di-*tert*-butyl-dicarbonate (Boc$_2$O) (2.58 mL, 11.24 mmol, 1.2 eq) and the reaction mixture was stirred at rt under N$_2$ for 12 h. Then the solvent was evaporated under reduced pressure. The obtained residue was dissolved in EA (15.0 mL) and washed with H$_2$O (10.0 mL) for three times. The organic layer was dried with

MgSO$_4$, filtered and concentrated. The crude product was purified by column chromatography on silica gel with EA/hexane = 1/3 (R$_f$ = 0.5), giving the corresponding final product **102** as a colorless oil (2.13 g, 98%). ^{1}H NMR (400 MHz, CDCl$_3$) δ 1.43 (s, 9H), 2.04 (tt, J = 8.0, 4.0 Hz, 2H), 3.26 (br, 2H), 3.43 (t, J = 8.0 Hz, 2H), 4.67 (br, 1H); ^{13}H NMR (100 MHz, CDCl$_3$) δ 27.24, 28.29, 30.76, 32.77, 38.88, 156.03; HRMS (FAB): calcd for C$_8$H$_{16}$BrNO$_2$ [M]$^+$ 237.0364; found at m/z 237.0360.

Synthesis of 41
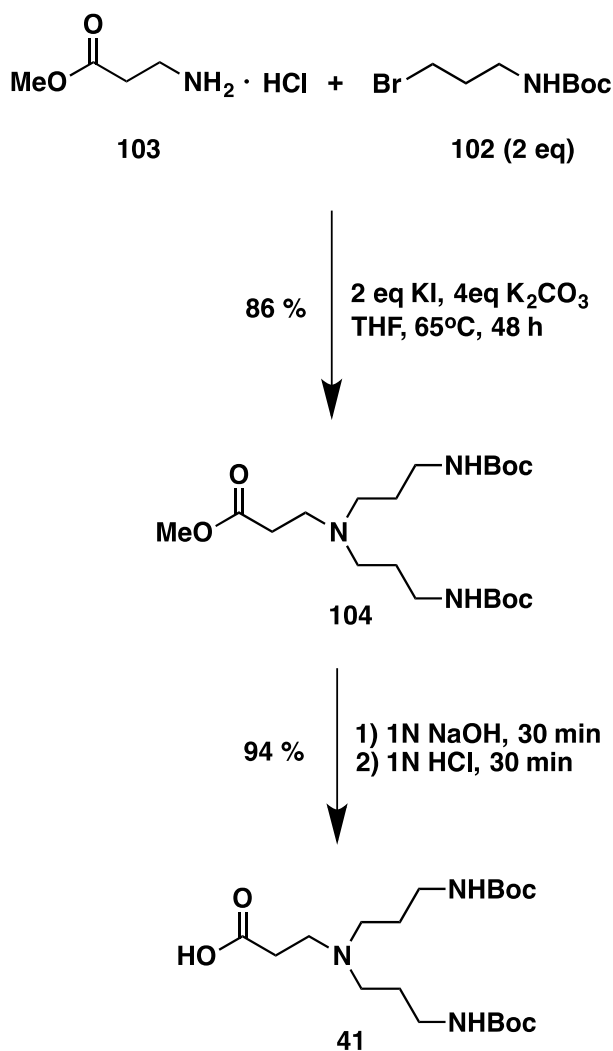
To the solution of **103** (4.01 g, 16.92 mmol) in THF was added KI (2.80 g, 16.86 mmol, 1 eq). The reaction mixture was stirred at rt under N_2 for 30 min, then heating to 65°C. To the resulting solution was added compound **102** (1.21 g, 8.61 mmol, 0.5 eq) and K_2CO_3 (4.68 g, 33.86 mmol, 2 eq). The reaction mixture was stirred at 65 °C under N_2 for 48 h. Then the resulting solution with precipitate was filtered and the filtrate was concentrated under reduced pressure. The obtained residue was partitioned between DCM and H_2O. The organic layer was dried with $MgSO_4$, filtrated and concentrated. The crude product was purified by column chromatography on silica gel with EA/hexane = 3/1, DCM/MeOH = 20/1 (R_f = 0.3; DCM/MeOH = 20/1), giving the corresponding final product **104** as a brownish oil (2.54 g, 86%). ^{1}H NMR (400 MHz, CDCl$_3$) δ 1.42 (s, 18H), 1.64 (m, 4H), 2.47 (m, 6H), 2.75 (m, 2H), 3.14 (m, 4H), 3.67 (s, 3H), 5.16 (br, 2H); ^{13}C NMR (100 MHz, CDCl$_3$) δ 26.74, 28.21, 32.05, 38.76, 49.17, 51.31, 51.39, 78.51, 155.86, 172.88. HRMS (FAB): calcd for $C_{20}H_{39}N_3O_6$ $[M]^+$ 417.2839; found at *m/z* 417.2840.

Hydrolysis of 104 to obtain 41

To the solution of **104** (2.54. g, 6.09 mmol) in EtOH (R_f = 0.3; DCM/MeOH = 20/1) was added 1 N NaOH$_{(aq)}$ until the pH equal to 12. After being stirred at rt for 30 min, the resulting solution was added with 1N HCl$_{(aq)}$ until the pH of solution equal to 3 and stirred at rt for additional 30 min. (R_f = 0.1; DCM/MeOH = 10/1) The resulting solution was concentrated under reduced pressure to remove EtOH. The resulting solution was partitioned between DCM and H_2O. The aqueous layer was concentrated in vacuum to give yellowish oil with white solid. The mixture was dissolved in EtOH and stand for 30 min. After filtration to remove the residues, the filtrate was concentrated under reduced pressure and dried under high vacuum, giving the corresponding final product **41** as a yellowish solid (2.31 g, 94%). ^{1}H NMR (400 MHz, DMSO) δ 1.37 (s, 18H), 1.61 (tt, *J* = 8.0, 4.0 Hz, 4H), 2.50 (m, 2H) 2.65 (t, *J* = 8.0 Hz, 4H), 2.87-2.96 (m, 6H), 6.86 (br, 2H); ^{13}C NMR (100 MHz, DMSO) δ 25.23, 28.26, 30.00, 37.70, 48.43, 50.08, 77.55, 155.61, 172.82; HRMS (FAB): calcd for $C_{19}H_{37}N_3O_6$ $[M]^+$ 403.2682; found at *m/z* 403.2682.

General procedure of solid-phase synthesis

The suspension of Kaiser oxime resin (0.22 g, 0.2 mmol) in RV bottle was added DMF/DCM (10/1, v/v) under N_2 and bubbled with N_2 overnight. After removal of DMF, the following resin in RV bottle was added the solution of **41** (2 eq) in DMF, PyBOP (2 eq) and 0.4 M *N*-methylmorpholine (NMM). The following mixture was bubbled with N_2 for 8 h (for the first introduction of **41**) or 4 h (for rest of introduction of **41**). After reaction, the solvent was removed and the resulting mixture was washed with DMF three times. As the dendrimer generation increased, the amount of reagents used was doubled. To the resulting solution was added acetic anhydride in DMF (100μL, 10% v/v solution). After washed with DMF three times, the reaction mixture was added was trifluoroacetic acid (TFA) in DCM (30 %, 10 mL) for deprotection. After 1 h of reaction, the solution was removed and the mixture was washed with DCM and DMF three times.

General procedure of 50% loading capacity for G6 and G7 inverse PAMAM dendrimers (108 and 109)

The suspension of oxime resin (0.22 g, 0.2 mmol) in RV bottle was added 5 mL of DMF/DCM (10/1, v/v) under N_2 and bubbled with N_2 overnight. After removal of DMF, the following resin in RV bottle was added the solution of **41** (0.5 eq), PyBOP (0.5 eq) and 0.4 M *N*-methylmorpholine (NMM) in DMF. The following mixture was bubbled with N_2 for 8 h. After reaction, the solvent was removed and the resulting mixture was washed with DMF three times. To the resulting solution was added acetic anhydride in DMF (100μL, 10% v/v solution). Then the later dendrimer growth was following the general procedure of SPDS.

Cleavage from Resin

The reaction mixture was added 1N NaOH/dioxane = 1/3 (v/v, 20 mL/mmol) and shaked from 0 °C to rt for 30 min. After filtration, the filtrate was neutralized with 0.5 N HCl to pH 7 from 0 °C to rt. The following solid was washed with MeOH and DCM to give desire product.

(G:2)-*dendri*-inversePAMAM-(NH₂)₄ (G2, 106)
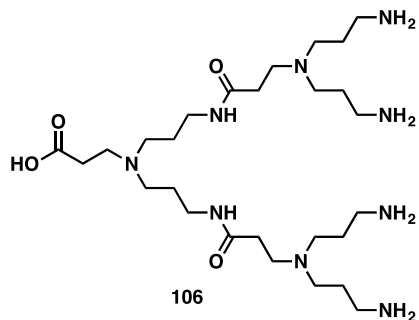
93 %. ^{1}H NMR (400 MHz, CD$_3$OD) δ 1.84 (m, 12H), 2.56 (m, 6H), 3.00 (m, 12H), 3.07 (t, J = 6.6 Hz, 6H), 3.16 (t, J = 6.4 Hz, 12H); MS (MALDI-TOF, matrix: 2,5-dihydroxybenzoic acid (DHB)/fucose = 10/1) calcd for C$_{28}$H$_{60}$N$_9$O$_4$ [M+H]$^+$ 574.5; found at m/z 575.2. PDI = 1.07.

(G:3)-*dendri*-inversePAMAM-(NH₂)₈ (G3, 107)
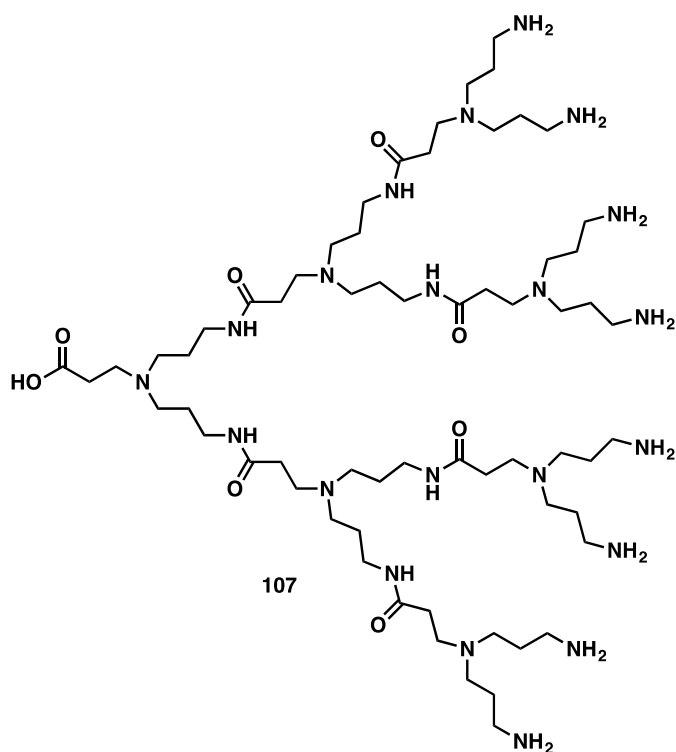
89 %. ¹H NMR (400 MHz, CD₃OD) δ 1.84 (dt, J = 13.6, 6.7 Hz, 28H), 2.62 (m, 14H), 3.00 (dd, J = 9.8, 5.2 Hz, 28H), 3.09 (t, J = 6.6 Hz, 14H), 3.16 (t, J = 6.5 Hz, 28H); MS (MALDI-TOF, matrix: DHB/fucose=10/1) calcd for $C_{64}H_{135}N_{21}O_8$ [M+H]⁺ 1315.1; found at *m/z* 1315.7. PDI = 1.09.

(G:4)-*dendri*-inversePAMAM-(NH₂)₁₆ (G4, 44)
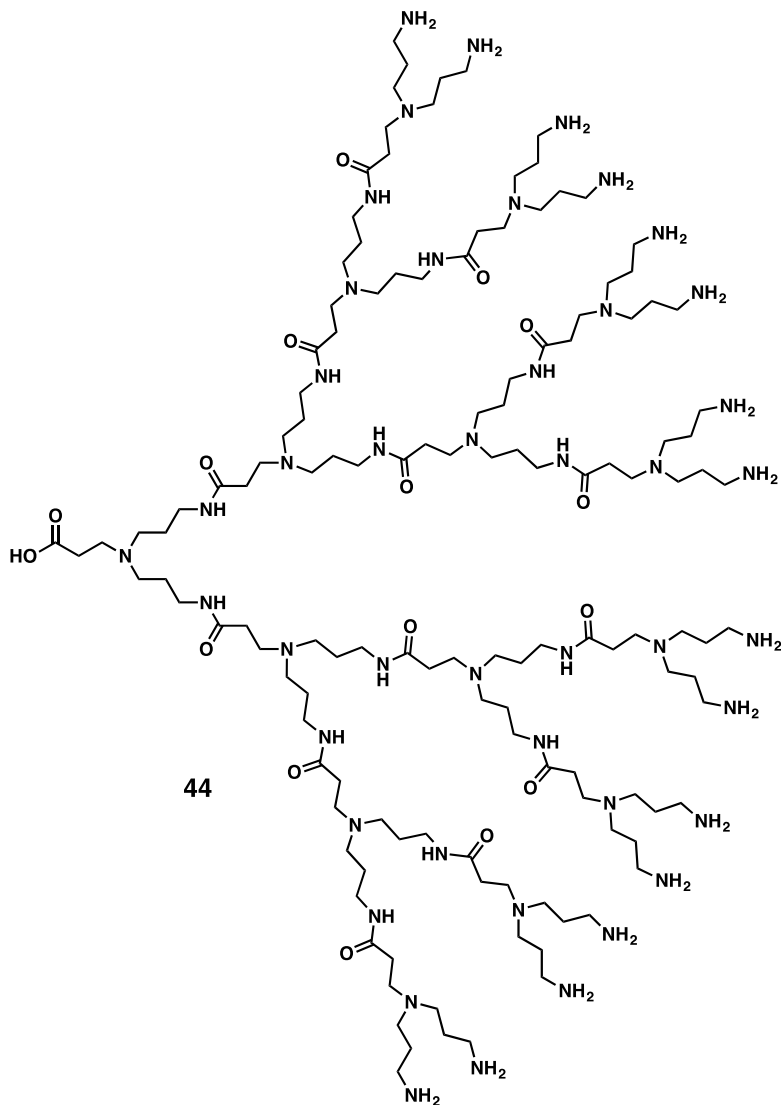
84 %. ^{1}H NMR (400 MHz, CD₃OD) δ 1.91 (m, 60H), 2.57 (m, 60H), 3.15 (m, 62H), 3.59 (m, 28H), 3.70 (m, 30H); MS (MALDI-TOF, matrix: DHB/fucose = 10/1) calcd for C₁₃₆H₂₈₉N₄₅O₁₆ [M+H]$^+$ 2796.3; found at *m/z* 2796.2. PDI = 1.10.

(G:5)-*dendri*-inversePAMAM-(NH$_2$)$_{32}$ (G5, 105)
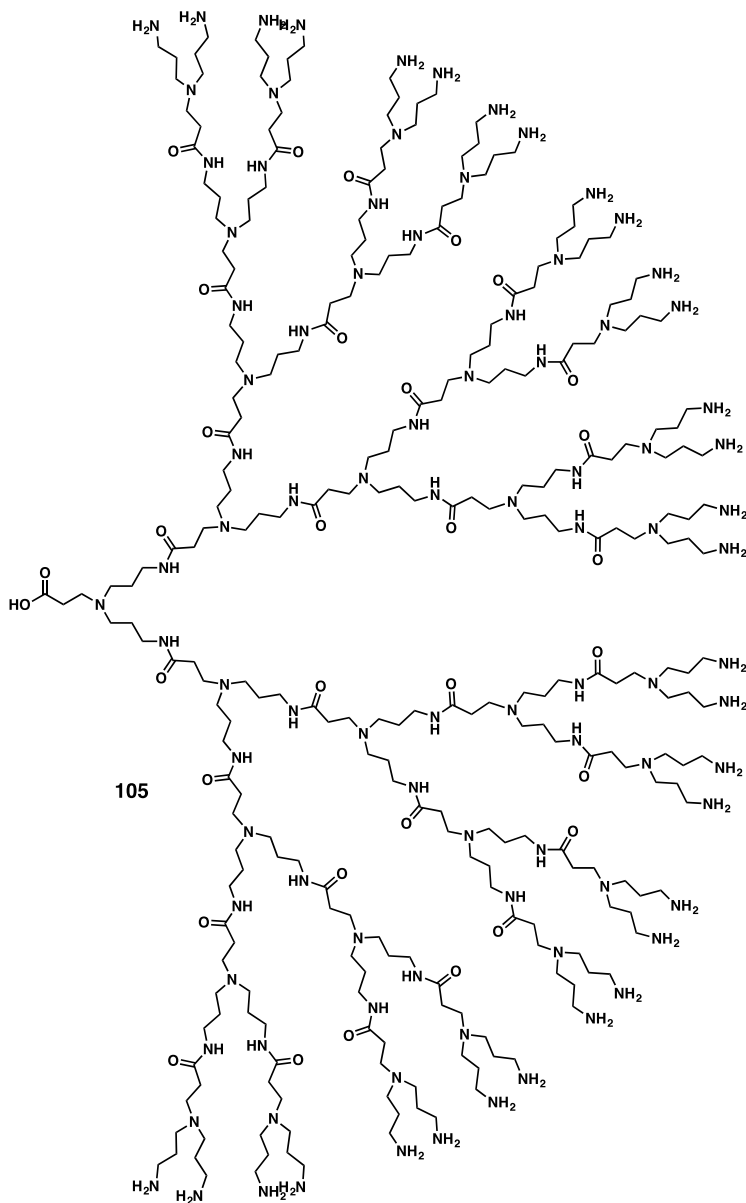
86 %. ^{1}H NMR (400 MHz, CD$_3$OD) δ 1.91 (m, 124H), 2.64 (m, 124H), 3.17 (m, 126H), 3.59 (m, 60H), 3.70 (m, 60H); MS (MALDI-TOF, matrix: DHB/fucose = 10/1) calcd for C$_{279}$H$_{590}$N$_{93}$O$_{32}$Na [M+Na]$^+$ 5782.7; found at *m/z* 5782.4. PDI = 1.18.

(G:6)-*dendri*-inversePAMAM-(NH$_2$)$_{64}$ (G6, 108)

108
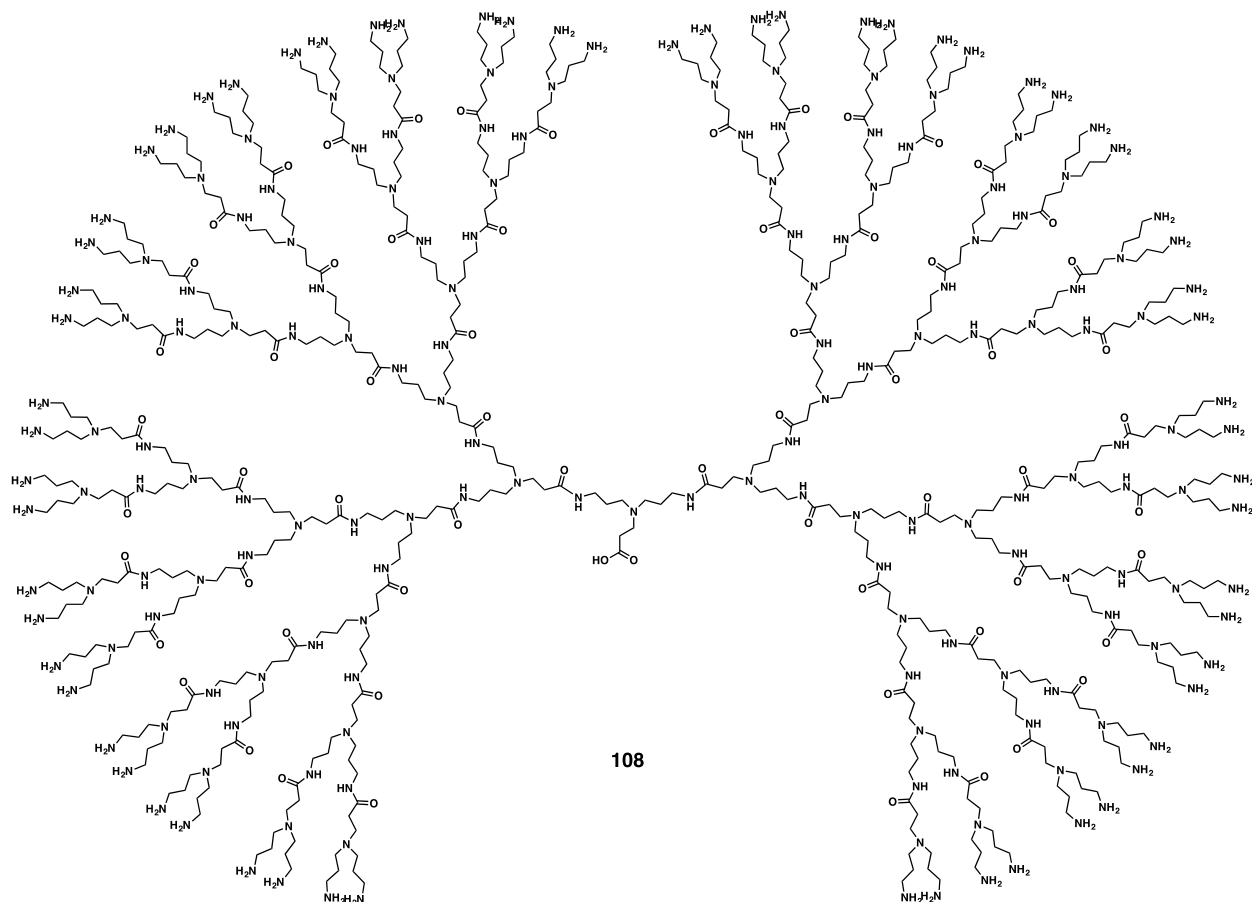
85 %. ^{1}H NMR (400 MHz, CD$_3$OD) δ 1.73-1.91(m, 22H), 2.29-2.40 (br, 230H), 2.54 (t, *J* = 8.0 Hz, 24H), 2.60 (br, 106H), 2.69 (t, *J* = 8.0 Hz, 20H), 2.81 (br, 228H), 2.90-3.14 (m, 154H), 3.27 (br, 98H), 3.35-3.50 (m, 126H); MS (MALDI-TOF, matrix: DHB/fucose = 10/1) cacld. for C$_{567}$H$_{1200}$N$_{189}$O$_{64}$ [M+H]$^{+}$ 11688.6; found at *m/z* 11691.8. PDI = 1.17.

(G:7)-*dendri*-inversePAMAM-(NH$_2$)$_{128}$ (G7, 109)

109
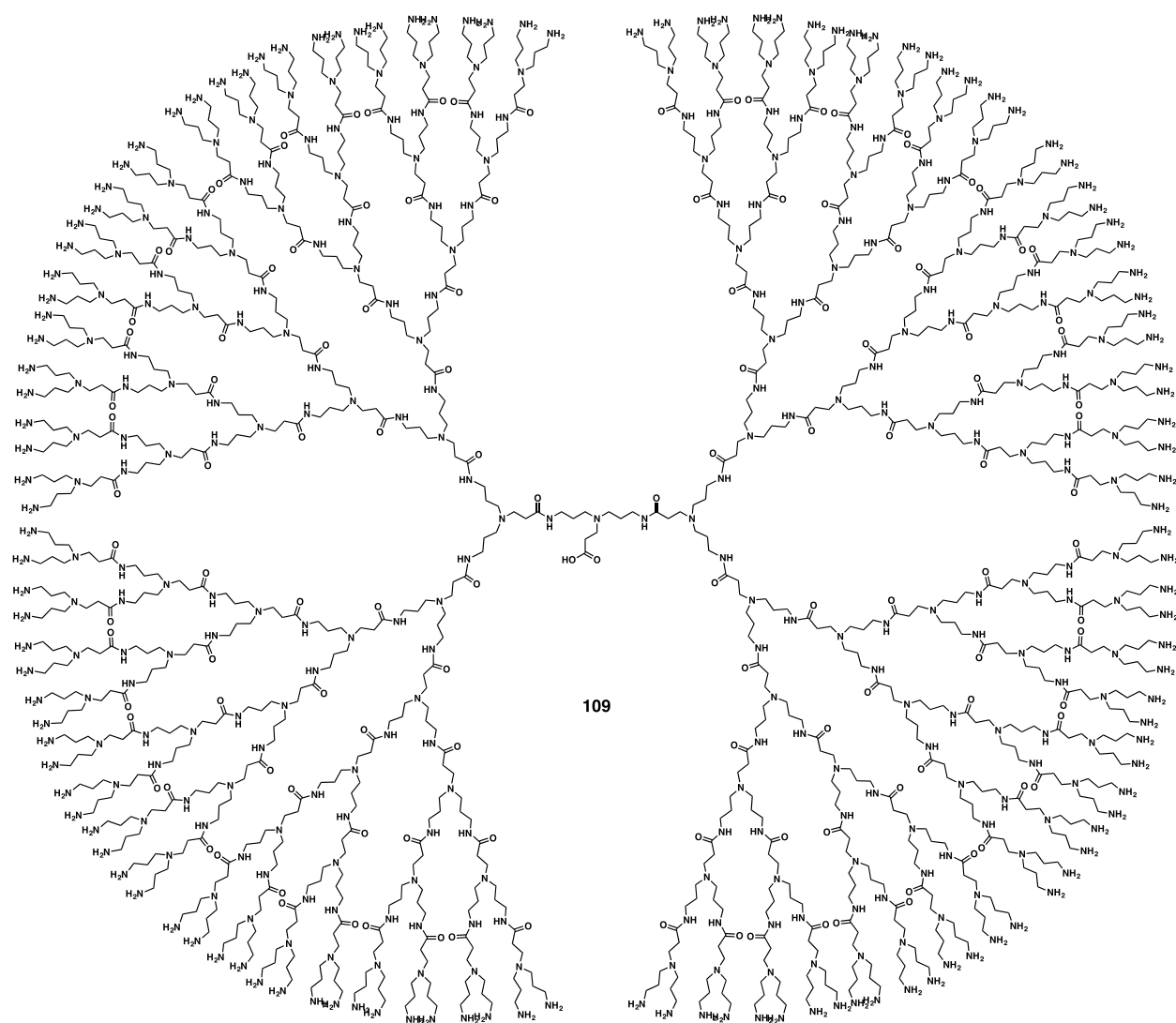
80 %. ^{1}H NMR (400 MHz, CD$_3$OD) δ 1.81 (tt, J = 6.0, 6.4 Hz, 42H), 2.15-2.22 (m, 120H), 2.32 (t, J = 6.4 Hz, 24H), 2.43 (br, 346H), 2.55 (t, J = 6.4 Hz, 72H), 2.62 (br, 208H), 2.69 (t, J = 6.4 Hz, 46H), 2.82 (br, 412H), 2.97-3.08 (m, 310H), 3.29 (br, 136H), 3.45 (br, 148H), 3.54 (t, J = 5.2 Hz, 106H); MS (MALDI-TOF, matrix: DHB/fucose = 10/1) cacld. for C$_{1143}$H$_{2415}$N$_{381}$O$_{128}$ [M]$^+$ 23532.4; found at *m/z* 23526.3. PDI = 1.18.

Gel permeation chromatography (GPC)

For analytic GPC of the dendrimers, a TSK-GEL G2000SW column (7.5x300 mm) was used with 90% MeOH and 10% water with 0.1% TFA (flow rate= 0.4 mL/min). UV detection was performed at 220 nm. These experiments were conducted at 25°C at a flow rate of 1.5 mL/min with PB buffer (10mM, pH 5.0) as eluent and detected at 220 nm. Polysaccharide standards with molecular weight range from 590 to 200,000 were used for dendrimer calibration. The GPC traces of inverse PAMAM dendrimers were followed with the figures that **106** (**G2**) (3.935 min; PDI= 1.07), **107** (**G3**) (3.828 min; PDI= 1.09), **44** (**G4**) (3.737 min; PDI= 1.10), **105** (**G5**) (3.706 min; PDI= 1.18), **108** (**G6**) (3.682 min; PDI= 1.17) and **109** (**G7**) (3.672 min; PDI= 1.18) are discovered.

General	PDI
106 (G2)	1.07
107 (G3)	1.09
44 (G4)	1.10
105 (G5)	1.18
108 (G6)	1.17
109 (G7)	1.18
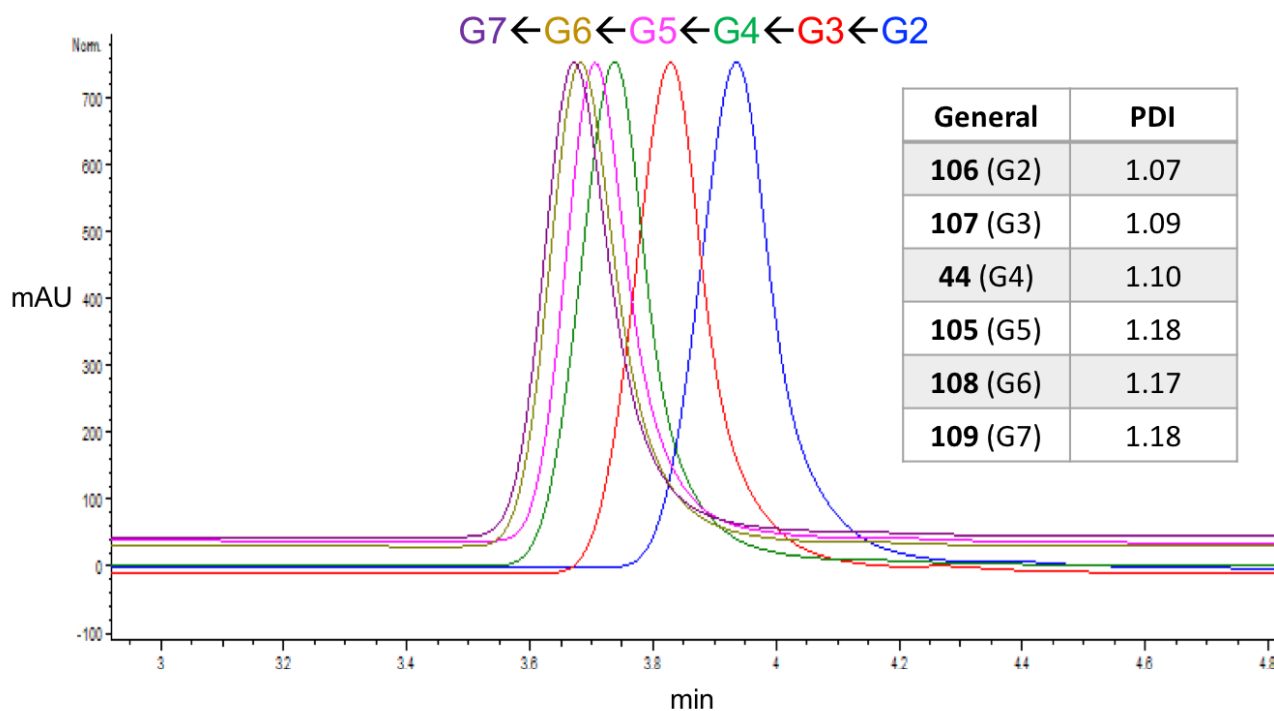
6. References

[1] D. A. Tomalia; H. Baker; J. Dewald; M. Hall; G. Kallos; S. Martin; J. Roeck; J. Ryder; P. Smith. A new class of polymers: Starburst-dendritic macromolecules. *Polym. J.*, **1985**, *17*, 117-132.

[2] R. Esfand; D. A. Tomalia. Poly(amidoamine) (PAMAM) dendrimers: From biomimicry to drug delivery and biomedical applications. *Drug Discovery Today*, **2001**, *6*, 427-436.

[3] B. K. Nanjwade; H. M. Bechra; G. K. Derkar; F. V. Manvi; V. K. Nanjwade. Dendrimers: Emerging polymers for drug-delivery systems. *Eur. J. Pharm. Sci.*, **2009**, *38*, 185-196.

[4] I. J. Majoros; A. Myc; T. Thomas; C. B. Mehta; J. R. Baker. PAMAM dendrimer-based multifunctional conjugate for cancer therapy: Synthesis, characterization, and functionality. *Biomacromolecules*, **2006**, *7*, 572-579.

[5] X. Shi; S. H. Wang; M. Shen; M. E. Antwerp; X. Chen; C. Li; E. J. Petersen; Q. Huang; W. J. Weber; J. R. Baker. Multifunctional dendrimer-modified multiwalled carbon nanotubes: Synthesis, characterization, and in vitro cancer cell targeting and imaging. *Biomacromolecules*, **2009**, *10*, 1744-1750.

[6] A. Nourse; D. B. Millar; A. P. Minton. Physicochemical characterization of generation 5 polyamidoamine dendrimers. *Biopolymers*, **2000**, *53*, 316-328.

[7] B. Huang; J. F. Kukowska-Latallo; S. Tang; H. Zong; K. B. Johnson; A. Desai; C. L. Gordon; P. R. Leroueil; J. R. Baker Jr. The facile synthesis of multifunctional PAMAM dendrimer conjugates through copper-free click chemistry. *Biorg. Med. Chem. Lett.*, **2012**, *22*, 3152-3156.

[8] Y. Kim; A. M. Klutz; K. A. Jacobson. Systematic investigation of polyamidoamine dendrimers surface-modified with poly(ethylene glycol) for drug delivery applications: Synthesis, characterization, and evaluation of cytotoxicity. *Bioconj. Chem.*, **2008**, *19*, 1660-1672.

[9] Y. Wang; R. Guo; X. Cao; M. Shen; X. Shi. Encapsulation of 2-methoxyestradiol within multifunctional poly(amidoamine) dendrimers for targeted cancer therapy. *Biomaterials*, **2011**, *32*, 3322-3329.

[10] Y. Wang; X. Cao; R. Guo; M. Shen; M. Zhang; M. Zhu; X. Shi. Targeted delivery of doxorubicin into cancer cells using a folic acid-dendrimer conjugate. *Polym. Chem.*, **2011**, *2*, 1754-1760.

[11] Y. Tang; Y.-B. Li; B. Wang; R.-Y. Lin; M. van Dongen; D. M. Zurcher; X.-Y. Gu; M. M. Banaszak Holl; G. Liu; R. Qi. Efficient in vitro siRNA delivery and intramuscular gene silencing using PEG-modified PAMAM dendrimers. *Mol. Pharm.*, **2012**, *9*, 1812-1821.

[12] M. M. Ali; M. Woods; P. Caravan; A. C. L. Opina; M. Spiller; J. C. Fettinger; A. D. Sherry. Synthesis and relaxometric studies of a dendrimer-based pH-responsive MRI contrast agent. *Chem. Eur. J.*, **2008**, *14*, 7250-7258.

[13] C. Peng; L. Zheng; Q. Chen; M. Shen; R. Guo; H. Wang; X. Cao; G. Zhang; X. Shi. PEGylated dendrimer-entrapped gold nanoparticles for in vivo blood pool and tumor imaging by computed tomography. *Biomaterials*, **2012**, *33*, 1107-1119.

[14] H. Wang; L. Zheng; C. Peng; M. Shen; X. Shi; G. Zhang. Folic acid-modified dendrimer-entrapped gold nanoparticles as nanoprobes for targeted CT imaging of human lung adencarcinoma. *Biomaterials*, **2013**, *34*, 470-480.

[15] D. A. Tomalia; A. M. Naylor; W. A. Goddard. Starburst dendrimers: Molecular-level control of size, shape, surface chemistry, topology, and flexibility from atoms to macroscopic matter. *Angew. Chem. Int. Ed. Engl.*, **1990**, *29*, 138-175.

[16] D. A. Tomalia; J. B. Christensen; U. Boas. Dendrimers, dendrons and dendritic polymers. Cambridge University Press: **2012**.

[17] D. A. Tomalia; H. D. Durst, Genealogically directed synthesis: Starburst/cascade dendrimers and hyperbranched structures. *Supramolecular chemistry I—Directed synthesis and molecular recognition*, Springer Berlin Heidelberg: **1993**.

[18] M. Munir; M. Hanif; N. M. Ranjha. Dendrimers and their applications: A review article. *Pak. J. Pharm. Sci.*, **2016**, *2*, 55-66.

[19] J. Peterson; V. Allikmaa; J. Subbi; T. Pehk; M. Lopp. Structural deviations in poly(amidoamine) dendrimers: A MALDI-TOF MS analysis. *Eur. Polym. J.*, **2003**, *39*, 33-42.

[20] V. Swali; N. J. Wells; G. J. Langley; M. Bradley. Solid-phase dendrimer synthesis and the generation of super-high-loading resin beads for combinatorial chemistry. *J. Org. Chem.*, **1997**, *62*, 4902-4903.

[21] A. Y.-T. Huang; C.-H. Tsai; H.-Y. Chen; H.-T. Chen; C.-Y. Lu; Y.-T. Lin; C.-L. Kao. Concise solid-phase synthesis of inverse poly(amidoamine) dendrons using AB_2 building blocks. *Chem. Commun.*, **2013**, *49*, 5784-5786.

[22] F. Zeng; S. C. Zimmerman. Dendrimers in supramolecular chemistry: From molecular recognition to self-assembly. *Chem. Rev.*, **1997**, *97*, 1681-1712.

[23] A. Basso; M. Bradley. Site–site interactions within high-loading PAMAM dendrimer resin beads. *Tetrahedron Lett.*, **2003**, *44*, 2699-2702.

[24] Y. Rio; G. Accorsi; H. Nierengarten; C. Bourgogne; J.-M. Strub; A. V. Dorsselaer; N. Armaroli; J.-F. Nierengarten. A fullerene core to probe dendritic shielding effects. *Tetrahedron*, **2003**, *59*, 3833-3844.

[25] R. Shi; F. Wang; B. Yan. Site–Site Isolation and Site–Site Interaction – Two Sides of the Same Coin. *Int. J. Pept. Res. Ther.*, **2007**, *13*, 213-219.

[26] P. P. Zweni; H. Alper. Dendrimer–Palladium complex catalyzed oxidation of terminal alkenes to methyl ketones. *Adv. Synth. Catal.*, **2004**, *346*, 849-854.

[27] C. Bouillon; G. Quéléver; L. Peng. Efficient synthesis of esters containing tertiary amine functionalities via active cyanomethyl ester intermediates. *Tetrahedron Lett.*, **2009**, *50*, 4346-4349.

[28] E. Kaiser; R. L. Colescott; C. D. Bossinger; P. I. Cook. Color test for detection of free terminal amino groups in the solid-phase synthesis of peptides. *Anal. Biochem.*, **1970**, *34*, 595-598.

[29] D. G. Mullen; A. Desai; M. A. van Dongen; M. Barash; J. R. Baker; M. M. Banaszak Holl. Best practices for purification and characterization of PAMAM dendrimer. *Macromolecules*, **2012**, *45*, 5316-5320.

# Section 3. Construction of triazine dendrimers and its focused library
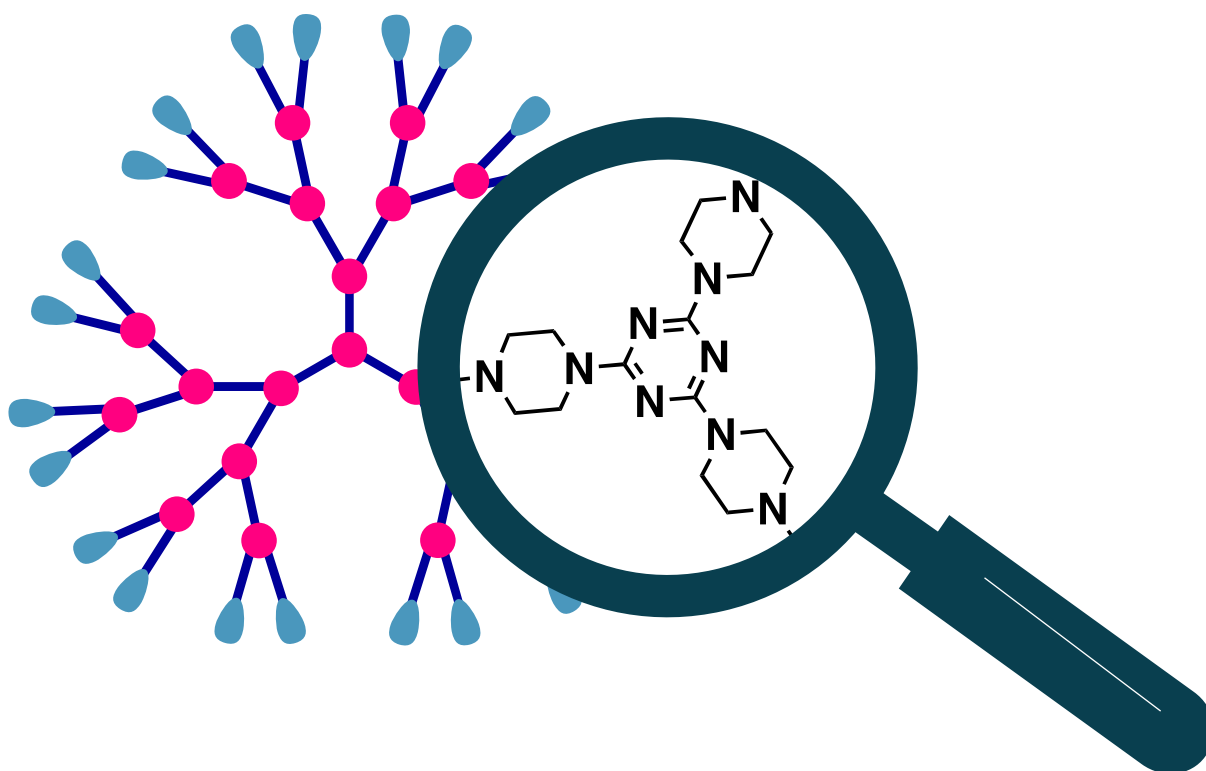
1. Background

1.1. Triazine dendrimers

Triazine dendrimers refers to the dendritic architectures incorporated triazine rings as the focal and branching points. Triazine dendrimers was first outlined in the patent filed by Meijer et al. in the 1990s.[1] Since then, accounts of triazine dendrimers have been synthesized for various

applications. Applications of triazine dendrimers can be characterized into several categories; molecular recognition and supramolecular self-assembly,[2-5] environmental remediation by attachment of triazine dendrons to solid supports[6-9] and biomedical applications.[10-16]

The characteristic entities of triazine dendrimer are triazine units, which are six-membered aromatic heterocycles composed of three carbon and three nitrogen atoms. The 1,3,5-triazine (**111**) is the most extensively studied isomer, giving symmetrical molecule among with the other two isomers, 1,2,3-triazine (**112**) and 1,2,4-triazine (**113**) (**Figure 3.1**). Triazines recognize other molecules by hydrogen bonds, metal chelation, and π-π interactions. This opportunity has enabled various supramolecular structures to be prepared on the basis of hydrogen bonding interactions to form ribbons and other types of interesting oligomers and polymers.[2-4] Another interest is the use of triazine dendrimers to modify silica surfaces or polystyrene supports for various purposes such as insoluble scavengers for removal of excess nucleophilic or electrophilic reagents from the reaction mixtures.[6-9]

111   **112**   **113**
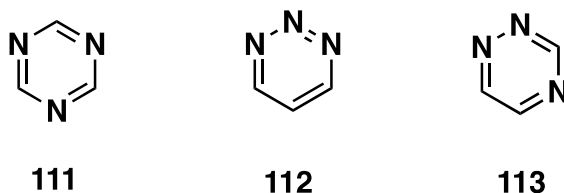
Figure 3.1. Triazine isomers: 1,3,5-triazine (**109**), 1,2,3-triazine (**110**) and 1,2,4-triazine (**111**).

Biologically relevant applications of triazine dendrimers have been a major focus with most investigations for drug delivery systems.[10-16] A significant advance in the application has been the preparation of triazine dendrimers that present disulfide linkages at the periphery for modulable and responsive drug delivery.[12,14] Triazine dendrimers have also been displayed antiviral activity[17] and a potential resin-bound antibiotic for single-bead screening.[11]

1.2. Synthesis of triazine dendrimers

Triazine dendrimer synthesis was mainly based on the characteristic chemistry of cyanuric chloride (**76**). Together with cyanuric acid (**114**) and melamine (**115**), cyanuric chloride is one of the most commonly used triazine derivatives (**Figure 3.2**).[18] Cyanuric chloride (**76**) is highly reactive and can be used in many organic transformations, such as serving as reagent for chlorination of alcohols/carboxylic acids to alkyl chlorides/acid chlorides[19] and dehydration of amides to nitriles/imines[20] as well as undergoing nucleophilic aromatic substitution (S_NAr). In particular, the three chlorides in **76** have differential reactivity for substitution reactions with nucleophiles during S_NAr, which can be achieved with temperature-dependent selectivity. Usually, the first substitution occurs at low temperatures (0 °C), the second substitution at approximately room temperature, and the third one at elevated temperatures (70-100 °C) (**Figure 3.3A**). This property allows sequential substitution of the three chlorides on the same triazine unit using various nucleophiles at different temperatures, providing a vast array of possible triazine derivatives and applications.[21,22]

76   **114**   **115**
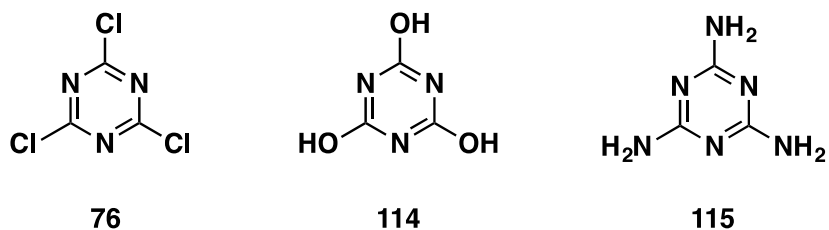
Figure 3.2. 1,3,5-triazine derivatives: cyanuric chloride (**76**), cyanuric acid (**114**) and melamine (**115**).

(A)

(B) Relatively reactivity of various amines

1	2	3	7	10	31	45	63	214	321

More reactive

(C)
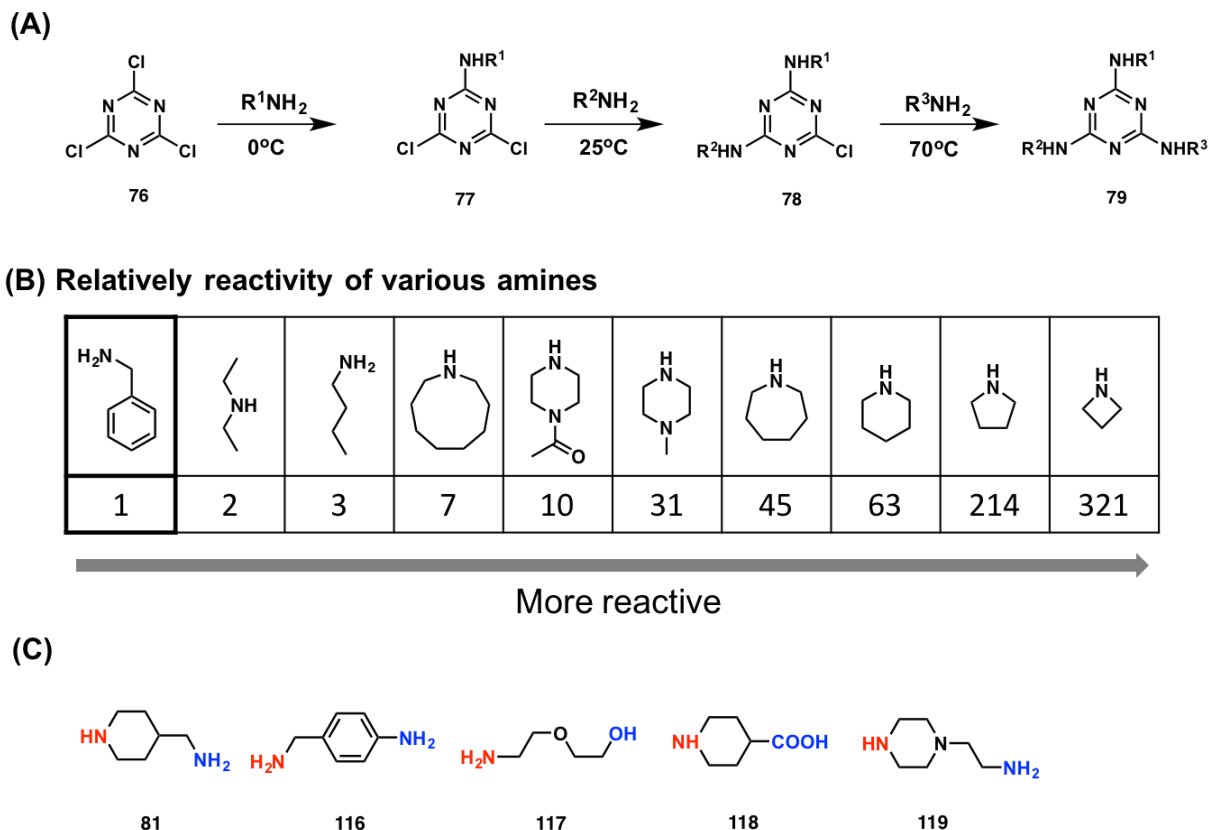
Figure 3.3. **(A)** Chemoselective reactivity of cyanuric chloride (**76**) depending on reaction temperatures; **(B)** Relative reactivity of various amines toward a monochlorotriazine; **(C)** Linkers containing two different reactive sites (Red: more reactive; blue: less reactive).

The unique reactive feature of **76** as substrate for S_NAr towards a wide variety of amine nucleophiles makes an ideal building unit for constructing triazine dendrimers (**Figure 3.3**).[21] The choice of diamines (**Figure 3.3C**, **81, 116-119**) used to link the triazine units into dendrimers is a critical issue. Differences in amine reactivity enable further control over the generalized reactivity that allow more efficient and reliable syntheses of dendrimers. (**Figure 3.3B**). Triazine dendrimers synthesized from **76** by nucleophilic aromatic substitutions were first published in 2000 by the Simanek group.[23] Other groups have since reported triazine dendrimers and this subject has been reviewed by Steffensen et al.[21] Until now, a variety of triazine dendrimers with different diamine linkers and surface functionalities has been established.[10,22-28]

Besides the solution-phase synthesis, [21] solid-phase approach for triazine dendrimer synthesis has also been explored using a series of insoluble supports, including silica,[7] nanoporous alumina[9] and polystyrene.[29-31] For example, Acosta et al reported the divergent synthesis on SBA-15 mesoporous silica to afford up to fourth-generation triazine dendrons, forming organic-inorganic hybrids that were extensively characterized. Also the convergent assembly of triazine dendrons in solution followed by focal point attachment onto silica gel was explored and compared with the divergent solid-phase synthesis.[7] These comparative studies showed that convergent method was able to produce well-defined dendritic structures but unfortunately not applicable to reach large dendrimers due to the steric hindrance.

Also, the trizaine dendrimers synthesized and attached on solid-phase can serve as supported materials for the separation of organics in an aqueous solution or gas streams.[32,33] Supported triazine dendrimers can served as scavengers for organic synthesis. Marsh et al. reported polystyrene-supported triazine dendrimers with amine terminals as insoluble scavengers to remove the excess of electrophiles.[34] They also prepared triazine dendrimers on various solid supports including polystyrene resin, SynPhase[TM] Lanterns and silica gel[35] as supported reagents, which can be endowed with multivalent properties yet easily recovered, regenerated and reused for environmentally friendly applications such as proton scavenger and protein library screening.[34]

Although triazine dendrimer synthesis can be scale up to kilogram quantity in solution synthesis,[36] the main impedance of triazine dendrimers for their applications still consist of the consuming preparation and purification, hence the lack of high quality dendrimers. The reported solid-phase synthesis of triazine dendrimers has limitation of constructing higher generation products and limited chemical diversity. In my PhD thesis, we would like to develop effective strategy which can (i) successfully synthesize triazine dendrimers on solid-phase, (ii) rapidly diversify interior and peripheral functionalities, and (iii) accomplish these steps with high fidelity.

2. Results and discussion

2.1. Triazine dendrimer synthesis

To realize solid-phase approach for triazine dendrimer synthesis, we used cyanuric chloride (**76**) as the triazine building unit because of its unique reactivity as mentioned in the introduction. We also chose the diamine 4-aminomethylpiperidine (4-AMP, **81**) as linking unit by virtue of its distinct reactivity between the constrained secondary amine and the primary amine, which differ by a factor of 20:1 in nucleophilic substitution.[37,38] In addition, this short, rigid linker was inexpensive and was less likely to undergo cross-linking with chlorides to form cycled defects.

We first attempted Wang-amide resin for solid-phase synthesis of triazine dendrimers. However, the use of Wang-amide resin gave rise to a by-product with an additional *p*-hydroxybenzyl group at the cleavage step, which corresponds to linker cleavage at the phenolic position instead of the usual benzylic position (**Figure 3.4**). The cleavage products were confirmed with MS analysis and were difficult to separate to obtain the desired product. We then turned to use the Rink-amide resin as a solid support for triazine dendrimer synthesis.
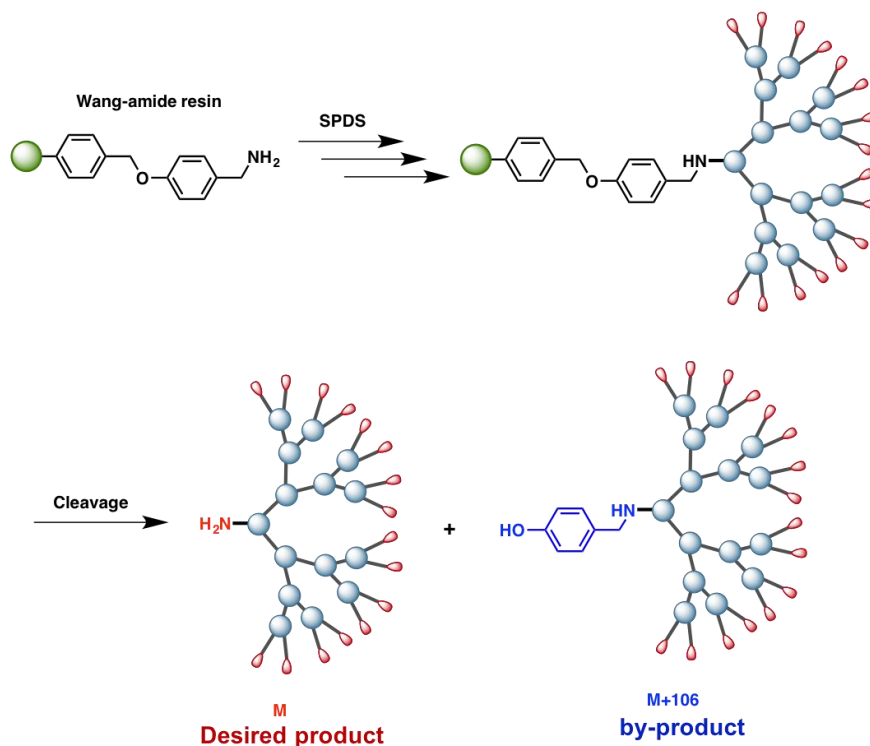

Figure 3.4. Two products bearing the amine and benzyl groups from Wang-amide resin cleavage.
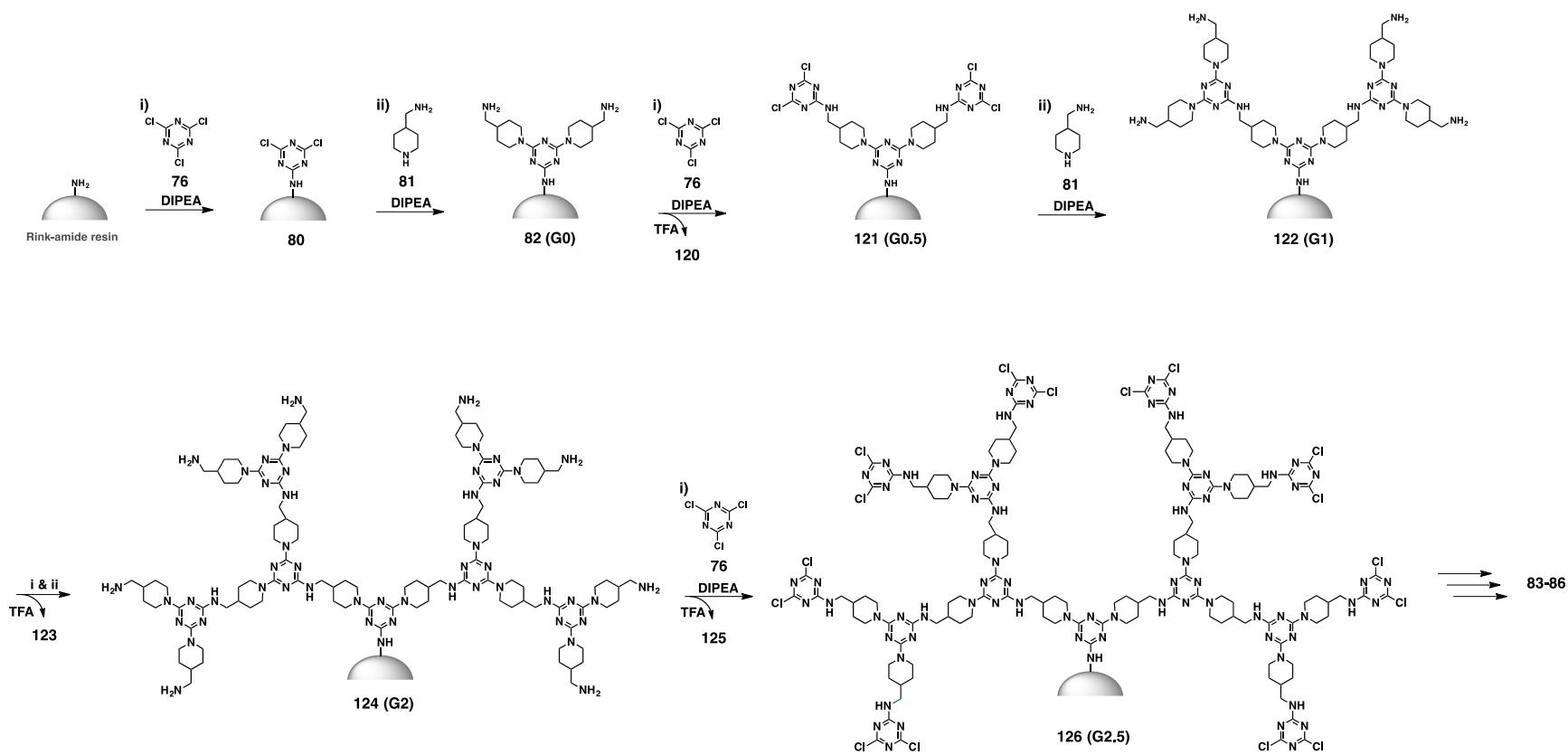
Scheme 3.1. Solid-phase synthesis of triazine dendrimers incorporating cyanuric chloride (**76**) and 4-AMP (**81**).

Scheme 3.1 illustrates the solid-phase strategy to build up triazine dendrimers with the iterative synthetic sequence composed of reaction with cyanuric chloride (**76**) and reaction with 4-AMP (**81**). The reaction of **76** with amines was optimized and involved the use of a two-fold excess of **76** relatives to the available terminal amine. A washing procedure with THF/MeOH was performed after each reaction and before repeating the cycle. The reaction progress was monitored using colorimetric tests. After accomplishing the synthesis, dendrimers were cleaved from the resin to afford triazine dendrimers (**120**), (**123**), (**125**), (83). Since NMR analysis was not informative because of the repeated chemical structures, MS spectral analysis was applied to characterized triazine dendrimers (**Figure 3.5**). However, only amine-terminated triazine dendrimers could be studied using MS, whereas the chlorinated triazine dendrimers were unstable under the MS spectra conditions, leading to the hydrolytic product and other unidentified products (**Figure 3.6**).
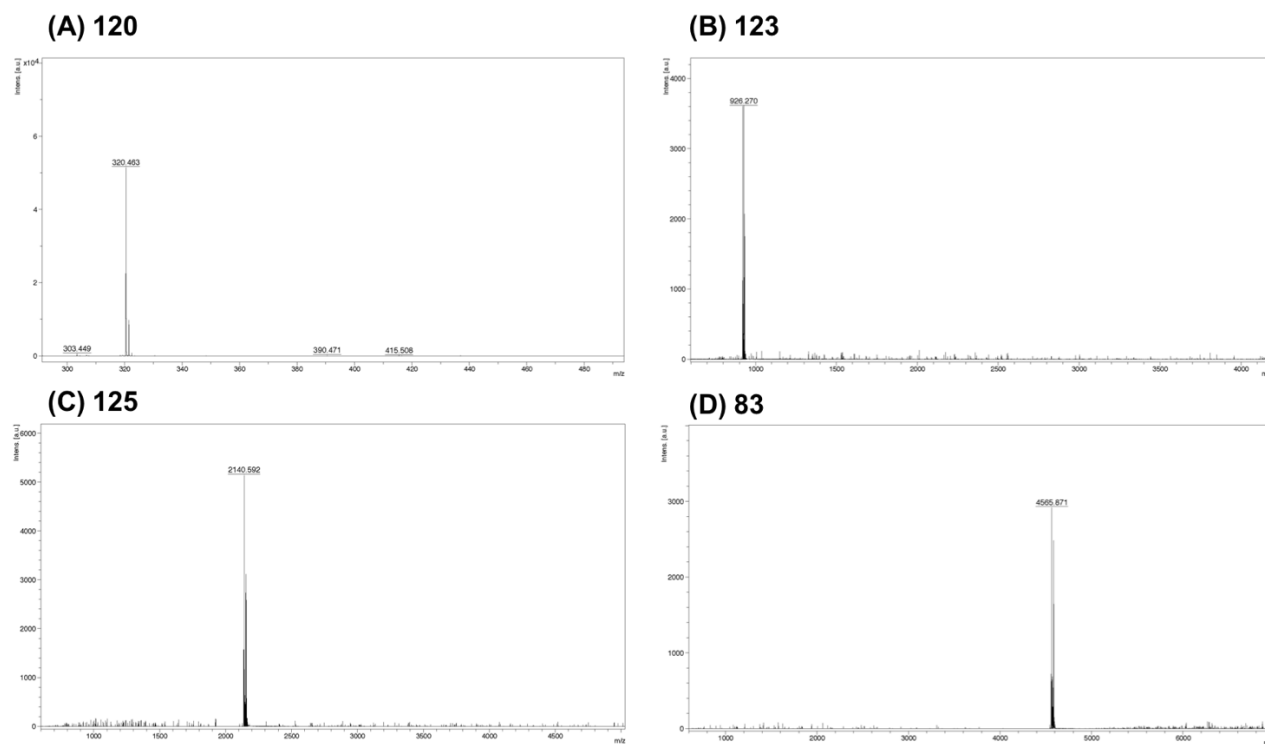
Figure 3.5. MALDI-TOF-MS spectra of triazine dendrimers **120**(G0), **123**(G1), **125**(G2) and **83**(G3).
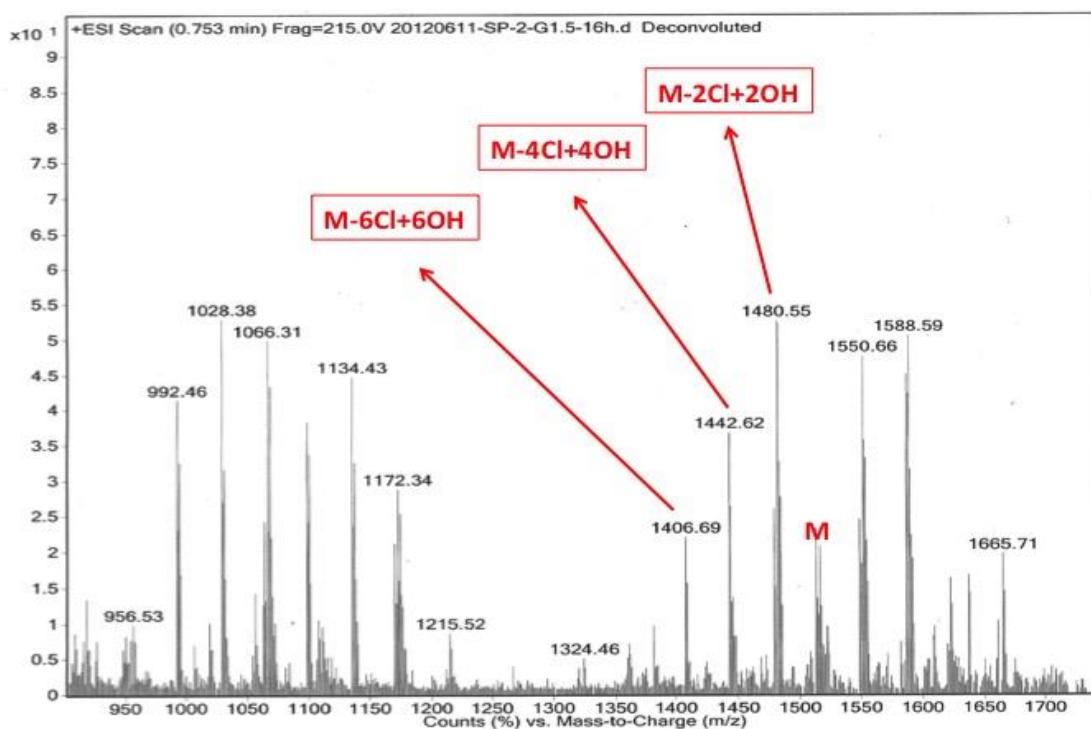
Figure 3.6. MS traces of chlorinated intermediate dendrimer (G1.5) with hydrolytic products.

2.2. Orthogonal staining methods for monitoring solid-phase reactions

An efficient and accurate method to track the reactions is crucial for ensuring the effective accomplishment of solid-phase synthesis. Among various methods proposed for monitoring solid-phase synthesis, colorimetric staining methods belongs to one of the easiest implemented approach yet being the most economical, hence the most frequently used in the practice.[39]

In the course of triazine dendrimer synthesis, the presence of chloride or amine terminal groups on the dendrimer surface constitutes the most significant characteristics for monitoring the dendrimer growth. Ninhydrin (**127**) is well-known for detecting the amine functionalities with its characteristic violent color,[40] and can be used for monitoring the steps of amine nucleophile conjugation in the synthesis of triazine dendrimers. Meanwhile, Alizarin R (AliR, **128**) can be employed to detect the presence of chloride substituent on the triazine during the progress of a nucleophilic reaction with chlorotriazine (**Figure 3.7A**). By adopting Taddei's procedure,[41] resin

109

beads harboring triazine chloride entities were mixed with AliR (**128**) solution in NMM/DMF followed by incubation for 5 min. The resulting resin appeared red in the presence of triazine chloride (**Figure 3.7B**). Accordingly, during solid-phase synthesis of triazine dendrimers, each step can be closely monitored using colorimetric assays based on Alizarin R (AliR, **128**) and ninhydrin (**127**) respectively. For example, using cyanuric acid to fully conjugate with all the dendrimer amine terminals should give a positive response in the AliR test but a negative result for the Kaiser test upon reaction completion, whereas using **81** to fully displace all the dendrimer chloride terminals will generate a positive result with Kaiser test but a negative response with the AliR test.
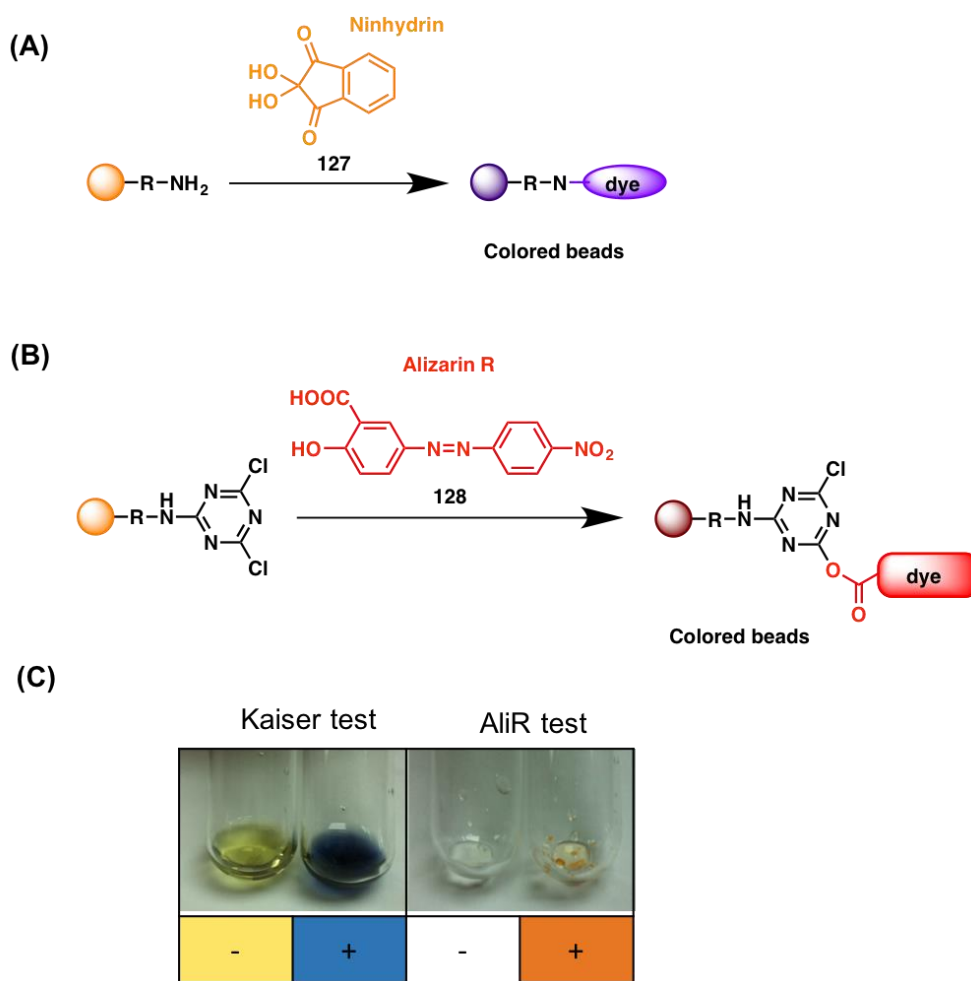
Figure 3.7. (A) Ninhydrin test; **(B)** AliR test; **(C)** Colorimetric results of the ninhydrin (**127**) and AliR (**128**) staining.

2.3. The construction of a focused library with four combinations of terminals

As the principle-demonstration model, we intended to create a small library of triazine dendrimers bearing various peripheral groups using SPDS. To do this, we started with the above synthesized supported triazine dendrimer **126**. Elaborating **126** into a small library of compounds relied on its conversion and the subsequent reactions with nucleophiles. **126** was reacted with the first nucleophile HX (**81, 129, 130** and **131**) to displace one of the two chlorides and generate a library of dendrimers with terminal triazine units bearing one chloride; these dendrimers were further reacted with the second nucleophile HY (**81** and **129**) to fully displace the chloride and provide the dendrimers bearing combinatorial amino acid terminals composed of g and h, and the cyclic amine terminals composed of e and f. Dendrimers with peripheral amino acids were considered as potential compounds for biomedical applications.[42]
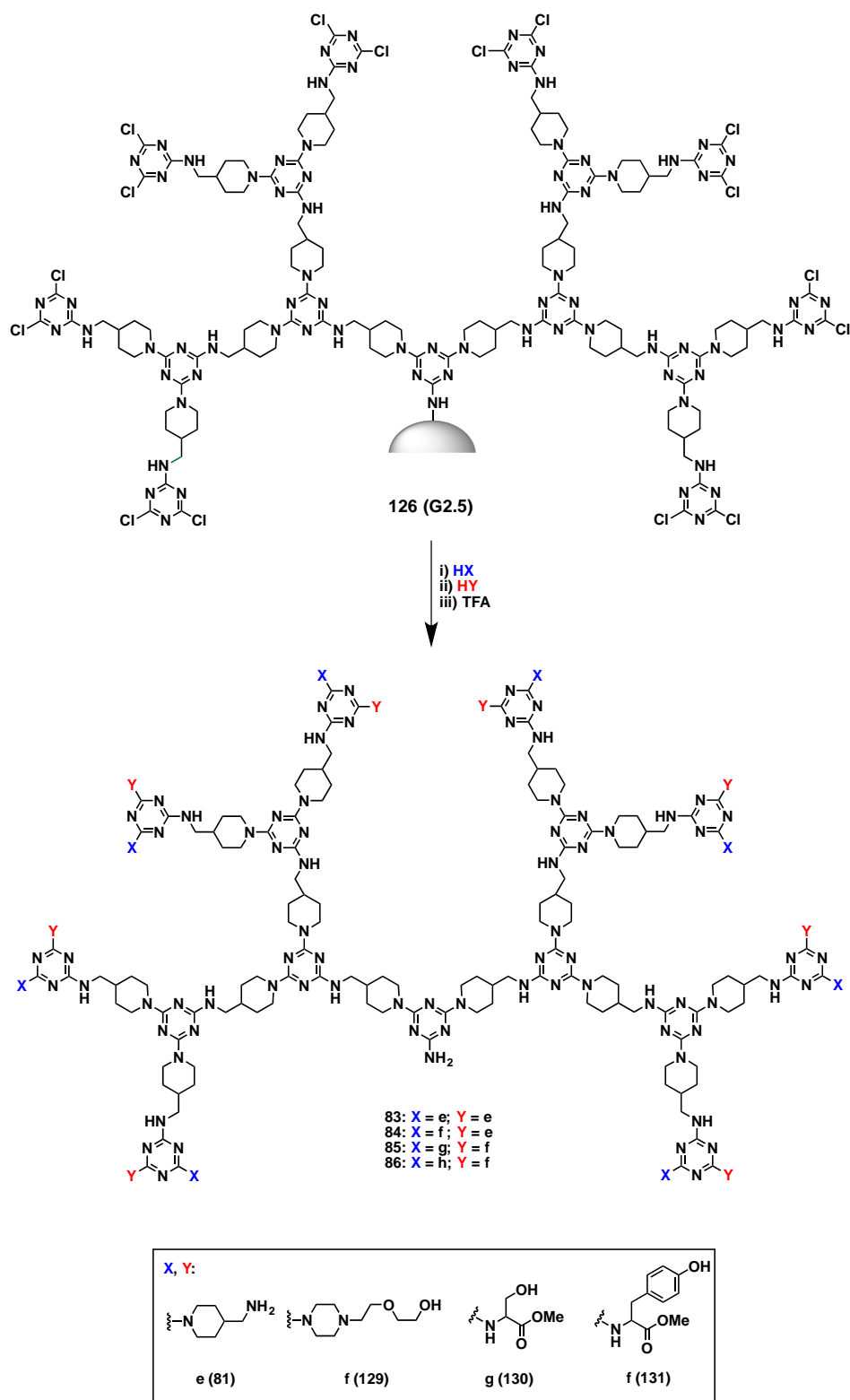
Scheme 3.2. The construction of triazine dendrimers **83-86** with four combinations of terminals starting from **126** (G2.5).

MALDI-TOF-MS confirmed the successful dendrimer synthesis and remained as a useful means to monitor the reaction progress. During the reaction of **132** with **129**, the mass spectra acquired after 12 h displayed signals corresponding to the desired product with eight substitutions of HEEP (**129**) and also the intermediate with only six substitutions (**Figure 3.8**). This finding indicated that the dendrimer growth reaction was not fully completed and longer reaction time was necessary. After another 12 h, only the signal corresponding to the fully substituted compound was observed, highlighting the completed reaction. Similarly, conversion into **84** yielded a single line corresponding to the product. Integration of the ^{1}H NMR spectrum confirmed the desired stoichiometry of the surface groups.
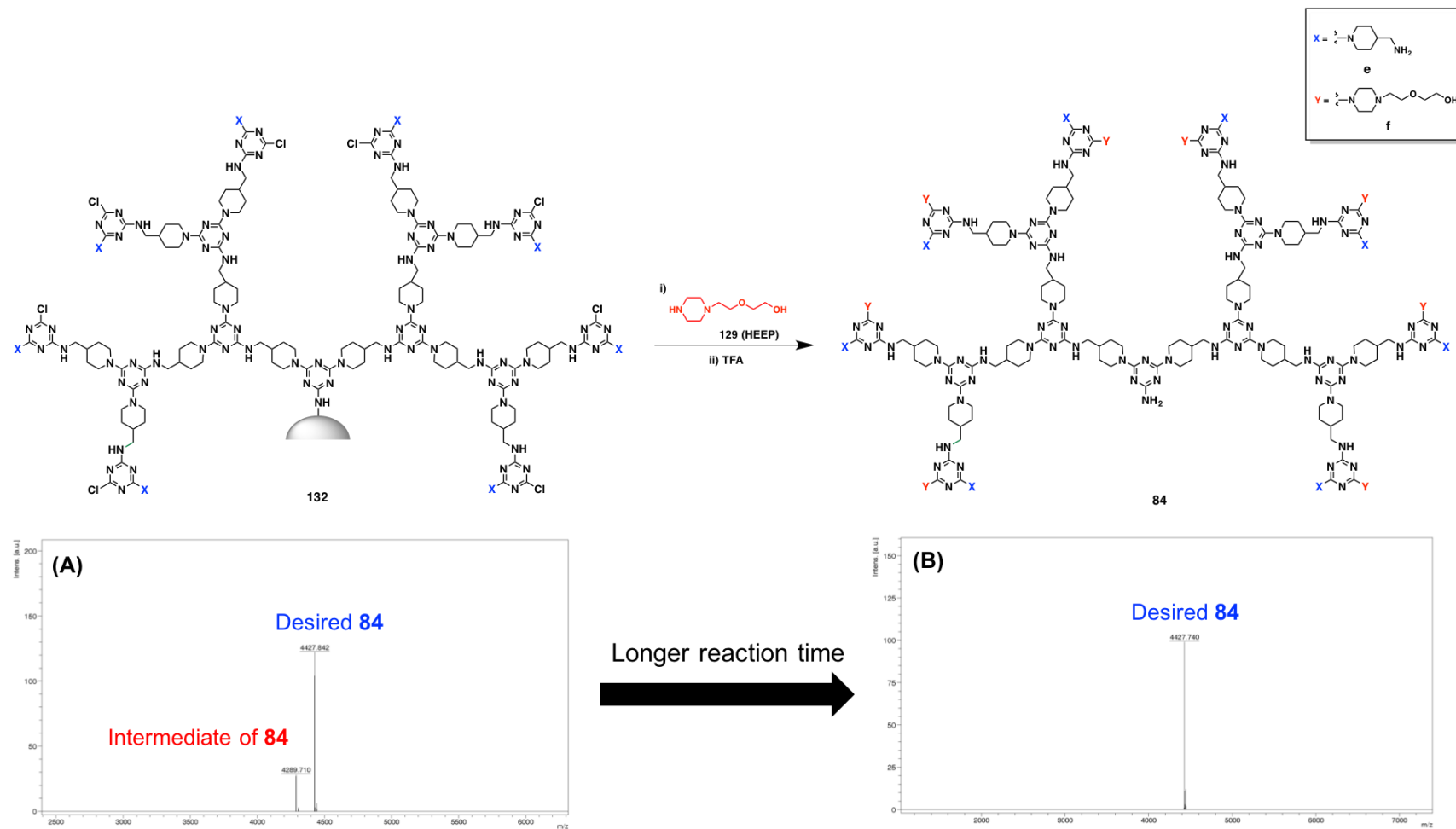
Figure 3.8. MALSI-TOF-MS tracking: **(A)** Intermediate of **84** after 12h reaction; **(B)** Desired disubstituted product of **84** after 24 h reaction.

It is to note that the secondary amine functionalities in 4-AMP (**81**) and HEEP (**129**) are more reactive than the primary amines in serine methyl ester (**130**) and tyrosine methyl ester (**131**) for nucleophilic substitution on triazine ring. Accordingly, during the preparation of (**85**) and (**86**), the amino acids reacted first to leverage the higher reactivity of the dichlorotriazine over the monochlorotriazine. This reaction was followed by the addition of (**129**) at room temperature for 24 h. The final compounds were collected by treating the resin with a solution of 95% TFA. The mixture was then shaken for 2 h at room temperature. The resin was removed by filtration and washed with DCM and THF. All filtrates were combined and the solvent was evaporated under reduced pressure. The overall yields for this series were 87%, 84%, 81% and 81% for dendrimers **83-86** respectively. In both serine methyl ester (**130**) and tyrosine methyl ester (**131**), the lower nucleophilicity of the primary amino groups was responsible for the lower yields.

During the construction of the triazine dendrimer library, each step was monitored using the orthogonal staining method described previously. The introduction of 1 equivalent of **81** to **84** gave a positive result in both tests due to the presence of amino and triazine chloride groups in the product. The final incorporation of **129** to give **84** via the substituted triazine chloride gave a negative AliR test but a positive Kaiser test. The same procedure was applied to the preparation of compounds **85** and **86** (**Table 3.1**).

Table 3.1. True table of colorimetric monitoring for triazine dendrimer library construction to reveal the primary amines and triazine chlorides.

83	Kaiser test	AliR test
Cl^a	-	+
e	+	-

84	Kaiser test	AliR test
e	+	+
f	+	-

85	Kaiser test	AliR test
g	-	+
f	-	-

86	Kaiser test	AliR test
h	-	+
f	-	-

^{a}: chloride of **72**

3. Summary

In this section, an efficient SPDS of triazine dendrimer was established and a small library of triazine dendrimers was conducted as a proof-of-concept study in the view of constructing a variety of dendrimers. This ability could extend the diversity for dendrimer applications. This library includes dendrimers with a variety of surface group compositions. Starting with Rink-amide resin, iterative reactions of cyanuric chloride (**76**) and a linking diamine, 4-AMP (**81**), provided the desired materials. Peripheral dichlorotriazines could react selectively with four different combinations of nucleophiles to yield a multifunctional surface (**83-86**) in a total yield of 81-87%. The whole preparation process could be accomplished within one week, which dramatically improves the preparation efficiency. In this study, we also developed and validated a pair of orthogonal staining methods involving the ninhydrin and AliR tests to monitor the presence of alkyl amines and triazine chlorides in the course of dendrimer synthesis. This combined staining method offered an efficient approach for monitoring the solid-phase synthesis of triazine dendrimers. The approach developed here will allow to rapidly access diverse dendrimers, providing an opportunity to exploit these dendrimers for specific screening purposes in biomedical applications.

4. Experimental Section

General

Wang-amide resin was obtained from Advanced ChemTech, Rink-amide resin was purchased from Merck and other chemicals, solvents, and reagents were obtained from Acros, Aldrich and TCI, and used without further purification. Mass spectra were acquired on either an Agilent ESI-MS-TOF and MALDI-MS-TOF (positive mode electrospray) mass spectrometer instrument as indicated. NMR spectra were obtained on a Varian 400MHz spectrometer. High-performance liquid chromatography (HPLC) and gel permeation chromatography (GPC) experiments were obtained using an Agilent HPLC system (1100 series).

General MALDI-TOF-MS protocol

A dendrimer solution was prepared by dissolving 1 mg of each final product in 1 ml of MeOH. Additionally, a 1:10 dilution of this solution was made. The matrix solution was prepared by dissolving 10 mg of matrix (2,5-dihydroxybenzoic acid, DHB) in 1 ml of MeOH. The analytical sample was prepared by mixing the dendrimer solution (0.5 μl) with the matrix solution (0.5 μl) on a stainless steel probe tip, and this mixture was allowed to dry at room temperature. MALDI-TOF-MS system (model Autoflex III Smartbeam) equipped with a 355 nm Nd: YAG laser was purchased from Bruker Daltonics (Billerica, MA, USA). Mass spectra were acquired in positive ion reflector mode for the summing of 600 laser shots and data was processed by FlexAnalysis software (Bruker Daltonics).

General procedure of solid-phase synthesis

Rink-amide resin (0.10 mmol) was allowed to swell in DMF for 4 h, then it was mixed with 20% piperidine in DMF for 10 min to remove the Fmoc protecting group. Deprotection was confirmed by ninhydrin assay. A solution of cyanuric chloride (4 eq) in THF (10 mL) was added to the swollen resin. The resulting mixture was treated with DIPEA and stirred at RT under N_2. After the reaction, the resin was washed with THF (30 mL) and MeOH (30 mL). Then, a solution of 4-AMP (4 eq) in THF (10 mL) was added to the resulting chlorinated resin. The reaction mixture was treated with DIPEA and stirred at rt under N_2. The resin was washed with THF (30 mL) and MeOH (30 mL). The ninhydrin and AliR tests were used to monitor the reaction progress. As the dendrimer generation increased, the amount of reagents used was doubled.

Cleavage from Resin

The resin-bound compounds (0.10 mmol) were treated with a solution of 95% TFA (5 mL), and the mixture was shaken for 2 h at rt. The solution was filtered and the resin was washed with EtOH (10 mL) and DCM (10 mL). The combined filtrates were evaporated in vacuo, and toluene (3x5 mL) was added to form an azeotropic mixture with any remaining TFA, which was removed under high vacuum to obtain the final compounds.

Colorimetric monitoring

Ninhydrin test for triazine amine: 10 beads of resin were taken from the reactor and transferred to a test tube, followed by an addition of 30 μl cocktail of ninhydrin reagent (50 mg/mL of ninhydrin (**127**) in EtOH, 4 g/mL of phenol in EtOH and pyridine). Then checking the color change after 5 min heating at 120°C. (Positive: violet; negative: yellow)

Alizarin R test for triazine chloride: 10 beads of resin were taken from the reactor and transferred to a test tube, followed by an addition of 1 mL AliR solution (5 mg of Alizarin R (**128**) with 1 mL of NMM in 3 mL of DMF). After 10 min of suspension at rt, the beads were washed several times with DMF and THF until the solution was no longer colored and observed the resin color. (Positive: red; negative: colorless)
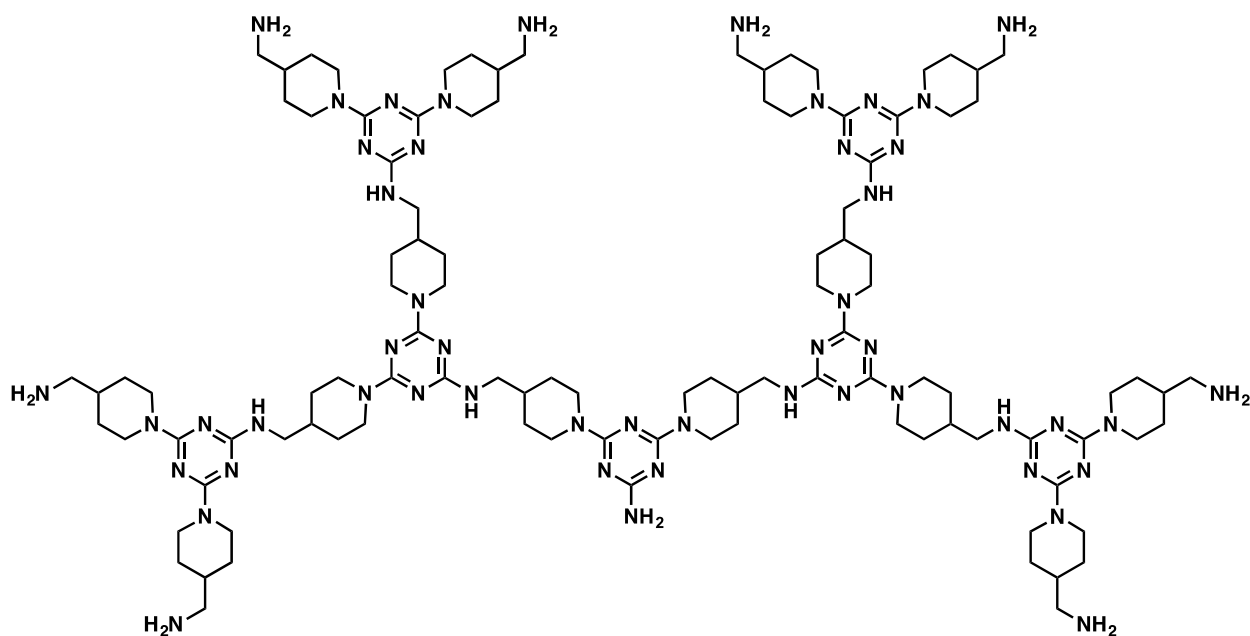
Triazine Dendrimer 120 (G0)
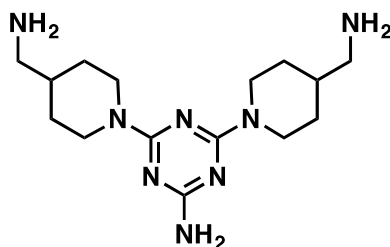
120

To swelling Rink-amide resin, cyanuric chloride ($C_3N_3Cl_3$, **76**) (79.10 mg, 0.43 mmol) in THF (10 mL) and DIPEA (59.30 mg, 0.46 mmol) was added and the mixture was incubated for 6 h. 4-AMP (**81**) (90.50 mg, 0.79 mmol) in THF (10 mL) and DIPEA (109.20 mg, 0.85 mmol) were then added, and the reaction was shaking for 8 h. Both reactions were stirred at rt under N_2. After the reactions had reached completion, cleavage from the 0.10 mmol resin afforded **120** as a yellow oil (30.20 mg, 94%). ^{1}H NMR (400 MHz, CD$_3$OD): δ 1.28 (m, 6H), 1.88 (m, 2H), 1.92 (m, 2H), 2.01 (m, 2H), 2.88 (m, 4H), 3.03 (t, J = 12 Hz, 6H), 4.65 (br s, 4H); ^{13}C NMR (100 MHz, CD$_3$OD): δ 30.1, 35.6, 45.3, 45.4, 159.0, 163.5; MS (MALDI-TOF, matrix: DHB): calcd for $C_{15}H_{28}N_8$ [M]$^+$ 320.2; found at *m/z* 320.5.

Triazine Dendrimer 123 (G1)

123

82 (Resin-bound G0) (0.10 mmol) was treated according to the general procedure involving cyanuric chloride (**72**) (0.16 g, 0.87 mmol) in THF (10 mL) and DIPEA (0.11 g, 0.86 mmol) over 12 h. 4-AMP (**81**) (0.18 g, 1.58 mmol) in THF (10 mL) and DIPEA (0.22 g, 1.70 mmol) were then added and the reaction was incubated for 8 h. Both reactions were stirred at rt under N_2. After the reactions had reached completion, cleavage from the resin afforded (**123**) as a yellow oil (85.40 mg, 92%). ^{1}H NMR (400 MHz, CD$_3$OD): δ 1.16 (m, 8H), 1.34 (m, 8H), 1.75–1.92 (m, 22H), 2.70 (m, 4H), 2.74 (m, 4H), 2.85 (m, 16H), 3.28 (m, 46H), 4.76 (br s, 8H); ^{13}C NMR (100 MHz, CD$_3$OD): δ 29.1, 30.6, 36.7, 37.7, 45.6, 46.7, 46.9, 54.4, 167.0, 172.7; MS (MALDI-TOF, matrix: DHB): calcd for C$_{45}$H$_{78}$N$_{22}$: [M]$^+$ 926.7; found at *m/z* 926.3.

Triazine Dendrimer 125 (G2)

125

122 (Resin-bound G1) (0.10 mmol) was treated according to the general procedure involving cyanuric chloride (**76**) (0.330 g, 1.79 mmol) in THF (15 mL) and DIPEA (0.249 g, 1.93 mmol) for 24 h. 4-AMP (**81**) (0.399 g, 3.50 mmol) in THF (15 mL) and DIPEA (0.45 g, 3.48 mmol) was then added and the reaction was incubated for 18 h. Both reactions were stirred at rt under N_2. After the latter reaction had reached completion, cleavage from the resin afforded **125** as a yellow oil (0.182 g, 86%). ^{1}H NMR (400 MHz, CD$_3$OD): δ 1.18 (m, 16 H), 1.52 (m, 8H), 1.79–2.00 (m, 62H), 2.77-2.90 (m, 56 H), 3.01 (t, J = 12.0 Hz, 8H), 3.43 (d, 12H), 4.76(br s, 16H); ^{13}C NMR (100 MHz, CD$_3$OD): δ 27.6, 30.4, 34.0, 36.1, 36.4, 43.9, 44.2, 44.7, 45.3, 45.7, 45.9, 153.1, 165.6, 166.3, 166.6; MS (MALDI-TOF, matrix: DHB): calcd for C$_{105}$H$_{178}$N$_{50}$ [M+H]$^+$ 2140.6; found at m/z 2140.6.

## Triazine Dendrimer 126 (Resin-bound G2.5)

124 (Resin-bound G2) (0.10 mmol) was treated according to the general procedure involving **76** (0.649 g, 3.52 mmol) in THF (15 mL) and DIPEA (0.510 g, 3.95 mmol) over 36 h. The reaction was stirred at rt under N_2 to afford the intermediated resin-bound **126**.
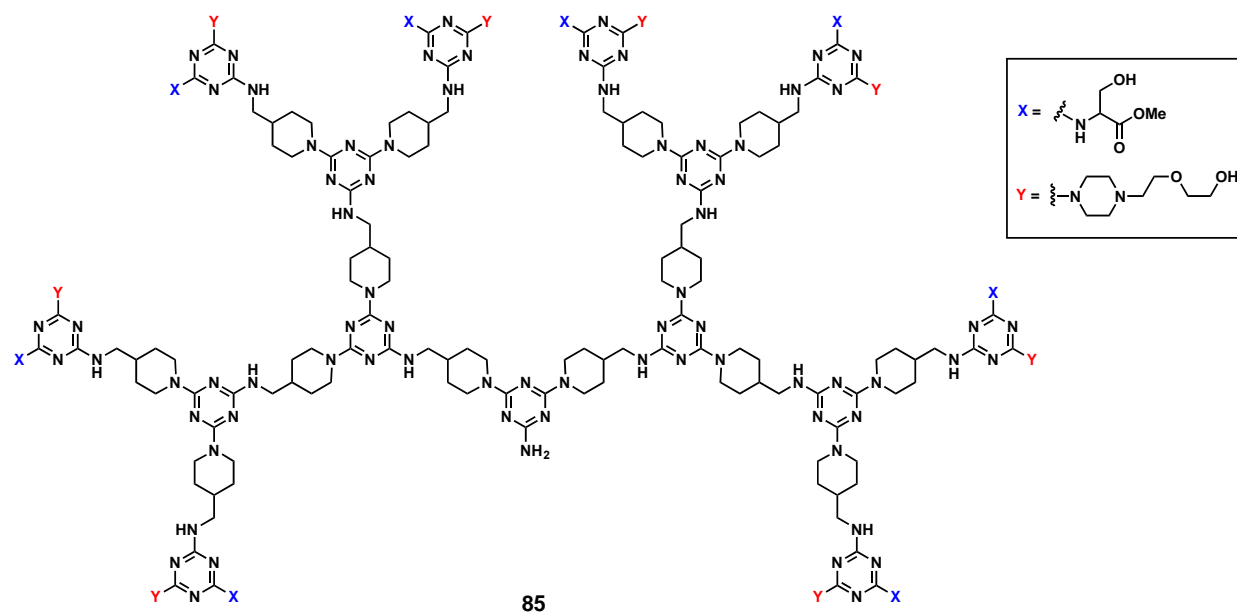
Triazine Dendrimer 83

83
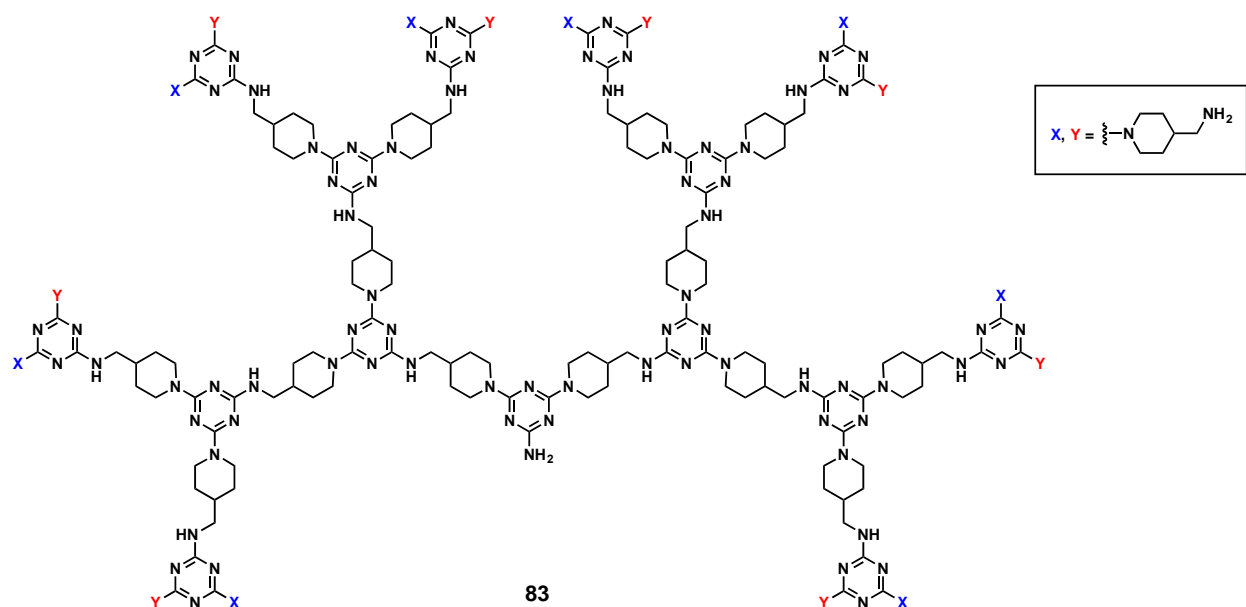
A solution of 4-AMP (**81**) (0.370 g, 3.24 mmol) in THF (15 mL) was added to a solution of the resin-bound **126** (0.10 mmol) in THF (5 mL). The reaction was treated with DIPEA (0.420 g, 3.25 mmol) and stirred for 36 h at rt under N_2. Then, the resin was washed with THF (15 mL) and MeOH (15 mL). Cleavage from the resin afforded **83** as a yellow oil (0.397 g, 87%). ^{1}H NMR (400 MHz, CD$_3$OD): δ 1.13–1.24 (m, 64 H), 1.51 (m, 16H), 1.73–1.83 (m, 64H), 1.95–2.01 (m, 40H), 2.83–2.89 (m, 88 H), 3.01 (t, J = 12.0 Hz, 16 H), 3.41 (d, J = 12.0 Hz, 12 H), 4.69 (br s, 32H); ^{13}C NMR (100 MHz, CD$_3$OD): δ 27.2, 30.1, 33.4, 35.6, 35.7, 37.6, 44.0, 44.4, 44.9, 45.4, 46.9, 151.7, 165.4, 170.7; MS (MALDI-TOF, matrix: DHB): calcd for C$_{225}$H$_{378}$N$_{106}$ [M]$^+$ 4565.3; found at m/z 4565.9.
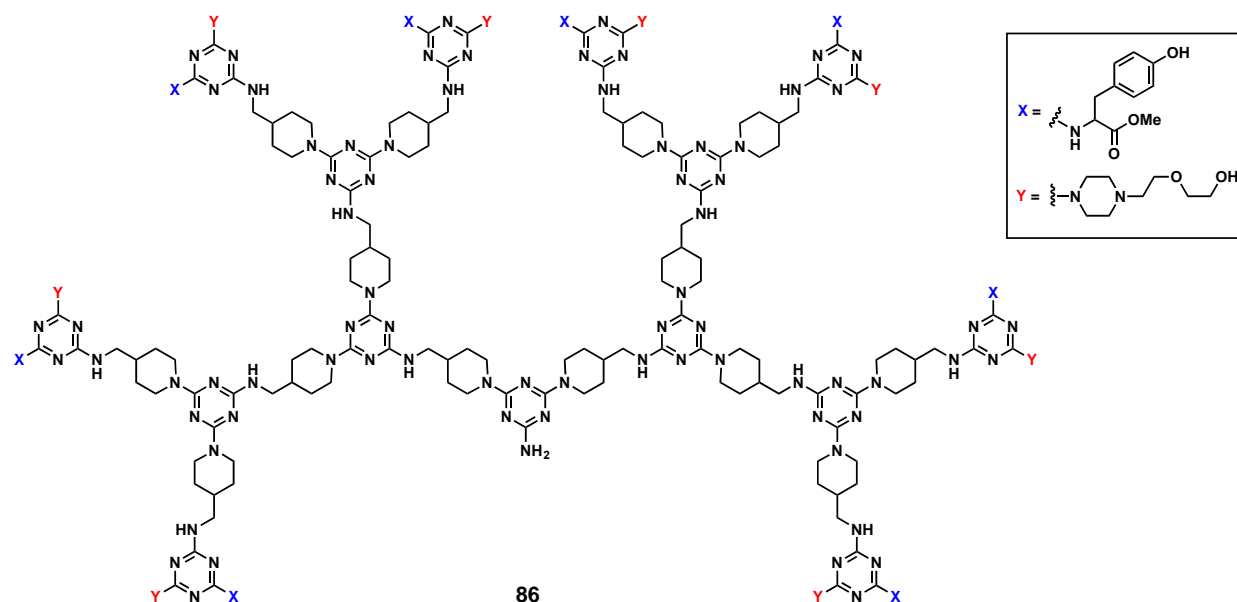
Triazine Dendrimer 84

84
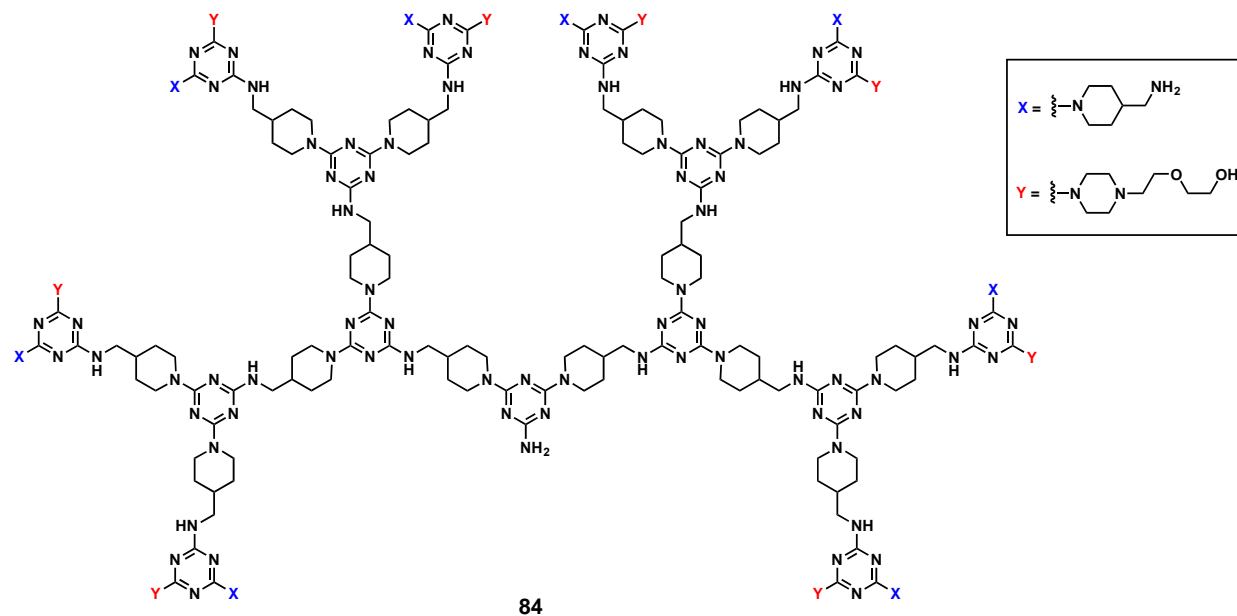
A solution of 4-AMP (**77**) (0.137 g, 1.20 mmol) in THF (15 mL) was added to a solution of resin-bound **126** (0.10 mmol) in THF (5 mL). The reaction was treated with DIPEA (0.156 g, 1.21 mmol) and stirred for 18 h at rt. Then, the resin was washed with THF (15 mL) and MeOH (15 mL). HEEP (**129**) (0.209 g, 1.20 mmol) was added and the reaction was stirred for 24 h at rt. Both reactions were performed under N_2. The resin was washed with THF (15 mL) and MeOH (15 mL). Cleavage from the resin afforded **84** as a yellow oil (0.424 g, 84%). ^{1}H NMR (400 MHz, CD$_3$OD): δ 1.08–1.16 (m, 24H), 1.22–1.31 (m, 32H), 1.63–1.72 (m, 24H), 1.78 (m, 22H), 1.86 (m, 32H), 2.54 (d, J = 12.0 Hz, 28H), 2.59–2.68 (m, 48 H), 2.77 (m, 64 H), 2.88 (t, J = 8 Hz, 32H), 3.22 (d, J = 8 Hz, 16 H), 3.54 (m, 16 H), 3.62–3.68 (m, 32H), 3.77 (br s, 16H), 4.77 ppm (d, J = 12 Hz, 16H); ^{13}C NMR (100 MHz, CD$_3$OD): δ 28.4, 29.5, 36.4, 37.36, 44.7, 44.7, 46.2, 53.3, 53.6, 57.8, 58.2, 61.1, 61.1, 67.7, 67.8, 72.3, 72.3, 165.3, 165.4, 186.5, 165.6 ppm; MS (MALDI-TOF, matrix: DHB): calcd for $C_{241}H_{411}N_{106}O_{16}$ [M]$^+$ 5046.5; found at m/z 5047.5.

Triazine Dendrimer 85

85

A solution of L-serine methyl ester hydrochloride (**130**) (0.146 g, 1.23 mmol) in THF/MeOH (1:1, 15 mL) was added to a solution of resin-bound **126** (0.10 mmol) in THF (5 mL). The reaction was treated with DIPEA (0.291 g, 2.25 mmol) and stirred for 36 h at rt. After 36 h, the resin was washed with THF (15 mL) and MeOH (15 mL). Then, HEEP (**127**) (0.211 g, 1.21 mmol) was added and the reaction was stirred for 24 h at rt. All reactions were performed under N_2. The resin was washed with THF (15 mL) and MeOH (15 mL). Cleavage from the resin afforded **85** as a yellow oil (0.411 g, 81%). ^{1}H NMR (400 MHz, CD$_3$OD): δ 1.14 (m, 12H), 1.28–1.41 (m, 24 H), 1.77–1.93 (m, 66 H), d 2.53 (t, J = 8.0 Hz, 12H), 2.62 (m, 36H), 2.72 (d, J = 8.0 Hz, 16H), 2.77 (d, J = 8.0 Hz, 12H), 2.85 (m, 24H), 2.95 (t, J = 4 Hz, 32 H), 3.53 (m, 16 H), 3.65 (m, 40 H), 3.74 (s, 24H), 3.79 (m, 16H); ^{13}C NMR (100 MHz, CD$_3$OD): δ 27.2, 27.6, 29.3, 34.6, 35.1, 36.1, 42.5, 42.8, 44.1, 44.2, 44.4, 45.3, 45.5, 48.7, 51.4, 52.9, 53.2, 56.0, 56.7, 57.6, 57.8, 58.0, 61.1, 61.1, 63.7, 64.4, 67.8, 67.8,72.3, 156.2, 165.3, 165.4, 165.5, 165.6, 174.; MS (MALDI-TOF, matrix: DHB): calcd for $C_{217}H_{354}N_{98}O_{40}$ [M]$^+$ 5085.0; found at m/z 5084.9.

Triazine Dendrimer 86

86

A solution of L-tyrosine methyl ester hydrochloride (**131**) (0.240 g, 1.23 mmol) in THF/MeOH (1:1, 15 mL) was added to a solution of resin-bound **126** (0.10 mmol) in THF (5 mL). The reaction was treated with DIPEA (0.291 g, 2.25 mmol) and stirred for 36 h at rt. After 36 h, the resin was washed with THF (15 mL) and MeOH (15 mL). Then, HEEP (**129**) (0.211 g, 1.21 mmol) was added and the reaction was stirred for 24 h at rt. All reactions were performed under N_2. The resin was removed by filtration and washed with THF (15 mL) and MeOH (15 mL). Cleavage from the resin afforded **86** as a yellow oil (0.461 g, 81 %). ^{1}H NMR (400 MHz, CD$_3$OD): δ 1.13–1.19 (m, 12 H), 1.44–1.53 (m, 24H), 1.70–2.00 (m, 66H), 2.55 (m, 8H), 2.65 (m, 32H), 2.72 (t, J = 8.0 Hz, 8H), 2.84 (d, J = 8.0 Hz, 24 H), 2.97 (m, 24H), 3.09 (t, J = 4 Hz, 32H), 3.39 (d, J = 12.0 Hz, 12 H), 3.55 (m, 16H), 3.62–3.71 (m, 64 H), 3.78 (br s, 24 H), 6.73 (d, J = 8.0 Hz, 16 H), 7.00 (d, J=8.0 Hz, 16H); ^{13}C NMR (100 MHz, CD$_3$OD): δ 27.9, 30.5, 4.6, 36.5, 40.7, 43.7, 43.9, 44.9, 45.1, 45.7, 52.5, 52.5, 54.5, 56.7, 58.7, 59.0, 62.3, 62.3, 68.9, 69.1, 73.5, 116.5, 128.6, 131.4, 131.6, 157.6, 166.5, 166.7, 176.1; MS (MALDI-TOF, matrix: DHB): calcd for $C_{265}H_{386}N_{98}O_{40}$ [M]$^+$ 5693.2; found at *m/z* 5693.8.

5. References

[1] E. W. Meijer; H. J. M. Bosman; F. H. A. M. Vandenbooren; E. De Brabander-van Den Berg; A. M. C. F. Castelijns; H. C. J. De Man; R. W. E. G. Reintjens; C. J. C. Stoelwinder; A. J. Nijenhuis U.S. Patent, DSM N. V., 1996.

[2] H. Sauriat-Dorizon; T. Maris; J. D. Wuest; G. D. Enright. Molecular tectonics. Construction of porous hydrogen-bonded networks from bisketals of pentaerythritol. *J. Org. Chem.*, **2003**, *68*, 240-246.

[3] N. Malek; T. Maris; M. Simard; J. D. Wuest. Molecular tectonics. Selective exchange of cations in porous anionic hydrogen-bonded networks built from derivatives of tetraphenylborate. *J. Am. Chem. Soc.*, **2005**, *127*, 5910-5916.

[4] P. Brunet; E. Demers; T. Maris; G. D. Enright; J. D. Wuest. Designing permeable molecular crystals that react with external agents to give crystalline products. *Angew. Chem. Int. Ed.*, **2003**, *42*, 5303-5306.

[5] W. T. S. Huck; R. Hulst; P. Timmerman; F. C. J. M. van Veggel; D. N. Reinhoudt. Noncovalent synthesis of nanostructures: Combining coordination chemistry and hydrogen bonding. *Angew. Chem. Int. Ed. Engl.*, **1997**, *36*, 1006-1008.

[6] X. Wu; P. Liu; Q. Pu; Z. Su. FAAS determination of platinum using an on-line separation and preconcentration system with a polymelamine dendrimer immobilized silica gel. *Anal. Lett.*, **2003**, *36*, 2229-2241.

[7] E. J. Acosta; S. O. Gonzalez; E. E. Simanek. Synthesis, characterization, and application of melamine-based dendrimers supported on silica gel. *J. Polym. Sci., Part A: Polym. Chem.*, **2005**, *43*, 168-177.

[8] P. Gamez; P. de Hoog; M. Lutz; A. L. Spek; J. Reedijk. Coordination compounds from 1,3,5-triazine-derived multi-directional ligands: application in oxidation catalysis. *Inorg. Chim. Acta*, **2003**, *351*, 319-325.

[9] E. J. Acosta; C. S. Carr; E. E. Simanek; D. F. Shantz. Engineering nanospaces: Iterative synthesis of melamine-based dendrimers on amine-functionalized SBA-15 leading to complex hybrids with controllable chemistry and porosity. *Adv. Mater.*, **2004**, *16*, 985-989.

[10] J. Lim; G. M. Pavan; O. Annunziata; E. E. Simanek. Experimental and computational evidence for an inversion in guest capacity in high-generation triazine dendrimer hosts. *J. Am. Chem. Soc.*, **2012**, *134*, 1942-1945.

[11] S. Lebreton; N. Newcombe; M. Bradley. Antibacterial single-bead screening. *Tetrahedron*, **2003**, *59*, 10213-10222.

[12] W. Zhang; S. E. Tichy; L. M. Pérez; G. C. Maria; P. A. Lindahl; E. E. Simanek. Evaluation of multivalent dendrimers based on melamine: Kinetics of thiol−disulfide exchange depends on the structure of the dendrimer. *J. Am. Chem. Soc.*, **2003**, *125*, 5086-5094.

[13] S. A. Bell; M. E. McLean; S.-K. Oh; S. E. Tichy; W. Zhang; R. M. Corn; R. M. Crooks; E. E. Simanek. Synthesis and characterization of covalently linked single-stranded DNA oligonucleotide-dendron conjugates. *Bioconj. Chem.*, **2003**, *14*, 488-493.

[14] A. P. Umali; E. E. Simanek. Thiol−disulfide exchange yields multivalent dendrimers of melamine. *Org. Lett.*, **2003**, *5*, 1245-1247.

[15] M. F. Neerman; H.-T. Chen; A. R. Parrish; E. E. Simanek. Reduction of drug toxicity using dendrimers based on melamine. *Mol. Pharm.*, **2004**, *1*, 390-393.

[16] C. Lee; S.-T. Lo; J. Lim; V. C. P. da Costa; S. Ramezani; O. K. Öz; G. M. Pavan; O. Annunziata; X. Sun; E. E. Simanek. Design, synthesis and biological assessment of a triazine dendrimer with approximately 16 paclitaxel groups and 8 PEG groups. *Mol. Pharm.*, **2013**, *10*, 4452-4461.

[17] S. da Silva Santos; E. Igne Ferreira; J. Giarolla. Dendrimer prodrugs. *Molecules*, **2016**, *21*, 686.

[18] E. M. Smolin; L. Rapoport. Chemistry of heterocyclic compounds: s-Triazines and derivatives. John Wiley & Sons, Inc.: **2008**.

[19] G. Blotny. Recent applications of 2,4,6-trichloro-1,3,5-triazine and its derivatives in organic synthesis. *Tetrahedron*, **2006**, *62*, 9507-9522.

[20] K. P. Haval; S. B. Mhaske; N. P. Argade. Cyanuric chloride: Decent dehydrating agent for an exclusive and efficient synthesis of kinetically controlled isomaleimides. *Tetrahedron*, **2006**, *62*, 937-942.

[21] M. B. Steffensen; E. Hollink; F. Kuschel; M. Bauer; E. E. Simanek. Dendrimers based on [1,3,5]-triazines. *J. Polym. Sci. A Polym. Chem.*, **2006**, *44*, 3411-3433.

[22] E. E. Simanek; H. Abdou; S. Lalwani; J. Lim; M. Mintzer; V. J. Venditto; B. Vittur. The 8 year thicket of triazine dendrimers: strategies, targets and applications. *Proc. R. Soc. A*, **2010**, *466*, 1445-1468.

[23] W. Zhang; E. E. Simanek. Dendrimers based on melamine. Divergent and orthogonal, convergent syntheses of a G3 dendrimer. *Org. Lett.*, **2000**, *2*, 843-845.

[24] W. Zhang; D. T. Nowlan; L. M. Thomson; W. M. Lackowski; E. E. Simanek. Orthogonal, convergent syntheses of dendrimers based on melamine with one or two unique surface sites for manipulation. *J. Am. Chem. Soc.*, **2001**, *123*, 8914-8922.

[25] H.-T. Chen; M. F. Neerman; A. R. Parrish; E. E. Simanek. Cytotoxicity, Hemolysis, and Acute in Vivo Toxicity of Dendrimers Based on Melamine, Candidate Vehicles for Drug Delivery. *J. Am. Chem. Soc.*, **2004**, *126*, 10044-10048.

[26] O. M. Merkel; M. A. Mintzer; J. Sitterberg; U. Bakowsky; E. E. Simanek; T. Kissel. Triazine dendrimers as nonviral gene delivery systems: Effects of molecular structure on biological activity. *Bioconj. Chem.*, **2009**, *20*, 1799-1806.

[27] S. Patra; B. Kozura; A. Y. T. Huang; A. E. Enciso; X. Sun; J.-T. Hsieh; C.-L. Kao; H.-T. Chen; E. E. Simanek. Dendrimers terminated with dichlorotriazine groups provide a route to compositional diversity. *Org. Lett.*, **2013**, *15*, 3808-3811.

[28] C. Lee; K. Ji; E. Simanek. Functionalization of a triazine dendrimer presenting four maleimides on the periphery and a DOTA group at the core. *Molecules*, **2016**, *21*, 335.

[29] E. Hollink; S. E. Tichy; E. E. Simanek. Piperidine-functionalized supports sequester atrazine from solution. *Ind. Eng. Chem. Res.*, **2005**, *44*, 1634-1639.

[30] S. O. Gonzalez; S. Furyk; C. Li; S. E. Tichy; D. E. Bergbreiter; E. E. Simanek. Latent solid-phase extraction with thermoresponsive soluble polymers. *J. Polym. Sci., Part A: Polym. Chem.*, **2004**, *42*, 6309-6317.

[31] E. J. Acosta; M. B. Steffensen; S. E. Tichy; E. E. Simanek. Removal of atrazine from water using covalent sequestration. *J. Agric. Food. Chem.*, **2004**, *52*, 545-549.

[32] A. Javaid; S. O. Gonzalez; E. E. Simanek; D. M. Ford. Nanocomposite membranes of chemisorbed and physisorbed molecules on porous alumina for environmentally important separations. *J. Membr. Sci.*, **2006**, *275*, 255-260.

[33] S. Yoo; J. D. Lunn; S. Gonzalez; J. A. Ristich; E. E. Simanek; D. F. Shantz. Engineering nanospaces: OMS/dendrimer hybrids possessing controllable chemistry and porosity. *Chem. Mater.*, **2006**, *18*, 2935-2942.

[34] A. Marsh; S. J. Carlisle; S. C. Smith. High-loading scavenger resins for combinatorial chemistry. *Tetrahedron Lett.*, **2001**, *42*, 493-496.

[35] S. J. Dilly; M. P. Beecham; S. P. Brown; J. M. Griffin; A. J. Clark; C. D. Griffin; J. Marshall; R. M. Napier; P. C. Taylor; A. Marsh. Novel tertiary amine oxide surfaces that resist nonspecific protein adsorption. *Langmuir*, **2006**, *22*, 8144-8150.

[36] A. Chouai; E. E. Simanek. Kilogram-scale synthesis of a second-generation dendrimer based on 1,3,5-triazine using green and industrially compatible methods with a single chromatographic step. *J. Org. Chem.*, **2008**, *73*, 2357-2366.

[37] M. B. Steffensen; E. E. Simanek. Chemoselective building blocks for dendrimers from relative reactivity data. *Org. Lett.*, **2003**, *5*, 2359-2361.

[38] K. X. Moreno; E. E. Simanek. Identification of diamine linkers with differing reactivity and their application in the synthesis of a melamine sendrimers. *Tetrahedron Lett.*, **2008**, *49*, 1152-1154.

[39] G. Dey; A. Gupta; T. Mukherjee; P. Gaur; A. Chaudhary; S. K. Mukhopadhyay; C. K. Nandi; S. Ghosh. Functional molecular lumino-materials to probe serum albumins: Solid phase selective staining through noncovalent fluorescent labeling. *ACS Appl. Mater. Interfaces*, **2014**, *6*, 10231-10237.

[40] E. Kaiser; R. L. Colescott; C. D. Bossinger; P. I. Cook. Color test for detection of free terminal amino groups in the solid-phase synthesis of peptides. *Anal. Biochem.*, **1970**, *34*, 595-598.

[41] M. E. Attardi; M. Taddei. A sensitive visual test for detection of OH groups on resin. *Tetrahedron Lett.*, **2000**, *41*, 7395-7399.

[42] L. Crespo; G. Sanclimens; M. Pons; E. Giralt; M. Royo; F. Albericio. Peptide and amide bond-containing dendrimers. *Chem. Rev.*, **2005**, *105*, 1663-1682.

Section4. Poly(aminoester) dendrimer synthesis and its challenges
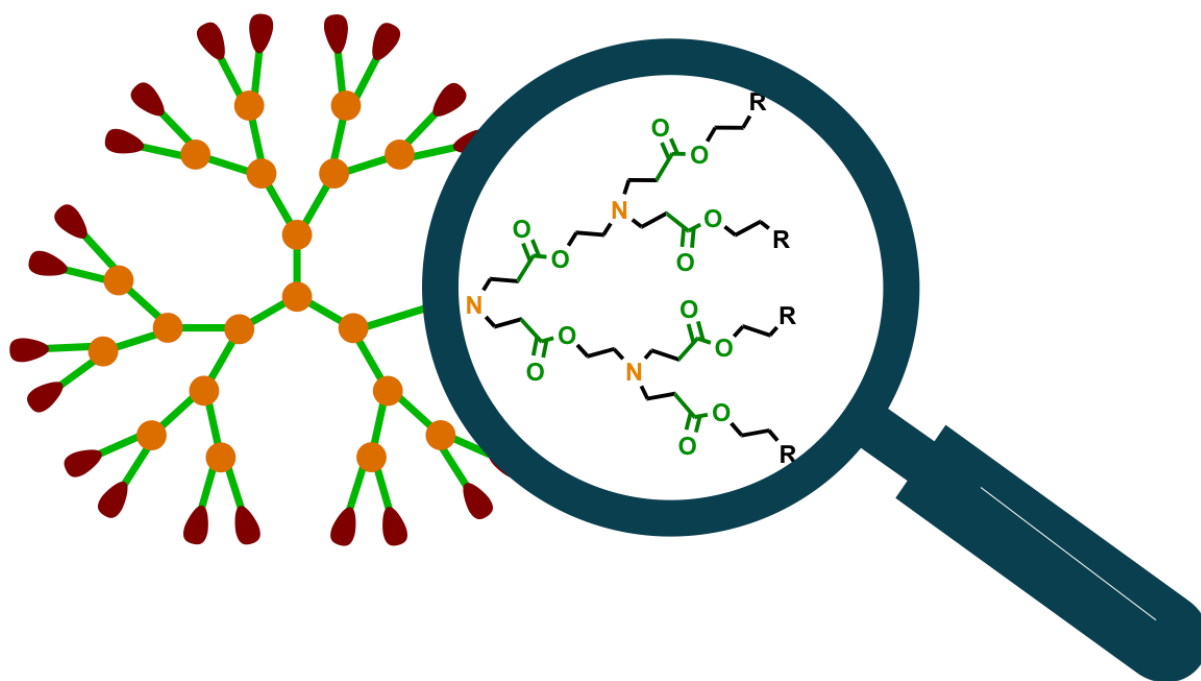
1. Background

1.1. Poly(aminoester) dendrimers

Poly(aminoester) dendrimers are characterized by the dual presence of both amine entities and ester functions. Poly(aminoester) dendrimers are particularly appealing for drug delivery in biomedical applications due to their multiple advantageous features.[1,2] First of all, poly(aminoester) dendrimers are biodegradable because of the labile ester linkages which can be readily hydrolyzed in acidic or basic conditions or via the action of enzymes, allowing effective degradation under

mild conditions. Secondly, the amine functionalities present in the poly(aminoester) dendrimers can serve as buffers to neutralize the acids generated from the ester hydrolysis, creating a benign and nonaggressive environment during dendrimer degradation. Furthermore, the large amount of ester and amine functionalities presented within the dendrimer may facilitate the formation of hydrogen bonds and interactions with the drug molecules, which in turn enforce the encapsulation to improve drug solubility and delivery. Last but not least, both terminal amine and ester functions in poly(aminoester) dendrimers can be easily transformed to various other functionalities in order to meet the special needs of various biomedical applications. In spite of the poly(aminoester) dendrimers having such superior properties compared to other families of dendrimers, their applications in drug delivery have rarely been revealed because of the limited methodologies available for reliable synthesis.

1.2.　Challenges for synthesizing poly(aminoester) dendrimers

The synthesis of poly(aminoester) dendrimers is by no means trivial and the main challenge lies in the simultaneous presence of both ester and amine functionalities.[2] Concerning the ester groups, not only are they labile in acid/basic conditions and in the presence of enzymes, but they can also be easily attacked by nucleophiles and readily undergo various derivations even under mild conditions. Regarding to the amine groups, they can easily form zwitterions or hydrogen bonds with carboxylic acid functions during the synthesis, hence reducing the reactivity of carboxylic acids for esterification. In addition, the amine functionalities can impart high polarity and water solubility to the dendrimers, which complicate the subsequent separation and purification procedures. Thus, the synthesis of reliable and high quality poly(aminoester) dendrimers constitutes a great challenge for synthetic chemists.[1,3]

Several synthetic strategies for preparing poly(aminoester) dendrimers in solution have been reported include the amine branching approach,[4,5] the ester formation strategy,[6] and the combination of both methods[1,7,8] along with the emerging click chemistry based synthesis.[3,9] All four strategies have their own advantages and limitations, and need further improvements to generate defect-free dendrimers for biomedical applications (**Scheme 4.1**).
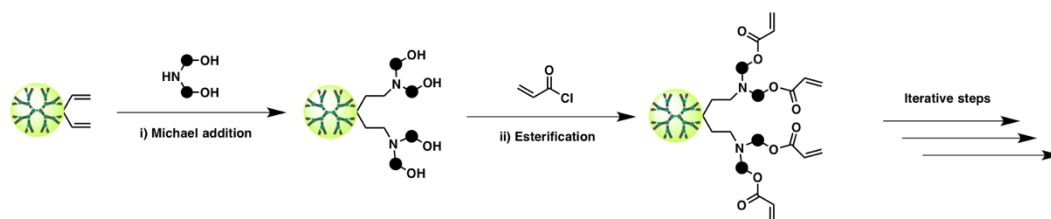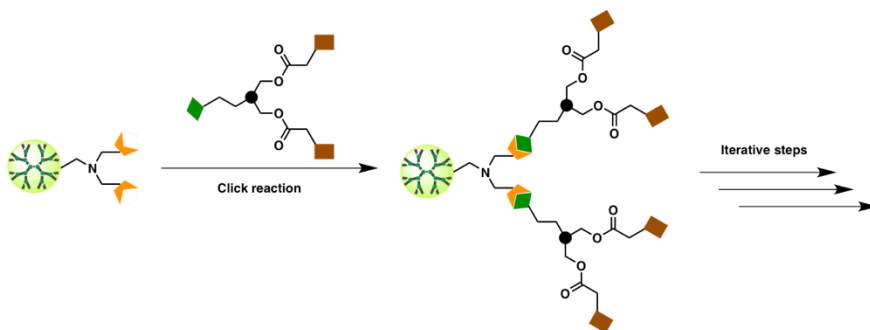
(A) Amine branching
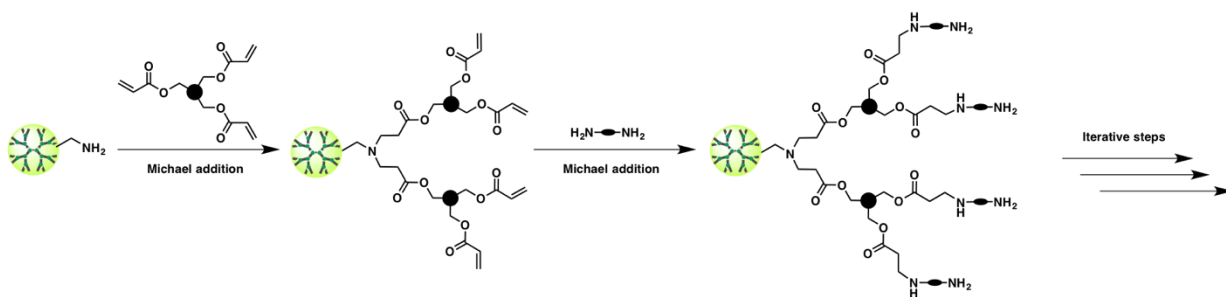
(B) Direct ester bond formation

(C) Combination of A+B

(D) Click chemistry

Scheme 4.1. Strategies for the synthesis of poly(aminoester) dendrimers via **(A)** amine branching, **(B)** direct ester bond formation, **(C)** combined ester bond formation and amine branching, and **(D)** click chemistry.

Alternatively, the solid-phase synthesis may provide a promising strategy with the simple separation and purification steps, hence offering a rapid achievement of poly(aminoester) dendrimers. Recently, Kang et al reported the solid-phase synthesis of poly(aminoester) dendrimers (**Figure 4.1**). They enclosed Fe_3O_4 nanoparticles within a poly(aminoester) dendrimer shell in the view of developing Fe_3O_4 as a magnetic resonance imaging agent for biomedical applications.[10]
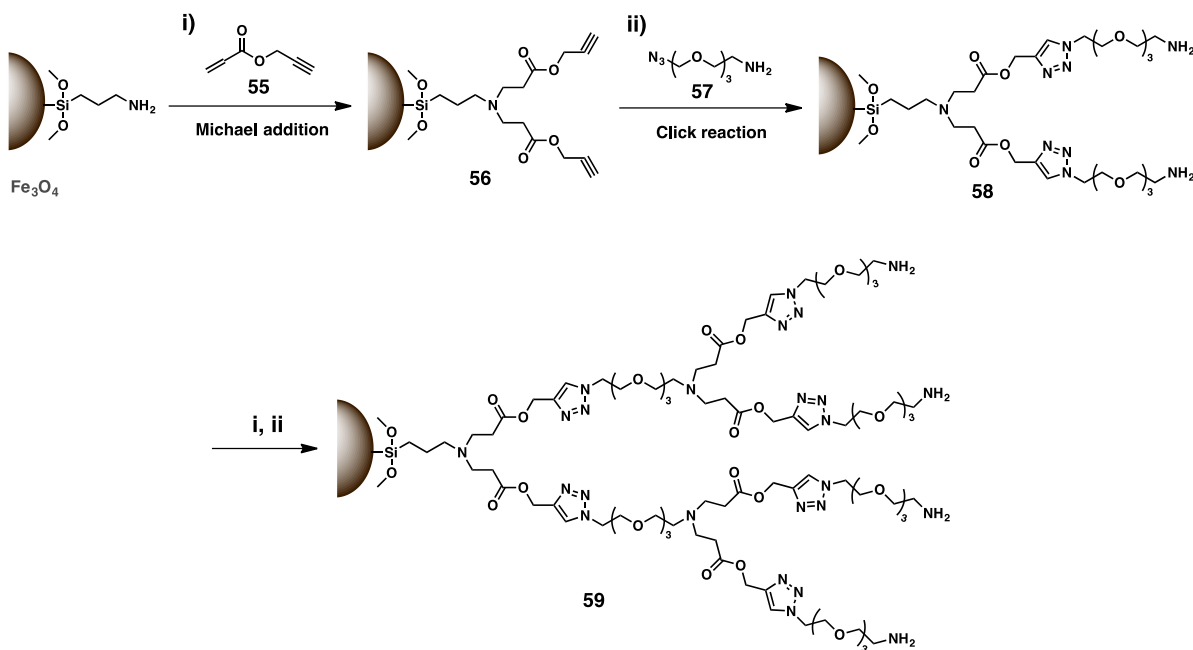
Figure 4.1. Solid-phase synthesis of poly(aminoester) dendrimers onto Fe_3O_4 nanoparticles.

Encouraged by our successful solid-phase synthesis of inverse PAMAM dendrimers[11] and triazine dendrimers[12] as well as Kang's report on solid-phase synthesis of poly(amino)ester dendrons on Fe_3O_4,[10] we would like to elaborate a general solid-phase method for synthesizing poly(aminoester) dendrimers.

As the only difference between poly(aminoester) and PAMAM dendrimers is the amide functions in PAMAM dendrimers being replaced by ester linkages, we therefore envisioned an allied synthetic strategy similar to what we developed for solid-phase synthesis of PAMAM dendrimers for creating poly(aminoester) dendrimers, specifically, we would like to construct

poly(aminoester) dendrimers via ester bonding formation instead of amide bond formation used in PAMAM dendrimer synthesis. In this way, we expected that solid-phase synthesis could facilitate the preparation of poly(aminoester) dendrimers with highly efficient coupling/deprotection reactions yet easy and effective purification procedures.

2. Results and discussion

2.1. Molecular design and preparation of building blocks

Similar to the solid-phase synthesis of PAMAM dendrimers, we were in need of the AB_2 type repeating units capable of building poly(aminoester) dendrimers via stepwise ester bond formation. We therefore conceived and prepared two building blocks **133** and **136** (**Figure 4.2**). **133** bearing free carboxylic acid functionality was designed for attachment to Kaiser oxime resin as the first residue, whereas **136** harboring free hydroxyl group was devised to serve as the repeating unit for dendrimer growth. The hydroxyl group in **136** were able to form ester with the carboxylic acid terminals of the dendrimer attached onto the resin for dendrimer growth, followed by hydrolysis to release the acid terminals for next reaction cycle to construct next generation dendrimers. The iterative integration of the repeating unit **136** and final resin cleavage reaction were expected to provide the desired dendrimers (**Scheme 4.2**).
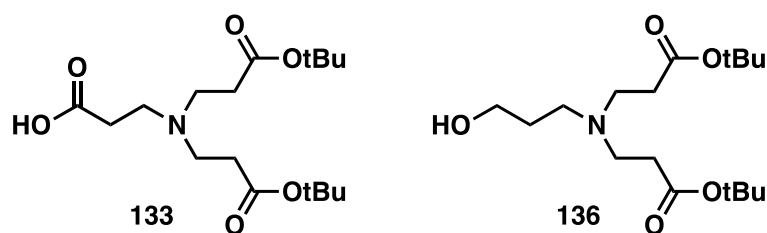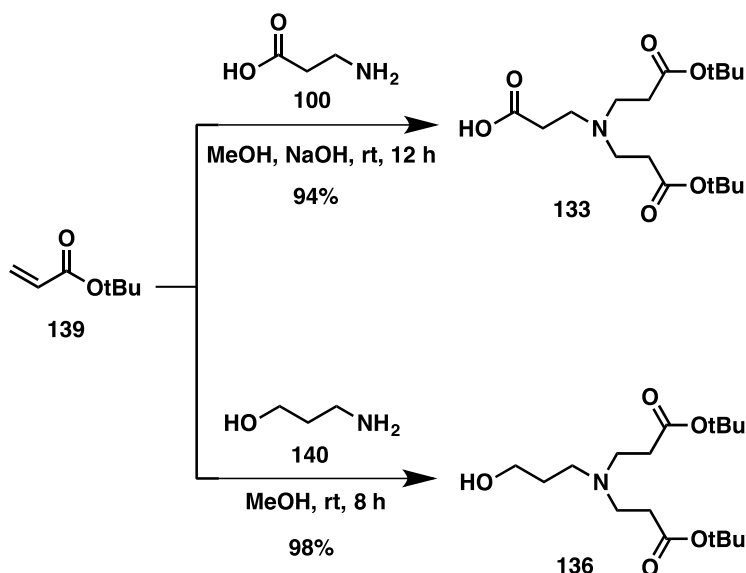

Figure 4.2. Two building blocks, **133** and **136**, for solid-phase synthesis of poly(aminoester) dendrimers.
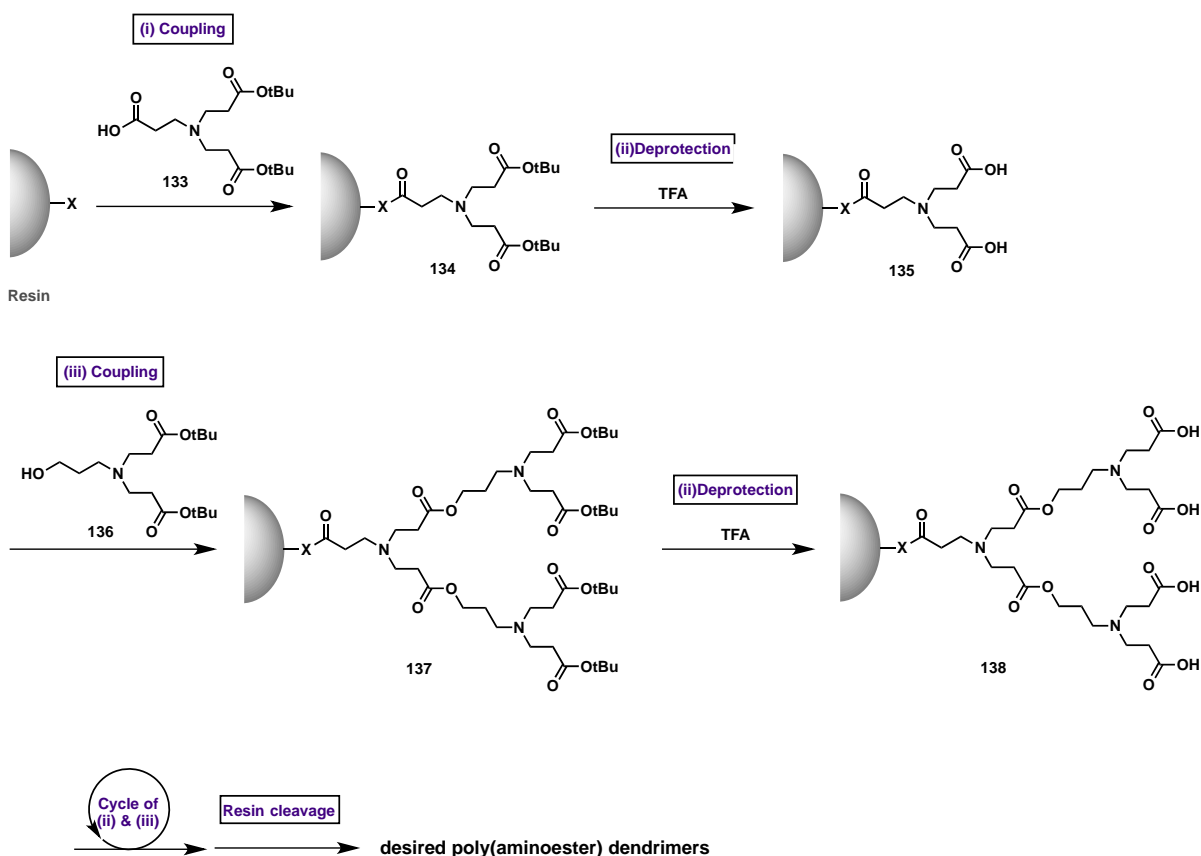
Scheme 4.2. Synthetic plan for Solid-phase synthesis of poly(aminoester) dendrimers using two designed AB$_2$ constructing units (**133** and **136**).

The preparation of building block **133** proceeded through Michael addition of free β-alanine (**100**) onto the corresponding *tert*-butyl acrylate **139**. Likewise, Michael reaction between the acrylate (**139**) and 3-aminopropanol (**140**) yielded the building block **136**. It is to note that no protection of the acid and hydroxyl group is necessary for the preparation of **133** and **136**. Both **133** and **136** were purified by chromatography easily with high yields and could be obtained in 20-gram scale (**Scheme 4.3**).

Scheme 4.3. Preparations of building blocks **133** and **136** for poly(aminoester) dendrimer constructions.

2.2. Solid-phase synthesis of biodegradable poly(aminoester) dendrimers

With the building blocks **133** and **136** in hands, we first carried out solid-phase synthesis of poly(aminoester) dendrimers using Kaiser oxime resin. The resin was first stood in anhydrous DMF for more than 4 hours of swelling before being conjugated with **133** via an ester bond linkage to yield **141**. The swelling process is very important in order to fully expose the reactive sites on the resin and offer the access to the reagent for resin coupling. Without this swelling procedure, the coupling of the resin with **133** decreased dramatically from 95% to 50% yield. Following the successful attachment of **131** onto the resin, the obtained **141** underwent further deprotection in TFA to generate **142**, which bears two carboxylic acid terminals and will serve as the focal core for the construction of poly(amidoamine) dendrimers on the solid support (**Scheme 4.4**).
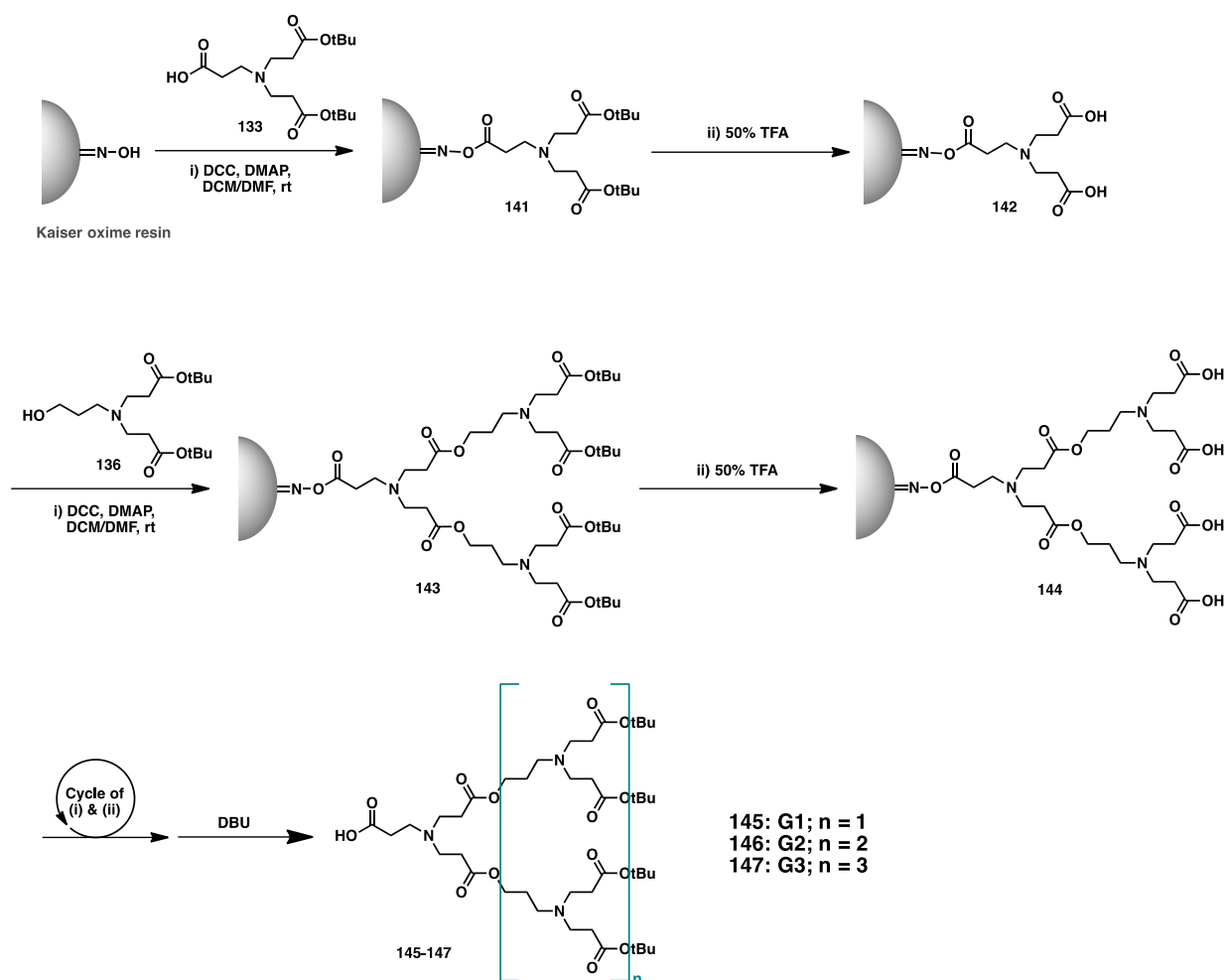
Scheme 4.4. Solid-phase synthesis of G1-G3 poly(aminoester) dendrimers **145-147** using building blocks **133** and **136**.
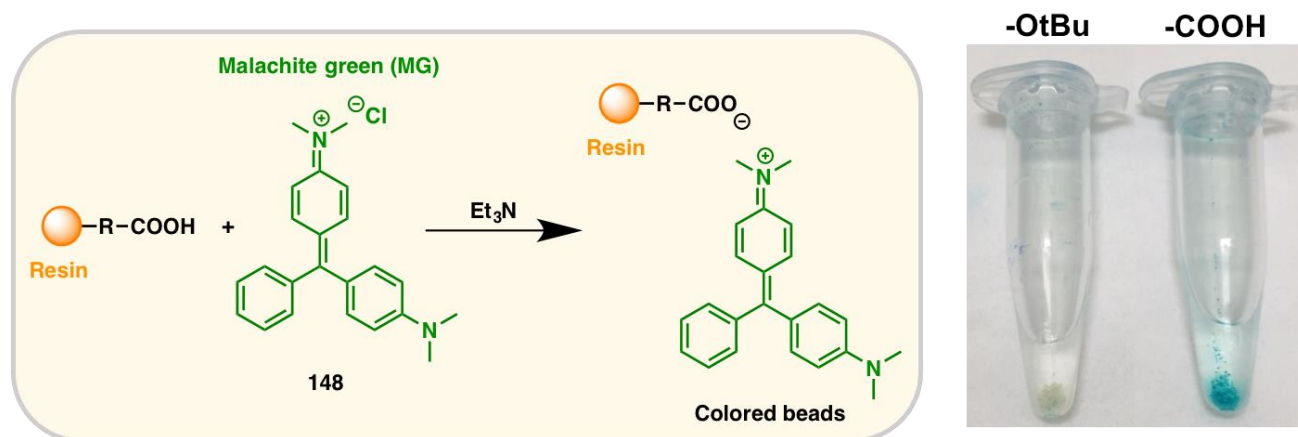
Figure 4.3. Malachite green (MG, **148**) reagent as colorimetric test for poly(aminoester) dendrimer synthesis monitoring to reveal carboxylic acids.

Coupling the acid-terminated **142** with the free hydroxyl group in building block **136** was achieved in the presence of DCC/DMAP, providing the first generation of poly(aminoester) dendrimer **145**. A color test sensitive to carboxylic acid is used to monitor this reaction. Namely, mixing the resin with malachite green solution in the presence of TEA,[13] appearance of green resin suggesting the existence of carboxylic acids, whereas no green color appearance highlighting resin harboring ester-terminating dendrimer (**Figure 4.3**). Further deprotection of the terminal ester functionalities in **143** offered the acid-terminating dendrimer **146** ready for next cycle of dendrimer growth. Iteration of the coupling and deprotection procedures generated effectively higher generation dendrimers up to G3 (**Scheme 4.4**).

Nevertheless, the cleavage of poly(aminoester) dendrimers from Kaiser oxime resin is the most challenging step since the ester linkages are labile not only in acid or base conditions but also in the presence of nucleophiles. We tried various cleavage conditions which were commonly used and reported for Kaiser oxime resin cleavage such as TEA in MeOH/DMF, NaOH in dioxane and 1,8-diazabicyclo[5.4.0]undec-7-ene (DBU) in THF/H$_2$O. Subjecting the dendrimer-bearing resin to the cleavage reagent of TEA in MeOH/DMF, no desired product could be identified. These findings suggested that a strong base is necessary for the cleavage of synthesized dendrimers from the resin whereas TEA is not strong enough. Thereafter, a typical cleavage reagent, NaOH, for Kaiser oxime resin was used but no reproducible results could be obtained. This might be ascribed to the labile ester functionalities within the dendrimers which can be hydrolyzed under alkaline condition. Notably, an organic base DBU, which is weaker than NaOH, was used to replace NaOH in order to reduce or suppress the possible hydrolysis. We used NMR to analyze the reaction products (**Figure 4.4**), and found out that there were indeed NMR signals for the expected dendrimers, which were mixed with DBU and dicyclohexyl urea (DCU), both of which were difficult to remove.[14] We tried multiple purification methods to remove these impurities. Unfortunately, none of them were successful, the final compounds were either degraded or completely disappeared. Also to note, building blocks, were also revealed in the product mixture based on NMR analysis, suggesting the possible hydrolysis of the ester functions in the poly(aminoester) dendrimers during resin cleavage step, because these starting materials should have been eliminated during the solid-phase synthesis by washing and filtration. Consequently, our results indicated that the dendritic poly(aminoester) compounds might decompose at the last step of resin cleavage as a result of the labile ester bonds.
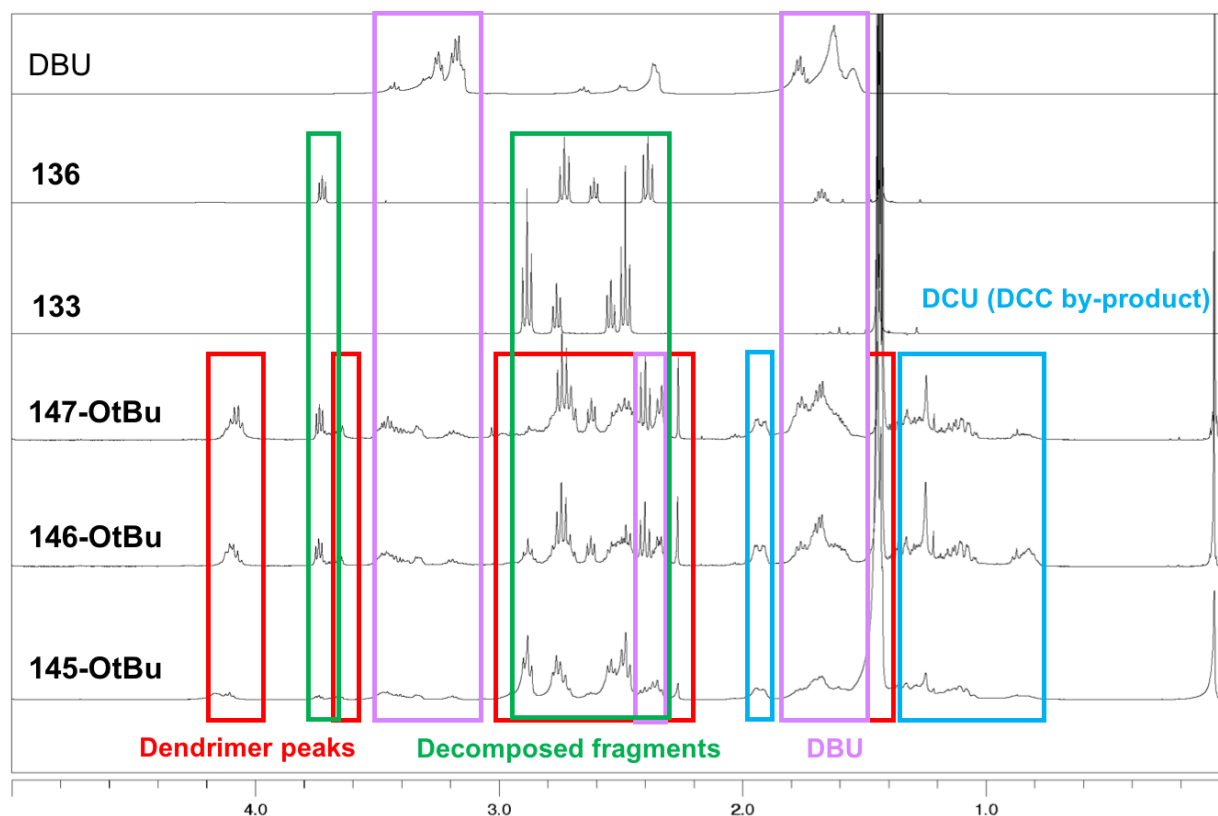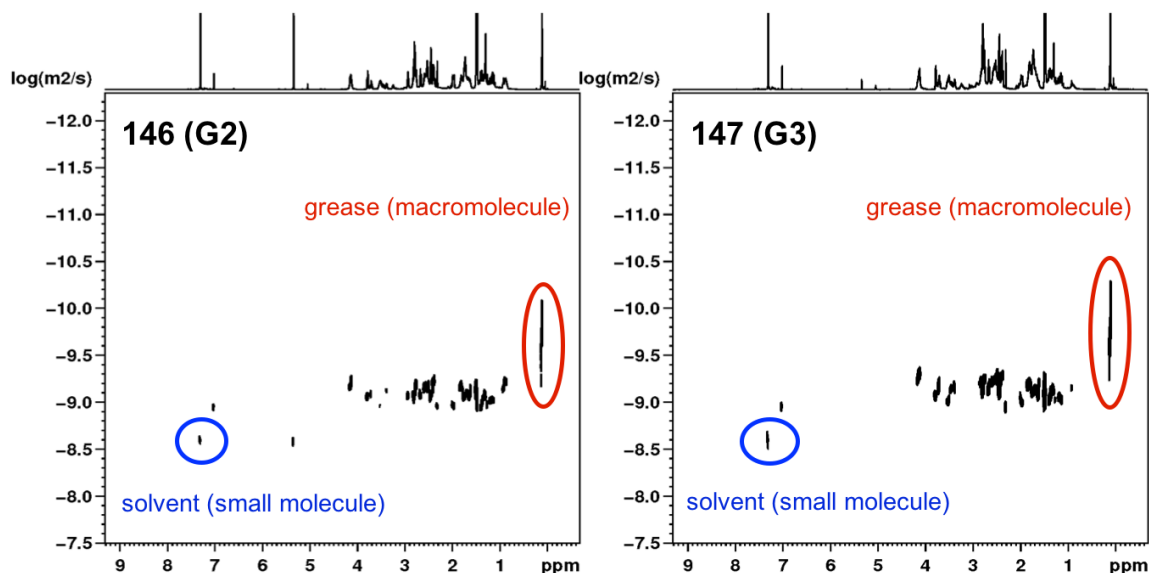
Figure 4.4. NMR traces of poly(aminoester) dendrimers **145-147** after resin cleavage treated with DBU (Signals: red-dendrimer; green-building blocks; violet-DBU; blue-DCU).

To further confirm the degradation of the poly(aminoester) dendrimer during the resin cleavage step, we performed ESI-TOF-MS (**Figure 4.5**) and 2D-DOSY analysis of the dendrimer products (**Figure 4.6**) collected from resin cleavage. HRMS measurements can provide information pertaining to the molecular weight and elemental composition whereas 2D-DOSY is a useful method to distinguish between the different components of a mixture based on their diffusion coefficients, depending on the size and shape of the molecules. Regarding to the MS analysis, we could notice only weak signals corresponding to G1 and G2 dendrimers **145** and **146**. The most intense MS signals belonged to building blocks **133**, **136**, DBU and the associated impurities. These results are consistent with those obtained from NMR studies. Further ^{1}H-DOSY analysis did not reveal any macromolecular species. The larger G2 and G3 dendrimers **146** and **147** were used as reference and no signal of macromolecules as dendrimers was identified (**Figure 4.6**). Collectively, these results confirmed the difficulty to get the intact poly(aminoester) dendrimers

from resin cleavage, highlighting the synthetic challenge for synthesizing poly(aminoester) dendrimers.
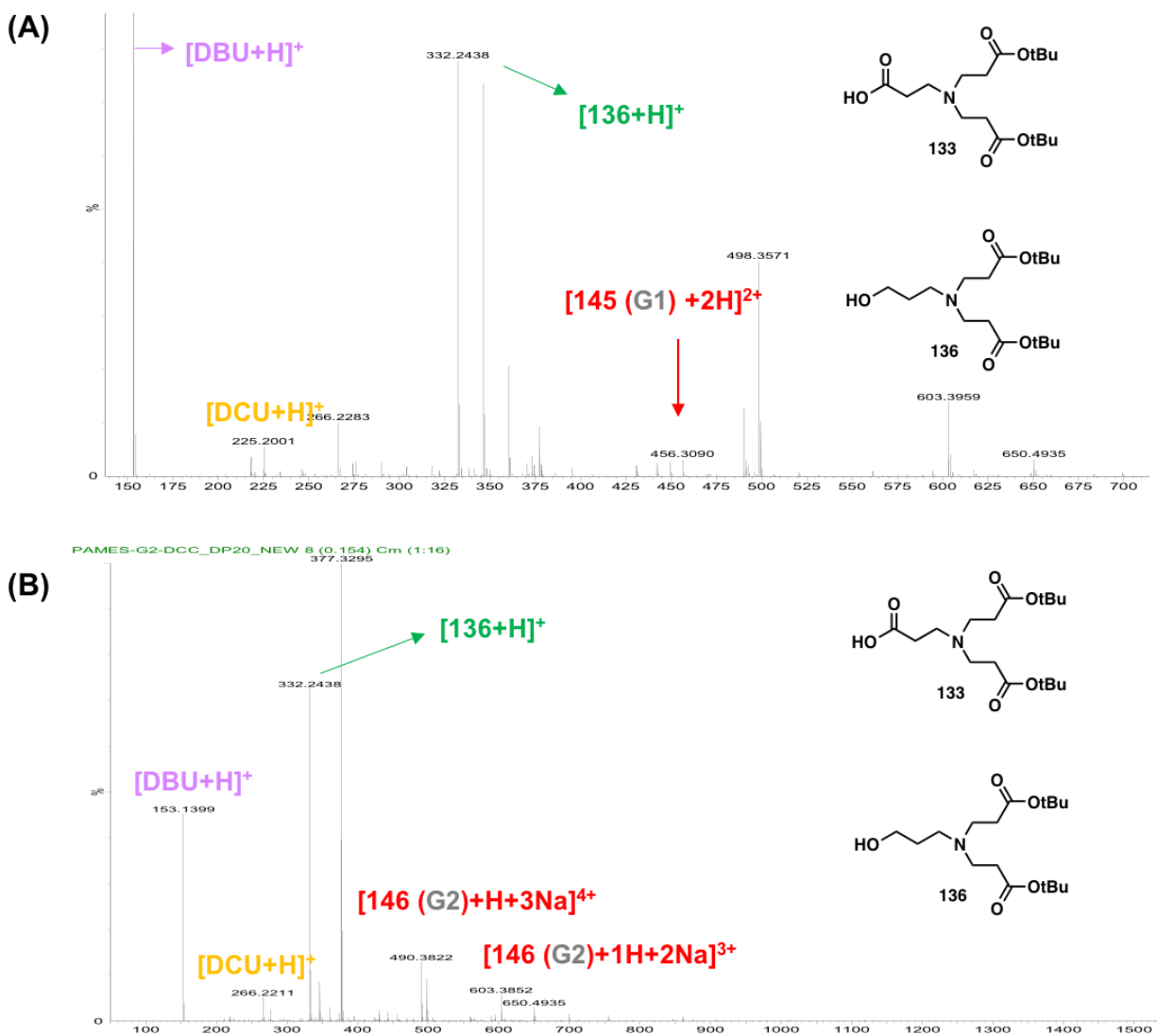
Figure 4.5. ESI-TOF-MS spectra of poly(aminoester) dendrimers **(A) 145** (G1) and **(B) 146** (G2) after DBU cleavage.

Figure 4.6. 2D-DOSY spectra of poly(aminoester) dendrimers **146** (G2) and **147** (G3) after DBU cleavage.

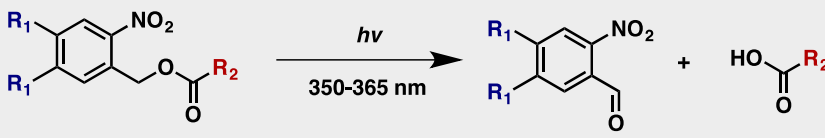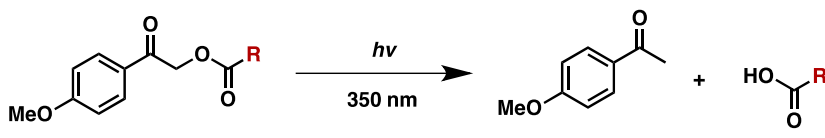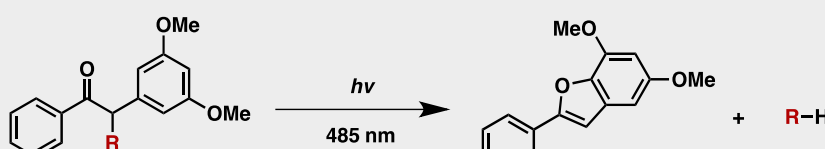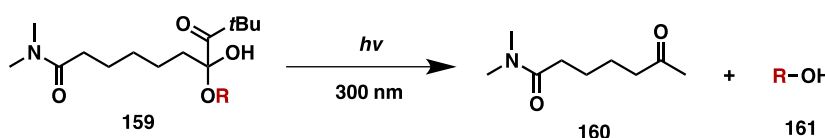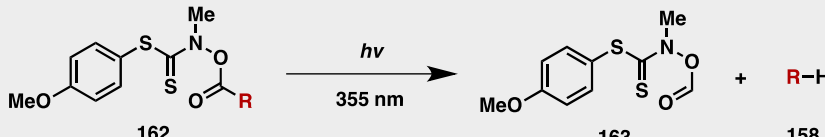## 2.3. Construction of poly(aminoester) dendrimers using photolabile resin

As presented above, Kaiser oxime resin appeared not suitable for poly(aminoester) dendrimer synthesis because the resin cleavage methods with either basic or nucleophilic reagents gave rise to the dendrimer degradation. Taking the consideration of the labile poly(aminoester) dendrimers, other solid resin requiring acidic cleavage may not be suitable either. Therefore, we turned to the photolabile resins in the hope that resin cleavage could be realized under specific light irradiation, which could avoid dendrimer degradation under strong acid or base cleavage cocktails. Photolabile resin bearing photoactivatable linkers have been shown considerable promise for releasing compounds such as peptides, oligonucleotides, carbohydrate derivatives and small molecules from solid supports.[15] They offer mild conditions of light irradiation for resin cleavage and the cleaved compounds can be directly applicable for biological testing. In addition, most photolabile resins are robust and stable in both acidic and basic conditions required for various chemical reactions.

Table 4.1 listed the most commonly used photolabile resins in solid-phase synthesis along with their photoactivatable linkers and the related photocleavage reactions. Early work on linkers mainly based on the *o*-nitrobenzyloxy group, and many variants of this kind of linkers have since

been reported. Resins with *o*-nitrobenzyloxy linkers are still one of the most popular photolabile resins nowadays. Cleavage of substrates from the *o*-nitrobenzyloxy linker (**Table 4.1**, *P1*) can be achieved by irradiating at 350-365 nm.[15-18] Also resins based on the photolabile phenacyl linker (**Table 4.1**, *P2*) have been developed. Similar to the nitrobenzyl linkers, cleavage from the phenacyl linker can be realized by irradiating at 350 nm.[19] In addition, photolabile groups such as the benzoin group[20,21](**Table 4.1**, *P3*), pivaloyl group[22] (**Table 4.1**, *P4*) and thiohydroxamic functionality (**Table 4.1**, *P5*) have all been adapted as linker units for resins used in solid-phase synthesis with varied degrees of success. Among all these photoremovable linkers listed in **Table 4.1**, *o*-nitrobenzyl based linkers have the advantages of fast release kinetics, hence being widely applied in SPS. Also, the increased electron density at the benzylic position caused bathochromic shift and allowed photoirradiation to be undertaken under longer UV wavelength, hence avoiding possible photodamage of the compounds.

In our synthesis of poly(aminoester) dendrimers, we employed a photolabile resin based on the *o*-nitroveratryl group (**Table 4.1**, *P1*), which is capable of releasing final product upon UV irradiation at 350-365 nm (**Scheme 4.4**). We also incorporated the amino acid phenylalanine to the resin, serving as an indicator, because phenylalanine has the characteristic UV absorption which facilitate product tracing using UV detection. Using the similar strategy as we developed for Kaiser oxime resin, we carried out the solid-phase synthesis of poly(aminoester) dendrimers with the phenylalanine pre-loaded resin. As a proof-of-concept study, we only performed synthesis of small generation dendrimers. Photolytic cleavage of the dendrimers from resins was performed with pulsed laser at 331 nm and UV lamp with 365 nm UV irradiation in MeOH/H_2O solution. The cleavage mixture was analyzed using NMR and HRMS. Unfortunately, we were not able to provide evidence for the desired poly(aminoester) dendrimers. Further efforts are necessary to clarify the underlying problems associated with photocleavage in order to identify the best condition to realize safe and effective dendrimer removal from the solid resin.

Table 4.1. Photolytic reactions of various photolabile linkers.

	Photoremovable linkers	Photolytic reactions
P1	Nitrobenzyl groups (NBOC/NVOC)	148: NBOC, R1= H 149: NVOC, R1= OMe → 150: R1= H 151: R1= OMe + 152
P2	Phenacyl group	153 → 154 + 155
P3	Benzoin group	156 → 157 + 158
P4	Pivaloyl group	159 → 160 + 161
P5	Thiohydroxamic group	162 → 163 + 158
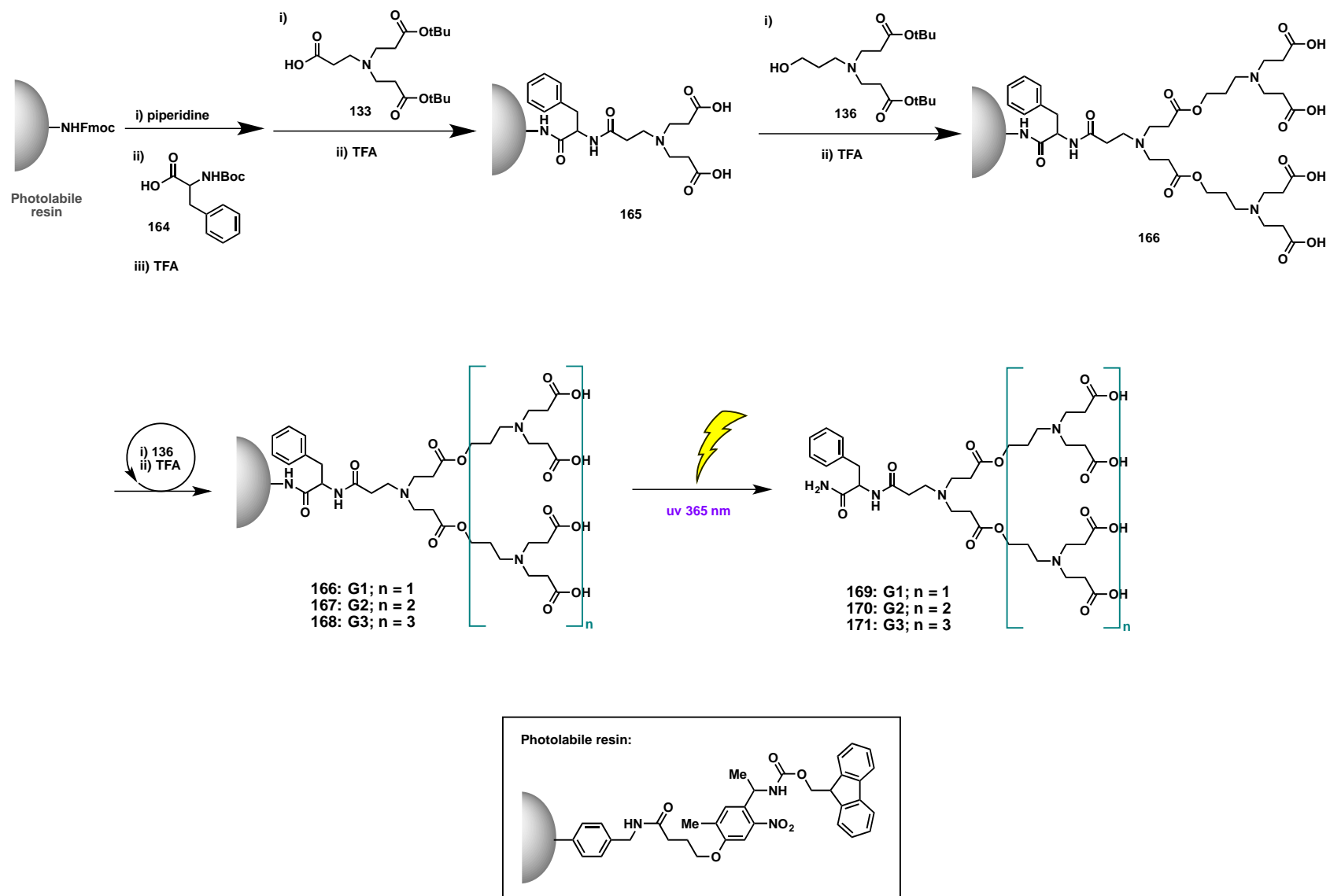
Scheme 4.5. Preparation of poly(aminoester) dendrimers using photolabile resin via photocleavage.

3. Summary

Poly(aminoester) dendrimers hold great promise as biodegradable nanocarriers for drug delivery thanks to their advantageous properties including biodegradability, potentially lower toxicity and possibility of diverse chemical conjugations. However, synthesis of such dendrimers is challenging because of the labile feature of numerous ester functionalities within the dendrimer backbones. Part of my PhD thesis has been dedicated to the synthesis of poly(aminoester) dendrimers using solid-phase synthesis in the view to overcome the limitation encountered during the solution-phase synthesis. We attempted to synthesize poly(aminoester) dendrimers using similar strategy which we developed for the solid-phase synthesis of inverse PAMAM dendrimers using Kaiser oxime resin. Regrettably, this method was not able to deliver the desired dendritic molecules because the labile poly(aminoester) dendrimers were degraded during the resin cleavage under either basic or nucleophilic conditions. We then turned to the photolabile resin for the solid-phase dendrimer synthesis in the hope that the final compounds could be safely cleaved from the resin via photo-irradiation, while avoiding the damage of amine and ester functionalities. Unfortunately, our current results were not successful to deliver the expected products. Further efforts with detailed studies are necessary to clarify the underlying problems associated with photochemical reactions. We are working in this direction.

4. Experimental section

General

Kaiser oxime resin was obtained from Merck and Fmoc photolabile resin was purchased from Iris Biotech GmbH. The other chemicals, solvents, and reagents were obtained from Acros, Aldrich and TCI, and used without further purification. Mass spectra were acquired on either an Agilent ESI-TOF-MS and MALDI-TOF-MS (positive mode electrospray) mass spectrometer instrument as indicated. The exact mass measurement was done in triplicate with a double internal calibration. ^{1}HNMR spectra were recorded at 400 or 500 MHz and ^{13}C NMR spectra recorded at 100 MHz on Bruker Avance III 400, Bruker Avance III 500 or JEOL ECS 400 spectrometers. High-performance liquid chromatography (HPLC) and gel permeation chromatography (GPC) experiments were obtained using an Agilent HPLC system (1100 series).

Synthesis of building blocks 133 and 136

Building block 133
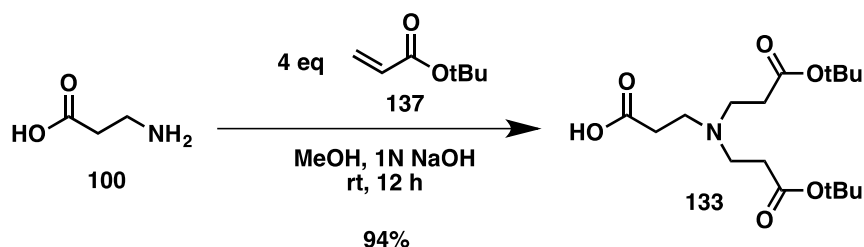
tert-Butyl acrylate (**139**, 7.2 g, 56.2 mmol) was treated with β-alanine (**100**) (2.0 g, 22.45 mmol) in MeOH (50 mL) and add 1N NaOH (20 mL, 1.65 mol). The reaction solution was stirred at rt under N_2 for 12h. The resulting mixture was partitioned between DCM and H_2O. The organic layer was washed with brine and evaporated under reduced pressure to give an oily mixture which was further purified by column chromatography (DCM/MeOH=12/1) to provide **133** as a white solid (7.2 g, 94%): R_f 0.65 (DCM/MeOH = 12/1, v/v); ^{1}H NMR (400 MHz, CDCl$_3$) δ 1.43 (s, 18H),

2.46 (t, J = 8.0 Hz, 4H), 2.52 (t, J = 8.0 Hz, 2H), 2.76 (t, J = 8.0 Hz, 2H), 2.87 (t, J = 8.0 Hz, 4H); ^{13}C NMR (100 MHz，CDCl$_3$) δ27.96, 30.20, 32.06, 48.15, 49.27, 81.36, 170.58; HRMS (FAB): calcd for C$_{17}$H$_{33}$NO$_6$ [M+H]$^+$ 346.2230; found at m/z 346.2233.

Building block 136
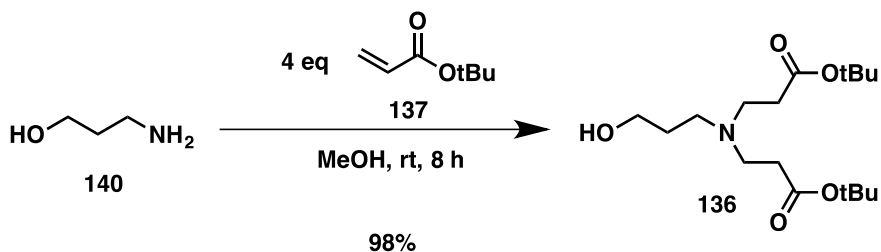
tert-Butyl acrylate (**139**, 8.54 g, 66.62 mmol) was treated with 3-amino-1-propanol (**140**) (2.0 g, 26.62 mmol) in MeOH (50 mL). After stirring at room temperature under N$_2$ for 8h. The resulting mixture was partitioned between DCM and H$_2$O. The organic layer was washed with brine and concentrated under reduced pressure to give an oily mixture which was further purified by column chromatography (DCM/MeOH = 15/1) to provide **136** as a pale amber oil (8.6 g, 98%): R$_f$ 0.6 (DCM/MeOH = 13/1, v/v); ^{1}H NMR (400 MHz, CDCl$_3$) δ 1.44 (s, 18H), 1.68 (tt, J = 4.0, 4.0 Hz, 2H), 2.40 (t, J = 8.0 Hz, 4H), 2.62 (t, J = 4.0 Hz, 2H), 2.74 (t, J = 8.0 Hz, 4H), 3.74 (t, J = 6.0 Hz, 2H); ^{13}C NMR (100 MHz, CDCl$_3$) δ 28.05, 28.27, 33.23, 49.29, 53.07, 63.22, 80.66, 171.71; HRMS (FAB): calcd for C$_{17}$H$_{35}$NO$_5$ [M+H]$^+$ 332.2437; found at m/z 332.2437.

General procedure of solid-phase synthesis for poly(aminoester) dendrimers

Using Kaiser oxime resin

The suspension of oxime resin (0.22 g, 0.2 mmol) in RV bottle was added DMF under Ar and bubbled with Ar for 2 h. After removal of DMF, the following resin in RV bottle was added the solution of **133** (2.0 eq) in DMF/DCM (4/1, v/v), DCC (2.0 eq) and DMAP (2.0 eq). The following mixture was bubbled with N_2 for 12 h (for the first introduction of **133**) or 4 h (for rest of introduction of **136**). After reaction, the solvent was removed and the resulting mixture was washed with DMF three times. To the resulting solution was added acetic anhydride in DMF (100μL, 10% v/v solution). After washed with DMF three times, the reaction mixture was added was trifluoroacetic acid (TFA) in DCM (50 %, 10 mL) for deprotection. After 1 h of reaction, the solution was removed and the mixture was washed with DCM and DMF three times.

Using Fmoc photolabile resin

The suspension of Fmoc photolabile resin (0.25 g, 0.2 mmol) in RV bottle was added DMF under Ar and bubbled with Ar for 2 h. After removal of DMF, the reagent of 20% piperidine in DMF was treated for 15 min for Fmoc deprotection. After washing with DMF, the following resin in RV bottle was added the solution of phenylalanine (2.0 eq) in DMF, PyBOP (2 eq) and 0.4 M *N*-methylmorpholine (NMM), shaken under Ar. After 8 h, the solvent was removed and the resulting resin was washed with DMF. Then a solution of **133** in DMF/DCM (4/1, v/v), DCC (2.0 eq) and DMAP (2.0 eq) was added. The following mixture was bubbled with Ar for 12 h (for the first introduction of **133**) or 4 h (for rest of introduction of **136**). After reaction, the solvent was removed and the resulting mixture was washed with DMF three times. To the resulting solution was added acetic anhydride in DMF (100μL, 10% v/v solution). After washed with DMF three times, the reaction mixture was added was trifluoroacetic acid (TFA) in DCM (50 %, 10 mL) for deprotection. After 1 h of reaction, the solution was removed and the mixture was washed with DCM and DMF three times.

Colorimetric monitoring

Ninhydrin test for aryl amine: 10 beads of resin were taken from the reactor and transferred to a test tube, followed by an addition of 30 μl cocktail of ninhydrin reagent (50 mg/mL of ninhydrin (**127**) in EtOH, 4 g/mL of phenol in EtOH and pyridine). Then checking the color change after 5 min heating at 120°C. (Positive: purple; negative: yellow)

MG test for carboxylic acid: 10 beads of resin were taken from the reactor and transferred to a test tube, followed by an addition of 0.3 mL MG solution (0.25% Malachite green (**148**) in EtOH) and 10 μL TEA. After 10 min of suspension at rt, the beads were washed several times with EtOH until the solution was no longer colored and observed the resin color. (Positive: green; negative: colorless)

Photolytic procedures

50 mg of resins bearing the deprotected dendrimers were placed in the plate and covered with a solution of MeOH/H$_2$O = 1/4 (v/v) A glass slide was fixed on the top of the plate, which was then irradiated at UV 365 nm for 3 h. After UV irradiation, the resulting mixture was concentrated under reduced pressure to give an oily mixture which was further determined by UV, NMR and HRMS spectra.

5. References

[1]   C. Bouillon; A. Tintaru; V. Monnier; L. Charles; G. Quélével; L. Peng. Synthesis of poly(amino)ester dendrimers via active cyanomethyl ester intermediates. *J. Org. Chem.*, **2010**, *75*, 8685-8688.

[2]   Y. Wang; G. Quélével; L. Peng. The seemingly trivial yet challenging synthesis of poly(aminoester) dendrimers. *Curr. Med. Chem.*, **2012**, *19*, 5011-5028.

[3]   P. Moreno; G. Quélével; L. Peng. Synthesis of poly(aminoester) dendrimers via 'click' chemistry in combination with the divergent and convergent strategies. *Tetrahedron Lett.*, **2015**, *56*, 4043-4046.

[4]   D. Xu; K. Zhang; X. Zhu. Fast growing dendritic poly(ester–amines) from alternate reaction of EDA and TMPTA. *Tetrahedron Lett.*, **2005**, *46*, 2503-2505.

[5]   Y. Shen; X. Ma; B. Zhang; Z. Zhou; Q. Sun; E. Jin; M. Sui; J. Tang; J. Wang; M. Fan. Degradable dual pH- and temperature-responsive photoluminescent dendrimers. *Chem. Eur. J.*, **2011**, *17*, 5319-5326.

[6]   D. Soto-Castro; J. A. Cruz-Morales; M. T. R. Apan; P. Guadarrama. Synthesis of non-cytotoxic poly(ester-amine) dendrimers as potential solubility enhancers for drugs: Methotrexate as a case study. *Molecules*, **2010**, *15*, 8082-8097.

[7]   Y. Sha; L. Shen; X. Hong. A divergent synthesis of new aliphatic poly(ester-amine) dendrimers bearing peripheral hydroxyl or acrylate groups. *Tetrahedron Lett.*, **2002**, *43*, 9417-9419.

[8]   D. Shi; Y. Sha; F. Wang; Q. Tian. Synthesis and photophysical properties of poly(ester−amine) dendrimers with focal 4-amino-N-benzylphthalimide, as sensitive media probes and switchable proton sensors. *Macromolecules*, **2008**, *41*, 7478-7484.

[9]   X. Ma; J. Tang; Y. Shen; M. Fan; H. Tang; M. Radosz. Facile synthesis of polyester dendrimers from sequential click coupling of asymmetrical monomers. *J. Am. Chem. Soc.*, **2009**, *131*, 14795-14803.

[10]   M. Li; L. Q. Xu; L. Wang; Y. P. Wu; J. Li; K.-G. Neoh; E.-T. Kang. Clickable poly(ester amine) dendrimer-grafted Fe3O4 nanoparticles prepared via successive Michael addition and alkyne-azide click chemistry. *Polym. Chem.*, **2011**, *2*, 1312-1321.

[11] A. Y.-T. Huang; C.-H. Tsai; H.-Y. Chen; H.-T. Chen; C.-Y. Lu; Y.-T. Lin; C.-L. Kao. Concise solid-phase synthesis of inverse poly(amidoamine) dendrons using AB2 building blocks. *Chem. Commun.*, **2013**, *49*, 5784-5786.

[12] A. Y.-T. Huang; S. Patra; H.-T. Chen; C.-L. Kao; E. E. Simanek. Solid-phase synthesis of libraries of triazine dendrimers and orthogonal staining methods for tracking reactions on resin. *Asian J. Org. Chem.*, **2016**, *5*, 860-864.

[13] M. E. Attardi; G. Porcu; M. Taddei. Malachite green, a valuable reagent to monitor the presence of free COOH on the solid-phase. *Tetrahedron Lett.*, **2000**, *41*, 7391-7394.

[14] M.-k. Leung; J.-L. Lai; K.-H. Lau; H.-h. Yu; H.-J. Hsiao. S,S-Dimethyl dithiocarbonate: A convenient reagent for the synthesis of symmetrical and unsymmetrical ureas. *J. Org. Chem.*, **1996**, *61*, 4175-4179.

[15] J. Tulla-Puche; F. Albericio. The power of functional resins in organic synthesis. John Wiley & Sons, Inc.: **2008**.

[16] C. P. Holmes. Model studies for new o-nitrobenzyl photolabile linkers: Substituent effects on the rates of photochemical cleavage. *J. Org. Chem.*, **1997**, *62*, 2370-2380.

[17] C. P. Holmes; D. G. Jones. Reagents for combinatorial organic synthesis: Development of a new o-nitrobenzyl photolabile linker for solid phase synthesis. *J. Org. Chem.*, **1995**, *60*, 2318-2319.

[18] B. Ruhland; A. Bhandari; E. M. Gordon; M. A. Gallop. Solid-supported combinatorial synthesis of structurally diverse β-lactams. *J. Am. Chem. Soc.*, **1996**, *118*, 253-254.

[19] S.-S. Wang. Solid phase synthesis of protected peptides via photolytic cleavage of the .alpha.-methylphenacyl ester anchoring linkage. *J. Org. Chem.*, **1976**, *41*, 3258-3261.

[20] A. Routledge; C. Abell; S. Balasubramanian. The use of a dithiane protected benzoin photolabile safety catch linker for solid-phase synthesis. *Tetrahedron Lett.*, **1997**, *38*, 1227-1230.

[21] H. B. Lee; S. Balasubramanian. Studies on a dithiane-protected benzoin photolabile safety catch linker for solid-phase synthesis. *J. Org. Chem.*, **1999**, *64*, 3454-3460.

[22] S. Peukert; B. Giese. The pivaloylglycol anchor group: A new platform for a photolabile linker in solid-phase synthesis. *J. Org. Chem.*, **1998**, *63*, 9045-9051.

# Chapter III: Self-assembly synthesis of supramolecular dendrimers

Section 5. Construction of supramolecular dendrimers as nanotheranostics
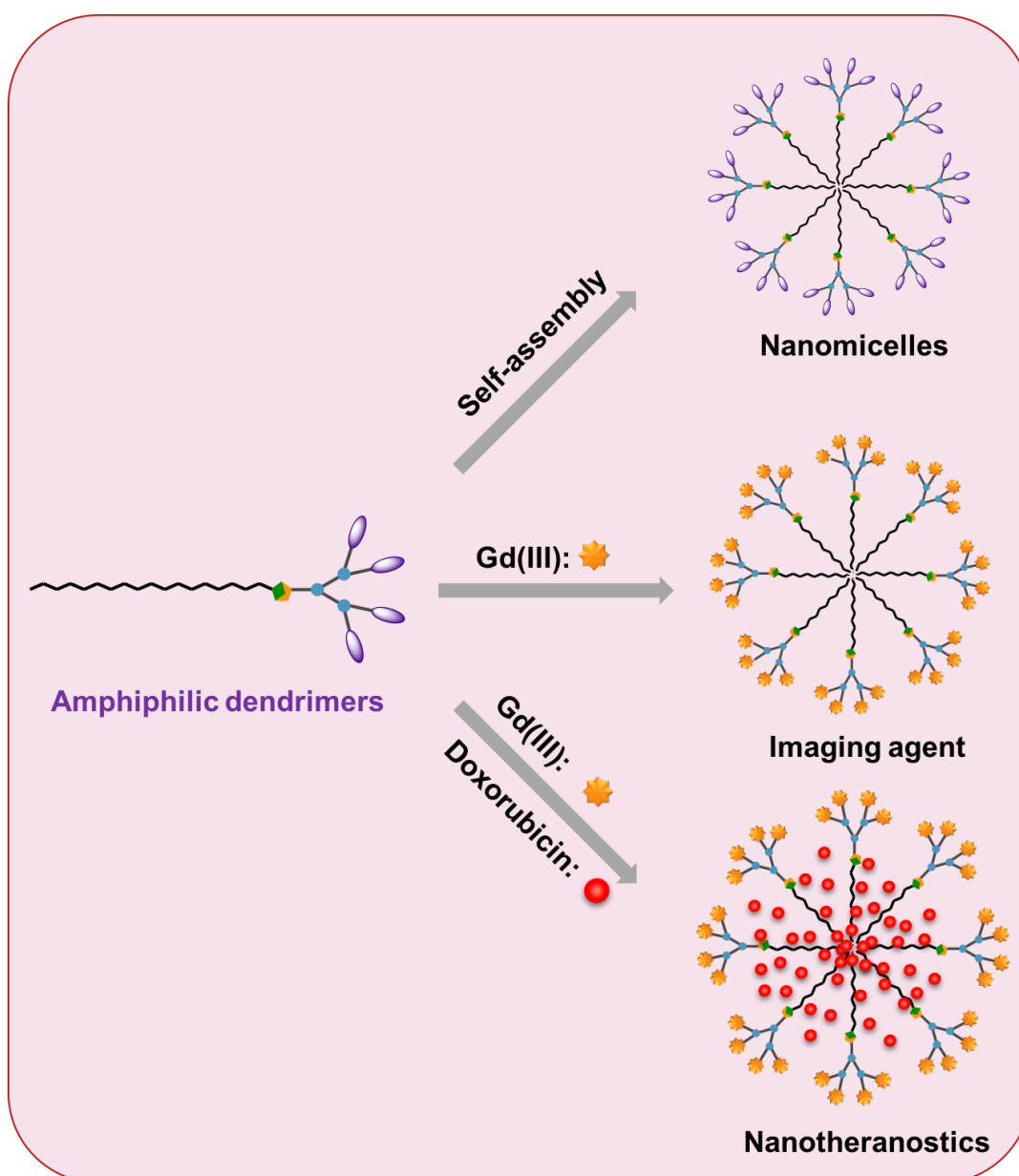
As aforementioned, conventional divergent and convergent methods for dendrimer synthesis (**Figure 5.1A** and **Figure 5.1B**) have their limitations, in particular for high generation dendrimers. Accordingly, alternative strategies such as solid-phase synthesis and self-assembly approach have been proposed for dendrimer synthesis as subjects of my PhD project. In the first part of my PhD program, we mainly focus on developing solid-phase dendrimer synthesis. The second part of my PhD thesis is dedicated to the self-assembly approach to build supramolecular dendrimers (**Figure 5.1C**) for elaborating nanosystems for bioimaging and drug delivery in the view to providing effective diagnostics and therapy for cancer management.

1. Introduction

Self-assembly is an emerging and powerful means to construct supramolecular architectures in modern molecular science.[1-3] Of particular value is the ability of self-assembled supramolecules to behave as more than the sum of their individual units, and show completely new properties.[4] In 1996, Zimmerman et al explored self-assembly of dendrons through hydrogen bonding to generate supramolecules.[5] Recently, Percec has extended the supramolecular dendrimersomes via self-assembly of amphiphilic dendrons.[6,7] Our group has successfully applied the self-assembly approach, by using small amphiphilic dendrons, to create various supramolecular dendrimer nanostructures for drug and nucleic acid delivery.[8,9] The employed small amphiphilic dendrons simply bear PAMAM dendritic wedges as polar heads and long alkyl chains as the non-polar portions. By varying the size, the generation and the chemistry of the polar dendrons as well as the nonpolar alkyl chains, the size, shape, our group have demonstrated that the function of the supramolecular dendrimer nanostructure can be modulated for controlled and on-demand delivery,[8-12] which has been proven to be very effective in various cancer models *in vitro* and *in vivo*, offering a new perspective in molecular engineering of functional dendrimers in nanotechnology-based biomedical applications.
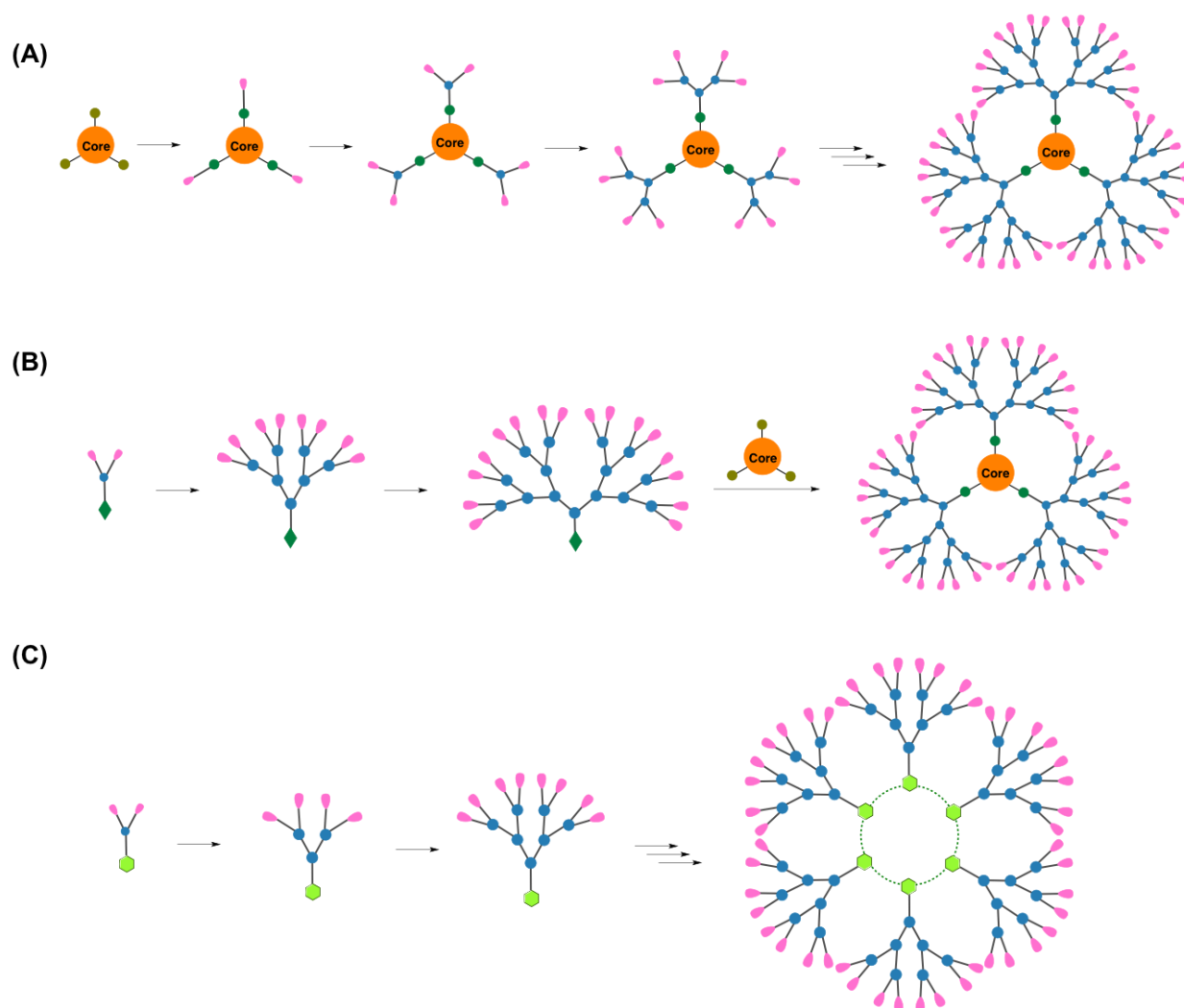
Figure 5.1. Illustrations of high generation dendrimer synthesis using: **(A)** Conventional divergent method; **(B)** Conventional convergent method; and **(C)** Self-assembly construction.
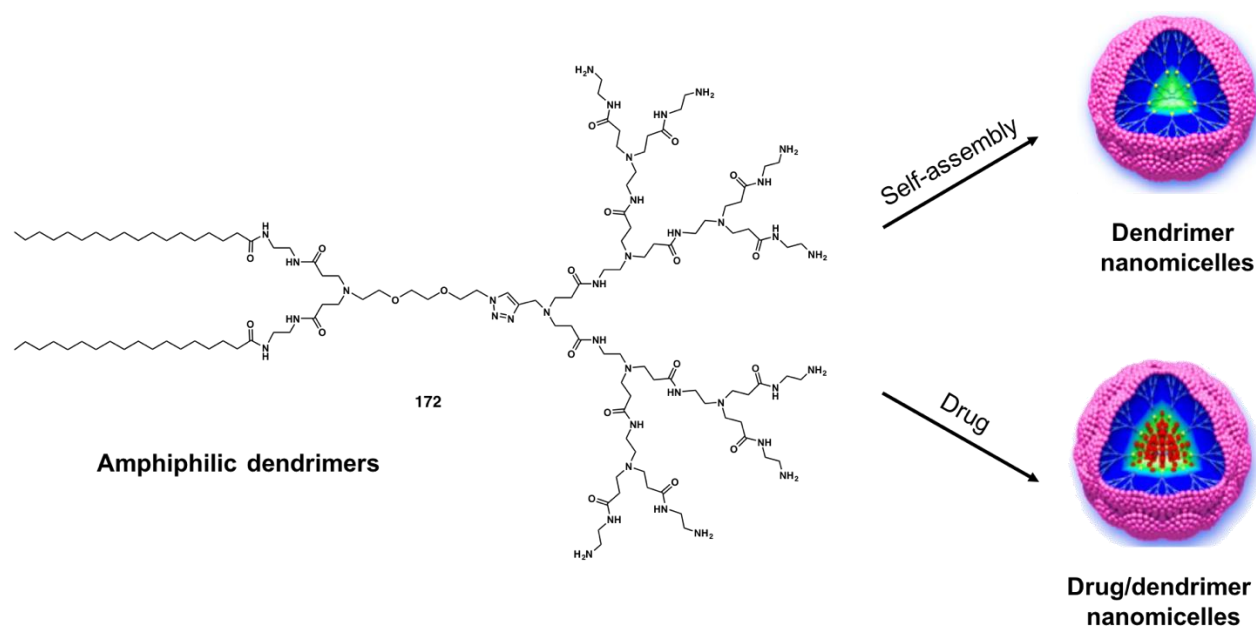
Figure 5.2. Schematic presentation of self-assembly of amphiphilic dendrimers into supramolecular dendrimers for gene and drug delivery.[9]

In particular, we have recently established an innovative drug delivery system based on self-assembled amphiphilic dendrimer supramolecular nanomicelles (**Figure 5.2**).[9] These nanomicelles have large void space in their core to encapsulate anticancer drug with high loading capacity. The resulting drug-encapsulated nanomicelles can effectively enhance drug potency and combat drug resistance by significantly promoting cellular uptake and decreasing efflux of the anticancer drug.[9] Moreover, this drug delivery system can remarkably reduce the drug toxicity. Motivated by the promising results obtained using these self-assembling supramolecular dendrimer nanomicelles for drug delivery, we would like to further integrate imaging platform in combination with therapeutic potency into our dendrimer nanomicelles to establish nanosystems for early and precise diagnosis along with safe and effective treatment for personalized medicine in cancer therapy.

It is well known that early and precise diagnosis is a key issue for successful management of cancer in addition to safe and effective treatment and that the application of nanotechnology for targeted delivery of diagnostic and therapeutic agents is widely expected to bring breakthrough for cancer treatment. This is because nanosized carriers with tailored properties can protect the diagnostic and/or therapeutic agents from degradation, increase their bioavailability, and most

importantly, deliver them selectively to tumor lesion via Enhanced Permeation and Retention (EPR) effect.[13] The EPR effect can increase local concentration of the agent at the tumor sites while sparing healthy tissues and organs, hence achieving better diagnostics sensitivity and resolution as well as therapeutic efficacy yet with considerably reduced toxicity. Particularly exciting are the recent efforts to engineer functional nanosystems to integrate therapeutic and diagnostic platforms into a combined "theranostic" approach, allowing diagnosing, grading, staging and treating cancer, and at the same time, monitoring treatment response to assess therapeutic efficacy for personalized medicine.[14]

On the basis of the promising perspective of nanotheranostics and the encouraging results with our self-assembling amphiphilic dendrimer nanomicelles, we would like to develop self-assembling dendrimer based nanotheranostics for cancer treatment (**Figure 5.3**). Among the different noninvasive tumor imaging modalities, magnetic resonance imaging (MRI) has superior resolution, with the potential to detect small tumor lesions. In my PhD project, we propose to develop self-assembling dendrimer nanomicelles for combined MRI and anticancer drug delivery with a view to establishing innovative theranostics for cancer therapy.
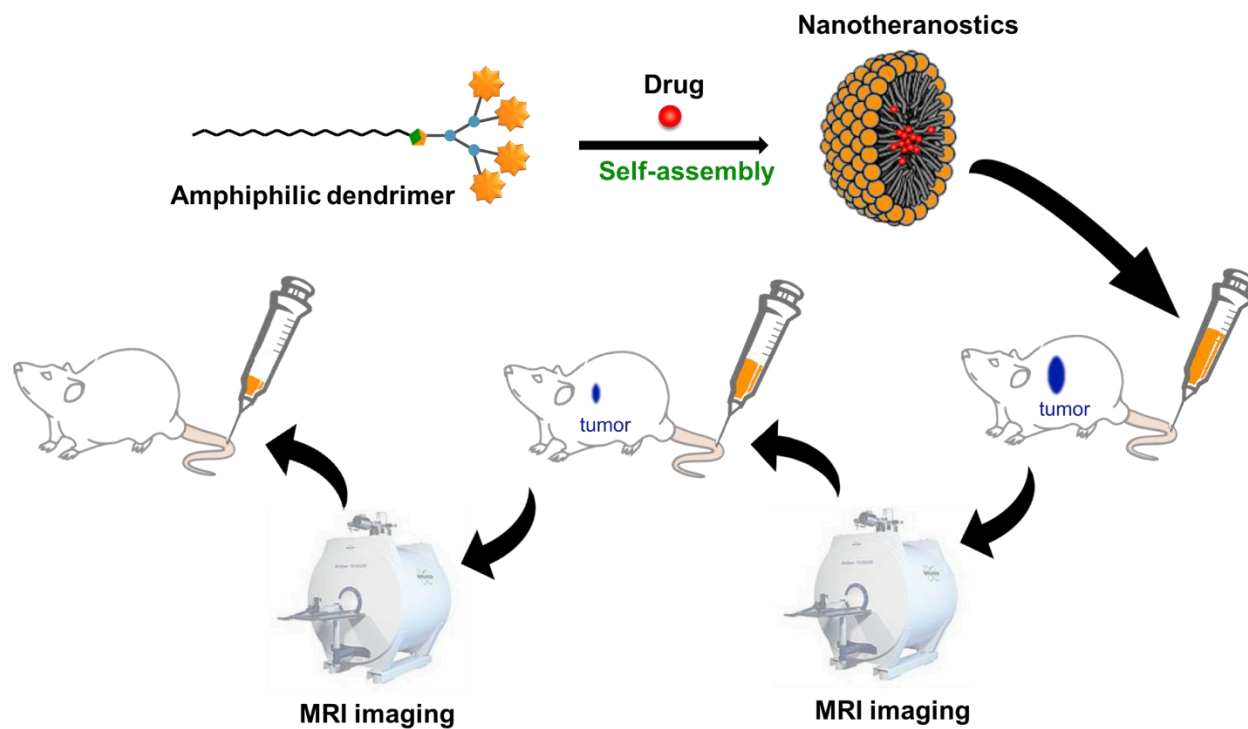
Figure 5.3. General concept of self-assembling amphiphilic dendrimers as nanotheranostics combining imaging diagnosis and therapy.

Magnetic resonance imaging (MRI)
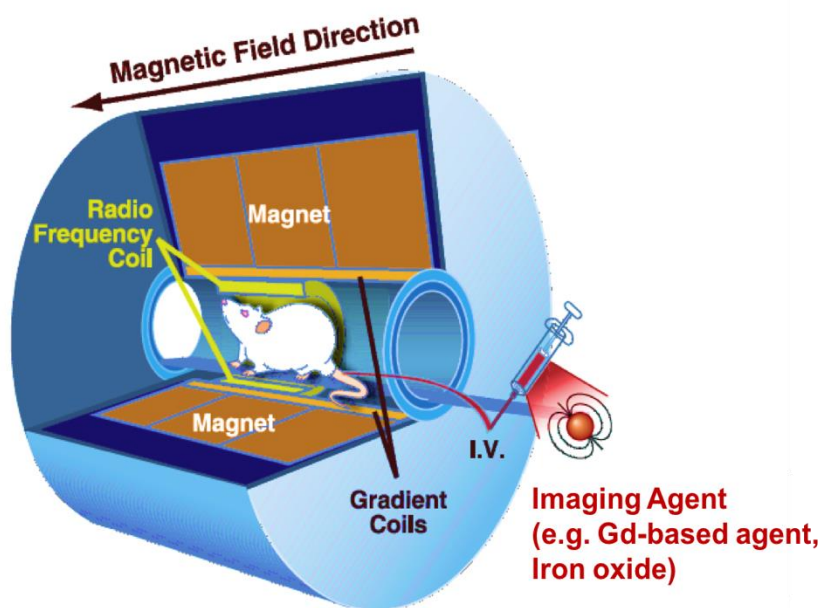
Figure 5.4. General principle of MRI imaging.[15]

Magnetic resonance imaging (MRI) is a powerful imaging tool that produces high resolution images without requiring the application of harmful radiation.[16] This technique is similar to nuclear magnetic resonance (NMR) where a proton density image of the tissue is studied to generate an MRI image. In general, the basis for MRI signal is the precession of water hydrogen nuclei within a small magnetic field. Under the effect of the external magnetic moment, the protons can return themselves to original aligned state after applied the radiofrequency (RF) pulses (**Figure 5.4**). The signal that is generated contains information on water density and its environment which will be reconstructed to images via a computer to generate MRI images.

In order to increase the imaging intensity, resolution and contrast, MRI contrast agent based on paramagnetic metal ions such as of manganese (Mn), iron (Fe), and gadolinium (Gd) have been used to shorten the relaxation parameters of water for better imaging.[17] Although MRI has good spatial resolution, it suffers from low sensitivity. To overcome this, it is necessary to use relatively high concentrations of contrast agents. However, the administration of high doses of these contrast agents leads to concerns over accumulation and toxicity such as Gd(III) MRI agents associated with slow excretion and toxicity due to long-term accumulation,[18] whilst ferric ions are not suitable

for certain body areas such as the gastrointestinal (GI) tract, which produces gastric irritation and slow clearance of the contrast agent.[19] Therefore, reagents (**Figure 5.5**) such as diethyltriaminepentaacetic acid (DTPA) and 1,4,7,10-tetraazacyclododecane-1,4,7,10-tetraacetic acid (DOTA) have been developed for chelating Gd(III) and marketed for MRI. DOTA has superior formation constant for the chelating with Gd(III) over DTPA, although Gd(III)/DOTA formation is slow and needs heating or microwave irradiation during complexation. In addition, DOTA was conjugated to monoclonal antibodies by attachment of one of the four carboxyl groups as an amide, with the remaining three carboxylate groups being available for strong complexation with the metal ions. Moreover, DOTA is a macrocyclic ligand which is entropically favorable for complexing with metal ions, allowing complex formation with high affinity and stability.[20-23] Example of clinically used MRI contrast agent based on Gd(III)/DOTA are Dotarem® (gadoterate, Gd-DOTA) and Prohance® (gadoteridol, Gd(HP-DOTA)), which distribute rapidly between plasma and interstitial spaces following intravascular injection. These are most effective in detection and diagnosis of disrupted blood-brain barrier in the central nervous system (CNS) such as multiple sclerosis and brain tumor.[24]

Similar to MRI contrast agents, DOTA and DTPA are also used in imaging contrast agents for PET/SPECT, where it functions as a strong chelating agent for the radioisotopes Ga^{3+}, $^{90}Y^{3+}$ and $^{111}In^{3+}$.[20-23] Yet, MRI and PET/SPECT provide measurement of different entities, in which MRI demonstrates anatomical alterations and PET/SPECT is commonly used to measure metabolism and the distribution of blood flow. As MRI has superior resolution and PET/SPECT have excellent sensitivity with the potential to detect tumor lesion, use of MRI is often in combination with PET/SPECT for cancer diagnosis. In my PhD project, we mainly propose to develop self-assembled dendrimer nanomicelles for MRI in combination with anticancer drug delivery in the view of establishing innovative theranostics for cancer therapy.
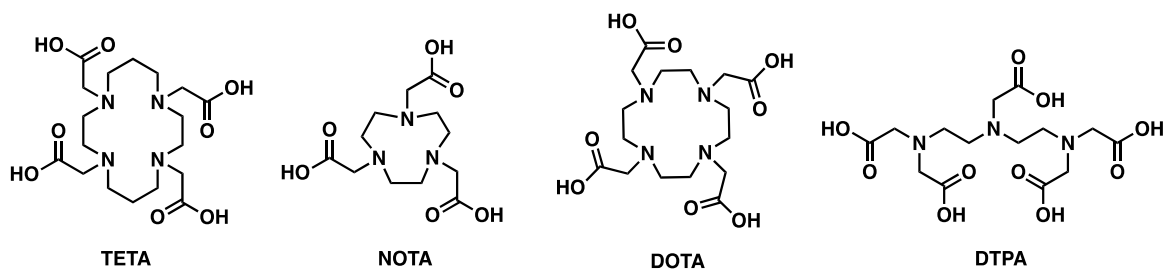

Figure 5.5. Commonly used macrocyclic chelators: TETA, NOTA, DOTA and DTPA.

2. Molecular design and synthetic strategy

Based on the above-mentioned characteristics for MRI imaging and the related imaging contrast agents alongside our expertise in self-assembled supramolecular dendrimers, we would like to propose dendrimer nanotheranostics based on small amphiphilic dendron capable for self-assembly to generate dendrimer nanostructures for drug delivery, and at the same time, bearing functional entities for MRI purpose. To do this, we conceived an amphiphilic dendron with a hydrophobic alkyl chain and a hydrophilic PAMAM dendritic wedge harboring four DOTA-conjugated terminals **C$_{18}$-G2-4DOTA** (**Figure 5.6**). This molecular design was intended to offer a balanced hydrophobicity *vs* hydrophilicity and functionality *vs* steric hindrance for self-assembling to create stable and robust supramolecular nanomicelles for drug encapsulation and at the same time MRI imaging.

The synthesis of **C$_{18}$-G2-4DOTA** was planned to start with **C$_{18}$-G2** (**Figure 5.7**) for conjugation with the DOTA reagent, followed with the chelation of metal ions Gd^{3+}, before self-assembling into supramolecular dendrimer nanomicelles for drug encapsulation to achieve the nanotheranostics construction (**Figure 5.8**). The so-built dendrimer nanotheranostics was expected to harness the large interior void of the supramolecular dendrimer for high drug loading to attain better therapeutic effect while making use of the multivalent accumulating effect of the dendrimer terminals for enhancing the local concentration of imaging agent for better imaging quality.
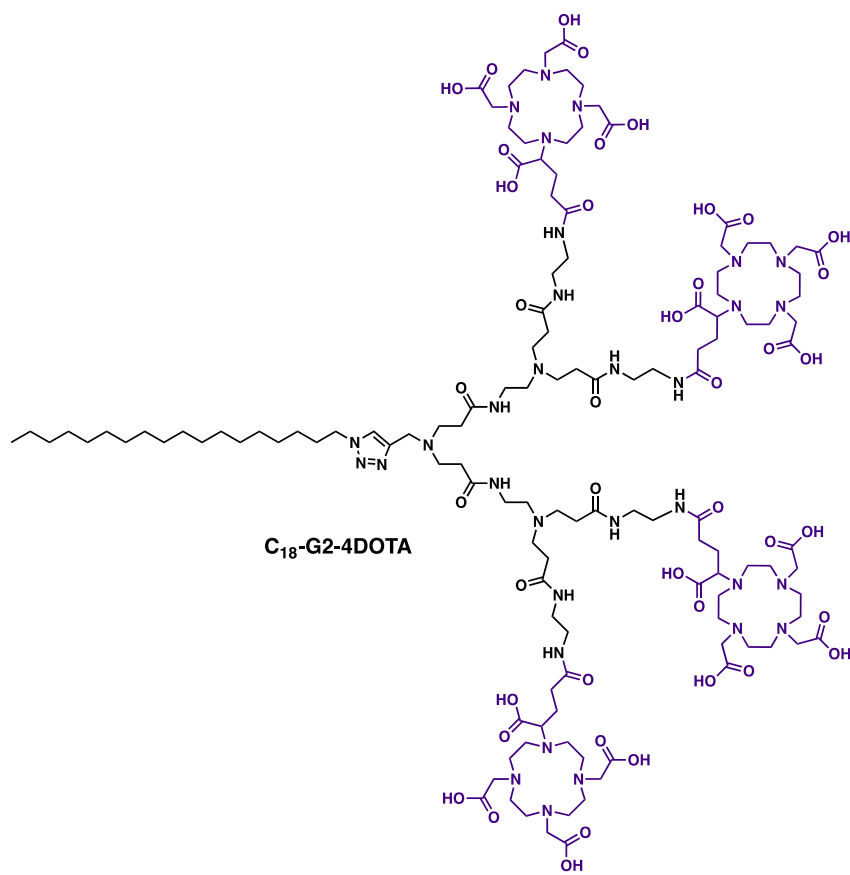
Figure 5.6. Amphiphilic dendron **C₁₈-G2-DOTA** with a hydrophobic alkyl chain and a hydrophilic PAMAM dendritic wedge harboring four DOTA-conjugated terminals.
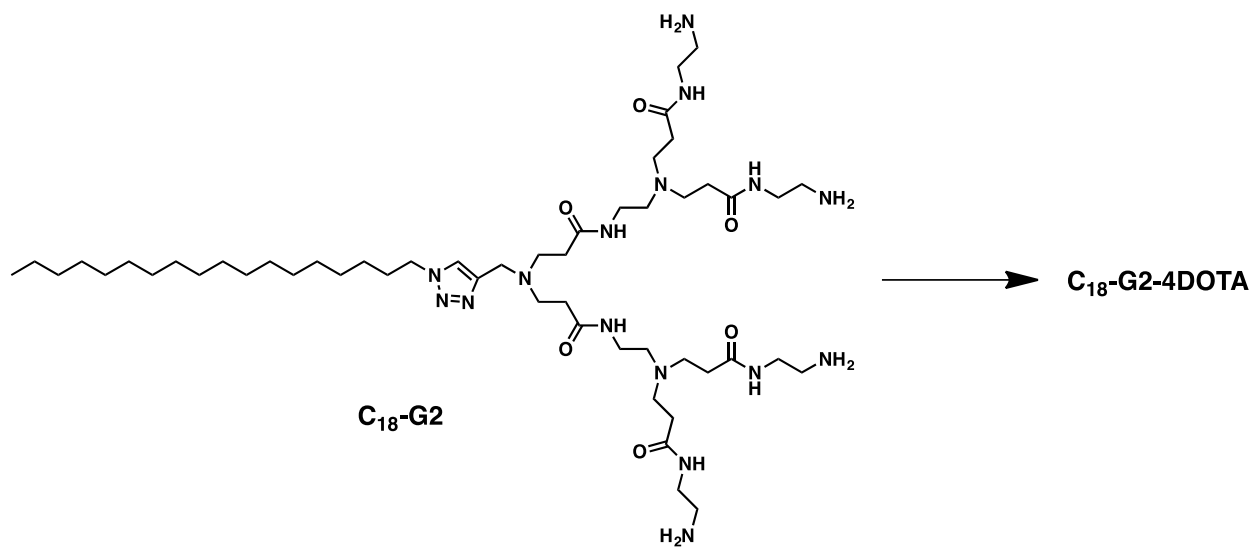
**Figure 5.7.** Amphiphilic G2 dendrimer with four amine terminals as the scaffold for further DOTA conjugations.
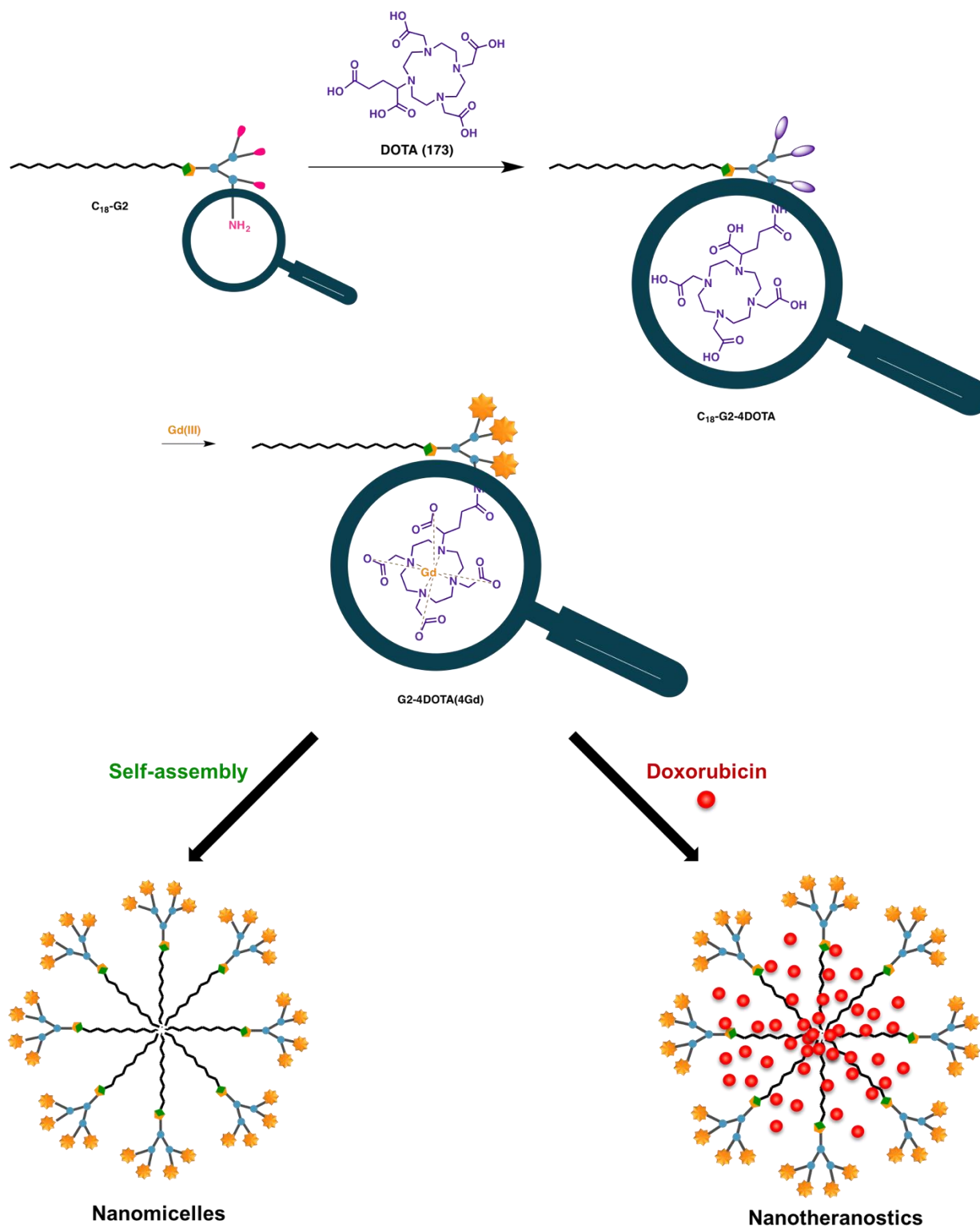
Figure 5.8. Molecular and synthetic design for preparing **C₁₈-G2-4DOTA**, **G2-4DOTA/Gd** and self-assembled nanomicelles.

3. Results and discussion
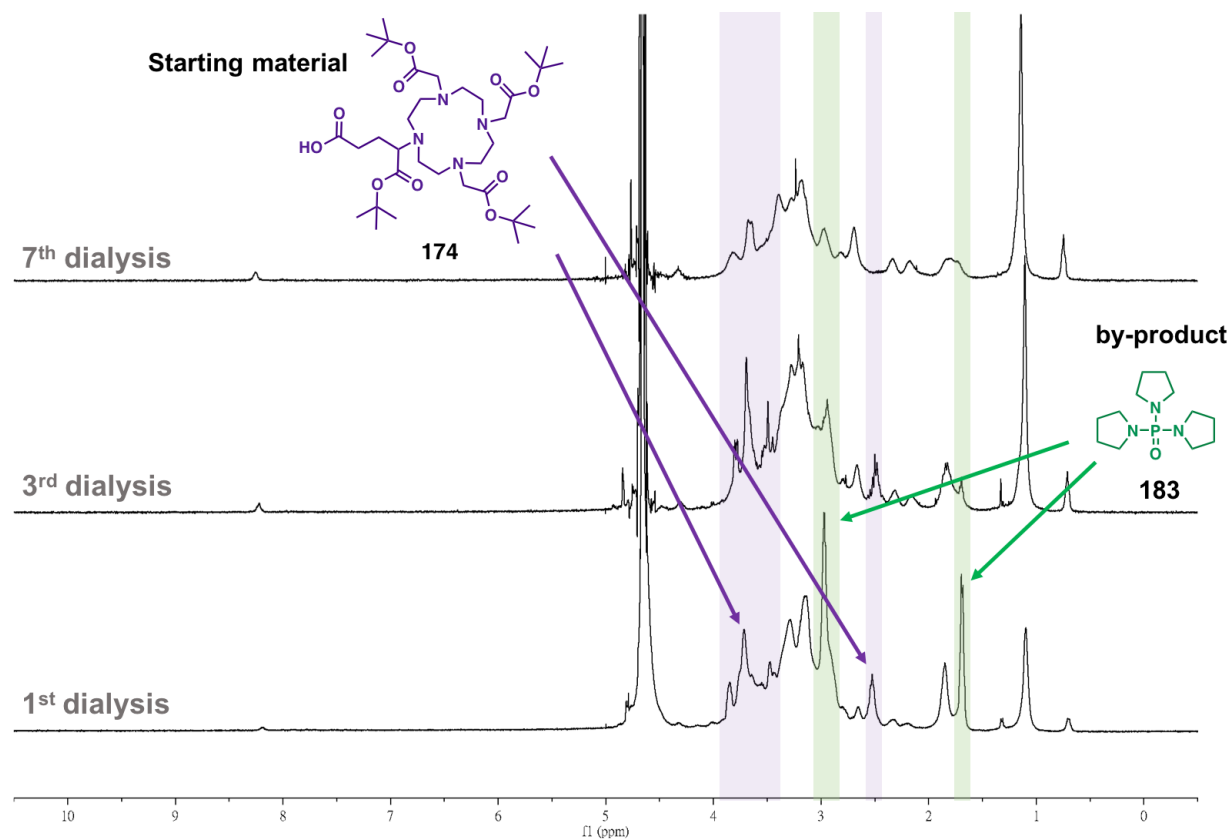
3.1. Synthesis of C$_{18}$-G2-4DOTA

As we mentioned previously, we chose the amphiphilic dendrimer scaffold **C$_{18}$-G2** with one hydrophobic alkyl chain and hydrophilic terminal dendritic wedge after considering the hydrophilic/hydrophobic balance and the possible steric hindrance during surface modification for conjugation with DOTA moiety (**Figure 5.7**).

Scheme 5.1 shows the synthesis of the dendrimer **C$_{18}$-G2-4DOTA,** starting from the 4 amine-terminated dendrimer **C$_{18}$-G2**, which was then conjugated with DOTA derivatives followed by deprotection. The amine-terminated dendrimer **C$_{18}$-G2** was prepared according to the protocols well-established in our group[25] and presented in the experimental section. Conjugation of the DOTA entities onto the terminal amines of **C$_{18}$-G2** was carried out using the *tert*-butyl (*t*Bu) protected DOTA derivative DOTA-GA(*t*Bu)$_4$ (**174**) with PyBOP as coupling agent, which proved to be very effective although the reaction was allowed to proceed via a long reaction time of 2 days. Subsequent deprotection of the *t*Bu groups was accomplished using TFA/DCM to deliver **C$_{18}$-G2-4DOTA** in 82% in 2 steps.

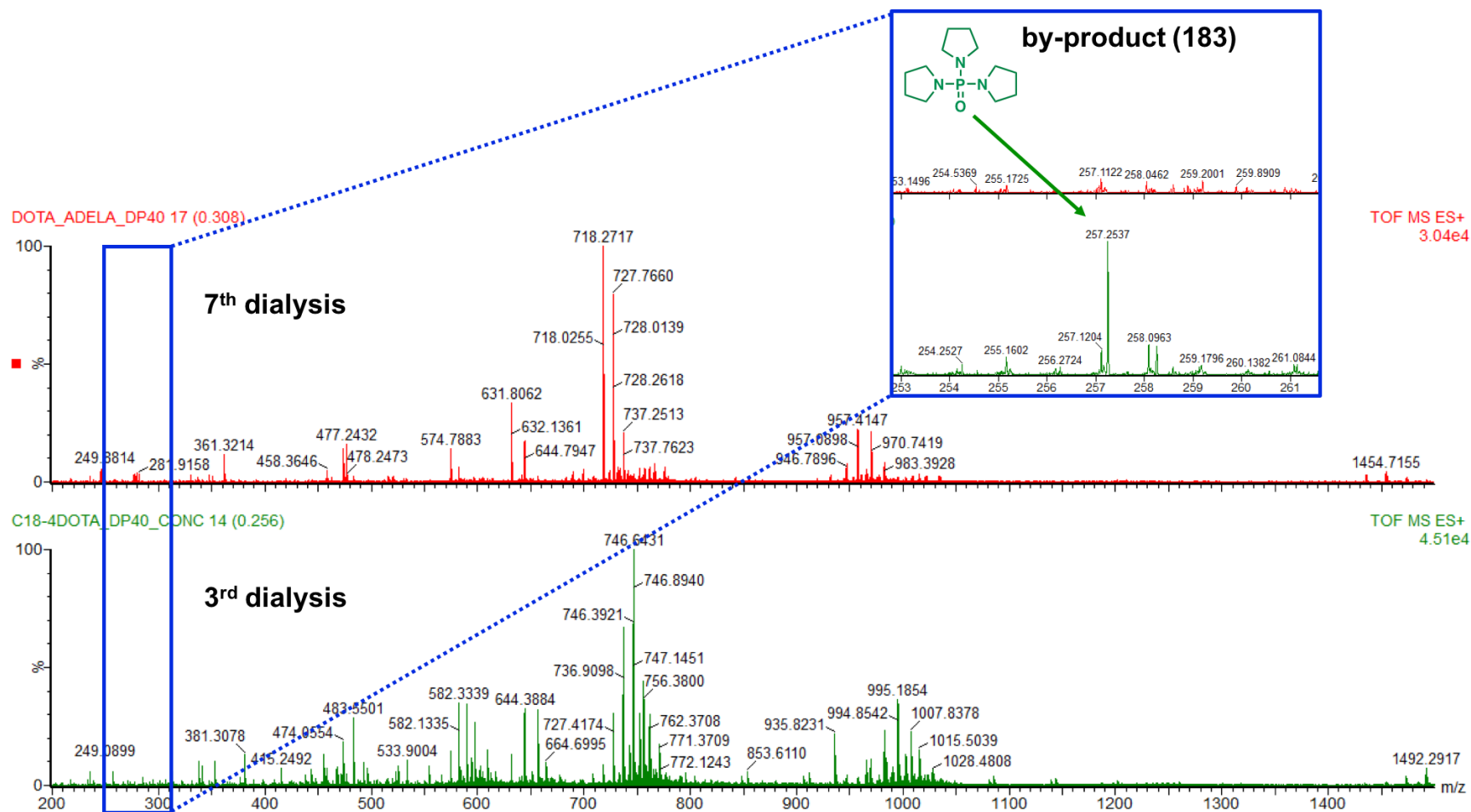**C₁₈-G2**

174

PyBOP, NMM, DMF

TFA/DCM
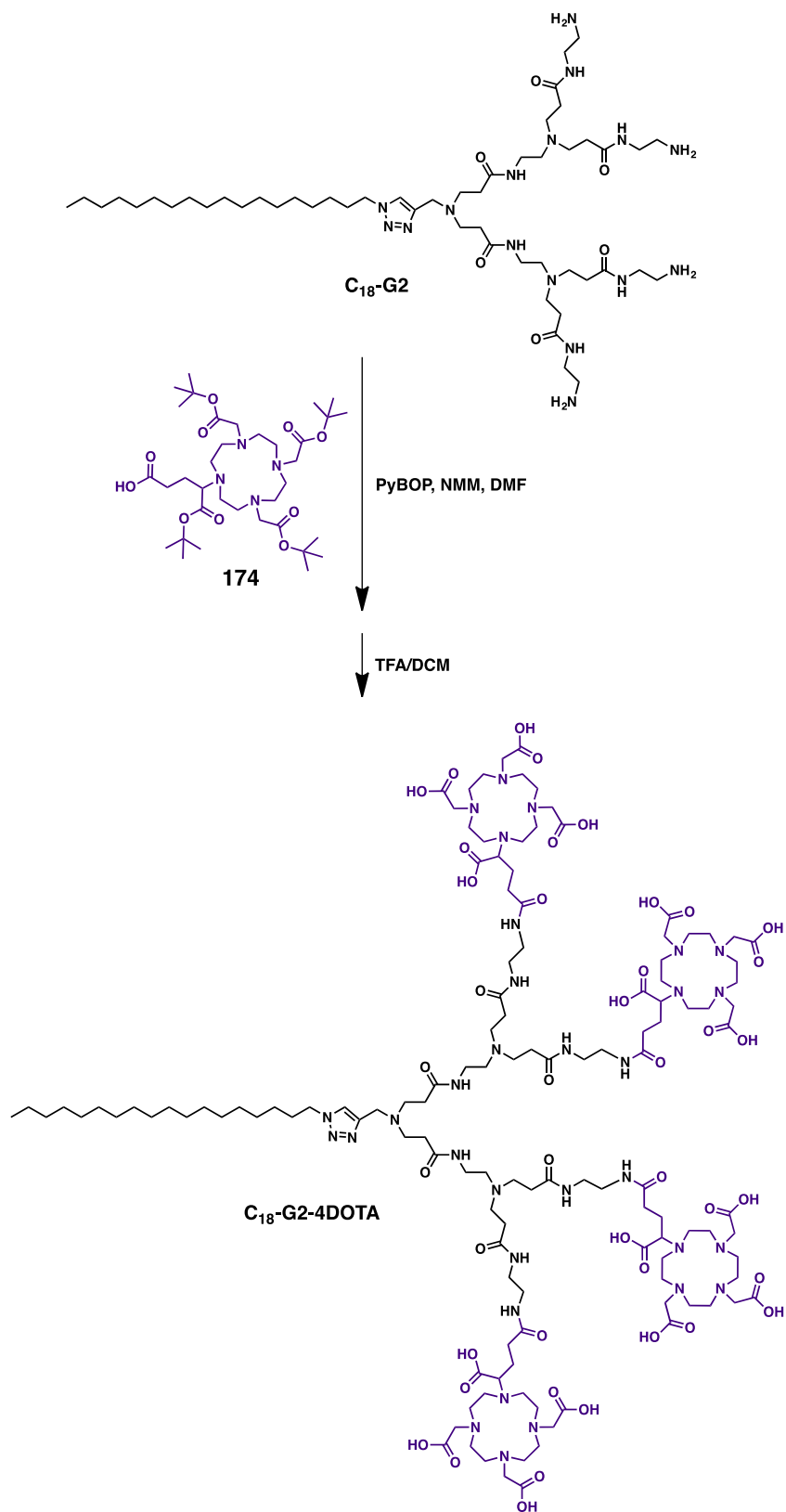
C₁₈-G2-4DOTA

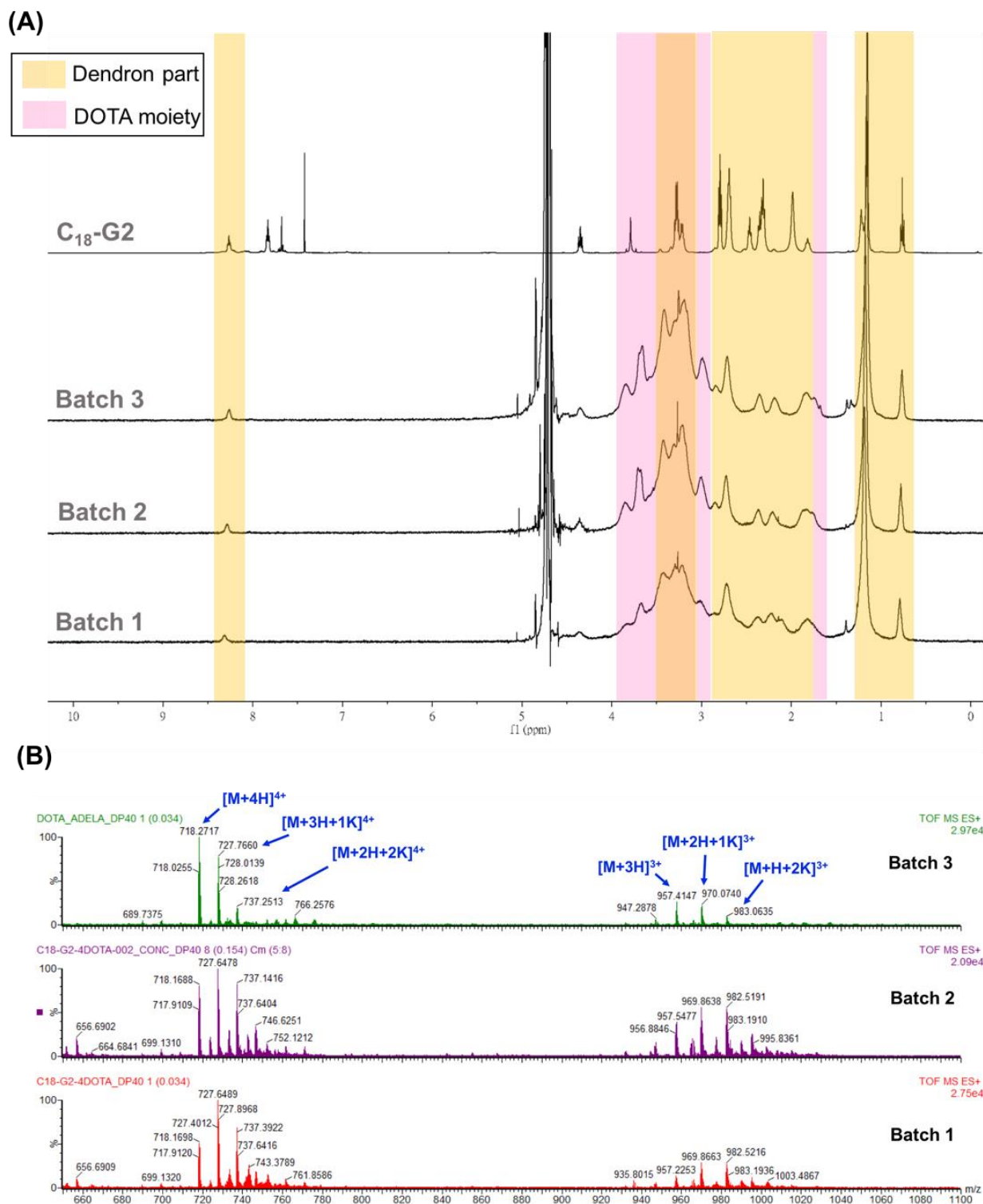**Scheme 5.1.** Synthesis of **C₁₈-G2-4DOTA**.

TLC, NMR and ESI-TOF-MS were employed to monitor and confirm the product formation. In particular, the obtained crude product was purified using sequential dialysis (replace fresh water per hour, 8 times per day) and lyophilization in order to get rid of the various impurities. It should be mentioned that the by-product, tris(pyrrolidinophosphine) oxide (**183**), originating from PyBOP was very difficult to separate, probably it was buried within the interior cavities of dendrimers (**Figure 5.9**, green highlighted). We therefore undertook extensively repeated dialysis/lyophilization purification cycles. After 7 cycles of dialysis/lyophilization, the by-product could be completely removed as demonstrated by MS analysis (**Figure 5.10**). The final product **C₁₈-G2-4DOTA** was obtained as beige amorphous solid. This optimized protocol was well-established, allowing dendrimer synthesis with reproducible yield and quality, as demonstrated by the NMR and ESI-MS analysis of three different batches of **C₁₈-G2-4DOTA** synthesized using this protocol (**Figure 5.11**).

**Figure 5.9.** NMR spectra of **C₁₈-G2-4DOTA** for impurity tracking after 1st, 3rd and 7th dialysis.

Figure 5.10. ESI-MS analysis to track the removal of **183** using dialysis and identify the complete synthesis of **C₁₈-G2-4DOTA**.

Figure 5.11. (A) NMR and **(B)** ESI-MS spectra of different batches of **C₁₈-G2-4DOTA** to show the consistence and reproducibility of synthesis.

^{1}H NMR and ^{13}C NMR were also used to identify the structure of **C18-G2-4DOTA**. Compared to the dendrimer **C18-G2**, both ^{1}H and ^{13}C NMR of **C18-G2-4DOTA** revealed the new and characteristic NMR signals corresponding to the DOTA moieties: 1.72, 2.18, 3.17, 3.39, 3.67 ppm in ^{1}H NMR, and 24.8, 27.8, 57.8, 66.3, 171.7, 175.3, 176.5 ppm in ^{13}C NMR (**Figure 5.12**). In addition, electrospray high-resolution mass spectrometry (HRMS) unveiled the signals assigned to **C18-G2-4DOTA** in multiple protonation states (from 2+ to 5+, **Figure 5.10**), effectively affirming its chemical structure.
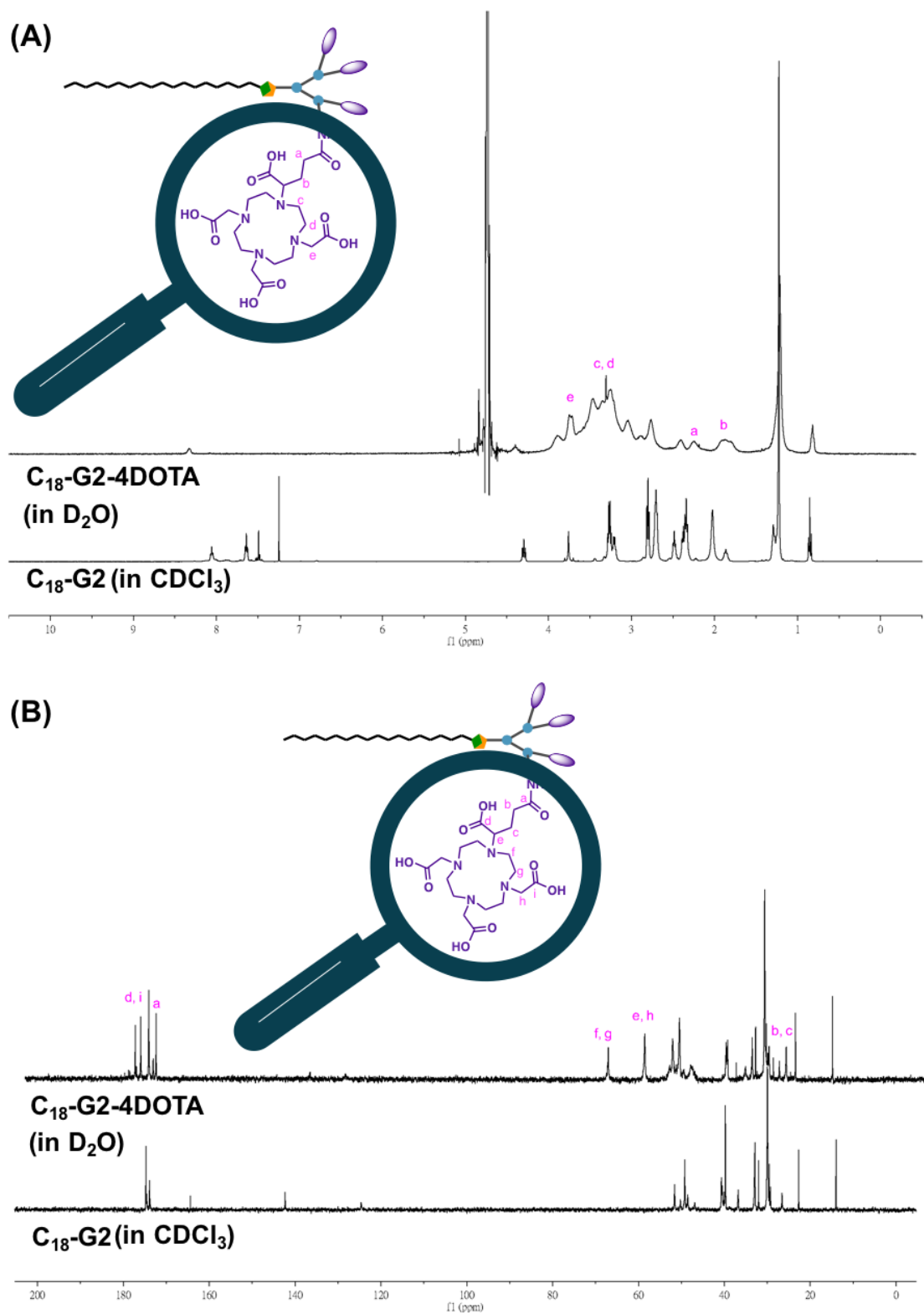
Figure 5.12. Comparison of the **(A)** ^{1}H NMR; and **(B)** ^{13}C NMR spectra **C₁₈-G2** and **C₁₈-G2-4DOTA**.

3.2.   Synthesis of Gd-chelated C$_{18}$-G2-4DOTA (G2-4DOTA/Gd)

The above synthesized **C$_{18}$-G2-4DOTA** was further chelate with Gd(III) in the view to establish imaging agent for MRI. **C$_{18}$-G2-4DOTA** was complexed with Gd(III) using an excess of GdCl$_3$ in order to ensure complete complexation of DOTA. GdCl$_3$ was added successively in several portions with pH adjusting to 6.5 after each addition. Precipitate was formed gradually when GdCl$_3$ was added, possibly due to the complexation with the carboxylate groups of DOTA with Gd^{3+} ions. After heating at 50°C for 24 h, the resulting reaction mixture for Gd(III) chelation was purified by dialysis, and then lyophilized to gain a white amorphous solid, **G2-4DOTA/Gd** (**Scheme 5.2**).
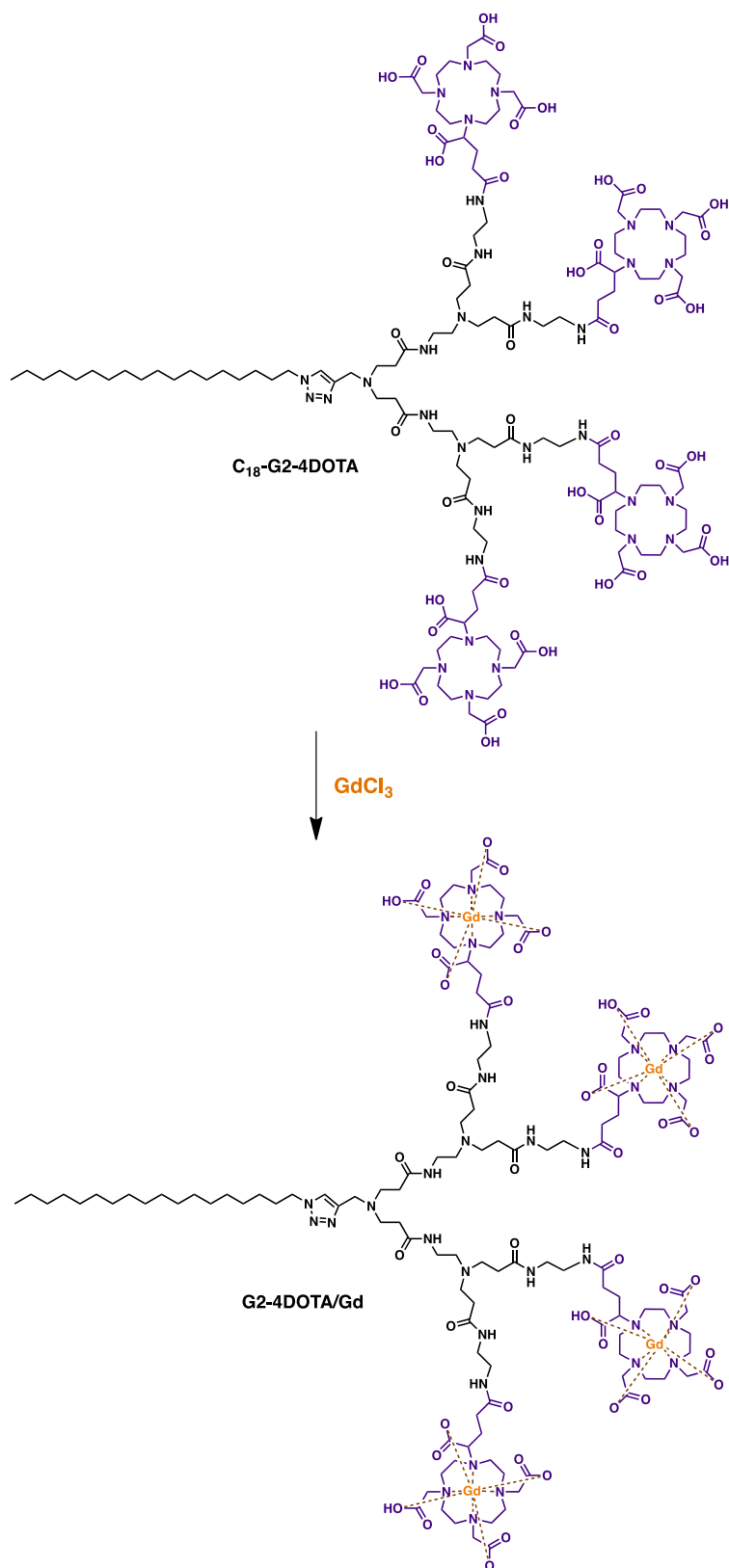
Scheme 5.2. Gd(III) chelation with DOTA-conjugated dendrimer, **G2-4DOTA/Gd**.

Due to the high paramagnetic properties of **G2-4DOTA/Gd**, we could not obtain reasonably resolved NMR spectra for the structural identification. Fortunately, ESI-MS is a powerful method, which allowed us to confirm the successful complexation between **C$_{18}$-G2-4DOTA** and Gd(III). As shown in **Figure 5.13**, two major signals assigned to **G2-4DOTA/Gd** in triple and quadruple protonation states (**Figure 5.13A** and **Figure 5.13B**) were observed. This finding indicates the fully complete chelation of four DOTA terminals in **C$_{18}$-G2-4DOTA** with Gd(III), to deliver **G2-4DOTA/Gd**.
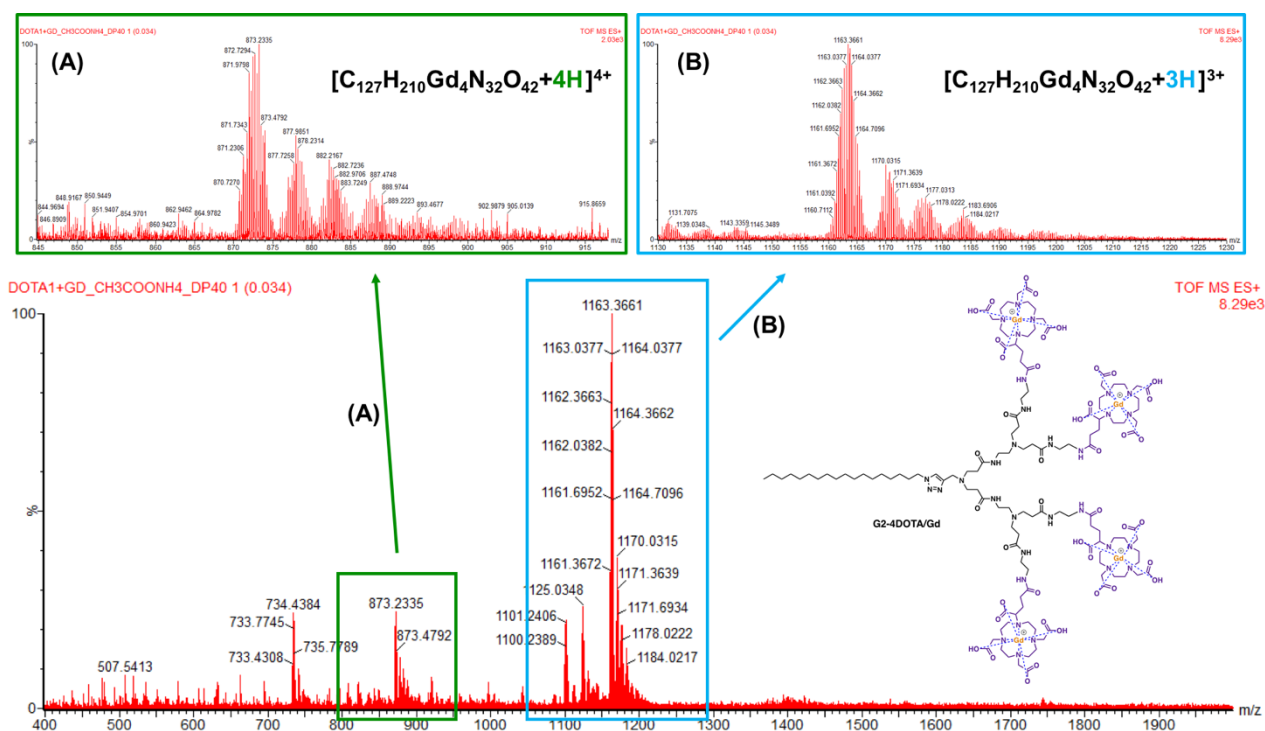
Figure 5.13. ESI-MS spectrum of DOTA dendrimer bonded with full Gd(III) ions.

It is known that Gd(III) possesses 7~9 coordination sites, and the exact coordination number depends on the ligand properties and availability. For the neutral, non-ionic **G2-4DOTA/Gd** [$C_{127}H_{210}Gd_4N_{32}O_{42}$], each Gd(III) chelated with the four nitrogen atoms, and the three carboxylate groups and the 1 protonate carboxylic acid of the DOTA unit, with Gd(III) having eight coordination sites (**Scheme 5.2**). For the quadruple charged **G2-4DOTA/Gd**$^{4+}$ [$C_{127}H_{214}Gd_4N_{32}O_{42}$]$^{4+}$ observed in HRMS, we proposed that each Gd(III) was coordinated with

the four nitrogen atoms, the two carboxylates and the two protonated carboxylates of each DOTA unit, hence also with eight coordination ligands (**Figure 5.14**). To further confirm this assumption, we doped our solution with sodium ions which would replace the labile protons in the complex structure (**Figure 5.14**). Indeed, upon the addition of sodium ions, the ionic peaks of $[C_{127}H_{214}Gd_4N_{32}O_{42}]^{4+}$ shifted to the new species $[C_{127}H_{206}Gd_4N_{32}O_{42}Na_8]^{4+}$. This result supports for the proposed coordination structure for the quadruple charged **G2-4DOTA/Gd**$^{4+}$ $[C_{127}H_{214}Gd_4N_{32}O_{42}]^{4+}$. In addition, the gadolinium ions were not influenced by sodium addition, indicating that their chelation with DOTA moieties was strong and robust.
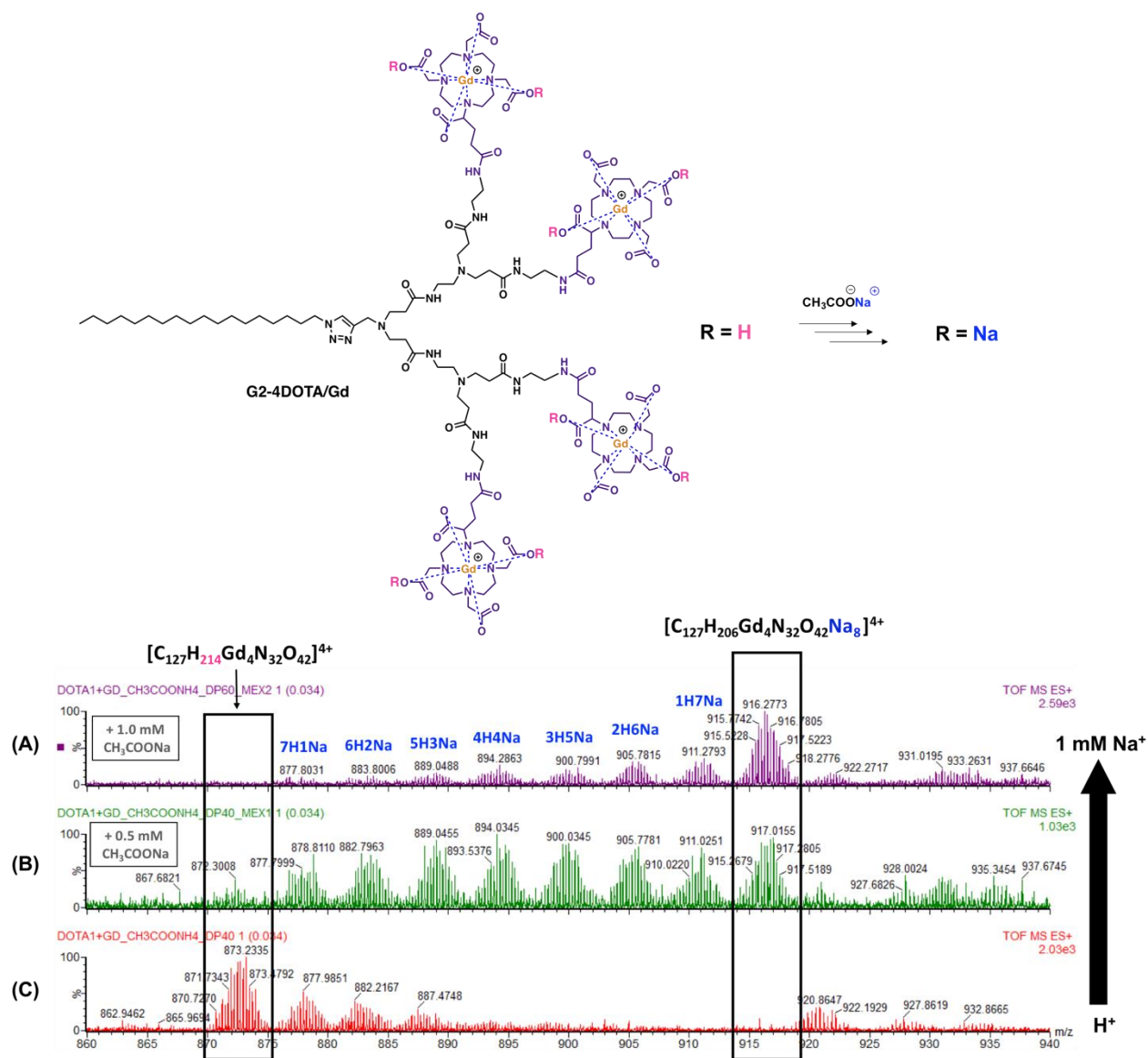
Figure 5.14. ESI-MS traces of **G2-4DOTA/Gd** with the addition of: **(A)** 1 mM of CH_3COONa; **(B)** 0.5 mM of CH_3COONa and **(C)** CH_3COONH_4.

### 3.3. Self-assembled nanosystems of C$_{18}$-G2-4DOTA and G2-4DOTA/Gd)

To verify the self-assembling properties of **C$_{18}$-G2-4DOTA** and **G2-4DOTA/Gd** to form supramolecular dendrimer nanostructures, we used film dispersion method to produce the corresponding nanomicelles issued from **C$_{18}$-G2-4DOTA** and **G2-4DOTA/Gd** respectively, and examined their hydrodynamic radius and their size distribution by using dynamic light scattering (DLS).[26] As shown in **Figure 5.15**, both **C$_{18}$-G2-4DOTA** and **G2-4DOTA/Gd** formed homogeneous nanoparticles with an average size of 6.3 nm and 7.1 nm, highlighting the formation of supramolecular dendrimer nanomicelles. The zeta potentials of the formed nanomicelles were further determined, with negative values of -24.7 mV and -12.5 mV for **C$_{18}$-G2-4DOTA** and **G2-4DOTA/Gd** at pH 6.4 and 8.6, respectively. As **C$_{18}$-G2-4DOTA** has all its carboxylate groups attached in DOTA moieties in deprotonated state, its nanomicelles have consequently high negative surface charge. Complexing the positively charged Gd(III) with the carboxylate groups in DOTA units, the nanomicelles issued from **G2-4DOTA/Gd** had hence less negatively zeta potential. Also, the zeta potential values around -24.7 mV and -12.5 mV implied formation of stable nanoparticle colloids. Indeed, the nanomicelles issued from both **C$_{18}$-G2-4DOTA** and **G2-4DOTA/Gd**, were stable in size and surface potential for at least 1 month.
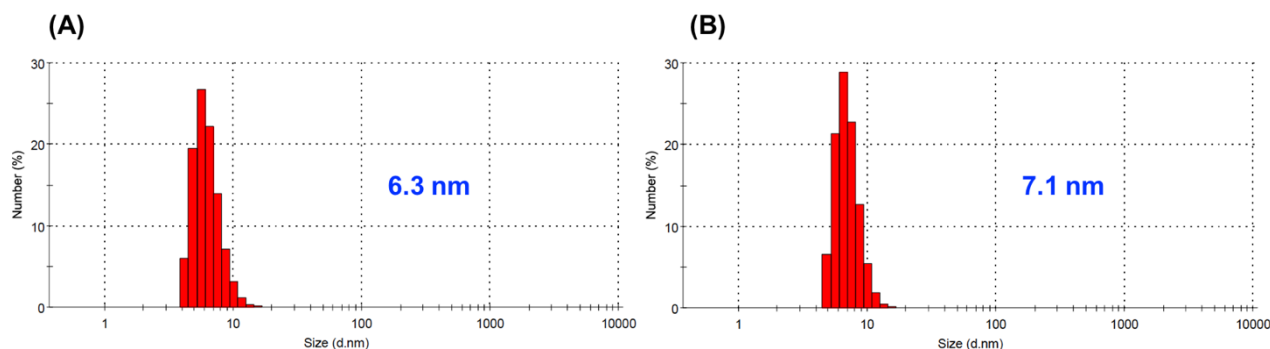
Figure 5.15. DLS results of **(A) C$_{18}$-G2-4DOTA** (1h) ;**(B) G2-4DOTA/Gd** (1h) in H$_2$O; **(C)** size and zeta tracking of **C$_{18}$-G2-4DOTA** and **(D)** size and zeta tracking of **G2-4DOTA/Gd**.

3.4. Construction of nanotheranostics (G2-4DOTA/Gd/DOX)

In order to further develop theranostics, we wanted to encapsulate the anticancer drug doxorubicin (**DOX**) within the nanomicelles of **G2-4DOTA/Gd**. Similarly, we used film dispersion method to prepare the **DOX**-encapsulating **G2-4DOTA/Gd** nanomicelles (**Figure 5.16**). We varied the ratio of **G2-4DOTA/Gd** and **DOX** from 1:2 (formulation [**A**]), 1:1 (formulation [**B**]) to 2:1 (formulation [**C**]) (**Figure 5.17** and **Figure 5.18**). To do this, the MeOH/CHCl$_3$ solutions of **C$_{18}$-G2-4DOTA** and **DOX** at the above-mentioned ratios were dried under vacuum to obtain homogeneous films, which were then hydrated using ultrasound sonication, followed by purification using dialysis. We denoted the so-obtained nanomicelles as **G2-4DOTA/Gd/DOX**.
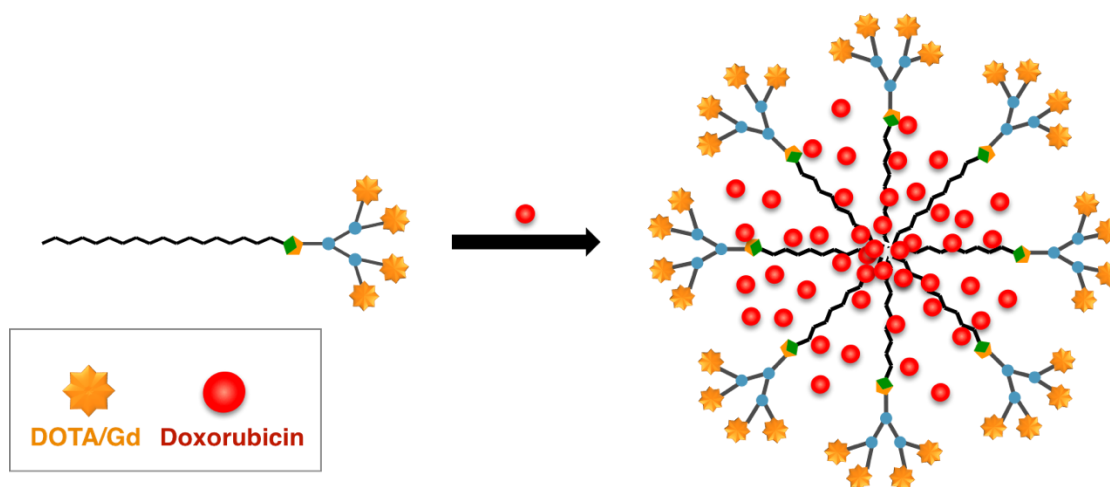
Figure 5.16. Self-assembly of doxorubicin-encapsulated nanomicelle **G2-4DOTA/Gd/DOX**.

The sizes and stability of these **DOX**-encapsulated nanomicelles were studied using dynamic light scattering (DLS) analysis. The sizes were steady except for the ratio of 1:1 of **G2-4DOTA/Gd** and **DOX** (formulation of [**B**]). However, the micelles formed with **G2-4DOTA/Gd**/**DOX** = 1:2 (formulation of [**A**]) were too small for being an effective delivery nanosystem for drug delivery (**Figure 5.17**). Furthermore, the most important parameter, zeta potential, remained hardly changed for at least one week indicating the good stability for the micelles formed with **G2-4DOTA/Gd**/ **DOX** at ratios of 1:1 (formulation of [**B**]) and 2:1 (formulation of [**C**]) (**Figure 5.18**).
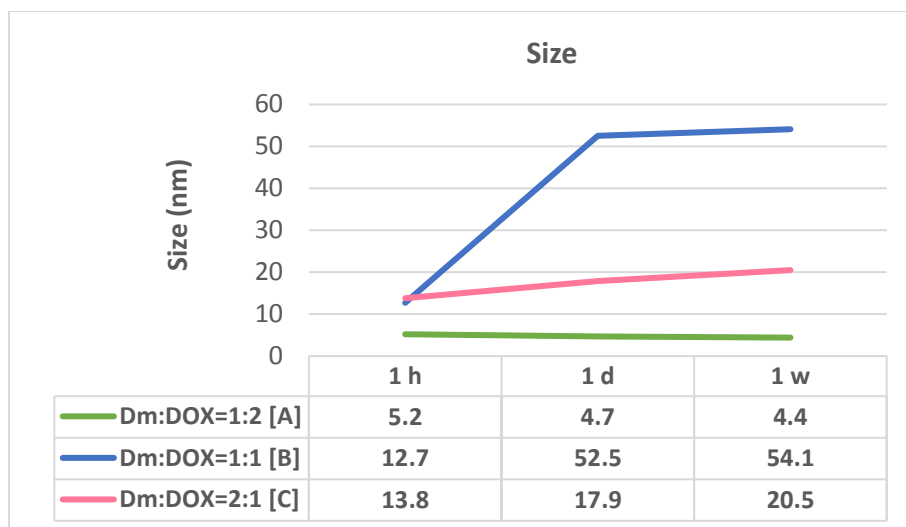
Figure 5.17. Sizes of **G2-4DOTA/Gd/DOX** with different NP formulation.
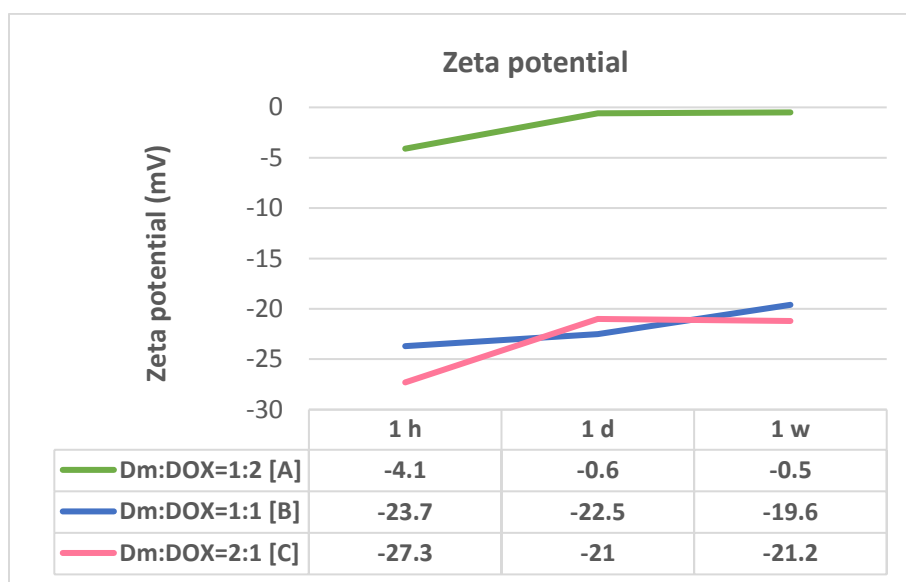
(Dm: **G2-4DOTA/Gd**)

Figure 5.18. Zeta potentials of **G2-4DOTA/Gd/DOX** with different NP formulation.

(Dm: **G2-4DOTA/Gd**)

We also investigated the drug loading capacity (DL) and encapsulation efficiency (EE) of **G2-4DOTA/Gd/DOX** from these three ratios of preparations (**Table 5.1**). Drug loading (DL) means the mass fraction of the active drug within the drug formulation, whereas drug encapsulation efficiency (EE) denotes the fraction of drug incorporated into the drug formulation compared with the total amount of drug that added for the preparation of drug formulation. The DL in formulation [**C**] appeared to be lower than the formulation [**B**] apparently, but the maximum of encapsulation efficiency (EE) were 54% and 69% for formulation [**B**] and [**C**] respectively. To summarize, the **G2-4DOTA/Gd/DOX** with the loading ratio of 2:1 was the best formulation, exhibiting promising stability with stable sizes and zeta potentials as well as the very good EE value.

Table 5.1. Drug loading capacity (DL) and encapsulation efficiency (EE) analysis of different NP ratios of **G2-4DOTA/Gd/DOX**.

Dm : DOX	[A] 1 : 2	[B] 1 : 1	[C] 2 : 1
DL (%)	49	17	18
EE (%)	65	54	69

In addition to the above approach for constructing the supramolecular dendrimer-based nanotheranostics, we also attempted another alternative route, namely, firstly self-assemble **C18-G2-4DOTA** encapsulated the anticancer drug **DOX**, followed by chelating with Gd(III) to establish the desired theranostics (**Figure 5.19A**). Interestingly, this construction route led to the formation of nanoparticles with size of 136 nm (**Figure 5.19B**) instead of small micellar nanoparticles. Also, the formed **C18-G2-4DOTA/DOX** complexes were of the size around 120 nm. Considering the observed size dimension of these nanosystems, we hypothesized that nanovesicles instead of nanomicelles were formed using this preparation method (**Figure 5.20**). Curiously, the so-formed nanosystems seemed not stable and rearranged into small micellar nanostructures after 1 day. These small micellar nanoassemblies appeared to be stable and retained this micellar size and zeta-potential of -15 mV even after 1 week. It is to note that the drug loading content was less than 1% when using route **II**. Therefore, route **II** is not a method of choice to recommend for constructing the desired nanotheranostics **G2-4DOTA/Gd/DOX** (**Figure 5.21**).
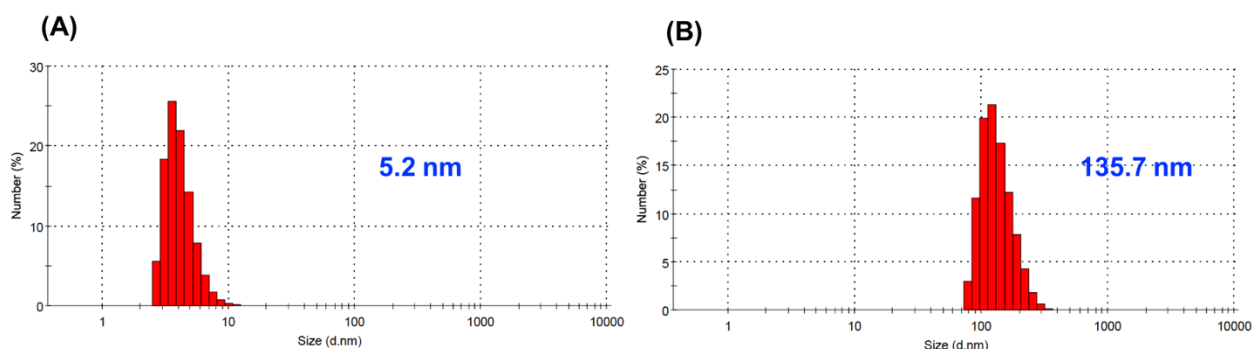
Figure 5.19. Sizes of **G2-4DOTA/Gd/DOX** prepared by **(A)** route **I** and **(B)** route **II**.
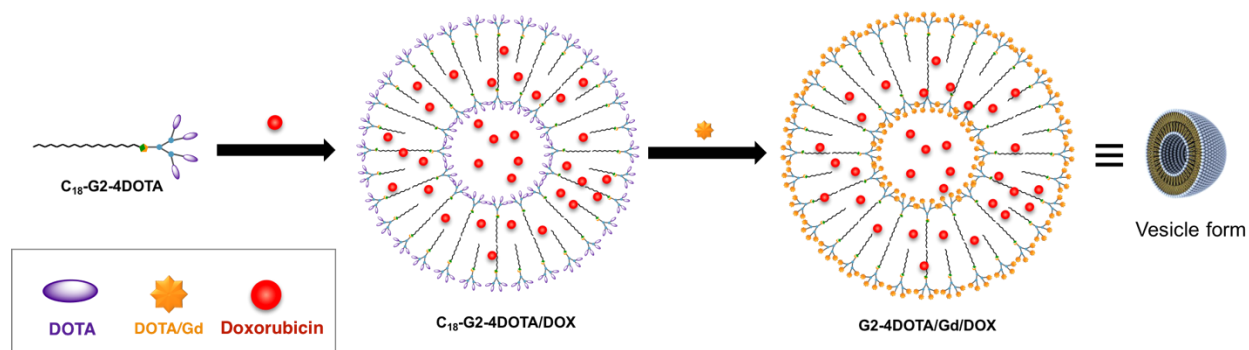
Figure 5.20. Hypothetic vesicle formation of **G2-4DOTA/Gd/DOX** via route **II**.
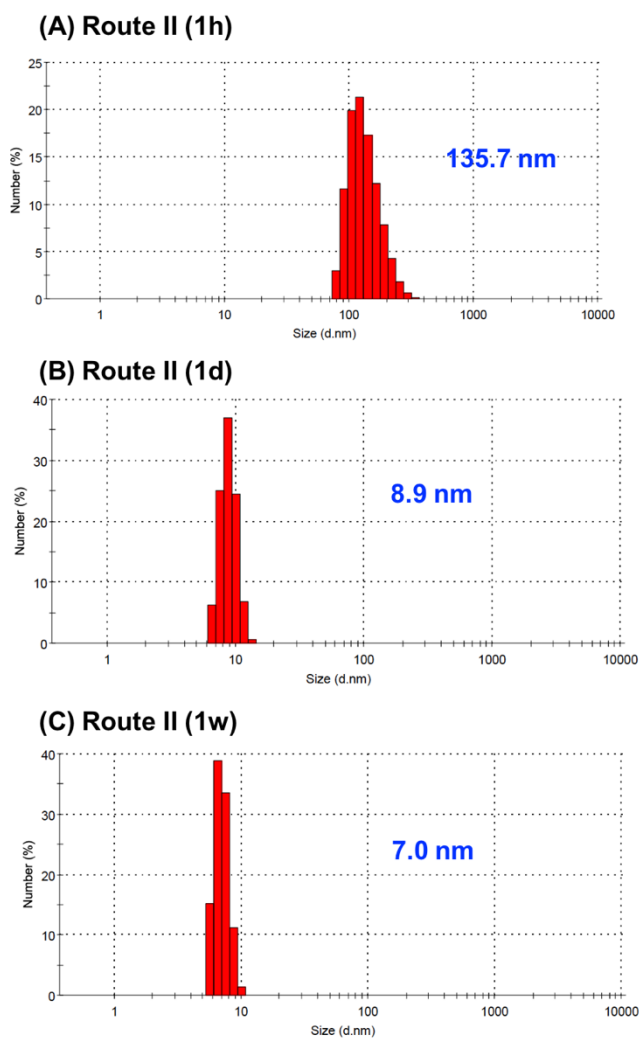
Figure 5.21. Stability analysis of **G2-4DOTA/Gd/DOX** via route **II** based on the DLS results standing after 1 h, 1 day (d) and 1 week (w), respectively.

4. Summary

In this chapter, we presented our rational and effort to explore self-assembly strategy to create supramolecular dendrimer nanostructure to construct theranostics with integration of diagnosis and therapeutic platform within our self-assembling supramolecular dendrimer nanosystems. To do this, a small amphiphilic dendron with a hydrophobic alkyl chain and a hydrophilic PAMAM dendritic wedge harboring four DOTA-conjugated terminals **C18-G2-4DOTA** was devised. The synthesis of **C18-G2-4DOTA** was achieved by conjugating the amine-terminating with DOTA-entities, followed with the chelation of metal ions of Gd(III) for MRI purpose, and finally self-assembled into supramolecular dendrimer nanomicelles encapsulated the anticancer drug doxorubicin (**DOX**) for constructing the nanotheranostics. The so-obtained dendrimer nanoassemblies were small in size (7.1 nm) yet with relatively high drug payload and being stable and robust for over 1 month. These nanosystems are intended to harness the large interior void of the supramolecular dendrimer for high drug loading to achieve better therapeutic effect while making use of the multivalent accumulating effect of the dendrimer terminals for enhancing the local concentration of imaging agent for better MRI quality. We hold great expectation for the self-assembly approach to construct supramolecular dendrimer nanosystems in nanotechnology-based biomedical applications for cancer treatment.

5. Experimental Section

General

The reagent DOTA-GA(*t*Bu)$_4$ (**174**) was purchased from CheMatech (Dijon, France) and other chemicals were purchased from Acros, Sigma Aldrich or Alfa Aesar. Methyl acrylate, ethylenediamine, trimethylamine, dichloromethane and methanol were dried according to the described methods and distilled before use. The other chemicals were used without further purification. Chromatography was prepared on silica gel (Merck 200-300 mesh). ^{1}H NMR spectra were recorded at 400 or 500 MHz and ^{13}C NMR spectra recorded at 100 MHz on Bruker Avance III 400, Bruker Avance III 500 or JEOL ECS 400 spectrometers. Chemical shifts (δ) are expressed in parts per million (ppm) with the residual peak of CDCl$_3$ at 7.26 ppm or CD$_3$OD at 3.31 as internal reference. The high-resolution mass spectra (ESI-MS) were obtained with an electrospray ionization (ESI) using mass spectrometer QStar Elite (Applied Biosystems SCIEX, Concord, Canada). The exact mass measurement was done in triplicate with a double internal calibration. IR spectra were recorded with an ALPHA FT-IR spectrometer (Bruker, France). Analytical thin layer chromatography (TLC) were performed using silica gel 60 F254 plates 0.2 mm thick with UV light (254 and 364 nm) as revelator.

General synthesis of PAMAM dendrons

G1.5 PAMAM dendron (178)

The precursors **G1.5** PAMAM dendron **178** and hydrophobic chain **181** (**C₁₈-N₃**) were synthesized according to processes reported by our group.[25]

To briefly summarize, **178** was synthesized by iterative Michael addition and amidation reactions starting from propargylamine (**175**). **175** was subjected to reaction with methyl acrylate (**35**) and produced the ester-terminated dendron **176** (**G0.5**) through Michael addition. After amidation with ethylenediamine (EDA, **88**) was transformed into the amine-terminated dendron **177** (**G1**). With a repeated cycle of Michael addition, desired product **158** was finally obtained in a good overall yield of 65%.
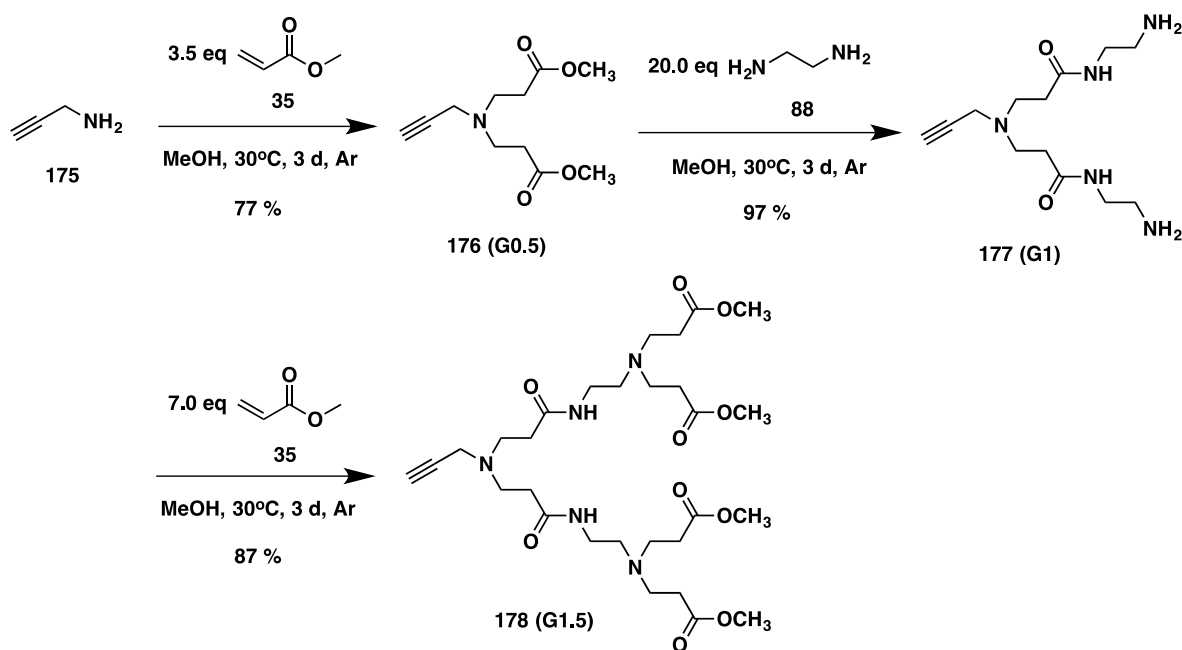
176 (G0.5)

^{1}H NMR (400 MHz, CDCl$_3$): δ 3.67 (s, 6H), 3.42 (s, 2H), 2.84 (t, 4H, J = 7.2 Hz), 2.47 (t, 4H, J = 6.8 Hz), 2.19 (s, 1H).

177 (G1)

^{1}H NMR (400 MHz, CDCl$_3$): δ 7.24 (br, 2H), 3.45 (s, 2H), 3.26-3.30 (m, 4H), 2.80-2.85 (m, 8H), 2.38 (t, 4H, J = 6.0 Hz); 2.22 (t, 1H, J = 2.4 Hz), 1.47 (br, 4H).

178 (G1.5)

^{1}H NMR (400MHz, CDCl$_3$): δ 7.09 (br, 2H), 3.67 (s, 12H), 3.46 (d, 2H, J = 2.0), 3.27-3.32 (m, 4H), 2.85 (t, 4H, J = 6.4 Hz), 2.76 (t, 8H, J = 6.8Hz), 2.54 (t, 4H, J = 6.0Hz), 2.37-2.45 (m, 12), 2.19 (br, 1H).

Synthesis of hydrophobic chains 181 (C$_{18}$-N$_3$)

For hydrophobic chain **181** (**C$_{18}$-N$_3$)**, it was easily achieved via a simple substitution reaction of octadecylamine (**179**) with imidazole-1-sulfonyl azide (**180**).
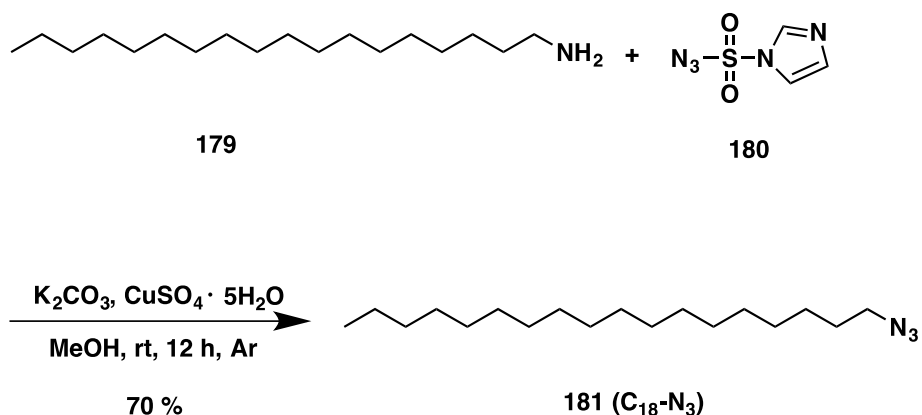
181 (C$_{18}$-N$_3$)

^{1}H NMR (400 MHz, CDCl$_3$): δ 3.25 (t, 2H, J = 6.8 Hz), 1.60 (m, 2H), 1.25(s, 30H), 0.88 (t, 3H, J = 6.4 Hz).

187

Synthesis of 163 (C$_{18}$-G1.5)

181 (C$_{18}$-N$_3$)

178 (G1.5)

84 %

5% CuSO$_4 \cdot$ 5H$_2$O
10% sodium ascorbate
THF/H$_2$O = 4/1
65ºC, 2 h, Ar

182 (C$_{18}$-G1.5)
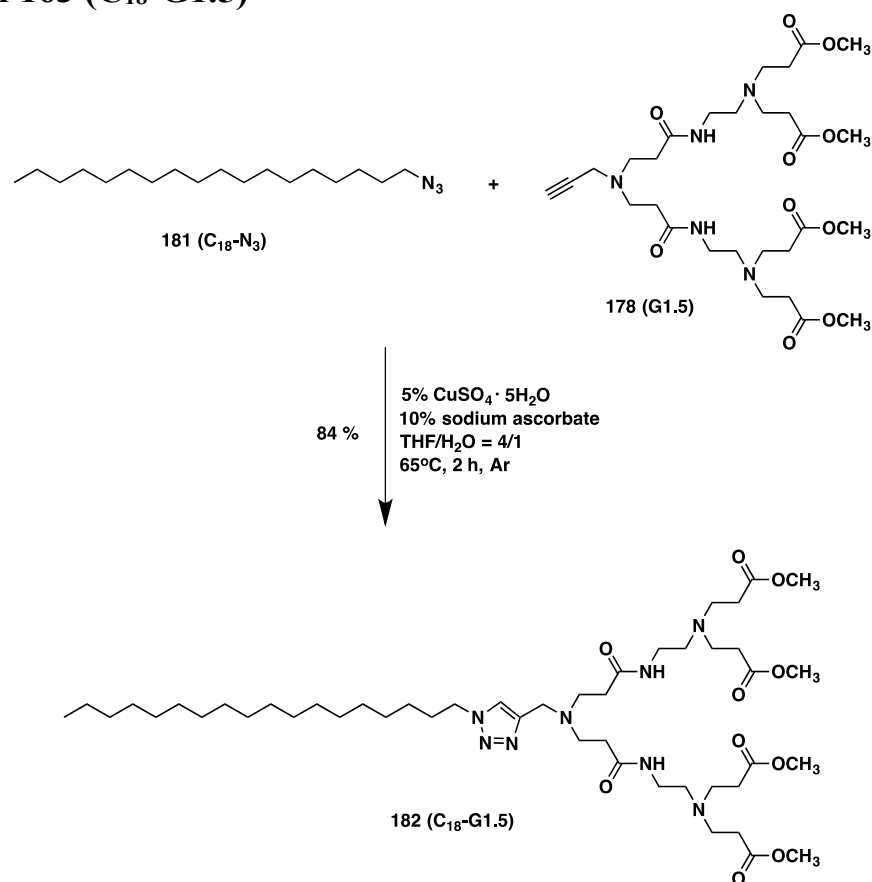
To a 25 mL two-neck round-bottom flask was sealed and purged with argon, a solution of **181** (**C$_{18}$-N$_3$**) (250.30 mg, 0.399 mmol) and **178** (**G1.5**) (129.4 mg, 0.438 mmol) in THF (8.00 mL) was added, followed by a solution of CuSO$_4 \cdot$ 5H$_2$O (4.98 mg, 0.020 mmol) in H$_2$O (2.00 mL). Then sodium ascorbate (7.89 mg, 0.040 mmol) was added. The resulting solution was stirred at 60 ºC for 2 h under argon until the reaction was completed indicated by TLC analysis. Then THF was removed under reduced pressure, the obtained residue was dissolved in 15.0 mL DCM and washed with saturated NH$_4$Cl$_{(aq)}$ (10.0 mLx3). The organic phase was dried with MgSO$_4$, filtrated and concentrated. The crude product was purified by column chromatography on silica gel with DCM/MeOH = 20/1, giving the corresponding **182** (**C$_{18}$-G1.5**) as a colorless oil (311.20 mg, 84%). ^{1}H NMR (400 MHz, CDCl$_3$): δ 7.51 (s, 1H), 7.13 (br, 2H), 4.29 (t, 2H, J = 7.2 Hz), 3.81 (s, 2H), 3.64 (s, 12H), 3.24-3.28 (m, 4H), 2.71-2.78 (m, 12H), 2.51 (t, 4H, J = 6.0 Hz), 2.39-2.43 (m, 12H), 1.86 (br, 2H), 0.97 (br, 30H), 0.60 (t, 3H, J = 6.8 Hz).

Synthesis of C$_{18}$-G2

182 (C$_{18}$-G1.5)

20.0 eq

89 %

H$_2$N $\sim$ NH$_2$

88

MeOH, 30°C, 3 d, Ar

C$_{18}$-G2
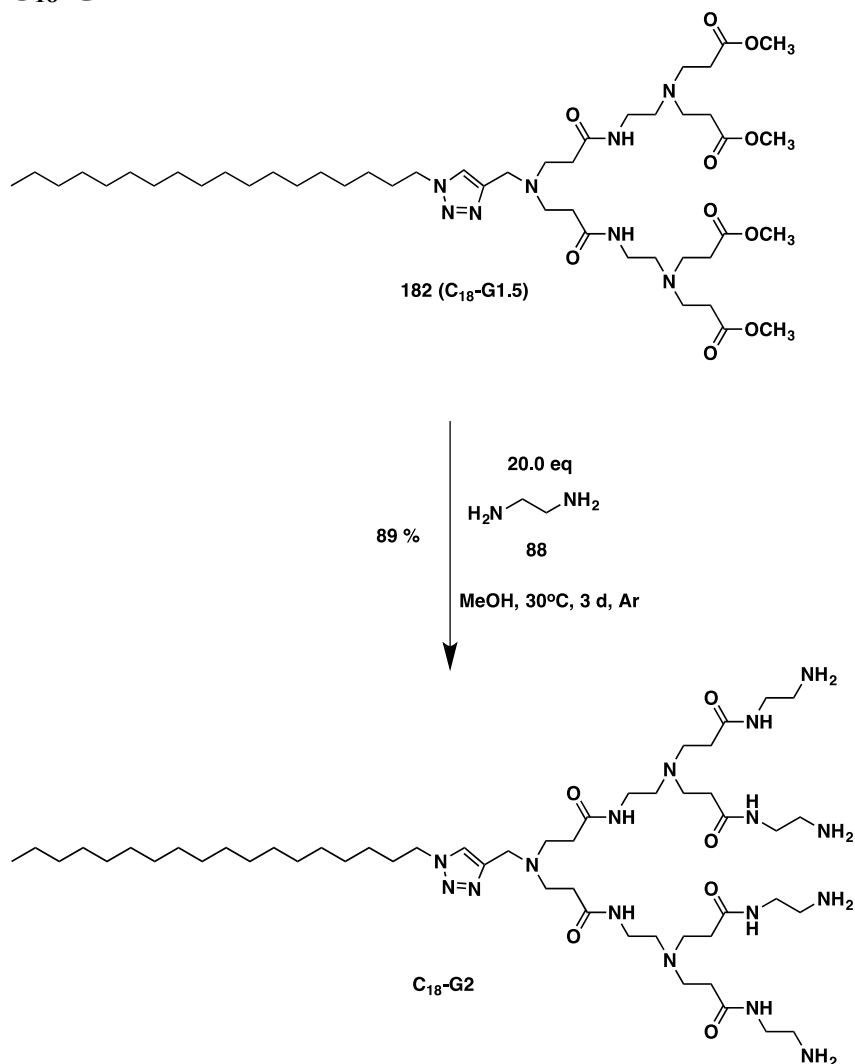
To a solution of **182** (**C$_{18}$-G1.5**) (298 mg, 0.323 mmol) in MeOH (4.00 mL) under argon, was added EDA (**88**) (1.50 mL, 22.4 mmol) slowly. The reaction mixture was stirred at 30 °C for 3 days until the reaction was completed indicated by IR analysis. Then the solvent was evaporated under reduced pressure, the obtained residue was purified by dialysis using dialysis tube of MWCO 500 in deionized water (800-1000 mL) (dialysis protocol: the water was changed every 1 h for seven times). The product was lyophilized to yield the corresponding **C$_{18}$-G2** as a lightly yellowish solid (313.20 mg, yield: 90%). ^{1}H NMR (400 MHz, CDCl$_3$): δ 8.06 (br, 2H), 7.64 (br, 4H), 7.49 (s, 1H), 4.30 (t, 2H, J = 8.0 Hz), 3.76 (s, 2H), 3.20-3.29 (m, 20H), 2.70-2.82 (m, 12H), 2.33-2.38 (m, 20H), 2.02 (br, 8H), 1.86 (br, 2H), 1.22 (s, 30H), 0.85 (t, 3H, J = 8.0 Hz).

Preparation of DOTA-conjugated dendrimer C₁₈-G2-4DOTA

C₁₈-G2

174

i) 16.0 eq DOTA(OtBu)₄
   16.0 eq PyBOP, 20 eq NMM
   DMF, 30°C, 3 d, Ar

ii) TFA/DCM = 3/1, rt, 24 h, Ar
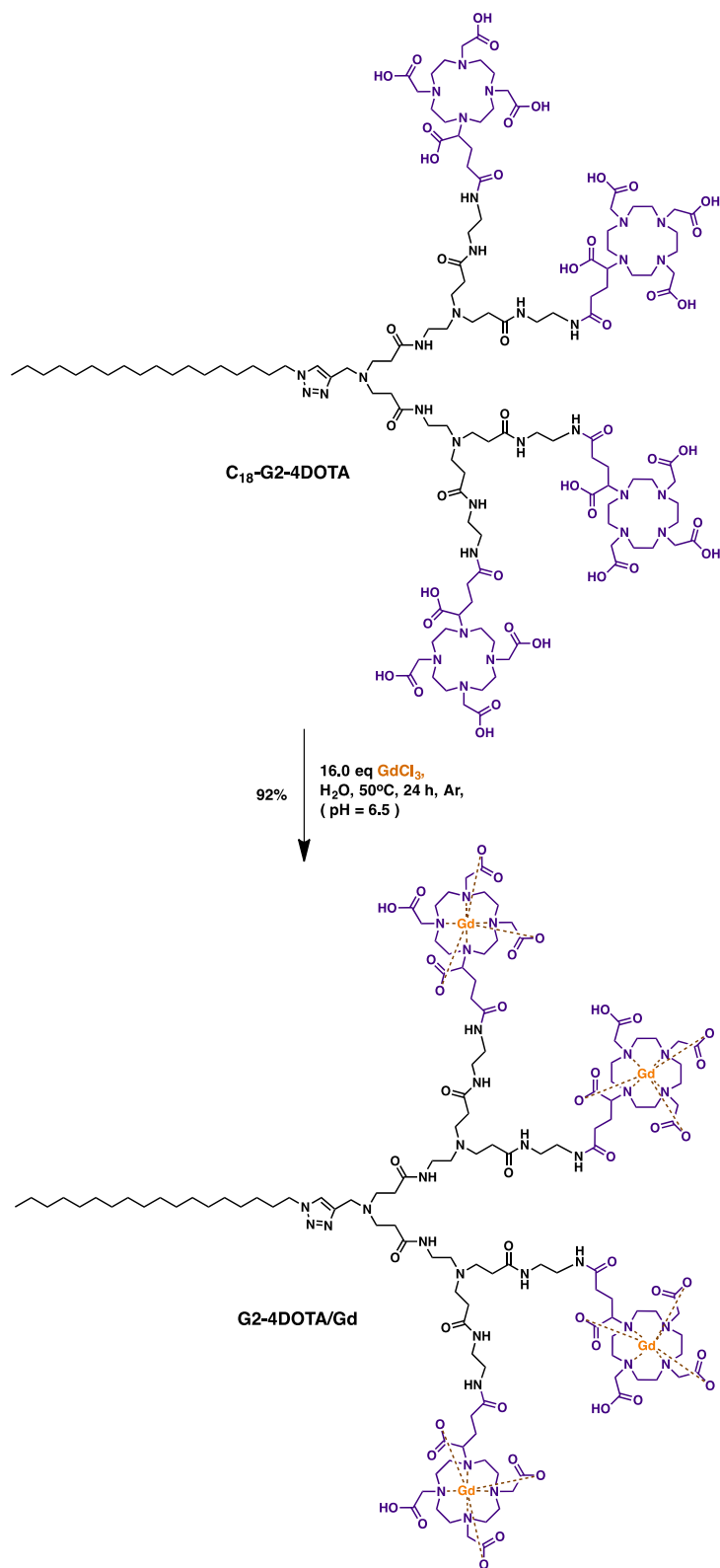
82% (2 steps)

C₁₈-G2-4DOTA
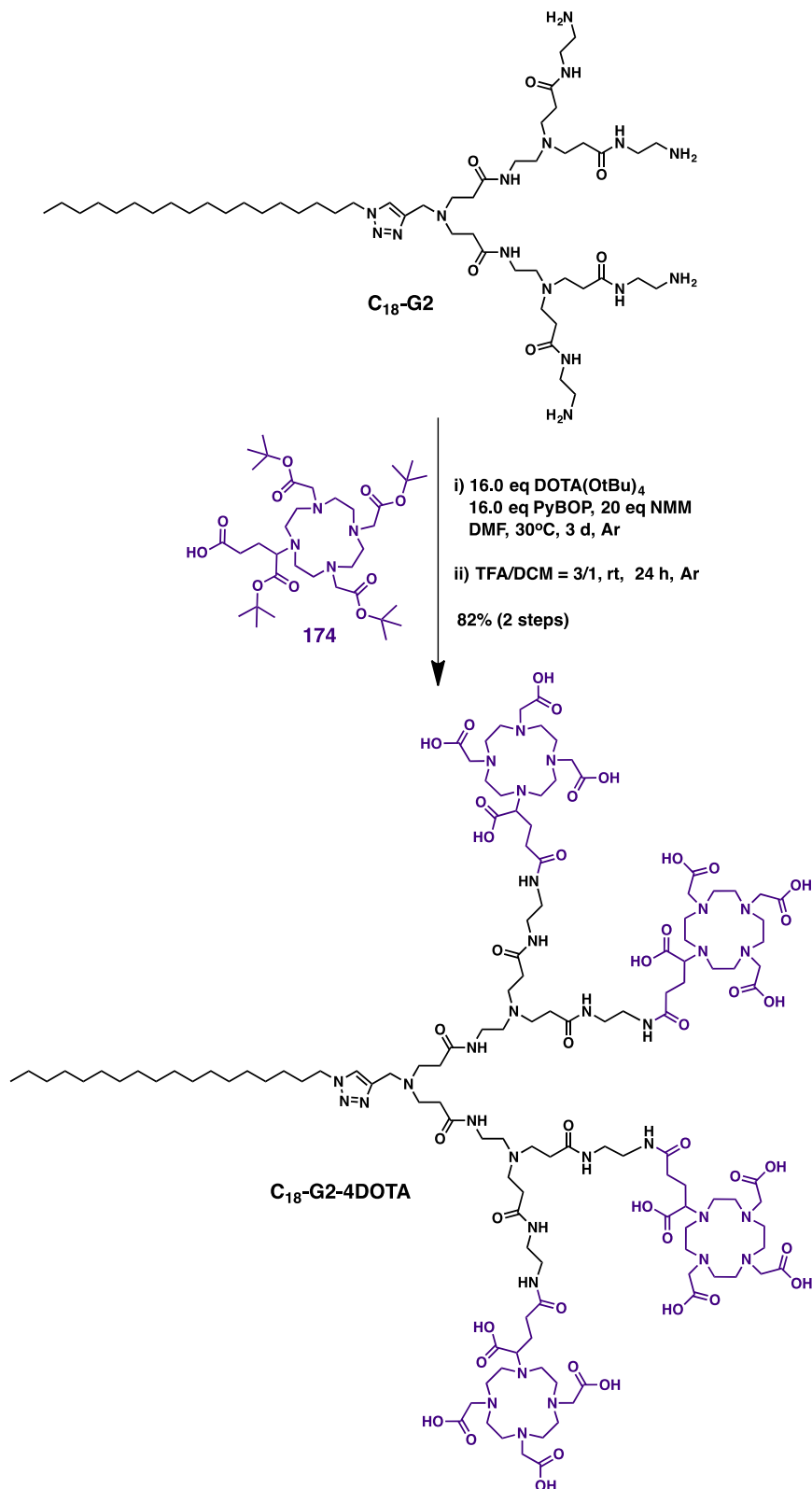
To a solution of DOTA-GA(*t*Bu)$_4$ (**174**) (325.0 mg, 0.464 mmol) in DMF (4.00 mL), was added PyBOP (242.1 mg, 0.465 mmol) and NMM (82.0 mg, 0.583 mmol). The mixture was stirred for 5 min and then **C$_{18}$-G2** (31.0 mg, 0.030 mmol) in DMF (2.00 mL) was added and the solution was stirred at 30 °C for 3 days under argon. Thereafter, saturated NaHCO$_3$ (20.0 mL) was added to the solution and EA (15.0 mLx3) was used for extraction. The organic layer was collected, dried with MgSO$_4$, filtrated and evaporated. Next this crude product was dissolved in TFA/DCM (3.00 mL, v/v = 1/1) mixture and stirred at rt for 24 h under argon. After evaporating the solvent, the obtained crude product was purified by dialysis (dialysis tubing, MWCO 2000) and lyophilized. Repeating the operation of dialysis and lyophilization 7 times, the product was lyophilized to yield the corresponding **C$_{18}$-G2-4DOTA** as a brownish solid (72.2 mg, yield: 84%). ^{1}H NMR (400 MHz, D$_2$O): δ 8.27 (s, 1H), 4.50 (br, 2H), 4.34 (br, 2H) 3.83-2.70 (m, 138H), 2.34 (br, 4H), 2.18 (br, 4H), 1.86 (br, 12H), 1.15 (br, 30H), 0.75 (s, 3H); ^{13}C NMR (100 MHz, D$_2$O) δ 176.5, 175.3, 173.4, 172.4, 171.7, 135.8, 127.5, 66.3, 57.8, 51.3, 49.7, 47.1, 46.9, 38.9, 38.5, 36.5, 32.8, 32.0, 29.9, 29.5, 29.1, 28.8, 27.8, 26.4, 24.8, 22.7, 14.1. ESI(+)-HRMS: calcd for C$_{127}$H$_{226}$N$_{32}$O$_{42}$$^{4+}$ [M+4H]$^{4+}$ 718.1634; found at *m/z* .718.1633 (error: -0.1 ppm).

DLS study

To prepare the DLS samples, 2.8 mg of **C$_{18}$-G2-4DOTA** was first dissolved in MeOH/CHCl$_3$ (v/v = 6/1, 2 mL) in a 10 mL of round bottom flask, followed by evaporation of the solvent with a rotary evaporator to form a thin film on the inner wall of the flask. 5 mL of deionized H$_2$O was then added and the solution was submitted to ultrasound to facilitate the dendrimer dispersion in the aqueous medium with the final concentration of dendrimers was 195 μM. The resulting solution was filtered by a Nylon membrane (0.45 μm with polypropylene housing, Whatman^{TM}) The size distribution of nanoparticles was determined by DLS using Zetasizer Nano-ZS (Malvern, Ltd.) with a He-Ne ion laser of 633 nm at 25°C.

Synthesis of Gd-chelated C₁₈-G2-4DOTA (G2-4DOTA/Gd)

C₁₈-G2-4DOTA

92%   **16.0 eq GdCl₃,**
H₂O, 50°C, 24 h, Ar,
(pH = 6.5)

G2-4DOTA/Gd

The solid **C$_{18}$-G2-4DOTA** (5.02 mg, 1.75 μmol) was dissolved in H$_2$O (5.00 mL) and the pH value adjusted to 6.5 with 1N NaOH. To this solution was added GdCl$_3$ (7.38 mg, 0.028 mmol) successively in three portions and the pH value was adjusted to 6.5 at each addition. The mixture was stirred for 24 h at 50 °C under Argon. Thereafter, the obtained crude product was purified by dialysis (dialysis tubing, MWCO 2000) and lyophilized to yield the corresponding **G2-4DOTA/Gd** as a white solid (5.56 mg, yield: 92%). ESI(+)-HRMS: calcd for C$_{127}$H$_{213}$Gd$_4$N$_{32}$O$_{42}$$^{3+}$ [M+3H]$^{3+}$ 1163.0835; found at *m/z* 1163.0825 (error: -0.9 ppm).

DLS study

To prepare the DLS samples, 5 mg of **G2-4DOTA/Gd** was first dissolved in MeOH/CHCl$_3$ (v/v = 4/1, 2 mL) in a 10 mL of round bottom flask, followed by evaporation of the solvent with a rotary evaporator to form a thin film on the inner wall of the flask. 5 mL of deionized H$_2$O was then added and the solution was submitted to ultrasound to facilitate the dendrimer dispersion in the aqueous medium. The final concentration of dendrimers was 287 μM. The resulting solution was filtered by a Nylon membrane (0.45 μm with polypropylene housing, Whatman^{TM}). The size distribution of nanoparticles was determined by DLS using Zetasizer Nano-ZS (Malvern, Ltd.) with a He-Ne ion laser of 633 nm at 25°C.

Doxorubicin encapsulation of G2-4DOTA/Gd(G2-4DOTA/Gd/DOX)

Route I. 1.7 mg (2.0 eq, 2.9 mmol) of doxorubicin hydrochloride (DOX・HCl) was dissolved in MeOH/CHCl$_3$ (v/v = 3/2, 0.5 mL) in a 10 mL of round bottom flask and treated with 3.0 eq Et$_3$N for 10 min. Then a MeOH/CHCl$_3$ (v/v = 3/2, 2.0 mL) solution of **G2-4DOTA/Gd** (5.1 mg, 1.0 eq, 1.5 mmol) was added, followed by evaporation of the solvent with a rotary evaporator to form a thin film on the inner wall of the flask. Afterward, 5.0 mL of deionized H$_2$O was then added and the solution was submitted to ultrasound to facilitate the dendrimer dispersion in the aqueous medium. The resulting solution was filtered by a Nylon membrane (0.45 μm with polypropylene housing, Whatman^{TM}). The size distribution of nanoparticles was determined by DLS using Zetasizer Nano-ZS (Malvern, Ltd.) with a He-Ne ion laser of 633 nm at 25°C.

*Different ratios of formulation were followed this procedure with different drug loading accordingly.

Route II. 1.3 mg (2.0 eq, 2.2 mmol) of doxorubicin hydrochloride (DOX・HCl) was dissolved in MeOH/CHCl$_3$ (v/v = 3/2, 0.5 mL) in a 10 mL of round bottom flask and treated with 3.0 eq Et$_3$N for 10 min. Then a MeOH/CHCl$_3$ (v/v = 6/1, 2.0 mL) solution of **C$_{18}$-G2-4DOTA** (3.2 mg, 1.0 eq, 1.1 mmol) was added, followed by evaporation of the solvent with a rotary evaporator to form a thin film on the inner wall of the flask. Afterward, 5.0 mL of deionized H$_2$O was then added and the solution was submitted to ultrasound to facilitate the dendrimer dispersion in the aqueous medium and adjusted the pH value to 6.5 with 1N NaOH. To this solution was added GdCl$_3$ (4.7 mg, 17.8 mmol) successively in three portions and the pH value was adjusted to 6.5 at each addition. The mixture was stirred for 24 h at 50 ^{o}C under Argon. Thereafter, the obtained crude product was purified by dialysis (dialysis tubing, MWCO 2000). The resulting solution was filtered by a Nylon membrane (0.45 μm with polypropylene housing, Whatman^{TM}). The size distribution of nanoparticles was determined by DLS using Zetasizer Nano-ZS (Malvern, Ltd.) with a He-Ne ion laser of 633 nm at 25°C.

6. References

[1] J.-M. Lehn. Toward self-organization and complex matter. *Science*, **2002**, *295*, 2400-2403.

[2] M. J. Webber; E. A. Appel; E. W. Meijer; R. Langer. Supramolecular biomaterials. *Nat. Mater.*, **2016**, *15*, 13-26.

[3] T. Aida; E. W. Meijer; S. I. Stupp. Functional supramolecular polymers. *Science*, **2012**, *335*, 813-817.

[4] A. Whitty. Cooperativity and biological complexity. *Nat. Chem. Biol.*, **2008**, *4*, 435-439.

[5] S. C. Zimmerman; F. Zeng; D. E. C. Reichert; S. V. Kolotuchin. Self-assembling dendrimers. *Science*, **1996**, *271*, 1095-1098.

[6] V. Percec; D. A. Wilson; P. Leowanawat; C. J. Wilson; A. D. Hughes; M. S. Kaucher; D. A. Hammer; D. H. Levine; A. J. Kim; F. S. Bates; K. P. Davis; T. P. Lodge; M. L. Klein; R. H. DeVane; E. Aqad; B. M. Rosen; A. O. Argintaru; M. J. Sienkowska; K. Rissanen; S. Nummelin; J. Ropponen. Self-assembly of Janus dendrimers into uniform dendrimersomes and other complex architectures. *Science*, **2010**, *328*, 1009-1014.

[7] H.-J. Sun; S. Zhang; V. Percec. From structure to function via complex supramolecular dendrimer systems. *Chem. Soc. Rev.*, **2015**, *44*, 3900-3923.

[8] C. Chen; P. Posocco; X. Liu; Q. Cheng; E. Laurini; J. Zhou; C. Liu; Y. Wang; J. Tang; V. D. Col; T. Yu; S. Giorgio; M. Fermeglia; F. Qu; Z. Liang; J. J. Rossi; M. Liu; P. Rocchi; S. Pricl; L. Peng. Mastering dendrimer self-assembly for efficient siRNA delivery: From conceptual design to in vivo efficient gene silencing. *Small*, **2016**, *12*, 3667-3676.

[9] T. Wei; C. Chen; J. Liu; C. Liu; P. Posocco; X. Liu; Q. Cheng; S. Huo; Z. Liang; M. Fermeglia; S. Pricl; X.-J. Liang; P. Rocchi; L. Peng. Anticancer drug nanomicelles formed by self-assembling amphiphilic dendrimer to combat cancer drug resistance. *PNAS*, **2015**, *112*, 2978-2983.

[10] X. Liu; J. Zhou; T. Yu; C. Chen; Q. Cheng; K. Sengupta; Y. Huang; H. Li; C. Liu; Y. Wang; P. Posocco; M. Wang; Q. Cui; S. Giorgio; M. Fermeglia; F. Qu; S. Pricl; Y. Shi; Z. Liang; P. Rocchi; J. J. Rossi; L. Peng. Adaptive amphiphilic dendrimer-based nanoassemblies as robust and versatile siRNA delivery systems. *Angew. Chem. Int. Ed.*, **2014**, *53*, 11822-11827.

[11] X. Liu; Y. Wang; C. Chen; A. Tintaru; Y. Cao; J. Liu; F. Ziarelli; J. Tang; H. Guo; R. Rosas; S. Giorgio; L. Charles; P. Rocchi; L. Peng. siRNA delivery: A fluorinated bola-amphiphilic

dendrimer for on-demand delivery of siRNA, via specific response to reactive oxygen species. *Adv. Funct. Mater.*, **2016**, *26*, 8565-8565.

[12] Y. Cao; X. Liu; L. Peng. Molecular engineering of dendrimer nanovectors for siRNA delivery and gene silencing. *Front. Chem. Sci. Eng.*, **2017**, In Press, DOI: 10.1007/s11705-11017-11623-11705

[13] V. P. Chauhan; R. K. Jain. Strategies for advancing cancer nanomedicine. *Nature materials*, **2013**, *12*, 958-962.

[14] E. K.-H. Chow; D. Ho. Cancer nanomedicine: From drug delivery to imaging. *Sci. Transl. Med.*, **2013**, *5*, 216rv214.

[15] M. L. James; S. S. Gambhir. A molecular imaging primer: Modalities, imaging agents, and applications. *Physiol. Rev.*, **2012**, *92*, 897-965.

[16] C. S. S. R. Kumar. Nanomaterials for cancer diagnosis. John Wiley & Sons, Inc.: **2007**.

[17] W. J. Schempp. Magnetic resonance imaging: Mathematical foundations and applications. John Wiley & Sons, Inc.: **1998**.

[18] C. Corot; J.-M. Idee; A.-M. Hentsch; R. Santus; C. Mallet; V. Goulas; B. Bonnemain; D. Meyer. Structure-activity relationship of macrocyclic and linear gadolinium chelates: Investigation of transmetallation effect on the zinc-dependent metallopeptidase angiotensin-converting enzyme. *J. Magn. Reson. Imaging*, **1998**, *8*, 695-702.

[19] J. Bremerich; J. M. Colet; G. B. Giovenzana; S. Aime; K. Scheffler; S. Laurent; G. Bongartz; R. N. Muller. Slow clearance gadolinium-based extracellular and intravascular contrast media for three-dimensional MR angiography. *J. Magn. Reson. Imaging*, **2001**, *13*, 588-593.

[20] D. A. Tomalia; L. A. Reyna; S. Svenson. Dendrimers as multi-purpose nanodevices for oncology drug delivery and diagnostic imaging. *Biochem. Soc. Trans.*, **2007**, *35*, 61-67.

[21] P. Caravan; J. J. Ellison; T. J. McMurry; R. B. Lauffer. Gadolinium(III) chelates as MRI contrast agents: Structure, dynamics, and applications. *Chem. Rev.*, **1999**, *99*, 2293-2352.

[22] H. Kobayashi; M. W. Brechbiel. Nano-sized MRI contrast agents with dendrimer cores. *Adv. Drug Del. Rev.*, **2005**, *57*, 2271-2286.

[23] K. N. Raymond; V. C. Pierre. Next generation, high relaxivity Gadolinium MRI agents. *Bioconj. Chem.*, **2005**, *16*, 3-8.

[24] Z. Zhou; Z.-R. Lu. Gadolinium-based contrast agents for MR cancer imaging. *Wiley interdisciplinary reviews. Nanomedicine and nanobiotechnology*, **2013**, *5*, 1-18.

[25] T. Yu; X. Liu; A.-L. Bolcato-Bellemin; Y. Wang; C. Liu; P. Erbacher; F. Qu; P. Rocchi; J.-P. Behr; L. Peng. An amphiphilic dendrimer for effective delivery of small interfering RNA and gene silencing in vitro and in vivo. *Angew. Chem. Int. Ed.*, **2012**, *51*, 8478-8484.

[26] Z. Zhang; G. Huang. Micro- and nano-carrier mediated intra-articular drug delivery systems for the treatment of osteoarthritis. *J. Nanotechnol.*, **2012**, *2012*, 1-11.

Chapter IV: Conclusions and perspectives

1. Conclusions

Dendrimers hold great promise for a wide range of applications by virtue of their distinct ramified architecture, well-defined structure and multivalent cooperativity. Unfortunately, dendrimer synthesis suffers from inherent problems of structural defects caused by incomplete reactions and difficulties associated with dendrimer purification because of the presence of side-products with similar properties. For these reasons, alternative synthetic approaches to overcome the limitations of current dendrimer synthesis are in high demand. The objective of my PhD thesis is to contribute to this area and advance dendrimer synthesis by exploring solid-phase and self-assembly approaches to complement current dendrimer synthesis techniques and enable the creation of structurally diverse dendrimers as new molecular paradigms and functional materials for a wide range of applications.

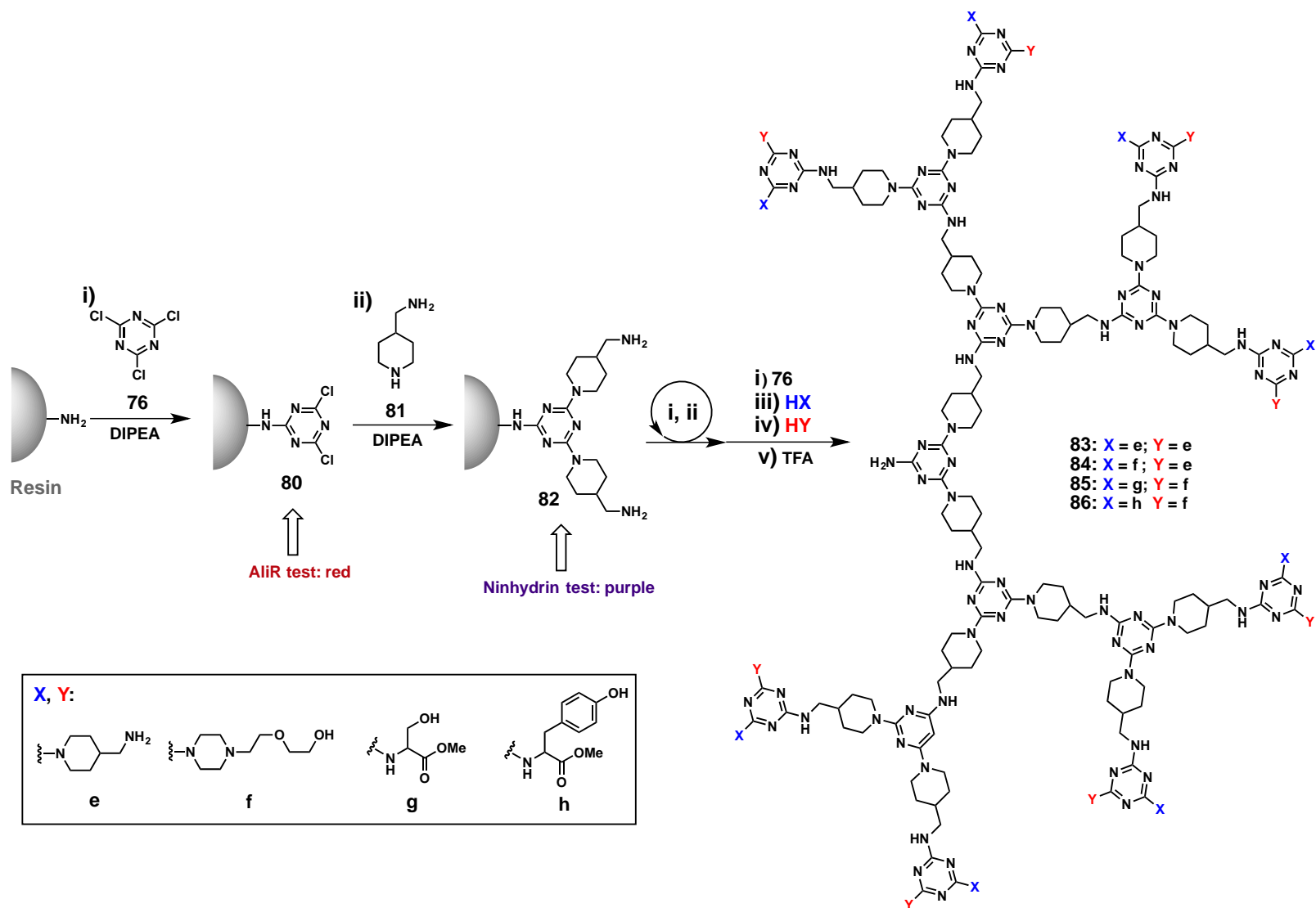### 1.1. Solid-phase synthesis of various dendrimers

The first part of my PhD project mainly focused on solid-phase dendrimer synthesis (SPDS). First of all, we presented a brief overview to highlight the current state of solid-phase dendrimer synthesis. In order to overcome the limitations associated with PAMAM dendrimer synthesis using traditional iterative steps of Michael addition and amidation, we established a novel and convenient approach for the solid-phase synthesis of inverse PAMAM dendrimers via amide bond formation using peptide synthesis chemistry. The synthesis was achieved by using the AB_2 type building block (**41**), which harbors both a carboxylic acid terminal and an amine terminal along with a tertiary amine branch point. As the synthetic approach was based on amide bond formation, it effectively precluded the formation of side-products that are typically associated with the Michael addition and amidation in the traditional synthesis of PAMAM dendrimers (**Scheme 1**).

A comparison with the conventional approach revealed that fewer reaction steps were needed and a smaller amount of the building blocks was required to obtain dendrimers of similar generation with high yields. In addition, reducing the loading ratio of the resin allowed effective synthesis of the high-generation dendrimers G6 and G7, highlighting that the steric hindrance among neighboring molecules on the solid support is the major obstacle in solid-phase synthesis of higher generations of dendrimers. Hence, reducing the loading ratio of the resin constitutes an effective solution for preparing high-generation dendrimers.
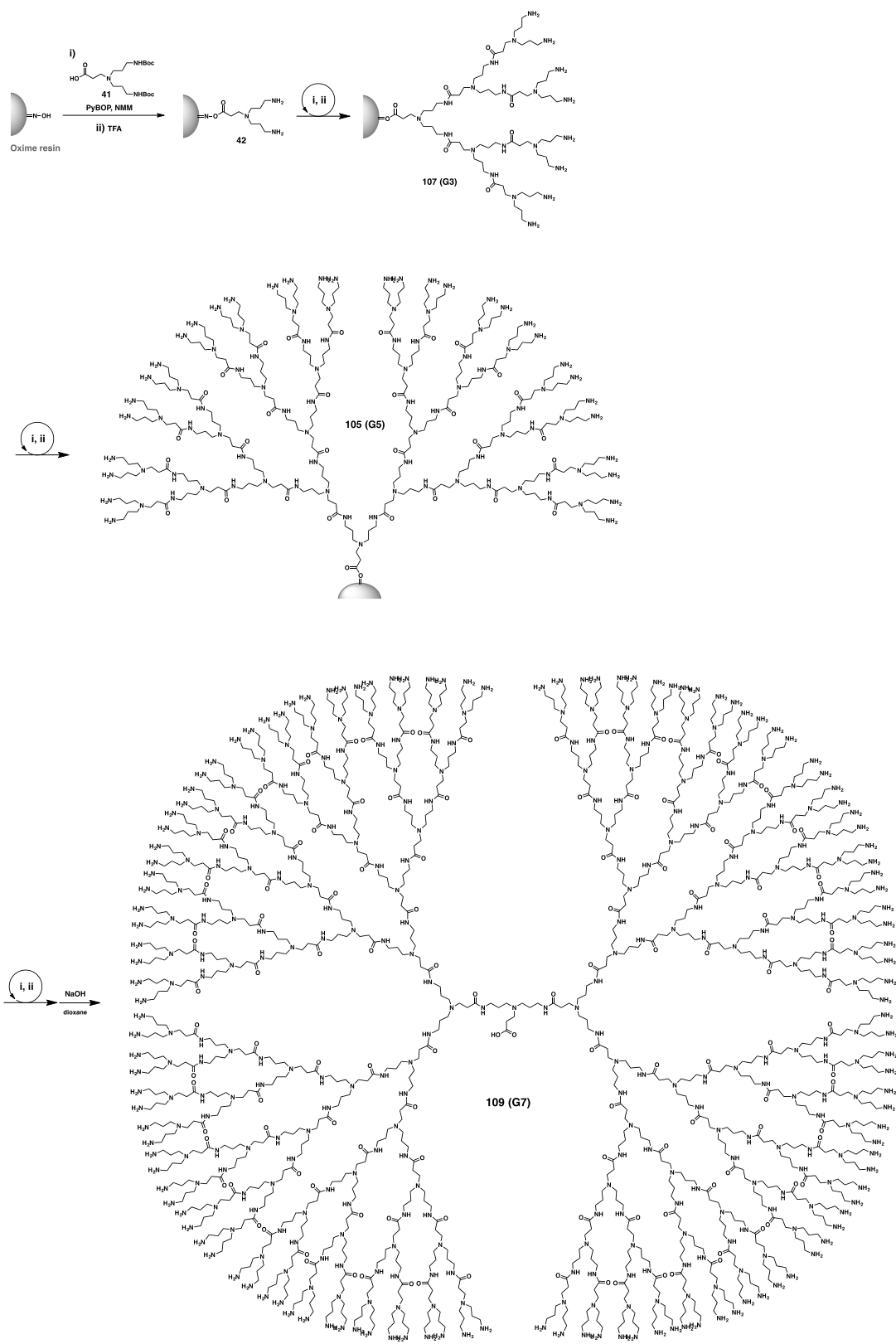
Scheme 1. PAMAM dendrimer synthesis through a solid-phase approach using the designed building block (**41**).

We next performed the solid-phase synthesis of a small library composed of triazine dendrimers bearing a variety of surface terminals (**Scheme 2**). Starting with Rink-amide resin, iterative reactions with the cyanuric chloride (**76**) and the diamine linker (**81**) allowed dendrimer growth to proceed steadily. In addition, the amine- and dichlorotriazine-terminated dendrimers could be tracked and revealed using the Kaiser test and the AliR test respectively. This offers an efficient approach to monitor the reaction process and hence the dendrimer growth. Notably, dichlorotriazine-terminated dendrimers could react selectively with four different combinations (**83-86**) of nucleophiles, generating a library of triazine dendrimers with multifunctional surfaces in a total yield of 81-87%. The whole preparation process was accomplished within one week. The approach developed in this work can also be applied to rapidly access various triazine dendrimers and construct a large library of diverse triazine dendrimers for various applications.

Scheme 2. Solid-phase synthesis of triazine dendrimer libraries with four combinations of terminals.

Key labels within the scheme:

i) 76, DIPEA

ii) 81, DIPEA

80 — AliR test: red

82 — Ninhydrin test: purple

i) 76
iii) HX
iv) HY
v) TFA

83: X = e; Y = e
84: X = f ; Y = e
85: X = g; Y = f
86: X = h Y = f

X, Y:
e   f   g   h

Encouraged by the promising results, we further explored the solid-phase approach to synthesize poly(aminoester) dendrimers. The only difference between poly(aminoester) and PAMAM dendrimers is that the amide functions in PAMAM dendrimers are replaced by ester linkages. Therefore, we attempted to synthesize poly(aminoester) dendrimers using a strategy similar to the one we developed for the solid-phase synthesis of PAMAM dendrimers, except that we adapted it for ester formation by using the AB_2 type building units with Kaiser oxime resin (**Scheme 3**). Regrettably, this method was not able to yield the desired dendritic molecules, presumably because the labile ester linkages were damaged during the resin cleavage. We then turned to the photolabile resin in the hope that the resin cleavage could be accomplished using photo-irradiation, thus avoiding the damage to the ester functionalities. Unfortunately, our pilot study using this approach was not yet successful in delivering the expected dendrimers. Further studies are necessary to clarify the underlying problems associated with poly(aminoester) dendrimers upon photo-irradiation.
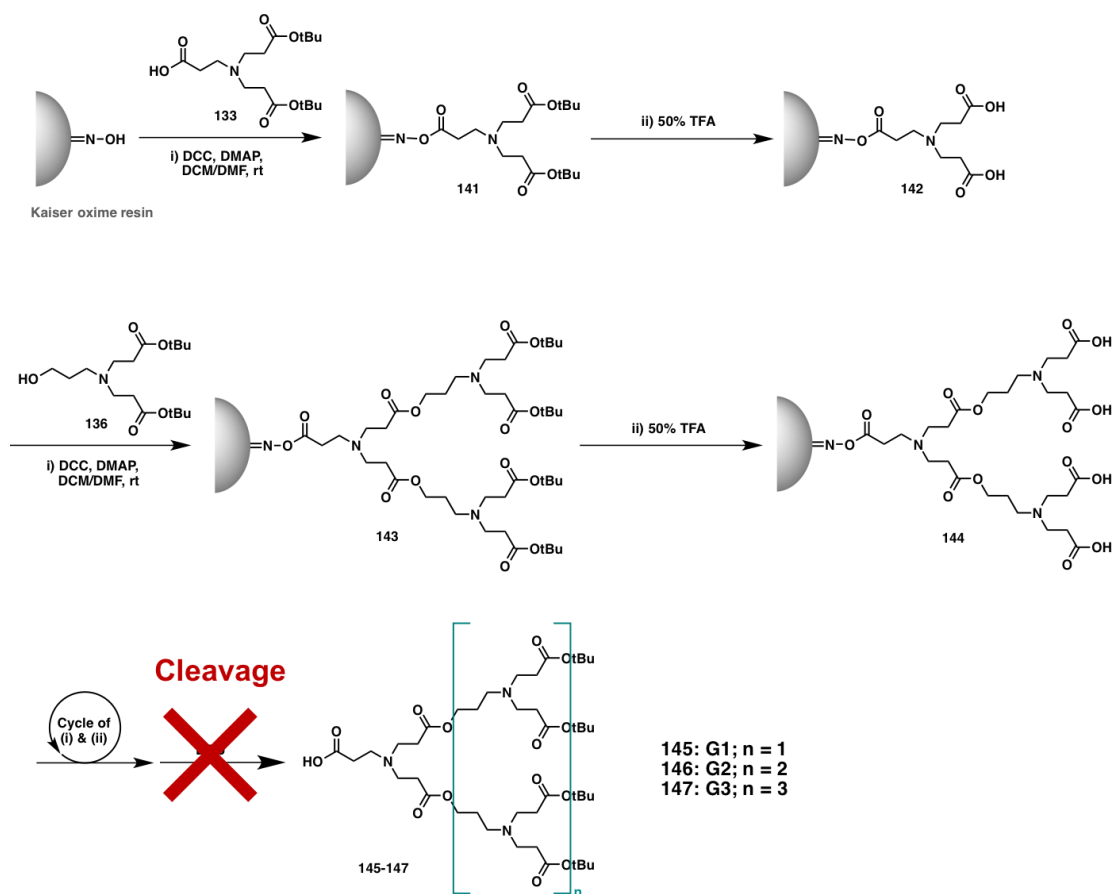
Scheme 3. Solid-phase synthesis of poly(aminoester) dendrimers, which failed due to decomposition at the cleavage step.

In conclusion, solid-phase synthesis sets the stage for the construction of diversified dendrimers in a concise and rapid manner. Practical implementation of solid-phase synthesis in both academic research and industrial production may further expand the applications of dendrimer chemistry. We expect that further research will deliver more effective methods for solid-phase dendrimer synthesis, which can be extended into the area of biomedical and material sciences.

1.2. Self-assembly synthesis of supramolecular dendrimers as nanotheranostics

The second topic of my PhD project is to use the self-assembly approach to construct supramolecular dendrimers as nanotheranostics for bioimaging and drug delivery (**Figure 8**). For this purpose, a DOTA-conjugated amphiphilic dendrimer **C$_{18}$-G2-4DOTA** was established. The synthesis of **C$_{18}$-G2-4DOTA** was achieved by conjugation of the amine-terminating PAMAM dendrimer **C$_{18}$-G2** with DOTA-entities, followed by chelation of Gd(III) metal ions for MRI purposes, and finally self-assembly of the molecules into supramolecular dendrimer nanomicelles to encapsulate the anticancer drug doxorubicin (**DOX**), thus delivering the nanotheranostic. The so-built dendrimer nanoassemblies were small in size (6-7 nm), yet with a relatively high drug payload, and were stable and robust. Collectively, our results demonstrate that the self-assembly approach constitutes a promising new means to build up supramolecular dendrimer nanosystems for constructing multifunctional nanoparticles for diagnosis and therapy. The self-assembly synthetic strategy is not only a milestone in creating supramolecular dendrimers, but also holds great promise for generating functional nanosystems for biomedical applications in general.
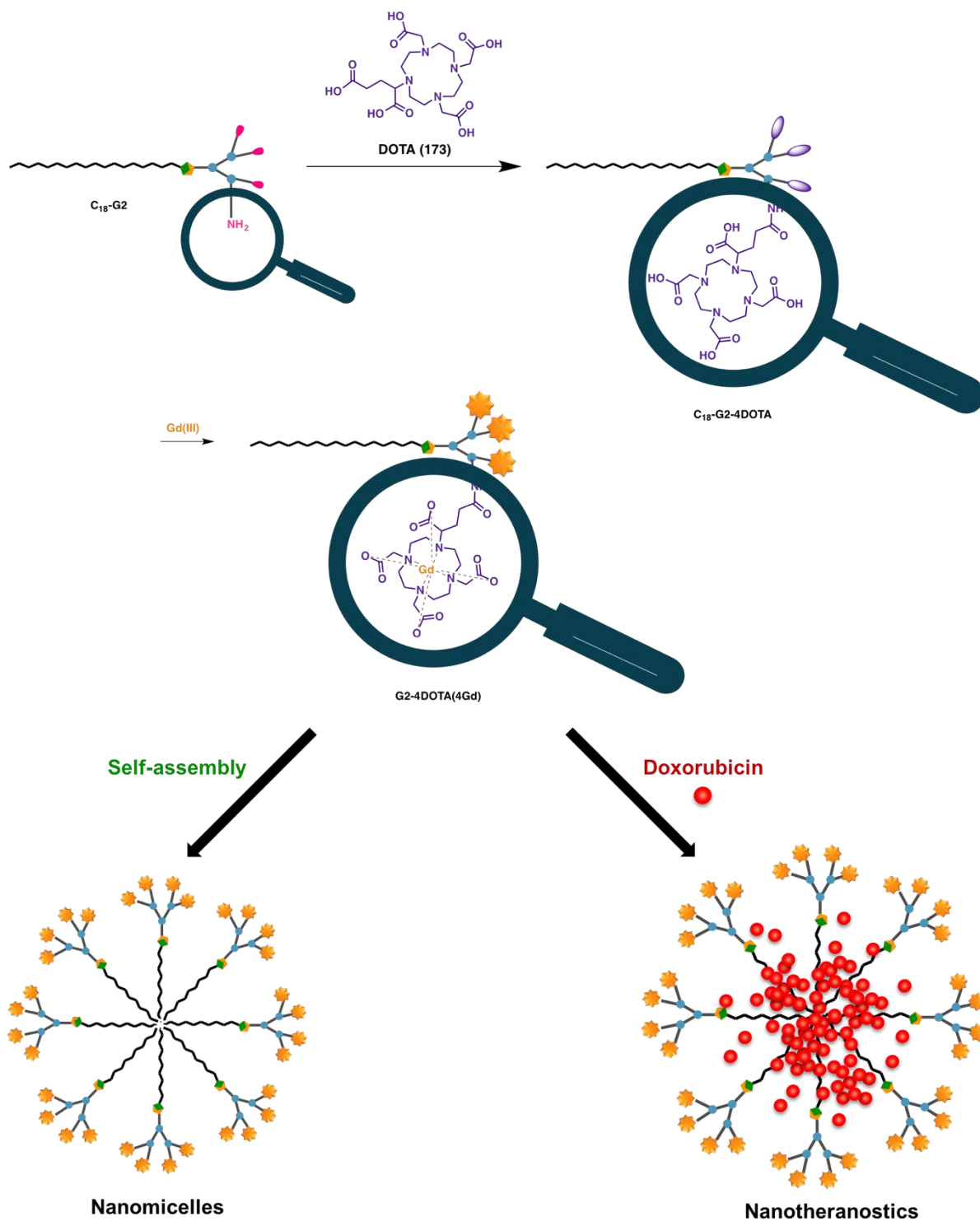
Figure 8. Synthesis of **C18-G2-4DOTA**, **G2-4DOTA/Gd/**, and then **DOX**-encapsulated nanomicelles **G2-4DOTA/Gd/DOX**, via the self-assembly approach.

2. Perspectives

Construction of functional molecules with novel composition, architecture and properties is one of the principal missions for chemists. Dendrimers, with their distinct ramified architecture, well-defined structure and multivalent cooperativity, constitute an extremely interesting class of molecules with unique properties for scientists to exploit in various applications including energy production, environmental protection, health care etc. Since its conception three decades ago, the characteristic multi-step process for dendrimer synthesis still requires tremendous effort, which greatly handicaps the development of dendrimers and limits their applications. Continuing improvements in dendrimer synthesis are in high demand. In my PhD thesis, we have explored both solid-phase and self-assembly approaches for dendrimer synthesis, which proved to be effective and enabled the creation of dendrimers for further specific applications. This provides us with the following perspectives:

2.1. Dendrimer synthesis and library construction via the solid-phase approach

The growing importance of solid-phase chemistry in organic chemistry has resulted in remarkable technological and synthetic advances in the field.[1] Over the past decade, the great majority of studies on dendrimer library construction have been based on peptide chemistry, which has been well elaborated by Reymond and co-workers. In their work, they developed a general method for synthesizing and decoding diversified peptide dendrimer libraries, and the resulting dendrimers have been used as versatile synthetic enzyme models as well as for drug delivery.[2-6]

Based on the results of solid-phase construction of a small triazine dendrimer library obtained during this PhD project, we will continue our efforts in dendrimer synthesis and library construction via the solid-phase approach (**Scheme 4**). We would like to build up triazine dendrimers with various linkers (groups **A** and **B**) as branching units, in order to diversify both the interior and surface functionalities. These versatile terminal and interior functionalities are well-suited for host-guest interactions and catalysis where the functional motifs are important. Preliminary work has shown encouraging results, suggesting that a low-generation dendrimer library with mixed interior branches can be constructed.
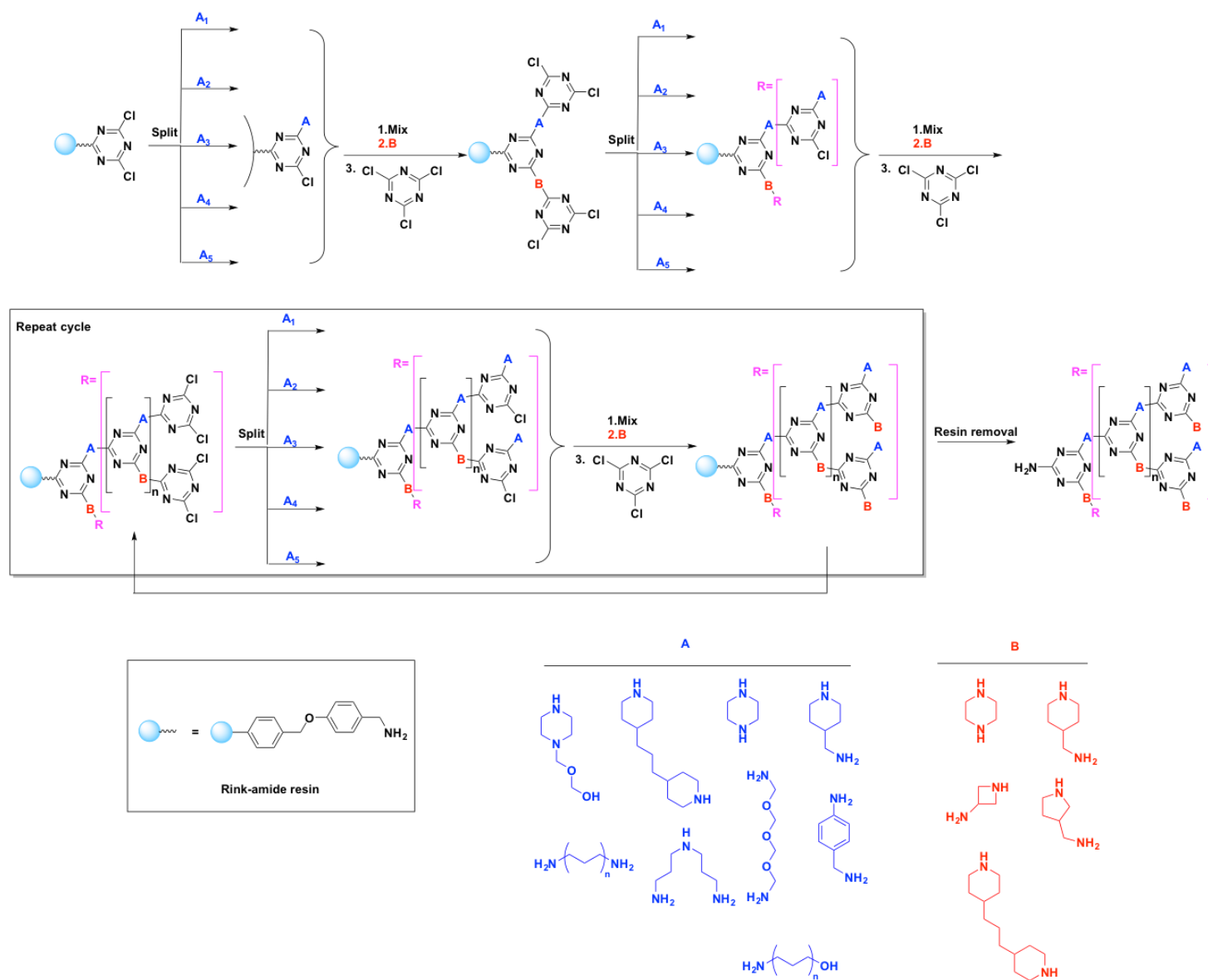
Scheme 4. Solid-phase synthesis of a triazine dendrimer library with versatile interior branching units (groups **A** and **B**).

2.2. Self-assembling supramolecular nanotheranostics for MRI and PET/SPECT imaging

In my PhD project, we used an ingenious self-assembly approach to successfully construct dendrimer nanosystems for theranostic purposes (**Figure 9**). These nanosystems facilitate MRI-based cancer imaging in combination with doxorubicin-based cancer chemotherapy. The building unit for constructing such a supramolecular dendrimer nanosystem is simply a small amphiphilic dendrimer **C18-G2-4DOTA**, which is composed of a hydrophobic alkyl chain and a hydrophilic PAMAM dendritic wedge with four DOTA-conjugated terminals. By chelating the DOTA units with Gd(III), we established supramolecular dendrimers for MRI-based imaging. Alternatively, we can also chelate DOTA with radionuclides such as Ga^{3+}, $^{90}Y^{3+}$ and $^{111}In^{3+}$ for PET/SPECT-based cancer imaging. While MRI has superior resolution with the potential to detect small tumor lesions, PET/SPECT is the most sensitive method for cancer imaging. A combination of MRI with PET/SPECT thereby offers multimodal imaging with both high resolution and high sensitivity. Using the same amphiphilic dendrimer **C18-G2-4DOTA** to chelate with different metal ions, we can achieve different imaging modalities, hence realizing combined MRI- and PET/SPECT-based multimodal imaging for accurate, sensitive cancer imaging and early, precise cancer diagnosis.

Similar to the supramolecular dendrimer nanoassembly **G2-4DOTA/Gd/DOX** that we developed for MRI-based theranostics, we can also encapsulate the anticancer drug doxorubicin within the **G2-4DOTA/Ga** or **G2-4DOTA/In** nanosystems for PET- or SPECT-based theranostics. These supramolecular dendrimer nanoassemblies integrate therapeutic and diagnostic platforms, allowing us to diagnose and treat cancer at the same time as well as to assess the therapeutic efficacy for personalized medicine.[7-9] We hope to reach a better understanding of the use of nanotheranostics in integrating multimodal imaging and therapeutic platforms for cancer treatment in general, moving our research results towards clinical applications.
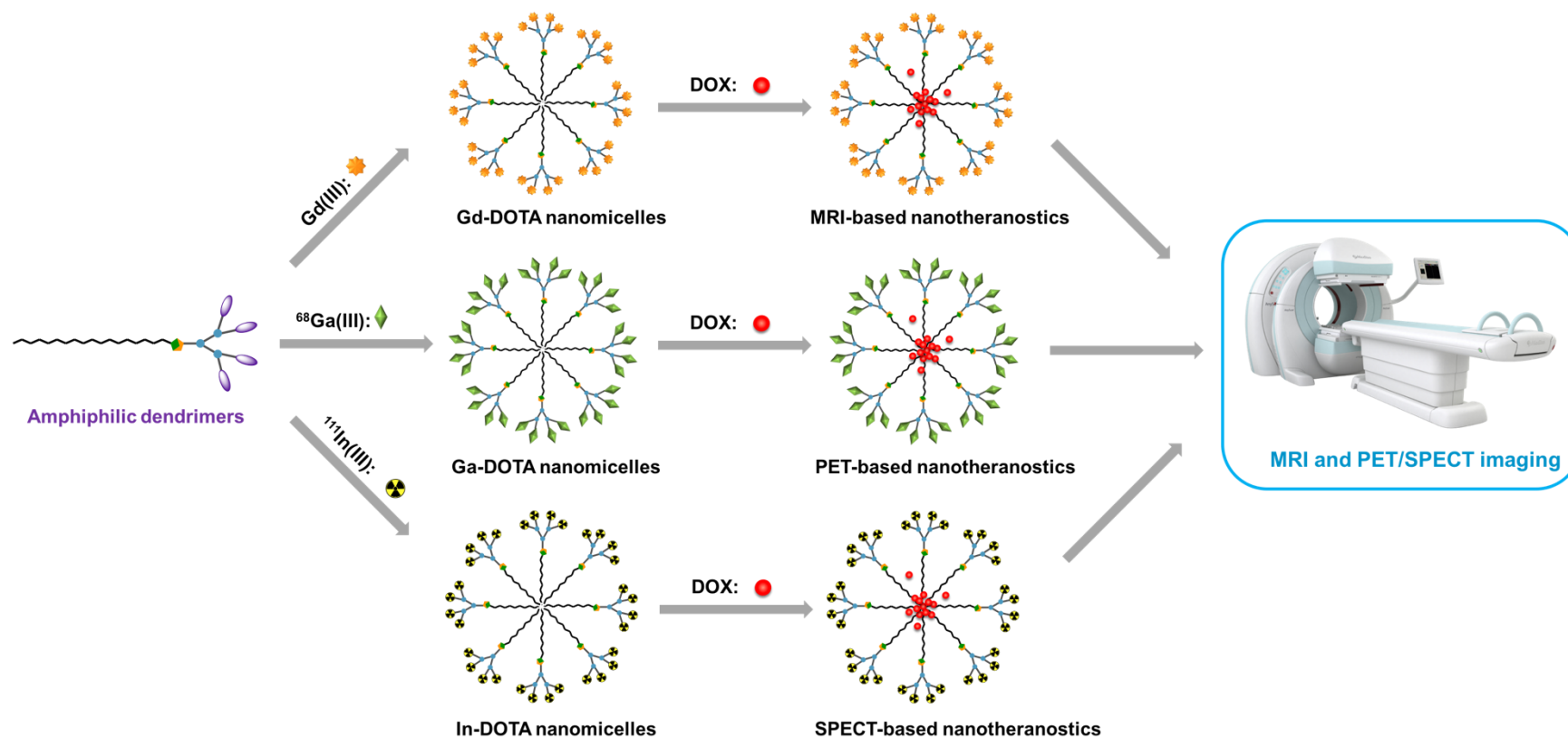
Figure 9. Gd-, Ga-, and In-based nanotheranostics **G2-4DOTA/Gd/DOX**, **G2-4DOTA/Ga/DOX** and **G2-4DOTA/In/DOX** for MRI and PET/SPECT imaging

3. References

[1] W. Bannwarth; B. Hinzen. Combinatorial chemistry: From theory to application. John Wiley & Sons, Inc.: **2006**.

[2] M. Stach; T. N. Siriwardena; T. Köhler; C. van Delden; T. Darbre; J.-L. Reymond. Combining topology and sequence design for the discovery of potent antimicrobial peptide dendrimers against multidrug-resistant *Pseudomonas aeruginosa*. *Angew. Chem. Int. Ed.*, **2014**, *53*, 12827-12831.

[3] N. Maillard; A. Clouet; T. Darbre; J.-L. Reymond. Combinatorial libraries of peptide dendrimers: Design, synthesis, on-bead high-throughput screening, bead decoding and characterization. *Nat. Protocols*, **2009**, *4*, 132-142.

[4] E. M. V. Johansson; E. Kolomiets; F. Rosenau; K.-E. Jaeger; T. Darbre; J.-L. Reymond. Combinatorial variation of branching length and multivalency in a large (390 625 member) glycopeptide dendrimer library: Ligands for fucose-specific lectins. *New J. Chem.*, **2007**, *31*, 1291-1299.

[5] J. Kofoed; T. Darbre; J.-L. Reymond. Artificial aldolases from peptide dendrimer combinatorial libraries. *Org. Biomol. Chem.*, **2006**, *4*, 3268-3281.

[6] T. Darbre; J.-L. Reymond. Peptide dendrimers as artificial enzymes, receptors, and drug-delivery agents. *Acc. Chem. Res.*, **2006**, *39*, 925-934.

[7] S. M. Janib; A. S. Moses; J. A. MacKay. Imaging and drug delivery using theranostic nanoparticles. *Adv. Drug Del. Rev.*, **2010**, *62*, 1052-1063.

[8] J. Xie; S. Lee; X. Chen. Nanoparticle-based theranostic agents. *Adv. Drug Del. Rev.*, **2010**, *62*, 1064-1079.

[9] E. K.-H. Chow; D. Ho. Cancer nanomedicine: From drug delivery to imaging. *Sci. Transl. Med.*, **2013**, *5*, 216rv214.